Joint 5th Central-European Mineralogical Conference and 7th Mineral Sciences in the Carpathians Conference

Book of Contributions and Abstracts

Banská Štiavnica
June 26 – 30, 2018

Comenius University in Bratislava

Mineralogical Society of Slovakia (SMS) and Slovak Mining Museum (SBM)

Joint 5th Central-European Mineralogical Conference and 7th Mineral Sciences in the Carpathians Conference

Book of Contributions and Abstracts

Mineralogical Society of Slovakia 2018 ISBN 978-80-223-4548-4

Joint 5th Central-European Mineralogical Conference and 7th Mineral Sciences in the Carpathians Conference

Editors:
Martin Ondrejka Jan Cempírek and Peter Bačík

The manuscripts have been reviewed by:
Khaled Abdelfadil, Peter Bačík, Igor Broska, Jan Cempírek, Andreas Ertl, Štefan Ferenc, Radek Hanus, Monika Huraiová, Marian Janák, Stanislav Jeleň, Ján Kráľ, Otília Lintnerová, Zděnek Losos, Juraj Majzlan, Milan Novák, Martin Ondrejka, Daniel Ozdín, Igor Petrík, Jaroslav Pršek, René Putiška, Jiří Sejkora, Radek Škoda, Martin Števko, Pavel Uher, Peter Uhlík, Anna Vozárová

The English was not reviewed

Published by:
Comenius University in Bratislava

Printed in:
Comenius University in Bratislava

Mineralogical Society of Slovakia 2018 ISBN 978-80-223-4548-4

Table of Contents

Evidence for rare-metal occurrences in the post-orogenic Pan-African Aswan pegmatite (southern Egypt): mineralogy, geochemistry and monazite dating

[1,3]Khaled M. Abdelfadil[#], [2]Moustafa E. Gharib, [3]Marian Putiš and [3]Pavel Uher

[1] Sohag University, Faculty of Science, Department of Geology, 82524 Sohag, Egypt
[#]khaled.abdelfadeel@science.sohag.edu.eg
[2] Helwan University, Faculty of Science, Geology Department, 11795 Cairo, Egypt
[3] Comenius University, Faculty of Natural Sciences, Department of Mineralogy and Petrology, Mlynská dolina, Ilkovičova 6, 842 15 Bratislava, Slovakia

Key words: rare metal, Aswan pegmatite, Pan-African, columbite, monazite

Pegmatite-hosted, rare-metal mineralization from Aswan area, southern Egypt, intruded the post-orogenic Pan-African granitic rocks and the associated tonalitic gneisses and biotite schists. Most of the pegmatites show a regular pattern of concentric zoning and present affinity to NYF (Nb-Y-F) family. These pegmatites consist mainly of K-feldspar, albite, quartz, and subordinate muscovite, while the accessory minerals include columbite-(Fe), monazite-(Ce), xenotime-(Y), zircon, fluorapatite, and magnetite. Compositions of Nb-Ta minerals show enrichment of Ti, Sc and fractionation Fe/Mn and Nb/Ta. These features indicate primary magmatic fractionation of these elements into the highly evolved pegmatite melts, rather than to assimilation from the country rocks. Chemical U-Th-Pb dating of monazite from the studied pegmatites yielded post-orogenic Pan-African age (578 ± 5 Ma). This age is younger than the previously estimated U-Pb zircon ages for the tonalitic gneisses and the associated granitic country rocks of the Aswan area (622 ± 11 Ma- 595 ± 11 Ma; Finger et al. 2008) which the studied pegmatite intruded all of them. The analysed monazite-(Ce) displays the dominant LREE phosphate end-member composition and show large variations in composition from the border to the core zone of the studied pegmatites. Monazite-(Ce) from the border zone has higher ThO_2 (2.7–9.5 wt.%), Y_2O_3 (0.1–3.9 wt.%), Nd_2O_3 (11.0–14.3 wt.%), Sm_2O_3 (2.4–3.9 wt.%), Gd_2O_3 (1.3–3.1 wt.%) with marked lowering in La_2O_3 (9.3–12.8 wt.%), Ce_2O_3 (23.2–29.4 wt.%) and slightly negative Eu anomalies relative to the monazite-(Ce) from core zone. This data proved the effective role of fractional crystallization in formation of the studied pegmatites.

Acknowledgment: This work was supported by the Slovak Research and Development Agency under contract No. APVV-15-0050 and VEGA Agency 1/0079/15.

REFERENCES

Finger F. et al. (2008): Min Petrol 93:153–183.

Pan-African rare-earth bearing paragneiss, South-eastern desert, Egypt: geochemistry and monazite age dating

[1,2]Khaled M. Abdelfadil[#], [2]Marian Putiš, [2]Martin Ondrejka and [3]Gehad Saleh

[1] Sohag University, Faculty of Science, Department of Geology, 82524 Sohag, Egypt
[#]khaled.abdelfadeel@science.sohag.edu.eg
[2] Comenius University, Faculty of Natural Sciences, Department of Mineralogy and Petrology, Mlynská dolina, Ilkovičova 6, 842 15 Bratislava, Slovakia
[3] Nuclear Materials Authority, P.O. Box 530, El Maadi, Cairo, Egypt

Key words: monazite, gneiss, zircon, xenotime, columbite

The studied gneiss of Abu Rusheid is located about 90 km SW from Marsa Alam City (South-eastern desert, Egypt) covering about 3 km^2 with low to medium facies metamorphism. It accommodates rare-element (Nb, Sn, Zr, and REE) mineralization. Chemical composition of the samples was determined by ICP-ES and ICP-MS and detailed mineralogical study using EPMA and LA-ICP-MS have been achieved.

The gneiss is strongly enriched in REE. Chondrite-normalized REE patterns illustrated enrichment in HREE in studied rock relative to LRRE and strong Eu negative anomalies. The enrichment in HREE relative to LREE reflects the abundant presence of zircon, monazite-(Ce), xenotime-(Y), and fluorite.

Zircon contains high Hf, Th and Yb contents. Columbite is homogenous and weakly zoned and classified as columbite-(Fe) with moderate Mn/(Mn+Fe) ratio (0.35–0.49) and very low Ta/(Ta+Nb) (0.01–0.07) ratio.

The EMPA U–Th–Pb dating on monazite from the studied gneiss yields two ages: (i) deformation age of 659 ± 3.5 Ma recorded by monazite cores, and (ii) younger age of 575 ± 2.1 Ma obtained from its rims. The older age is comparable with previous age determination of zircon reported from similar rocks in the Eastern desert, indicating a thermal metamorphic peak at about 560 Ma during the convergence between East and West Gondwana, with simultaneously widespread calc-alkaline granitic intrusions (Loizenbauer et al. 2001). The younger age might represent a later event associated with the emplacement of post Pan-African granitic intrusions (Abdallah 2006, and references therein).

Acknowledgment: This work was supported by the Slovak Research and Development Agency under contract No. APVV-15-0050 and VEGA Agency 1/0079/15.

References

Abdallah M. (2006): Res Geol 56:365–370.

Loizenbauer J. et al. (2001): Precamb Res 110:357–383.

The Jahn-Teller distortion influences the cation distribution in Fe^{2+}-bearing tourmalines

[1,2]Peter Bačík[#]

[1] Comenius University, Faculty of Natural Sciences, Department of Mineralogy and Petrology, Ilkovičova 6, 842 15 Bratislava, Slovakia [#]peter.bacik@uniba.sk
[2] Earth Science Institute of the Slovak Academy of Sciences, Dúbravská cesta 9, 840 05 Bratislava, Slovak Republic

Key words: tourmaline supergroup minerals, octahedron, metrics, bond length

Two types of octahedral sites are present in the structure of tourmaline-supergroup minerals. The ZO_6 octahedron is smaller and more distorted than the YO_6 octahedron.

The goal of this contribution is the study of the octahedral metrics and their dependency on the chemical composition unconstrained on the *Y*-*Z*-site disorder assignment. For this purpose, published chemical compositional and structural data were collected from the American Mineralogist Crystal Structure Database for tourmaline samples belonging to dravite-schorl, schorl-elbaite (including tsilaisite) and schorl(±dravite)-olenite series.

Correlation analysis of this dataset showed the cation distribution between sites. Of studied cations, Al and Mg are disordered between *Z* and *Y* sites, while Fe (mostly ferrous), Li and Mn strongly prefer the *Y* site. An irregular cation distribution influences the variable metrics of both octahedra in tourmalines. It is a function of well-balanced and intertwined relations between cations at octahedral and neighbouring sites, based on bond-valence variations due to different ionic charges.

There is a strong dependence of the cation charge difference and the octahedral metrics. The largest irregularity of both octahedra was observed in elbaite samples with the largest charge difference between Li and Al. However, *buergerite* samples with trivalent Fe and Al at both octahedral sites have both octahedra almost isometric in the sense of bond lengths. Schorl and dravite samples display an increasing metric irregularity dependent on the Al and Mg content; decrease in Mg increases octahedral irregularity because Mg is distributed among both octahedral sites balancing charge difference.

In contrast, Fe-rich and Al-rich schorl samples have larger irregularity, which likely results on selective Fe^{2+} incorporation into the *Y* site. In olenite samples, the irregularity of both octahedra decreases with an increasing Al content.

These variations result from the shared edge between the ZO_6 and YO_6 octahedra, including both O3 and O6 sites, where bonds of both anions balance bond-valence requirements for a stable electroneutral structure.

In addition to the bond-valence relations, effects of the atomic shells internal geometry should be also taken into account, i.e. the Jahn-Teller distortion. Such a distortion can be a decisive factor for the cation occupancy; Fe^{2+} can be very selective in favour of the YO_6 octahedron not only due to a larger ionic radius compared to Mg and Al, but also because the prolonged tetragonal dipyramidal geometry is more favourable for Fe^{2+} in a $(t_{2g})^4(e_g)^2$ configuration.

Acknowledgment: This work was supported by the Slovak Research and Development Agency under the contracts No. APVV-14-0278, APVV-15-0050 and APVV-17-0134, and the Ministry of Education of Slovak Republic grant agency under the contracts VEGA-1/0079/15 and VEGA-1/0499/16.

Dravite and schorl stability in (U)HP conditions: evidence from myrmekitic tourmaline and quartz intergrowth in eclogite-hosting gneisses of the Tso Morari UHP metamorphic terrane (Eastern Ladakh Himalaya, India)

[1]Igor Broska[#], [1,2]Peter Bačík, [3]Santosh Kumar, [1]Marian Janák and [1]Sergiy Kurylo

[1] Slovak Academy of science, Earth Science Institute, Dúbravská cesta 9, 89009 Bratislava, Slovakia
[#]igor.broska@savba.sk
[2] Department of Mineralogy and Petrology, Faculty of Natural Science, Comenius University, Ilkovičova 6, 842 15 Bratislava, Slovakia
[3] Department of Geology, Centre of Advanced Study, Kumaun University, Nainital 263002, India

Key words: tourmaline, orthogneiss, (U)HP regime, uplift, dissolution, reprecipitation

INTRODUCTION

Dravitic tourmaline is reported from many ultra-high pressure (UHP) metamorphic localities, while schorlitic tourmaline formed under (U)HP conditions is scarce. Although UHP dravitic tourmaline is known from the Western Alps, Dora Maira, Kokchetav massif, schorlitic tourmaline is reported only from Erzgebirge (Ertl et al. 2010). Tso Morari UHP Crystalline Complex (TMCC), Eastern Ladakh Himalaya, offers an unique opportunity to investigate behaviour of both tourmaline compositional types, dravite vs schorl in such metamorphic conditions. The tourmaline-bearing gneisses hosting the (U)HP eclogites in TMCC shared the same tectono-metamorphic conditions as the eclogites during the Tertiary collision of Indian and Eurasian plates.

SCHORLITIC vs DRAVITIC TOURMALINES

Schorlitic tourmaline forms oriented and highly disintegrated crystals in the orthogneisses of TMCC. Tourmaline shows no distinct zoning, but contains numerous inclusions of quartz, albite, potassium feldspar as well as REE-rich apatite, indicating its high-pressure origin. Some segments of tourmaline crystals are rich in myrmekitic quartz intergrowth. The vermicular quartz inclusions are usually ca. 50 – 100 μm long. Tourmaline can be characterized as alkali-schorlitic Al-deficient with low *X*-site vacancies. Two types of quartz inclusion in tourmalines can be clearly observed: (1) matrix quartz co-existed with tourmaline, and (2) tiny vermicular quartz within tourmaline crystals. The tiny vermicular quartz inclusions are enriched in Fe (up to 0.5 wt. %) with elevated Al (0.04 wt. %) and Ti content. Temperatures of its origin using the quartz thermometer are in the range of 650 – 700 °C. Other large quartz inclusions in tourmaline are compositionally similar to those observed in the rock matrix: low contents of Fe, Al and Ti.

Secondary tourmaline crystals should have been formed either by re-precipitation within large tourmaline grains along the *c* axis as small acicular or needle–shaped crystals or by dissolution and re-precipitation of older host tourmaline resulted in "patchy" or "mosaic" zoning. Secondary tourmaline may also crystallize from anatectic melt in the veins. Secondary tourmaline often shows an increase of vacancies at the *X*-site connected with increasing Al.

Dravitic tourmaline occurs in the melanosome rocks. This tourmaline forms an envelope shaped crystals without any signature of alteration. The cores of the tourmaline are more Mg-rich in comparison to those samples from the margins, which indicates a dcereasing temperature during its growth. This tourmaline is slightly Al deficient.

TOURMALINE-QUARTZ INTERGROWTH

Schorlitic tourmaline shows tiny vermicular-shaped myrmekitic quartz intergrowth commonly developed locally within tourmaline. Vermicular quartz is enriched in Fe, Al and Ti. The investigated

myrmekitic texture in tourmaline is interpreted as expulsion of silica from tourmaline or as product of decompression during the M3 stage according to St-Onge et al. (2013). Relatively large-sized vermicular quartz is formed because of dynamic Ostwald ripening process, which occurred after expulsion. The exsolved vermicular silica from tourmaline at least points to elevated content of silica in the former tourmaline crystals at high pressure prior to exsolution. Silica oversaturation at UHP conditions is known from many minerals (e.g. omphacite, majorite garnet) and is also known from experimental works on tourmaline (e.g. Wunder et al. 2015).

Besides quartz intergrowth, potassic feldspar also forms tiny inclusions in tourmaline. Fig. 1 demonstrates the segments of tourmaline occupied with quartz exsolution and the formation of secondary tourmaline. Fig. 2 shows a distribution of tiny quartz and potassic feldspar grains as products of tourmaline decomposition during decompression.

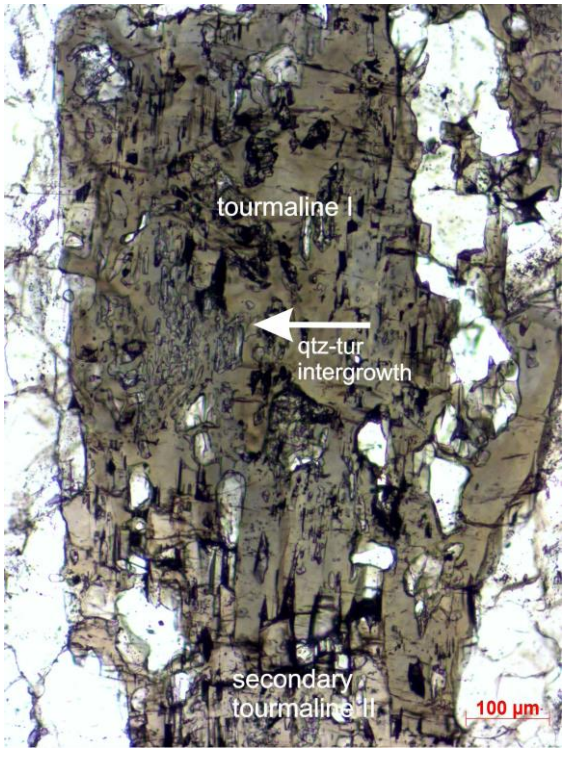

Fig. 1: Schorlitic tourmaline in transmitted light shows inclusions and exsolved quartz in one segment ("qtz-tur intergrowth"). Secondary tourmaline (bottom) forms crystals oriented parallel to the *c* axis in tourmaline (parallel nicols).

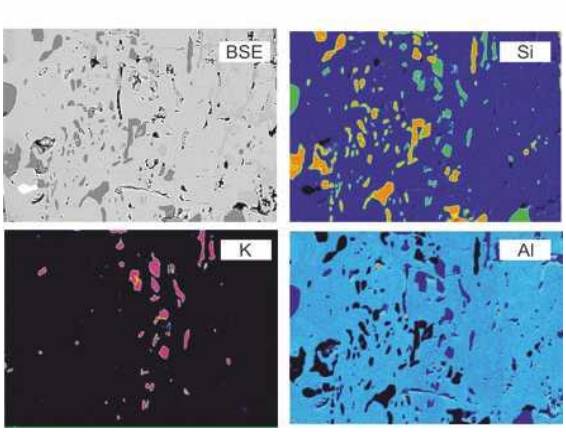

Fig. 2: Back-scattered electron image and element (Si-K-Al) maps of the "quartz-tur intergrowth" area from the tourmaline sample shown in Fig. 1. Tiny quartz and probably also Kfs are the result of tourmaline destabilisation during decompression.

FORMER TOURMALINE COMPOSITION

The detailed structural analysis, based on X-ray diffraction (XRD) and electron microprobe, has been carried out for the reconstruction of former primary tourmaline composition. Silicon formerly entered the octahedral *Z* site of the tourmaline crystal structure under high pressure conditions, most probably prior to the beginning of the decompression. Silicon located at the *Z* site produces bond-length shortening detected from the obtained XRD patterns. Former octahedral Si at the *Z* site will produce a significantly shorter bond length in the Al^{3+}-occupied ZO_6 octahedron. During decompression, the exsolution of silica from the tourmaline's octahedral site formed new quartz making the entire system more stable. After being released from the *Z* site, Si was replaced by Fe^{3+} and Mg, which are evidenced by an increase in the <Z-O> bond length calculated from the XRD pattern using empirical formula (Bačík 2015). An estimated content of quartz exsolved from tourmaline was calculated based on the BSE images on the volume content of quartz in tourmaline. The theoretically Z-site occupancy can be written as: $^{Z}(Al_{5.38}Si_{0.62})$.

Schorlitic tourmaline is slightly enriched in K and a possible expulsion of K from tourmaline structure could be expected as well. Potassium forms a large cation and usually does not fit into the tourmaline structure. However, an entry of K into the tourmaline structure during the compression stage would be possible.

Several tourmaline types occur in the gneisses of TMCC. Schorlitic tourmaline is a successor of magmatic Ordovician (?) tourmaline, which underwent a Tertiary continental subduction event. The former theoretical composition of schorlitic tourmaline can be derived from the HP stage or from a very early stage of decompression. The high-pressure origin of tourmalines is further strengthened by the observed association of gneissic host rocks containing UHP eclogites, and from the mineralogical point of view i.e. association with REE-rich apatite which during exhumation decomposed into a newly-formed apatite, monazite-(Ce) and xenotime-(Y). Similar behaviour of apatite is known from various (U)HP terrains (e.g. Krenn et al. 2009). The composition of schorlitic tourmaline has been modified during retrogression and now corresponds to slightly Al-deficient schorlitic tourmaline with exsolved vermicular quartz intergrowths. It is proposed that Si (at the octahedral site) in former tourmaline was later substituted by Mg and Fe^{3+} and probably due to a prevailed oxidation or an increase of temperature, which induced the expansion of the unit cell. During uplift of the host rock, schorl dissolved/ re-precipitated to schorlitic tourmaline with an increase of the Mg content. Dravite (Al-deficient tourmaline) from the melanosome rock contemporaneously precipitated along with schorl in orthogneiss. But the melanosome composition formed a more stable environment for dravitic tourmaline, and therefore it could not be disintegrated. It can be summarized that dravitic tourmaline is more stable in HP conditions than schorlitic.

Acknowledgements: This work was financed by projects by the Slovak Scientific Grant Agency (VEGA-0084/17). The fieldwork was partly supported under academic exchange programme between INSA, New Delhi and SAV, Bratislava, and partly from UGC-CAS-I grant sanctioned to Geology Department of Kumaun University.

REFERENCES

Bačík P. (2015): Can Min 53:571–590.
Ertl A. et al. (2010): Am Min 95:1–10.
Krenn E. et al. (2009): Am Min 94:801–815.
St-Onge M.R. et al. (2013): J Met Geol 31:469–504.
Wunder et al. (2015): Am Min 100:250–256.

Geochemical studies of lignite and its decomposition products: Insight from the laboratory biodegradation experiment

[1,2]Michał Bucha[#], [1]Leszek Marynowski, [2]Mariusz-Orion Jędrysek and [3]Mieczysław Błaszczyk

[1] University of Silesia, Faculty of Earth Sciences, Będzińska 60, 41-200 Sosnowiec, Poland
[#]michal.bucha@gmail.com
[2] University of Wroclaw, Institute of Geological Sciences, Max Born. Sq. 205, 50-205 Wrocław, Poland
[3] Warsaw University of Life Sciences, Faculty of Agriculture and Biology, Nowoursynowska 166, 02-787 Warszawa, Poland

Key words: lignite, biodegradation, methanogenesis, molecular study, GCMS

Miocene lignite from Konin area (Central Poland) was incubated in the laboratory to obtain CH_4 and evaluate its biogasification potential. As a result of incubation CH_4-rich biogas was produced by microbial community. Changes of total organic carbon (TOC) and the $\delta^{13}C$ value were observed in biodegraded lignite as compared to the lignite substrate. Nevertheless, it was not conclusively proven that lignite was decomposed. The aim of this study was to confirm lignite biodegradation and determine molecular composition and distribution caused by microbial impact. For this purpose fresh lignite used for fermentation, lignite from abiotic control and biodegraded lignite from incubation experiment were extracted and analysed using gas chromatography - mass spectrometry (GC-MS).

Our results showed that molecular composition of biodegraded lignite changed significantly, when compared to fresh lignite. These changes were not observed in the lignite from the abiotic control. The distribution of *n*-alkanes was similar for biodegraded and non-biodegraded samples. In both cases, *n*-alkanes (C_{23}–C_{35}) of high molecular weight occurred with very characteristic odd-over-even homologue preponderance. Only slight differences in the distribution of *n*-alkanes were observed via the lower abundance of C_{23}–C_{26} *n*-alkanes in biodegraded lignite. Their relative abundance was significantly lower in biodegraded lignite. The major compound in non-biodegraded lignite is 6,7-dehydroferruginol. Friedelan-3-one, *β*-tocopherol, and C31 (22R-17α(H),21β(H)-homohopane) are also highly abundant. Low molecular weight compounds, such as borneol, vanillin, calamine, or cadalene, are relatively small (3 to 5 % of major peaks). Compounds with molecular mass >300 did not change in biodegraded lignite. Surprisingly, pronounced differences are observed in case of ferruginol, sugiol or 6,7-dehydroferruginol. It seems that biomolecules (including *α*- and *β*-amirin and *α*- and *β*-tocopherol) are more susceptible on bacterial impact, than their geological counterparts.

In extract of biodegraded lignite, *p*-cresol and *n*-(2-acetylphenyl)formamide were identified. Occurrence of high relative concentration of *p*-cresol is most possibly connected with biodegradation of lignin, the cross-linked phenolic biopolymer (e.g. Kong et al. 2014). The presence of *p*-cresol confirmed that the degradation of macromolecules from lignite took place during incubation. The *n*-(2-acetylphenyl)formamide can be by-product of bacterial degradation of lignin, but also bacteria remnant (Peters et al. 2005).

Acknowledgment: This study was supported by Narodowe Centrum Nauki (NCN) [National Science Center] Grant DEC-2015/16/S/ST10/00430 to Michał Bucha.

REFERENCES

Kong J. et al. (2014): Fuel Sci Technol 127: 41–46.

Peters K.E. et al. (2005): The Biomarker Guide vol. 2. Cambridge University Press.

Tungsten mineralization in quartz veins at the Cetoraz deposit, Czech Republic

[1]Lenka Buřivalová[#] and [1]Zdeněk Losos

[1] Masaryk University, Department of Geological Sciences, Kotlářská 2, 612 37 Brno, Czech Republic [#]lenka@burival.com

Key words: W-mineralization, metamorphosis, ferberite, garnet, Moldanubicum

The Cetoraz deposit (ca. 25 km east of Tábor, Czech Republic) is characterized by tungsten mineralization present in quartz veins; the locality is situated in central part of the Moldanubian Zone. The deposit was studied in 1970's (Němec and Tenčík 1976; Němec and Páša 1986); the presented new data summarize several recent studies by Losertová et al. (2013; 2014).

The small Cetoraz deposit is related to the Pacov two mica orthogneiss body, which is surrounded by biote and sillimanite-biotite paragneisses. W-mineralization (ferberite, scheelite) occurs in quartz vein swarms in leucocratic orthogneiss, situated at the southern margin of Pacov orthogneiss body (Němec and Tenčík 1976; Němec and Páša 1986). Muscovite and muscovite-quartz greisens are located around quartz veins. W-mineralization is accompanied by muscovite-feldspar-quartz veins with gahnite. All these types of greisens contain sillimanite.

Ore mineralization is represented by scheelite and two generations of ferberite. Presence of garnet and sillimanite in assemblage with wolframite and scheelite in quartz veins is typical for this locality. These minerals are associated with minor amount of pyrite, chalcopyrite, galena, native bismuth and secondary minerals of W and Bi.

Primary ferberite forms tabular crystals or aggregates <10 cm in size. It is replaced by scheelite and secondary ferberite. Primary ferberite crystals are chemically homogeneous with an elevated content of Mn (<0.225 apfu), Mg (<0.044 apfu) and Nb (<0.027 apfu). Trace elements (LA-ICP-MS) include: Na, Al, Si, Ca, Sc, Ti, Zn, Y, Zr, In, Sn, Ta (10's to <1000 ppm).

Scheelite forms grains ca. <5 mm in size and replaces older primary ferberite, and it is replaced by younger secondary ferberite. Trace elements (LA-ICP-MS) include: V, K, Na, Mn, Fe, Sr, Y, Nb, Sn (10's to <1000 ppm).

Secondary ferberite forms very fine-grained aggregates, composed of tiny fibrous grains about 1 μm in size replacing both scheelite (reinite variety) and primary ferberite. It corresponds to almost pure ferberite with minor amount of Al (0.005–0.021 apfu).

Garnet (almandine-spessartine) occurs in quartz veins, either separately or associated with wolframite and scheelite aggregates. It has apparent chemical zonality, caused by changes particularly in Ca and Mn contents. Trace elements (LA-ICP-MS) include: Ti, Y, P (100's to <1000 ppm).

Unusual presence of garnet, gahnite, and sillimanite in greisens, together with structural deformation in both microscopic and macroscopic scale, support the multi-stage magmatic-metamorphic evolution of the original greisen and quartz veins.

Acknowledgment: Analytical work was financially supported by means of specific research of the Department of Geological Sciences, Masaryk University.

References

Losertová et al. (2013): Bull Mineral-petrol Odd Národního muzea v Praze 21:47–51.

Losertová et al. (2014): Bull Mineral-petrol Odd Národního muzea v Praze 22:269–273.

Němec D. and Tenčík I. (1976): Min Deposita 11:210–217.

Němec D. and Páša J. (1986): Min Deposita 21:12–21.

Comparing in situ U-Pb zircon and Th-Pb monazite ages from High Tatra granitoids, Slovakia

[1]Elizabeth J. Catlos[#], [1]Saloni Tandon, [1]Thomas M. Etzel, [2]Milan Kohút, [2]Igor Broska, [1]Daniel Stockli, [3]Brent A. Elliott, [1]Kimberly Aguilera and [1]Zoe Yin

[1] The University of Texas at Austin, Department of Geological Sciences, 23 San Jacinto Blvd. & E 23rd Street, Austin, TX 78712, USA [#]ejcatlos@jsg.utexas.edu
[2] Earth Science Institute, Slovak Academy of Science, Dubravska cesta 9, 840 05 Bratislava, Slovakia
[3] The University of Texas at Austin, Bureau of Economic Geology, 10611 Exploration Way, Austin, TX 78758, USA

Key words: High Tatra Mountains, zircon, monazite, geochronology

The focus of this contribution is constraining the timing of the tectonic evolution of the High Tatra Mountains in Slovakia, which are located in the Western Carpathian Mountains. Both monazite [$(REE,Th)PO_4$] and zircon ($ZrSiO_4$) grains were dated in rock thin section from the same samples of High Tatra granitoids to understand not only the tectonic evolution of the range but also to compare the timing information provided by these accessory minerals.

Overall, zircon and monazite grains were dated in five samples from the vicinity of Lomnický štít (Table 1). Zircon grains were analyzed using Laser Ablation-Inductively Coupled Plasma Mass Spectrometry (LA-ICP-MS) at UT Austin, whereas monazite grains from the same samples were dated in thin section using Secondary Ion Mass Spectrometry (SIMS) at UCLA. Entire rock thin sections were then imaged in cathodoluminescence after dating to decipher the textures and deformation history of the samples.

We present the ages of the oldest and youngest zircon and monazite grains from each sample in the table. Most yield ages as expected for the High Tatras, which has been reported to largely record events centering around the Carboniferous (e.g., Burda et al., 2013). Zircons, as expected, record older ages than the monazite, although, in many cases they overlap. The oldest zircon age is Early Devonian (n=2), whereas the oldest monazite are Middle to Late Devonian (n=4). Some monazite grains (n=4) yield Permian results, up to 60 m.y. younger than the time frame suggested to record the final stages of Variscan collision in the range. The younger monazite ages are ~30 m.y. older than K-feldspar $^{40}Ar/^{39}Ar$ step-heating results of ~221 Ma reported by Etzel et al. (2018) in this volume and provide important constraints to decipher the thermal history of the range.

Table 1: Oldest and youngest U-Pb zircon and Th-Pb monazite ages from High Tatra samples

Zircon age (^{238}U-^{206}Pb) (±2σ)	Monazite Th-Pb age (±1 σ)
HT01A (49°11'19.98"N, 20°13'58.90"E)	
387±19 Ma	348±18 Ma
343±22 Ma	316±13 Ma
HT01B (49°11'19.98"N, 20°13'58.90"E)	
353±13 Ma	331±15 Ma
333±15 Ma	299±29 Ma
HT02 (49°11'42.80"N, 20°12'47.90"E)	
n.m	380±17 Ma
n.m	254±28 Ma
HT03 (49° 9'55.50"N, 20°13'15.60"E)	
410±14 Ma	377±22 Ma
321±14 Ma	276±12 Ma
HT04 (49° 9'46.90"N, 20°13'12.90"E)	
415±41 Ma	351±14 Ma
358±16 ma	323±15 Ma

Note: HT01A, HT01B, and HT03 are granodiorite, HT02 is a syenite, and HT03 is a granite, n.m. = not measured.

Acknowledgment: This material is based upon work supported by the NSF under grant no. OISE 1460050. The SIMS facility UCLA acknowledges support through NSF Instrumentation and Facilities. We appreciate field assistance facilitated by Dusan Catlos.

REFERENCES

Burda J. et al. (2013): Geochronometria 40:134–144.

Joint 5th Central-European Mineralogical Conference and
7th Mineral Sciences in the Carpathians Conference
Banská Štiavnica 2018

Special cation ordering at octahedral *M*3 sites in natural epidote-supergroup minerals

[1]Peter Cibula[#], [1]Peter Bačík, [1]Petra Kozáková, [2]Marcel Miglierini, [1]Klaudia Lásková and [1]Filip Lednický

[1] Comenius University in Bratislava, Faculty of Natural Sciences, Department of Mineralogy and Petrology, Ilkovičova 6, 842 15 Bratislava, Slovak Republic [#]peter.cibula@uniba.sk
[2] Slovak University of Technology in Bratislava, Faculty of Electrical Engineering and Information Technology, Institute of Nuclear and Physical Engineering, Ilkovičova 3, 812 19 Bratislava, Slovak Republic

Key words: epidote; clinozoisite; Mössbauer spectroscopy; muffle furnace

INTRODUCTION

Recent studies were focused on the dependence of chemical composition of epidote-supergroup minerals (ESM) on chemical composition of host rock and processes that caused crystallization of ESM. This knowledge is the most important in mineralogical research but our study is focused mainly on cation ordering in natural solid solution epidote-clinozoisite. This decision was made purposely because ordering of cations in structure of minerals depends on physical-chemical conditions during crystallization.

MATERIALS

Natural dark green epidote from Sobotín, Czech Republic (ES) and natural brown-green clinozoisite from Baluchistan, Pakistan (CP) were studied for crystal-chemical variations before and after heating. Two samples from each other were not heat treated and were used as a standard while the eight other parts were heated in the muffle furnace in the air atmosphere for 12 hours and then cooled down to the ambient temperature for 12 h.

ANALYTICAL METHODS

The chemical composition was determined with Cameca SX100 electron microprobe operated in wavelength-dispersion mode at the Masaryk University, Brno, Czech Republic, under the following conditions: accelerating voltage 15 kV, beam current 20 nA and beam diameter 5 μm. The samples were analysed with the following standards: wollastonite (SiKα. CaKα, TiO_2 (TiKα), Al_2O_3 (AlKα), pure Cr (CrKα), fayalite (FeKα), rhodonite (MnKα), MgO (Mg Kα), pure Ni (NiKα), albite (NaKα), orthoclase (KKα), $Rb_2ZnSi_5O_{12}$ glass (RbLα), pollucite (CsLα), barite (BaLα), $SrTiO_3$ (SrLα), BaF_2 (FKα) and NaCl (ClKα).

The chemical formula of ESM was calculated based on Σ (A + M + T) = 8 cations with the procedure employed by Armbruster et al. (2006).

Powder X-ray diffraction analyses were determined by BRUKER D8 Advance diffractometer (Laboratory of X-ray diffraction SOLIPHA, Comenius University in Bratislava, Faculty of Natural Sciences) under the following conditions: the Bragg–Brentano geometry (Theta–2Theta), Cu anticathode ($K\alpha_1$ = 1.5406 Å), accelerating voltage 40 kV and beam current 40 mA, Ni Kβ filters were used for stripping Kβ radiation, and data were obtained using the BRUKER LynxEye detector. The step size was 0.01° 2θ, the counting time was 3s per step and measurement ranged from 2 to 65° 2θ.

Analyzed scans were fitted, and lattice parameters were refined with DIFFRACplus TOPAS software (Bruker 2010) using the structural models for appropriate mineral phases. For epidote and clinozoisite were used the structural model by Comodi and Zanazzi (1997).

RESULTS

The average chemical composition of epidote in ES-0 – ES-9 is $Ca_{2.000}A1_{2.211}Fe_{0.742}Si_{2.994}O_{12}(OH)$ and clinozoisite (CP-0 – CP-9) is $Ca_{2.017}A1_{2.626}Fe_{0.319}Si_{3.002}O_{12}(OH)$. The main difference between samples is in Fe/Al

ratio. Epidote from Sobotín is $^{M3}Fe^{3+}$-dominant (0.68–0.80 apfu), while Fe^{3+} (between 0.29–0.33 apfu) is lower in clinozoisite samples. The content of other cations including Mg, Ti, V and Cr is very low or below the detection limit in both types of samples.

The unit-cell dimensions of both samples strongly depend on the Fe^{3+}-Al ratio. Original samples fall into the trend of epidote-clinozoisite solid solution very well (Fig. 1) with larger all *a*, *b*, *c* and *V* in Fe^{3+}-dominant ES sample compared to in CP sample.

However, in heated samples, deviations from the trend can be observed. It is better pronounced in the CP samples with a vertical trend of increase in all *a*, *b*, *c* and *V* in heated samples. This trend could be partly attributed to small variations in Fe^{3+}-Al ratio but interestingly, sample heated at 900°C display significant increase in *b*. In contrast, the ES samples displays similar vertical trend only in *c* and partly in *a*; variations in *b* and *V* have no significant vertical trend.

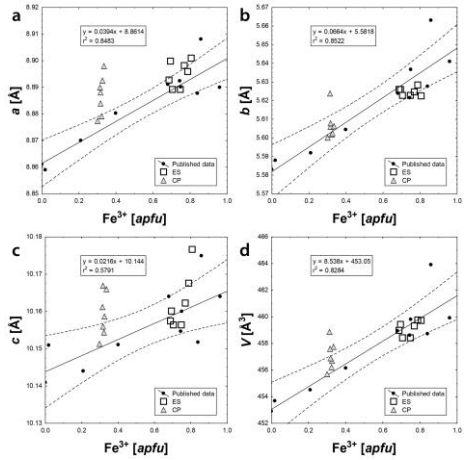

Fig. 1: Diagrams comparing lattice parameters versus Fe^{3+} apfu. Nonheated samples are consistent with the trend of epidote-clinozoisite solid solution based on the published data.

DISCUSSION

The position of Fe^{3+} in the epidote structure can be read from the Mössbauer spectra; spectra of both sample sets heated below 1000°C contain doublets related to Fe^{3+} in octahedral coordination. However, there is a slight difference in doublets if both sample sets are compared (Figs. 2; 3). The ES spectra are symmetrical and can be interpreted as one doublet of Fe^{3+} in the *M*3 site. However, CP samples display slight asymmetry of Mössbauer spectra. This can be explained by presence of more components in spectra. First two components have isomer shift (IS) and quadrupole splitting (QS) typical for *M*3 site.

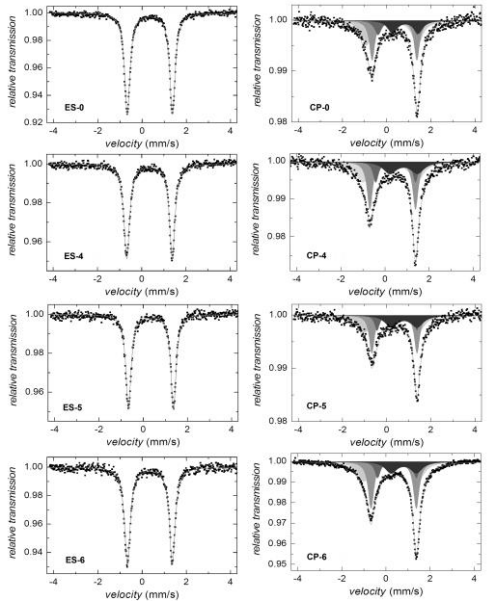

Fig. 2: Mössbauer spectra of samples ES and CP. Two of non-heated and other heated up to 600°C

Third doublet is close to Fe^{3+} in *M*1 site and takes area of 12-15 % corresponding to cca. 0.04 apfu in samples heated up to 500°C and increases up to 19 % (0.06 apfu) in samples heated at more than 500°C (Fig. 2; 3).

Incorporation of small amounts of Fe^{3+} in *M*2 can explain the presence of doublets with IS 0.31- 0.37 mm/s and QS 0.80-1.00 mm/s in the Mössbauer spectra of epidote-clinozoisite solid solution (Liebscher 2004). In our samples, doublets of the CP samples original and heated up to 800 °C have a similarly low QS but distinctly higher IS. Therefore, their interpretation as Fe^{3+} in *M*2 is not entirely clear but also not ruled out.

The *M*1 and *M*3 sites are connected by a common O1–O4 edge. The *M*1 octahedron is fairly regular and its mean bond length is about 1.90 to 1.94 Å (Franz & Liebscher 2004).

Up to about X_{Ep} = 0.6 the *M*1 octahedron exhibits only minor structural changes with increasing Fe content: the mean bond length, the volume, and the distance between the two apical O1 atoms slightly increase as response to the expansion of the attached *M*3 due to increased Fe content in *M*3 (Bonazzi and Menchetti 1995).

The *M*3 octahedron coordinates the oxygen atoms O1, O2, O4, and O8 and is the largest and most disorder site with the largest variability in occupancy (Ito et al. 1954; Grodzicki et al. 2001).

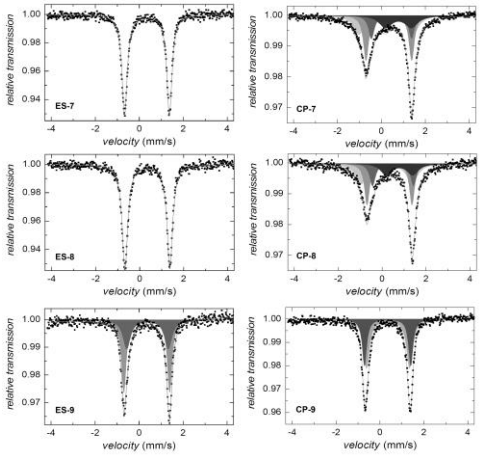

Fig. 3: Mössbauer spectra of ES and CP samples heated from 700 to 900°C

Increasing Fe content increases its mean bond length from 1.98 to 2.06 Å (Franz and Liebscher 2004). This mostly results from increase in the distance between the apical O4 and O8 due to the significant shift of O8; in clinozoisite it is considerable smaller than the comparable O1–O1 distance in epidote, but increases significantly with increasing Fe content. Structural changes of *M*3 are most pronounced for $X_{Ep} < 0.6$ and are in a clear linear relationship with Fe content. If X_{Ep} is higher than 0.6, the structural changes are less obvious and non-linear (Franz & Liebscher 2004).

In the Mössbauer spectra, Fe^{3+} in *M*1 is manifested by doublets with IS 0.22-0.36 mm/s and QS 1.46-1.67 mm/s (Bird et al. 1988; Fehr and Heuss-Assbichler 1997; Heuss-Assbichler 2000). Doublets in our CP-0 – CP-8 samples have slightly higher IS and QS but their interpretation as Fe^{3+} in *M*1 is relatively reasonable. Moreover, Fehr and Heuss-Assbichler (1997) observed two doublets in the Mössbauer spectra that both displayed the main characteristics of Fe^{3+} on *M*3 but with small differences in their QS. These were attributed to two slightly different *M*3 sites, labelled *M*3 and *M*3´, which belong to two different monoclinic epidote phases, one with Al-Fe^{3+} disorder on *M*3 (*M*3 doublet) and one with an ordered distribution of Al and Fe^{3+} at *M*3 (*M*3´ doublet); the latter represents the intermediate composition with $X_{Ep} = 0.5$ (Fehr and Heuss-Assbichler 1997; Heuss-Assbichler 2000).

CONCLUSION

However, this interpretation is relatively questionable, although, it can explain asymmetry of doublets in the CP samples very effectively. The Al-Fe^{3+} disorder between the *M*1 and *M*3 octahedral sites occurs at total Fe^{3+} contents higher than about $X_{Ep} = 0.6$ and is restricted to the *M*1 and *M*3 sites (Giuli et al. 1999). This obviously is not our case because CP clinozoisite contain only up to 0.3 Fe^{3+} apfu.

On the other hand, variable degree of disorder in specific areas of clinozoisite structure may result not only in occurrence of probable *M*1 doublet but also in above mentioned splitting of *M*3 doublets which may be interpreted for instance as *M*3 doublet for isolated $^{M3}Fe^{3+}$ and *M*3´ doublet for the pair of $^{M1}Fe^{3+}$ and $^{M3}Fe^{3+}$ in neighbouring octahedra.

Acknowledgment: This work was supported by the Ministry of Education, science, research and sport of Slovak Republic grant agency under the contracts VEGA-1/0079/15 and VEGA-1/0499/16.

REFERENCES

Armbruster Tet al. (2006): Eur J Min 18:551–567.

Bird D.K. et al. (1988): J Geophys Res 93:13135–13144.

Bonazzi P. and Menchetti S. (1995): Min Petrol 53:133–153.

Bruker (2010): DIFFRACplus TOPAS. http://www.bruker-axs.de/topas.html, date: 12. 3. 2015

Comodi P. and Zanazzi P.F. (1997): Am Min 82:61–68.

Fehr K.T. and Heuss-Assbichler S. (1997): Neues Jb Min Abh 172:43–76.

Franz G. and Liebscher A. (2004): Rev Min Geochem 56:1–82.

Giuli G. et al. (1999): Am Min 84:933–936.

Grodzicki M. et al. (2001): Phys Chem Min 28(9):675–681.

Heuss-Assbichler S. (2000): Habilitationthesis, Munich p105.

Ito T. et al. (1954): Acta Crystallogr 7:53–59.

Liebscher A. (2004): Rev Min Geochem 56: 125–170.

Mineralogical and structural aspects on the Geschieber structure in Jáchymov

[1]Michal Čurda[#], [1]Viktor Goliáš and [1]Jiří Zachariáš

[1] Institute of Geochemistry, Mineralogy and Mineral Resource, Charles University in Prague, Faculty of Science, Albertov 6, 128 43 Prague 2, Czech Republic [#]michalcurda@centrum.cz

Key words: Jáchymov, radioactive springs, structural, tectonic, mineralogy

The town of Jáchymov was founded in 1516, in the year when silver mineralisation was discovered here. Besides silver, non-ferrous metals and uranium were mined here, too (Ondruš et al. 2003). At present, radioactive thermal mineral water is pumped from the mine Svornost. The water is collected by several underground drill holes and distributed to the Jáchymov spa (Veselý 1986). The most important source is the HG-1 drilling, which is located in the vein structure Geschieber on the 12th level of the Svornost mine. This drilling was later named after the academic Běhounek. The total discharge of the source is 5 l/s with the activity around 10 kBq/l (Laboutka and Pačes 1966).

This work describes mineralogical character and structural-tectonic character regarding the radioactive water sources.

Measurements were performed on the 10th and 12th level of the Svornost mine. The results show monotonous orientation of the metamorphic foliation in mica-schist in the E-W direction dipping around 35° north (fall-line orientation is 356/36). The fracture system is orthogonal to the foliation direction and shows two prevailing directions: E-W and more often NNW-SSE, which is orthogonal to the foliation direction. NW-SE direction of the Geschieber vein structure differs from the NNW-SSE oriented fractures by approx. 20–30°. This can be explained by different age of the fractures and change of the stress field orientation in time.

Mineral composition of the "clay" filling in the cross adit to the drilling HG-1 was examined using X-ray diffraction analysis. Kaolinite, smectite group minerals (montmorillonite), quartz, gypsum, feldspar and micas dominate in the fracture zone. Cracks closest to the Geschieber zone contain also Co-Ni(As) supergene minerals. Some differences can be observed between fractures in massive granite (in the direction towards the HG-1 drilling) and the fracture zone in granite. Kaolinite dominates the fracture zone. Its presence decreases in the cracks in granite. The amount of quartz, micas and feldspar increases with distance. Total number of fractures also decreases in this direction.

REFERENCES

Ondruš P. et al. (2003): J Czech Geol Soc 48:3–18.

Veselý T. (1986): Sbor Geol Věd 27, ř Lož geol – mineral 9–109.

Laboutka M. and Pačes T. (1966): Sborn geol věd 4. HIG 59–112.

Arsenic mineralogy of near neutral soils and mining waste

[1]Petr Drahota[#], [1]Ondřej Kulakowski, [1]Adam Culka, [1]Magdaléna Knappová, [2]Jan Rohovec, [3]František Veselovský and [3]Martin Racek

[1] Charles University, Faculty of Science, Institute of Geochemistry, Mineralogy and Mineral Resources, Albertov 6, 128 43 Prague 2, Czech Republic [#]drahota@natur.cuni.cz
[2] The Czech Academy of Sciences, v.v.i., Institute of Geology, Rozvojová 269, 165 00 Prague 6, Czech Republic
[3] Czech Geological Survey, Geologická 6, 152 00 Prague 2, Czech Republic
[4] Charles University, Faculty of Science, Institute of Petrology and Structural Geology, Albertov 6, 128 43 Prague 2, Czech Republic

Key words: soil, mining waste, pharmacosiderite, yukonite, arseniosiderite

The mineralogical composition of mining wastes and contaminated soils is the key factor that controls the retention and release of pollutants. Herein (Drahota et al. 2018), we used bulk analyses, selective extractions, X-ray diffraction, electron microprobe, and Raman microspectrometry to determine the distribution and speciation of As as a function of depth in three slightly acidic to near-neutral soil and mining waste profiles at the Smolotely-Líšnice historical Au district (Czech Republic).

The soils there, which have developed from long-term weathering, exhibit As levels as high as 1.87 wt.% in the richest area; the 80 to 90 year old mining waste contains up to 0.87 wt.% As. In the soils and mining waste, the primary As ore (arsenopyrite) has almost completely oxidized to secondary As minerals: arseniosiderite ($Ca_3Fe_4(OH)_6(AsO_4)_4 \cdot 3H_2O$), bariopharmacosiderite ($Ba_{0.5}Fe_4(OH)_4(AsO_4)_3 \cdot 6H_2O$), yukonite ($Ca_2Fe_3(AsO_4)_3(OH)_4 \cdot 4H_2O$), and Fe (hydr)oxides (ferrihydrite, goethite, and hematite), with variable As_2O_5 and CaO concentrations (up to 27.5 and 3.8 wt.%, respectively). Arsenic distribution and speciation were found to vary with depth and bedrock type. Whereas the presence of multiple As-hosting phases that occurred in the mining waste and cambisol developed over a granodiorite, bariopharmacosiderite was absent in the cambisol overlying gabbrodiorite.

In light of the detailed mineralogical analyses, the geochemical behavior of As in the soil and mining waste at this site can be explained by a series of reactions beginning within the deep saprolite or unaltered mining waste material, respectively. Under the oxic condition of these environments, the arsenopyrite is not stable, and its oxidative dissolution leads to precipitation of bariopharmacosiderite or yukonite, likely depending on the activity of Ba and Ca. These initial secondary phases are not stable and transform into arseniosiderite, but the transformation kinetics are probably very low due to insufficient activity of Ca in the unsaturated soils and mining waste. As a result of this kinetic barrier, yukonite surprisingly is the dominant arsenate phase in the cambisol developed over a gabbrodiorite. Whereas crystalline arseniosiderite, bariopharmacosiderite, and Fe (hydr)oxides may be considered relatively stable over the long term, depending on the environmental conditions, the predominance of highly soluble yukonite and relatively unstable As-rich ferrihydrite in the natural systems suggest that As will be relatively mobile.

Acknowledgment: This study was supported by the Czech Science Foundation (GACR 16-09352S).

References

Drahota P. et al. (2018): Appl Geochem 89:243–254.

Unusual Li-bearing tourmalines from Austria

[1]Andreas Ertl[#]

[1] University of Vienna, Institut für Mineralogie und Kristallographie, Althanstrasse 14, 1090 Wien, Austria [#]andreas.ertl@a1.net

Key words: Lithium, tourmaline, crystallography, Austria

Crystal structures, chemical and spectral data were used to characterize coloured tourmalines from granitic pegmatites (Maigen, Blocherleitengraben) from the Moldanubian nappes, Lower Austria (Ertl et al. 2012). Pale-pink tourmaline from Maigen was classified as Mn-rich fluor-elbaite with a = 15.89, c = 7.12 Å and the crystal chemical formulae $\sim{}^{X}(Na_{0.9}\square_{0.1})\ {}^{Y}(Al_{1.3}Li_{0.8}Mn^{2+}_{0.7}\square_{0.2})\ {}^{Z}Al_6\ (BO_3)_3\ [Si_{5.9}Al_{0.1}O_{18}]\ {}^{V}(OH)_3\ {}^{W}[F_{0.8}(OH)_{0.2}]$. Dark-green tourmaline from Maigen was classified as Fe-, Mn- and Li-bearing olenite with a = 15.88, c = 7.11 Å and the formula ${}^{X}(Na_{0.6}\square_{0.4})\ {}^{Y}(Al_{1.3}Fe^{3+}_{0.5}Mn^{2+}_{0.4}\ Fe^{2+}_{0.2}Li_{0.2}\square_{0.4})\ {}^{Z}Al_6\ (BO_3)_3\ [Si_{5.6}Al_{0.3}B_{0.1}O_{18}]\ {}^{V}(OH)_3\ {}^{W}[(OH)_{0.7}F_{0.3}]$. Pink-coloured tourmaline (from a small pocket) from Blocherleitengraben was identified as Mn-bearing, B-rich fluor-elbaite with a = 15.84, c = 7.11 Å and the formula ${}^{X}(Na_{0.8}Ca_{0.1}\square_{0.1})\ {}^{Y}(Al_{1.5}Li_{0.7}Mn^{2+}_{0.4}Fe^{2+}_{0.1}\square_{0.3})\ {}^{Z}Al_6\ (BO_3)_3\ [Si_{5.7}B_{0.3}O_{18}]\ {}^{V}(OH)_3\ {}^{W}[F_{0.7}(OH)_{0.3}]$. A greenish-brown zone, rimming schorl, from Blocherleitengraben was classified as Fe- and Mn-bearing fluor-elbaite with a = 15.91, c = 7.13 Å and the formula ${}^{X}(Na_{0.9}Ca_{0.1})\ {}^{Y}(Al_{1.1}Li_{0.6}Fe^{2+}_{0.6}Mn^{2+}_{0.5}\square_{0.2})\ {}^{Z}Al_6\ (BO_3)_3\ [Si_{5.9}Al_{0.1}O_{18}]\ {}^{V}(OH)_3\ {}^{W}[F_{0.8}O_{0.2}]$. These pegmatites may have evolved as granitic pegmatitic melts during decompression from the surrounding country rocks in the frame of exhumation of the Moldanubian nappes after the peak of the Variscan metamorphism (Ertl et al. 2012).

Pale-green tourmaline from the border zone of a pegmatite of the Austroalpine basement units, from Altes Almhaus, Stubalpe, Styria, has been characterized by single-crystal structure determination and chemical analyses (Ertl et al. 2013). A crystal structure refinement of this Mn- and Fe-bearing fluor-liddicoatite in combination with the chemical analyses gave the optimized formula ${}^{X}(Ca_{0.5}Na_{0.4}\square_{0.1})\ {}^{Y}(Al_{1.3}Li_{0.8}Mn^{2+}_{0.4}Fe^{2+}_{0.2}\square_{0.3})\ {}^{Z}Al_6\ {}^{T}(Si_{5.7}Al_{0.3})O_{18}\ (BO_3)_3\ {}^{V}(OH)_3\ {}^{W}[F_{0.6}(OH)_{0.3}O_{0.1}]$, with a = 15.91, c = 7.12 Å. The tourmaline- and spodumen-bearing pegmatite crosscuts a marble from where Ca was mobilized, which is also responsible for the crystallization of this Ca-rich tourmaline. Pale-blue to pale-green tourmalines (dravite, fluor-dravite) from the border of Permian pegmatites (Rappold Complex, Styria) were found to contain small, but significant Li contents. The Li-richest tourmaline, found at Gleinalm with a = 15.92, c = 7.17 Å has the formula ${}^{X}(Na_{0.7}Ca_{0.2}\square_{0.1})\ {}^{Y}(Mg_{1.3}Al_{1.0}Fe^{2+}_{0.3}Li_{0.2}\ Ti^{4+}_{0.1}\square_{0.1})\ {}^{Z}(Al_{5.3}Mg_{0.7})\ (BO_3)_3\ Si_6O_{18}\ {}^{V}(OH)_3\ {}^{W}[F_{0.7}(OH)_{0.3}]$ (Ertl et al. 2010).

An unusual B-rich tourmaline, a Li-bearing olenite, was found in another pegmatite near Stoffhütte (Koralpe, Styria), which is also located within the Austroalpine basement complex of the Eastern Alps (Ertl et al. 1997). This pegmatite intruded discordantly into mylonitic garnet–biotite schists. The B-rich olenite can be pale-blue, pale-green or colouress. The latter one with a = 15.74, c = 7.07 Å has the formula ${}^{X}(Na_{0.4}Ca_{0.3}\square_{0.3})\ {}^{Y}(Al_{2.4}Li_{0.4}\square_{0.2})\ {}^{Z}Al_6\ (BO_3)_3\ {}^{T}[Si_{4.9}B_{0.8}Al_{0.3}]O_{18}\ {}^{V}(OH)_3\ {}^{W}[O_{0.6}(OH)_{0.3}\ F_{0.1}]$ (Ertl et al. 2007).

Acknowledgment: This work was supported by the Austrian Science Foundation (FWF) project no. P 31049-N29.

References

Ertl A. et al. (1997): Österr Akad Wiss, Math-naturw Kl, Anzeiger 134:3–10.
Ertl A. et al. (2007): Can Min 45:891–899.
Ertl A. et al. (2010): Min Petrol 99: 89–104.
Ertl A. et al. (2012): Eur J Min 24: 695–715.
Ertl A. et al. (2013): Abstractband, Deutsche Mineralogische Gesellschaft, Tübingen, Germany, Sept 16–19:80.

Dating the High Tatra Mountains, Slovakia: Tectonic Implications

[1]Thomas M. Etzel[#], [1]Elizabeth J. Catlos, [2]Milan Kohút, [2]Igor Broska, [3]Brent A. Elliott, [1]Daniel Stockli, [4]Daniel Miggins, [4]Tim O'Brien, [1]Saloni Tandon, [1]Kimberly Aguilera and [1]Zoe Yin

1 The University of Texas at Austin, Department of Geological Sciences, 23 San Jacinto Blvd. & E 23rd Street, Austin, TX 78712, USA [#]thomas.etzel@utexas.edu
2 Earth Science Institute, Slovak Academy of Science, Dubravská cesta 9, 840 05 Bratislava, Slovakia
3 The University of Texas at Austin, Bureau of Economic Geology, 10611 Exploration Way, Austin, TX 78758, USA
4 Oregon State University, Department of Geology and Geophysics, Corvallis, OR 97331, USA

Key words: High Tatra Mountains, argon geochronology, potassium feldspar, zircon

The High Tatra Mountains of northern Slovakia are a prominent segment of the Western Carpathian Mountain Belt. The range consists of polygenetic Variscan granitoid plutons emplaced during subduction and collision (e.g., Kohút and Janák, 1994). While crystallization is known to have occurred between ~370 Ma and ~340 Ma, uncertainties remain regarding its post-crystallization thermal evolution following the cessation of Variscan collision. This contribution presents new $^{40}Ar/^{39}Ar$ K-feldspar and zircon ^{238}U-^{206}Pb ages from calc-alkaline granodioritic samples from the High Tatras. Samples were collected from its western (IR41, just north of Štrbské Pleso), central (IR35, IR39, north of Velické Pleso) and eastern (IR27, IR30, south of Lomnický štít) portions.

K-feldspar separates from samples IR27, IR35, IR39, IR41 were dated at the Oregon State University Argon Geochronology Lab. Samples were step-heated using a CO_2 laser; gas released at each step was measured to produce an incremental age profile. Minimum measured $^{40}Ar/^{39}Ar$ step-heating ages from the central samples are 35.8±0.1 Ma (IR35) and 47.5±0.1 Ma (IR39). Eastern sample (IR27, 38.5±0.2 Ma) and western sample (IR41, 41.5±0.1 Ma) yield ages between these extremes. For samples IR27 and IR39 $^{40}Ar/^{39}Ar$ results are characterized by staircase age spectra that reach maximum ages (3-5 steps) ~215 Ma and ~221 Ma, respectively. Samples IR35 and IR41 retain younger average maximum ages of ~124 Ma and ~134 Ma, respectively.

Zircon separates from the same rocks were dated by Laser Ablation-Inductively Coupled Plasma Mass Spectrometry (LA-ICP-MS) in the Jackson School of Geosciences at UT Austin. For each sample, zircon ^{238}U-^{206}Pb ages are older than K-feldspar $^{40}Ar/^{39}Ar$ results. Most of these ages are similar to what has been observed for the range previously (351.4±1.5 Ma, IR27, n=17 spots; 349.4±1.0 Ma, IR35, n= 46 spots; 342.1±1.4 Ma, IR39, n=36 spots, 350.8±1.1 Ma, IR41, n= 36 spots; IR30, 350.8±1.3 Ma, n=38 spots). However, core ages from a subset of grains (n=9), are significantly older, and range from 458±18 Ma to 681±30 Ma.

Older zircon ages are likely xenocrystic grains or cores entrained in the magmas, and provide some understanding regarding the age of the lithosphere in which these magmas formed. The difference between zircon U-Pb and K-feldspar ^{40}Ar-^{39}Ar ages suggests these samples either remained at a depth below the argon retention zone of K-feldspar for ~230-130 m.y. after crystallization or experienced reburial. The age data also suggest the Late Triassic and Early Cretaceous should be considered important in terms of deciphering the tectonic history of the High Tatra Mountains. Further, the observed minimum Eocene ^{40}Ar-^{39}Ar ages are similar to those recorded in the Alps, and likely reflect the beginning of Miocene/Pleistocene exhumation.

Acknowledgment: This material is based upon work supported by the National Science Foundation under grant no. OISE 1460050.

References

Kohút M. and Janák M. (1994): Geol Carpath 45:301–311.

Polyphase solid inclusions in metamorphic minerals from mantle rocks, evidences for their recrystallization during pressure and/temperature change

[1]Shah Wali Faryad[#], [1]Radim Jedlicka, [2]Christoph Hauzenberger and [1]Martin Racik

[1] Charles University, Faculty of Science, Institute of Petrology and Structural Geology, Albertov 6, 128 43 Prague 2, Czech Republic [#]faryad@natur.cuni.cz
[2] Institute of Mineralogy and Petrology, Karl-Franzens University, Universitätplatz 2, 8010, Graz, Austria

Key words: eclogite-pyroxenite, prograde textures, polyphase inclusions, garnet, clinopyroxene

Solid phase inclusions are a powerful tool to investigate crystallization history of the host mineral and to reconstruct pressure-temperature changes during metamorphism of basement unit. In case of multistage evolution of the host rock, the enclosed phase (phases) in mineral may reflect change of the ambient pressure and temperature and recrystallize, mainly if the original phase(s) contained OH or other fluid-bearing component. The most challenging task is then to constrain the original phase(s) and to assess the responsible reaction for their formation. Except of possible interaction between inclusion and host mineral, the advance of such study is the closed system for reactions among phases compared to that occurring in the matrix, outside of the host mineral.

Mafic layer having transition between clinopyroxenite and eclogite within peridotite from felsic granulite in the Bohemian Massif (Lower Austria) has been investigated. Based on their bulk-rock major and trace elements chemistry, the layers formed by fluids migrated through the lithospheric mantle wedge above the subduction zone (Medaris et al. 2006). The origin of high-pressure minerals in the layers is however debated and questioned, whether, they crystallized direct from melt or recrystallized from the original igneous phases during subduction. Exsolution lamellae of garnet in pyroxenes from some coarse-grained pyroxenite indicated their formation by solid state recrystallization (Faryad et al. 2009). The mafic-ultramafic bodies shared common granulite facies metamorphism with hosting felsic rocks, but they still preserve evidence of eclogite facies event.

The layer is represented by the presence of omphacite in the core of coarse-grained clinopyroxene, while the fine-grained one in the matrix is diopside. In addition, garnet contains inclusions of omphacite, alkali feldspars, hydrous and other phases with halogens and/or CO_2. Textural relations along with compositional zoning in garnet from the clinopyroxenite-eclogite layers favour solid-state recrystallization of the precursor minerals in the inclusions and formation of garnet and omphacite during subduction. Textures and major and trace element distribution in garnet indicate two stages of garnet growth that record eclogite facies and subsequent granulite facies overprint. The possible model explaining the textural and compositional changes of mineral is that the granulite facies overprint occurred after formation and exhumation of the eclogite facies rocks.

Acknowledgment: This study is supported by the Czech Science Foundation (project. 18-03160S).

REFERENCES

Faryad S.W. et al. (2009): J Met Geol 27:601–845.

Medaris L.G. et al. (2006): Int Geol Rev 48:765–777.

The first crystal-chemical data of tourmalines from the Velence Granite Formation, Velence Mts., Hungary

[1]Béla Fehér[#]

[1] Herman Ottó Museum, Department of Mineralogy, Kossuth u. 13, H-3525 Miskolc, Hungary
[#]feherbela@upcmail.hu

Key words: tourmaline, granite, Velence Mts., Hungary

The Velence granitoid massif is located northwest of Lake Velence, over an area of approximately 20 x 6 km. Petrographically the A-type Variscan (280–300 Ma) Velence granitoids are mostly biotitic monzogranites, with minor granodiorites and alkaline-feldspar granites. The granitoid pluton intruded into Lower Paleozoic phyllites that show contact metamorphism along the igneous body (Uher and Broska 1994; Molnár 2004). The monzogranite intrusion is transected by syngenetic or slightly younger granite-porphyry and aplite dikes. Rare pegmatites occur as lenticular or nest-like, rounded-elongated bodies up to 1–2 m^3 in volume (Molnár et al. 1995).

Tourmaline, in small quantities, is very rarely found in the granite, aplites and pegmatites and their miarolitic cavities. However, locally considerable tourmalinization can be observed in the contact shales around the granite. In other words, tourmaline is relatively abundant at sites of mixing between magmatic and wallrock reservoirs, but only a minor accessory phase within the granite.

For obtaining chemical data, tourmalines were analysed by a JEOL JXA-8600 electron-microprobe in wavelength-dispersive mode. Localities of the analysed samples: Bence Hill, Velence (granite, aplite, contact), Sukoró pasture (pegmatite, miarolitic cavity), Tompos Hill, Pákozd (aplite), Sas Hill, Pákozd (miarolitic cavity), Antónia Hill, Lovasberény (contact) and Varga Hill, Pátka (contact).

In the granite, aplites and pegmatites, tourmaline forms pitch-black, disseminated crystals up to a few mm in size. On the BSE images this tourmaline is chemically homogeneous schorl, chemical zoning was not observed. Tourmalines of this type (i.e. disseminated, unzoned) can be related to the primary magmatic minerals, which crystallized from granitic melt (London and Manning 1995). The two most striking features of this tourmaline are its relatively low Al content (Al_{tot} = 5.43–6.11 apfu) and its significant ferric iron content [calculated from the equation $\Sigma(T+Z+Y)$ = 15 apfu]. The latter feature may indicate autometasomatic origin.

In miarolitic cavities tourmaline is an extremely rare mineral. It forms greenish-grey to black, stubby prismatic crystals up to a few mm in length. Chemically these tourmalines are schorl-elbaite solid solutions with an elevated fluorine content, but without chemical zoning.

In the contact metamorphic shales and the associated quartz-tourmaline veins tourmaline forms colourless, grey, brown to black, long prismatic to acicular crystals in massive or columnar to fibrous aggregates. On the BSE images this type of tourmaline shows oscillatory chemical zoning. This suggests growth in an environment where physical and chemical properties fluctuate rapidly. Compared to tourmaline from granites, aplites and pegmatites, such samples contain more Al, Mg and less Na, Fe, and can be assigned to the species schorl, dravite and foitite.

Acknowledgment: Thanks to the Mining and Geological Survey of Hungary (Budapest) for the tourmaline samples from Velence and Sukoró.

References

London D. and Manning D.A.C. (1995): Econ Geol 90:495–519.

Molnár F. (2004): Acta Min-Petrol 45:55–63.

Molnár F. et al. (1995): Acta Geol Hung 38:57–80.

Uher P. and Broska I. (1994): Acta Geol Hung 37:45–66.

Uraninite geochronometry – The spectacular return of an old method

[1] Fritz Finger[#] and [1] Michael Waitzinger

[1] University of Salzburg, Department of Chemistry and Physics of Materials, Jakob-Haringer-Strasse 2a, 5020 Salzburg, Austria [#]friedrich.finger@sbg.ac.at

Key words: uraninite, U-Pb geochronology, microcrystals, low-voltage electron beam analysis

The Pb content of uraninite and pitchblende is used as an index of age since more than 100 years (Boltwood 1907; Holmes 1911). In the very beginning, large crystals were needed for wet chemical analysis. Subsequently, the invention of electron microprobe analysis in the middle 20th century has provided a new powerful tool for in-situ analysis of uraninite (Parslow et al. 1985; Bowles 1990). Notably, U-Th-total Pb uraninite dating was successfully done before chemical U–Th–Pb dating of monazite became popular. To date, uraninite geochronometry has concentrated on "normal" accessory uraninite, i.e. grains that are typically ~ 10-100 μm in size. Such grains are rather rare in nature. Therefore, the method has reached only limited application and remained restricted to studies of uraninite and pitchblende in uranium deposits (Alexandre and Kyser 2005; Cross et al. 2011) and to accessory magmatic uraninite in granitic rocks (Förster 1999; Kempe 2003; Cocherie and Legendre 2007).

A spectacular new application results from the study of micron-sized uraninite grains that are < 3 μm. Our work shows that such microcrystals of uraninite are relatively abundant in metamorphic rocks, though being easily overlooked because of their small size. The potential of uraninite dating in metamorphic terranes will greatly depend on the robustness of the U-Th-Pb system in these small crystals. We can demonstrate that solid state Pb diffusion in uraninite is sluggish and creates no great problem for geochronology. Even very small uraninite crystals can easily survive an amphibolite facies overprint, preserving domains with U–Th–Pb ratios intact. However, uraninite is particularly prone to fluid-present low-T recrystallization by dissolution-reprecipitation. This is both a curse and a blessing at the same time. On the positive side, multiply recrystallized uraninite crystals provide a sensitive geological "hard disk" where several discrete thermal events of an area are stored (Finger et al. 2017). On the negative side, different age domains in recrystallized uraninite can be so small and intimately intergrown with each other that they are very difficult to resolve and to analyse. It is therefore imperative that uraninite age data always is collected in combination with detailed backscatter electron imagery and high-resolution compositional profiles across single grains. Low-voltage (8 kV) electron beam dating with an excitation volume of c. 300 nm diameter is the method of choice for submicron-scale uraninite geochronometry.

References

Alexandre P. and Kyser T.K. (2005): Can Min 43:1005–1017.

Boltwood B. (1907): Am J Sci 23:77–88.

Bowles J.F.W. (1990): Chem Geol 83:47–53.

Cocherie A. and Legendre O. (2007): Lithos 93:288–309.

Cross A. et al. (2011): Aus J Earth Sci 58:675–683.

Finger F. et al. (2017): Geology 45:991–994.

Förster H.J. (1999): Min Mag 63:239–252.

Holmes A. (1911): Proceed Royal Soc London 85:248–256.

Kempe U. (2003): Contrib Min Petrol 145:107–118.

Parslow G.R. et al. (1985): Can Min 23:543–551.

Different evolution of selenium mineralizations of the Bohemian Massif

[2]Tomáš Flégr[#], [1]Pavel Škácha, [1]Jiří Sejkora, [1]Luboš Vrtiška and [2]Jan Cempírek

[1] National Museum, National History Museum, Department of Mineralogy and Petrology, Cirkusová 1744, 193 00 Prague 20, Czech Republic [#]397248@mail.muni.cz
[2] Masaryk University, Faculty of Science, Department of Geological Sciences, Kotlářská 267/2, 611 37 Brno, Czech Republic

Key words: selenides, selenium, bohemian massif, West-Moravia, Příbram, Předbořice, Zálesí

INTRODUCTION

In the global scale, the Bohemian Massif belongs to the areas of anomalously abundant occurrences of selenides. Their importance is proved e.g. by newly found selenides on selected localities of this study (Fig. 1).

Western Moravian uranium deposits lies in Gföhl unit of the high Grade-Moldanubian domain (Kříbek et al. 2009). Region is characterized by numerous large or smaller deposits, however the richest Se-mineralization is present in Bukov, Habří and Petrovice (Kvaček 1973; Kvaček 1979). The Se-mineralization is bounded to the uranium mineralization formed predominantly by coffinite, uraninite (Kvaček 1973; Kvaček 1979; Kříbek et al. 2009).

The hydrothermal veins of the Příbram uranium district are situated in low grade metamorphic metasedimentary rocks of the Barrandian Unit. Most of the uranium mineralization is hosted in claystones, siltstones and sandstones of Neoproterozoic Dobříš group (Škácha et al. 2017). Some parts of the deposit, also lies in the tuffs and tuffites of underlying Davle group and lower Cambrian conglomerates of the Dobříš group (Škácha et al. 2017).

The Zálesí U-Ni-Co-As-Ag/Bi deposit comprise of 30 hydrothermal veins and 2 stockworks, hosted in early Paleozoic high-grade metamorphic rocks (Dolníček et al. 2009).

Small uranium mine Předbořice lies in the Krásnohorsko-Sedlčanský islet, the deposit comprises over 100 carbonate veins (Bindi et al. 2016) cross cutting complexes of contactly metamorphosed hornfels with graphitic schist lenses and marbles, which are intruded by orthogneisses (Prokop 1970).

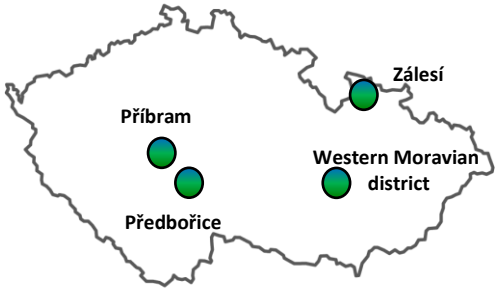

Fig. 1: Contour map of the Czech Republic showing studied localities.

MINERALOGY

Occurrences of selenides in Bohemian Massif are characterized by small accumulations embedded mostly in calcite or quartz veins with uraninite and coffinite, forming disseminated grains or aggregates, which are in close relationship with oxides and sulphides and the gangue minerals (Kvaček 1973; Paar et al. 2005; Dolníček et al. 2009), however large accumulation of selenium mineralization was described in some Moravian deposits (Kvaček 1973). Those accumulations are typical for Bukov and Habří, they are up to 50 cm thick and their mineral assemblages are mainly formed by dominant berzelianite (aggregates up to tenths cm) umangite, crookesite and clausthalite (usually a few mm in size), tyrrellite, athabascaite, hakite or permingeatite are associated as well (Kvaček 1973). Cu-selenides like berzelianite, umangite, crookesite or klockmannite are abundant (Fig. 2a) and extremely rare bellidoite was described in the Habří deposit as well (Montreuil 1975).

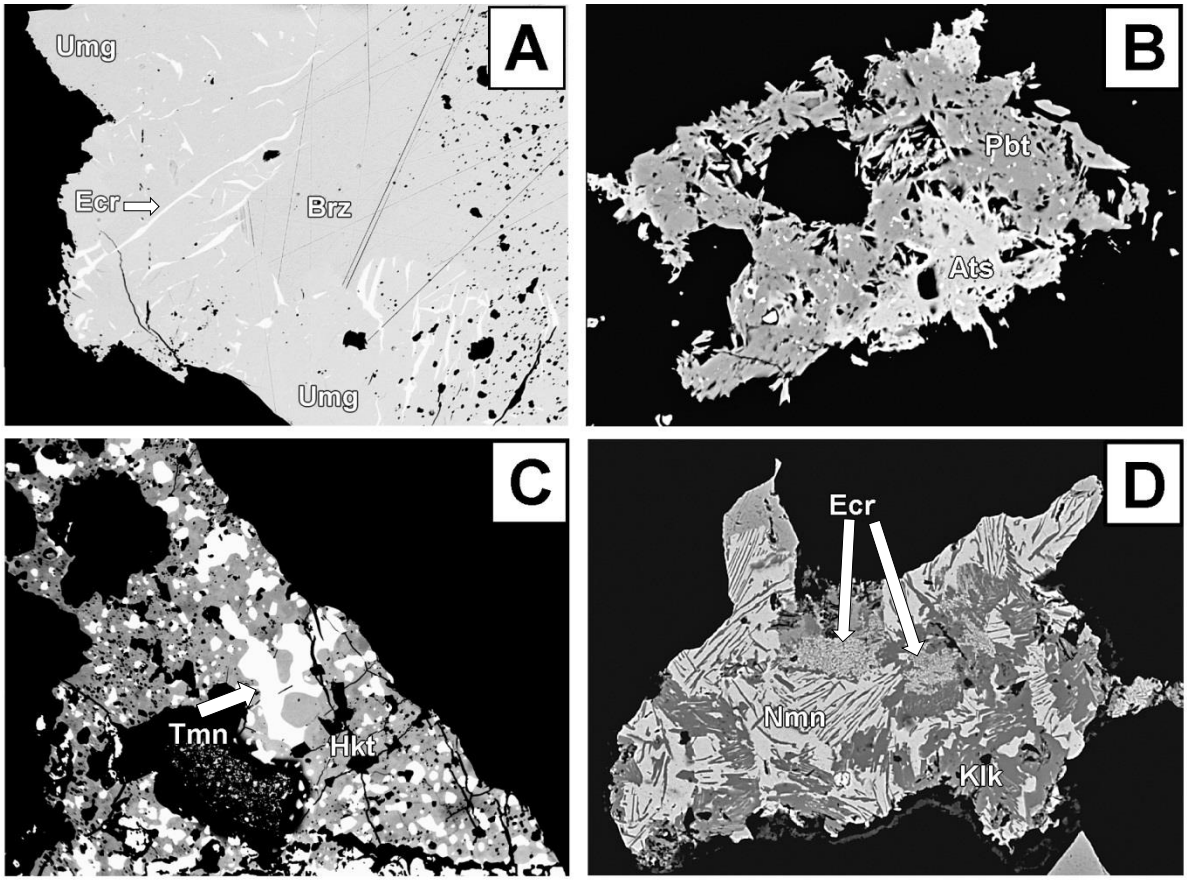

Fig. 2: BSE images, showing typical association of selenides. A) Xenomorphic grain of berzelianite and umangite intergrowth by eucairite from Habří (West-Moravian district), FOV 500 μm; B) Idiomorphic crystals of Příbramite associated with antimonselite from Příbram, FOV 120 μm; C) White xenomorphic grains of tiemannite embedded in grey hakite from Předbořice, FOV 500 μm; D) Aggregate of light grey crystals of naumannite replacing dark grey klockmannite, along his cleavage planes; it is associated with eucairite, Zálesí, FOV 200 μm.

In Příbram or Zálesí the amount of Pb, Hg, Ag selenides is higher compared to the Western Moravian localities (Sejkora et al. 2012; Škácha et al. 2017). The most typical for the Příbram district is the association of the Cu-Sb or Sb selenides – hakite, příbramite, bytízite and antimonselite (Fig. 2b). Common was clausthalite, berzelianite, umangite and tiemannite, however very rare was chaméanite, giraudite, dzharkenite, ferosellite and cadmoselite (Škácha et al. 2017). Příbram district is now with the 24 known selenides the most varied selenide locality on the world. In comparison Zálesí is more enriched in Bi, which is documented by Bi-bearing selenides like bohdanowiczite, litochlebite (Sejkora et al. 2011, 2014), watkinsonite (Topa et al. 2010) and Bi_4Se_3, whereas in Příbram Bi-bearing selenides are missing.

At the first sight the Se-mineralization from Předbořice looks similar especially to the Příbram district. Most abundant is clausthalite, than following eskebornite, umangite, eucairite, bukovite, berzelianite, ferroselite, hakite, naumannite, tiemannite, klockmannite (Fig. 2c), athabascaite, tyrrellite, permingeatite, aguilarite, chaméanite, giraudite. The mineralization is unique by presence of selenides bearing unusual elements (Au, Ag, Pd) or selenides which are missing on other studied localities including fischesserite, merenskyite, milotaite, chrisstanleyite, petříčekite, jolliffeite, kruťaite - trogtalite solid-solution and telargpalite (Johan 1987; Paar et al. 2005; Bindi et al. 2016).

DISCUSSION

At first we have to emphasize common features on studied localities. In general the localities are dominated by uraninite, coffinite, but the gangue minerals differ. The deposit formation conditions, corresponds to the low pressure and low temperatures on the studied

localities. Low temperatures (80 – 130°C), low pressure (<100 bars), low salinities and the fluids forming deposition recorded in Zálesí were mainly of meteoric origin (Dolníček et al. 2009). Also Škácha et al. (2017) noted that conditions of origin of selenides in the Příbram district probably corresponds to the temperatures around 100°C and admits that the solution involved in low salinity selenide precipitation, partially of the meteoric origin.

If we exclude the different sizes of the selenide accumulations on some localities, main difference between localities and its selenium mineralization is undoubtedly in the succession of individual phases, assemblages of selenides, sulphides and chemical composition of the selenides and different variety of phases in localities, caused by the fluids forming the minerals. We cannot negate that origin of the fluids was the same, but the composition could be different due to presumably different geological settings, the fluids were going through. If we consider, that the selenium mineralizations on the localities were formed in similar PT-conditions, the main difference was caused definitely by the different composition of the host rocks, e. g. the composition of the fluids in Zálesí is strongly dependent on the interaction of the initial brines and their country rocks (Dolníček et al. 2009).

On the other hand, if different composition of the host rock did not affect different composition of selenium mineralization, so did different PT-conditions, which could change the oxidation potential and stability of the elements in the fluids.

CONCLUSIONS

Different distribution of selenides in the Bohemian Massif is mostly probably caused by different composition of the reservoir entering the fluid forming the minerals and partly by the different host rock. Enormous predominance of Cu is visible in the Western Moravia, documented by berzelianite, umangite and eskebornite as the most abundant Se-phases. Příbram and Zálesí are characterized by clausthalite as the most abundant Se-phase, in Příbram clausthalite is followed by abundant berzelianite, eucairite and umangite.

Determination of succession of the selenides in Příbram and Zálesí is fairly complicated, due to material used for the studies, which was mostly collected as fragments from the dumps. However we can remark that, in both localities are visible increasingly higher amounts of Ag and Hg (also Sb in Příbram and Bi in Zálesí) in selenium mineralization compared to the Western Moravia. Příbram is also characterized by wide substitution by sulphur in selenides and rare Ag, Hg, Sb, As, Cd, Zn bearing selenides. In contrast with Příbram, the Zálesí is distinguishable by numerous of rare Bi bearing selenides. Nevertheless the most evolved and fractionated selenium mineralization is visible in Předbořice, where presence of PGE elements is indicated by merenskyite, the level of fractionation is also recorded by presence of rare selenides bearing Ag, Au, Pd, Te and Ni, which are mostly distinct in other studied localities.

ACKNOWLEDGEMENTS

The research of selenides was financially supported by internal grant of National Museum, Prague for TF, PŠ and LV. Further support was provided by the long-term project DKRVO 2018/02 of the Ministry of Culture of the Czech Republic (National Museum, 00023272) to JS.

REFERENCES

Bindi L. et al. (2016): Minerals 33:1–12.
Dolníček Z. et al. (2009): Min Deposita 44:81–97.
Johan, Z. (1987): Neues Jb Min 4:179–191.
Kříbek B. et al. (2009): Min Deposita 44: 99–128.
Kvaček M. (1973): Acta Uni Carolinae - Geol 1–2:15–38.
Kvaček M. (1979): Acta Uni Carolinae - Geol 1–2:13–36.
Montreuil L.A. (1975): Econ Geol 70:384–387.
Paar W.H. et al. (2005): Can Min 43:689–694.
Prokop L. (1970): MS, Czech Geol Surv Prague.
Sejkora J. et al. (2011): Can Min 49:639–650.
Sejkora J. et al. (2012): Bull Minerál-petrolog Odd Nár Muz 20:187–196.
Sejkora J. et al. (2014): Bull Mineral-petrolog Odd Nár Muz 22(2): 333–345.
Škácha P. et al. (2017): Minerals 7(6):91.
Topa D. et al. (2010): Can Min 48:1109–1118.

Varieties of magnetite associated with massive sulfides from the Morrison deposit

[1]Krzysztof Foltyn[#] and [1]Adam Piestrzyński

[1] AGH University of Science and Technology, Faculty of Geology, Geophysics and Environmental Protection, Department of Economic Geology, A. Mickiewicza Av. 30, 30-059 Kraków
[#]kfoltyn@agh.edu.pl

Key words: magnetite, magmatic sulfides, reaction rim, gold, electrum

Magmatic sulfide deposits are an important source of Ni, Cu as well as platinum group elements (PGE). Magnetite is a common accessory mineral present in the ore, forms primary grains in massive sulfides, and is interpreted to be a result of direct crystallization from an immiscible sulfide-rich melt (Fonseca et al. 2008). Secondary magnetite grains can be also formed during alteration of sulfide ore and host rock.

We report the presence of unusual types of magnetite from the footwall-type Morrison deposit (Ontario, Canada). It is a Cu-Ni-PGE deposit hosted within a zone of Sudbury Breccia in the Levack Gneiss Complex beneath the North Range of the Sudbury Igneous Complex. Magnetite is present as euhedral and subhedral crystals in massive sulfides but in some cases it also forms rims at the contact between thick sulfide vein and surrounding footwall rocks (granodiorite gneisses). Similar rims were recently described in the Munali Ni-sulfide deposit where they occur at the boundary between sulfide and silicate rocks. They are interpreted to have formed from melt interaction between sulfide liquid and a silicate melt generated by melting of the silicates by the hot sulfide liquid; or alternatively as a solid state disequilibrium reaction (Holwell et al. 2017). Spinel reaction rims have been also identified in many komatiite-hosted sulfide deposits (Staude et al. 2016), although in these cases the oxide is usually chromite. Footwall lithology in the Sudbury's North Range is mainly felsic so in the absence of significant chromium in the silicate rocks, such reaction will predominantly crystallize magnetite.

Additionally, some of the anhedral magnetite found at the sulfide – silicate contact and inside the massive sulfide ore, contains numerous sulfides inclusions (mainly chalcopyrite, pentlandite, pyrrhotite and bornite blebs), up to a few hundred μm in size. These inclusions might represent sulfide liquid trapped within the crystallizing magnetite grains. SEM and EMPA analysis reveal that oxide reaction rims and inclusion-rich magnetite contain numerous grains of gold, electrum and platinum group minerals which usually occur along cracks in the magnetite or at the contact with silicate rocks. This gold mineralisation is assumed to have precipitated from the hydrothermal fluids.

Magnetite rims and inclusion-rich magnetite might show a possible link between sulfide-silicate melt reaction and late hydrothermal fluids, which are usually considered to be a source of the low-sulfide Au-Pt-Pd-rich ores found around many footwall deposits in the Sudbury region.

REFERENCES

Holwell D. et al. (2017): Ore Geol Rev 90:553–575.

Staude S. et al. (2016): Geology 44:1047–1050.

Fonseca R. et al. (2008): Geochim Cosmochim Acta 72:2619–2635.

Crystal-chemical investigation on beryl from Namibia

[1]Jana Fridrichová[#], [1]Peter Bačík, [1]Pavel Uher, [1]Iveta Malíčková, [2]Valéria Bizovská, [3]Radek Škoda, [4]Marcel Miglierini and [4]Július Dekan

[1] Comenius University in Bratislava, Faculty of Natural Sciences, Department of Mineralogy and Petrology, Ilkovičova 6, 842 15 Bratislava, Slovakia [#]jana.fridrichova@uniba.sk
[2] Slovak Academy of Sciences, Institute of Inorganic Chemistry, Dúbravská cesta 9, 845 36 Bratislava 45, Slovakia
[3] Masaryk University, Department of Geological Sciences, Kotlářská 2, 611 37 Brno, Czech Republic
[4] Slovak University of Technology, Faculty of Electrical Engineering and Information Technology, Institute of Nuclear and Physical Engineering, Ilkovičova 3, 812 19 Bratislava, Slovak Republic

Key words: beryl, Namibia, crystal chemistry, trace elements, water types

Four beryl samples from various Namibian localities Etusis (ETU), Kudoberg (KUD), Baobismond (BAO) – Karibib and Engle Brecht (EN) – Strathmore) were investigated by wide spectrum of analytical methods.

The studied beryls are derived from complex-type petalite-subtype pegmatites of LCT family.

BAO and KUD samples are assigned to normal beryls (0.997-0.998 *c*/*a* ratio) and the other two samples (ETU and EN) are tetrahedral (0.999 *c*/*a* ratio) (Aurisicchio et al. 1988). The studied samples are relatively homogenous. The Fe contents in the most samples were below 0.1 wt. % FeO, only the KUD sample were enriched up to 0.6 wt. % FeO. Therefore, Mössbauer spectroscopy was performed only on this sample which proved mainly Fe^{2+} presence (86 %) at the octahedral site with variable assignment.

Samples are enriched in Na (up to 0.3 wt. % - EN sample), in Rb (up to 0.272 wt. % - EN sample) and Cs (up to 0.415 wt. % - EN sample). All of the samples exhibit relatively low K content (up to 0.032 wt. % - BAO sample). Based on the alkali content, KUD sample is alkali-free beryl, BAO is alkali-free to Na beryl, ETU is alkali-free – Rb-enriched beryl and EN is Na-Li beryl.

Trace element showed that the ETU sample has slightly increased Cr, Sc, Ga and Sr content, KUD is enriched in Ba, Cu, Ga, Sc, Sn, BAO has the highest content of Ba with slightly increased Cu, Ga, Sc and Sn, the EN sample has the lowest trace-element content, only Sr, Ga, Ni and Sc are in significant amount.

There were two types of water structural arrangement (H_2O I and H_2O II) detected in dependence of alkali presence. Powder IR spectroscopy proved that water type I was assigned to several bands: 1) symmetric stretching vibration ν_1 in range of 3630-3650 cm^{-1}; 2) asymmetric stretching mode ν_3 for 3695-3700 cm^{-1}; 3) bending vibration ν_2 for 1600-1610 cm^{-1}. Sodium is predominant cation coordinated to H_2O type II. Range for symmetric stretching mode of water type II ν_1 is 3595-3605 cm^{-1}, for asymmetric stretching ν_3 is 3660-3675 cm^{-1} and for bending vibration is 1630-1635 cm^{-1}.

Studied beryls contain relatively high Rb and Cs. Tetrahedral beryls (ETU and EN) are enriched in Li. The Li as a Be substituent enter the structure usually with Rb and Cs, which confirm highly fractionated pegmatite origin. This indicates that these beryls are derived from pegmatites, which are relatively well evolved.

Acknowledgment: This work was supported by the Slovak Research and Development Agency under the contracts No. APVV-14-0278, APVV-15-0050 and APVV-17-0134, and the Ministry of Education of Slovak Republic grant agency under the contracts VEGA-1/0079/15 and VEGA-1/0499/16.

REFERENCES

Aurisicchio C. et al. (1988): Am Min 73:826–837.

Joint 5th Central-European Mineralogical Conference and
7th Mineral Sciences in the Carpathians Conference
Banská Štiavnica 2018

Fluid inclusions and Ti-in-quartz thermometry of granulite from Monapo structure (Mozambique)

[1]Michaela Gajdošová[#], [1]Monika Huraiová and [2]Vratislav Hurai

[1] Department of Mineralogy and Petrology, Faculty of Natural Sciences, Mlynska dolina, Ilkovicova 6, 842 15 Bratislava, [#]michaela.gajdosova@uniba.sk
[2] Earth Science Institute, Slovak Academy of Sciences, Dubravská cesta 9, 840 05 Bratislava

Key words: granulite, fluid inclusions, Ti-in-quartz thermometry, Monapo structure

INTRODUCTION

The Monapo structure located in the north-east of Mozambique is a tectonic structure of an ellipsoidal shape with a size of 35 × 40 km. The structure forms part of the Mozambique orogene zone. There are three major groups of rocks: a) the metamorphic complex Metachéria; (b) the Mazerapane pluton; c) the Ramiane pluton. The Metachéria complex consists of orthogneisses, including mafic, felsic, pelitic and carbonate rocks. The Mazerapane pluton consists of ultramafic and mafic rocks with foids and intrudes into the western part of the Metachéria complex, while the Ramiane pluton is dominated by granite and syenite rocks without foids that enter the eastern half of the Metachéria complex (Macey et al. 2013).

The aim of the thesis is to determine the mineral composition of the granulite from the Monapo structure. Next to calculate the crystallization temperature of quartz based on Ti content. Following by determination of composition and density of fluid inclusions which will be used for reconstruction of the PT conditions of genesis.

METHODS

Two-sided polished plates with a thickness of 0.2 mm were used for the investigation of fluid inclusions in the quartz. Phase changes were measured using a LINKAM THMSG 600 microthermometric table with an Olympus BX-51 microscope with 10x, 20x, and 100x magnification mounted on. The temperature range of the microthermometric table is from -196 to 600 °C. On top of that, freezing, melting and homogenizing temperature values were measured.

Geothermometer "TitaniQ" (Wark and Watson 2006) was used to calculate the crystallization temperature of quartz. This geothermometer uses the substitution of titanium for silicon in quartz. In Ti oversaturated system, the Ti content in the quartz (in ppm) increases exponentially reciprocally to the temperature (°C) as:

$$T\,(^{\circ}C) = \frac{-3765}{\log(Ti[ppm]) - 5.69} - 273$$

The Raman spectra of fluid inclusions were generated using spectrometer Xplora (Horiba Ltd., Japan) at room temperature and pressure. Raman spectra were recorded using a 100x objective (NA = 0.8, WD = 3.4mm), a 628nm red laser produced by a 24mW laser diode, and a spectral grid with a density of 1800 scratches per mm.

MINERALOGICAL COMPOSITION AND FLUID INCLUSIONS

Researched sample is granulite from the Metacheria complex in Monapo structure. Mineral assemblage consists of quartz, albite, potassium feldspar, amphibole, magnetite, pyrrhotite and pyrite. Accessory minerals are small apatite and calcite grains, as well as titanite and monazite (Fig. 1). Monazites have increased content of LREE elements (0.81-1.00 apfu), most Ce (0.37-0.50 apfu), so we can label them as monazite-(Ce). Monazite grains were dated using in situ chemical dating. Model age of 6 monazite analyses is 573±13 Ma (Gajdošová et al. 2017). The cathodoluminescence of quartz was used to identify the zonation that indicates primary

crystallization at various PT conditions as well as recrystallization of quartz during metamorphism. Titanium content expressed in ppm is inserted in a formula for temperature calculation. The calculated crystallization temperature in the sample is in the range from 550 °C in the dark part of the grain up to 645 °C in the light part of the grain. The detection limit is in the range between 8-10 ppm. Findings correspond to an error in determining the temperature within ±5 °C.

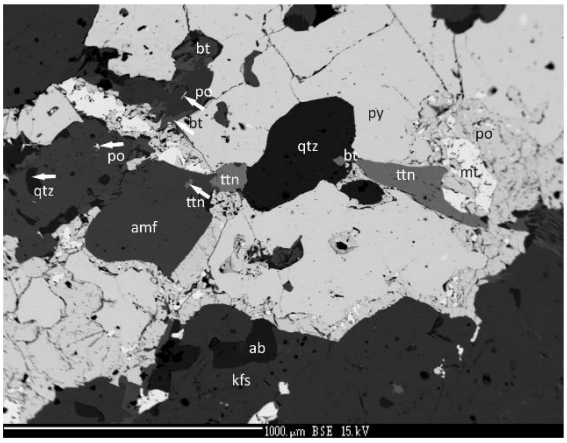

Fig. 1: Mineral composition of granulite is made by quartz-qtz, amphibole-amp, biotite-bt, albite-ab, potassium feldspar-kfs, pyrite-py, pyrrhotite-po, magnetite-mt and titanite-ttn.

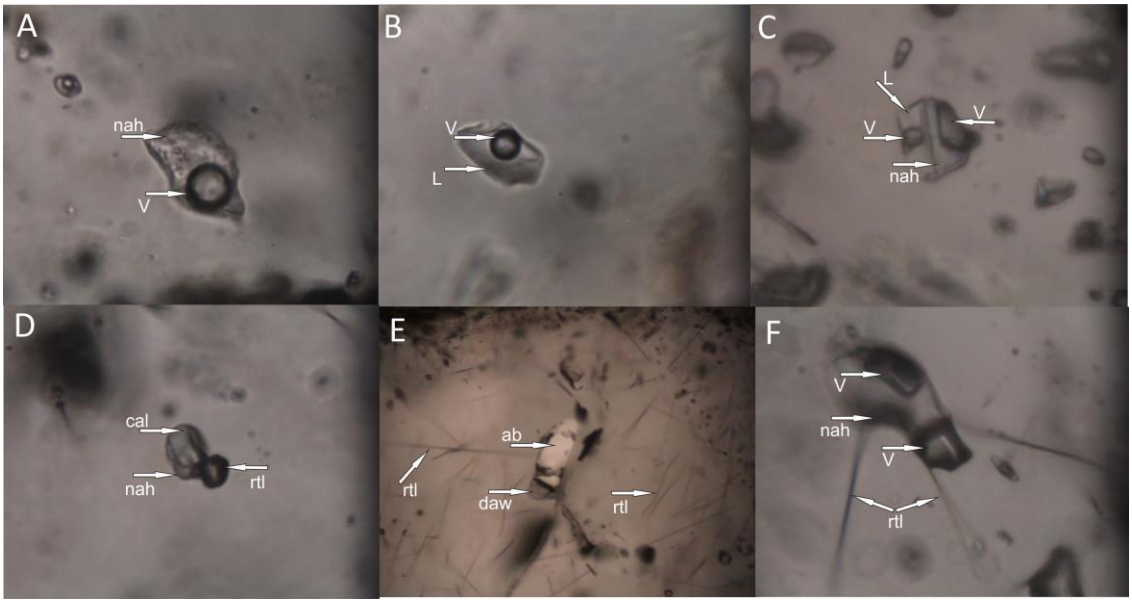

Fig. 2: A) CO_2 phase-V with nahcolite-nah (size 9x5 µm); B) water inclusion-L with CO_2 phase-V (size 7x4 µm); C) polyphase inclusion with water phase-L, gas phase-V and nahcolite-nah (size 5x5 µm); D) secondary inclusion with calcite-cal, rutile-rtl and nahcolite-nah (size 4x3 µm); E) inclusion of albite-ab with dawsonite-daw and marked rutile-rtl stick (size 3x2 µm); F) water inclusion with nahcolite-nah, CO_2 phase-V (size 11x5 µm).

Fluid inclusions were observed in 11 plates of quartz. In total 190 inclusions were measured. Fluid inclusions were further investigated for their size, shape, freezing temperature, melting and homogenization temperature. Inclusions size are from 1x0.8 µm to 10x16 µm and have regular round, oval or stick-shaped. The primary water inclusions contain the gas phase formed by N_2 and CO_2 and the solid phase. The homogenization temperature of the gas phase ranged from -31.5 °C to 21.8 °C with the highest frequency at -3.2 °C. The lower homogenization temperature corresponds to the higher density. Homogenization temperature in one inclusion was -57.4 °C, which corresponds to super-density gas with a density higher than the density of the liquid at the triple point. The melting point of the other inclusions ranged from -59 °C to -56.6 °C with the highest frequency at -56.7 °C. These melting points correspond to almost pure CO_2 with a low impurity N_2 and CH_4.

RAMAN SPECTRA

Raman spectrometry identified nahcolite, dawsonite and thenardite in fluid inclusions (Fig. 2). Secondary inclusions include calcite and rutile (Fig. 2D). Inclusions of albite and dawsonite were also observed in the quartz (Fig. 2E).

Raman spectrometer identified the gaseous components in the specific highest density inclusion (Fig. 3B). Size of this inclusion is 4x1.5 μm. The CO_2 vibration band is 1280 and 1384 cm^{-1}, for N_2 2327 cm^{-1}, and a vibration band for methane CH_4 at 2912 cm^{-1} was also observed. Nahcolite is carbonate ($NaHCO_3$), which has vibration bands at 1045 and 685 cm^{-1} (Fig. 3A). Next inclusion is 4.5x3.5 μm in size. Vibrating bands of the surrounding quartz are observed at 203 and 463 cm^{-1}. Dawsonite [$NaAlCO_3(OH)_2$] has typical vibration bands at 187, 257, 586 and 1091 cm^{-1}. The spectrum also includes vibration bands of surrounding quartz and CO_2 gas at 1280 and 1384 cm^{-1}. Inclusion of the thenardite (Na_2SO_4) in quartz has typical vibration bands at 452, 650 and 994 cm^{-1}.

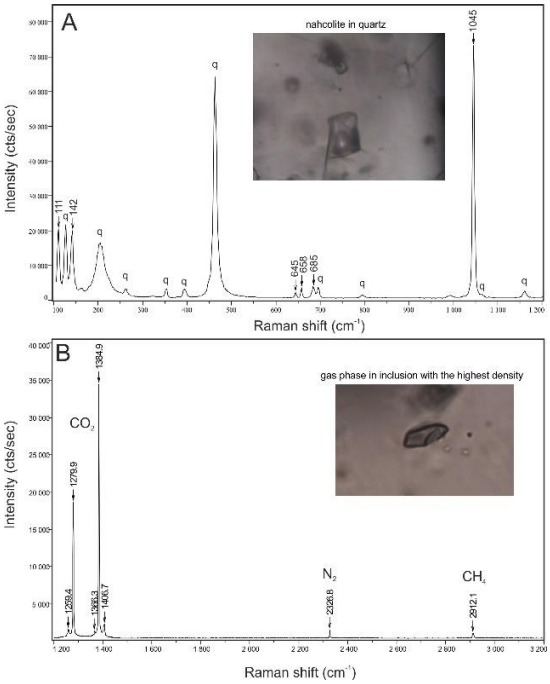

Fig. 3: A) Raman spectra of nahcolite in quartz. B) Raman spectra of superdensity CO_2-N_2-CH_4 gas.

CONCLUSION

Granulite from the Metachéria complex is the associated rock with the Evate carbonatite deposit in Mozambique. Granulite is composed of quartz, albite, potassium feldspar, biotite, amphibole, magnetite, pyrite and pyrrhotite. Accessory minerals are small grains of apatite and calcite, titanite and monazite. The age of monazite based on in situ chemical dating corresponds to 573 ± 13 Ma. The crystallization temperature of the quartz, calculated by Ti in quartz thermometry, is from 460 °C to 645 °C. N_2 and CO_2 gas phase were identified in the primary inclusions. The solid phases as nahcolite, dawsonite and thenardite indicating sulfate-carbonate fluids. In the secondary inclusions, calcite and rutile were present also albite inclusions were observed. Further research will focus on the thermodynamic conditions of quartz formation calculation, the reconstruction of the metamorphic pathway and the origin of the fluid migration through the Monapo structure during the pan-African orogenesis associated with the creation of the Gondwana supercontinent and its subsequent breakdown.

Acknowledgment: The work was supported by Comenius University grant under number UK/94/2018.

REFERENCES

Macey P.H. et al. (2013): Precamb Res 233:259–281.
Wark D.A. and Watson E.B. (2006): Contrib Min Petrol 152:743–754.
Gajdošová M. et al. (2017): Petros 2017, Book of Abstracts, Bratislava, 12–14.

Recent developments and the future of low-temperature calorimetric investigations: Consequences for thermodynamic calculations and thermodynamic data bases

[1]Charles A. Geiger[#] and [1]Edgar Dachs

[1] Salzburg University, Dept. of Chemistry and Physics of Materials, Jakob-Haringer-Straße 2a, A-5020, Salzburg, Austria [#]ca.geiger@sbg.ac.at

Key words: Calorimetry, Heat Capacity, Standard Entropy, Thermodynamics, Garnet

Low-temperature calorimetry is an experimental science that measures the thermodynamic function heat capacity, $C_p(T)$, from which the standard third-law entropy, $S°$, is calculated. The recent technological development of relaxation calorimetry allows new experimental strategies and types of C_p investigations that were previously not possible. Relaxation measurements are fast and automated and can be made on mg-sized mineralogical samples between 2 and 400 K. These advantages, when careful measurement procedures are used, permit better determinations and understanding of C_p behavior.

The C_p of synthetic single-crystal MgO was measured between 5 and 302 K and $S°$ calculated using relaxation calorimetry to further investigate its precision and accuracy.

Synthetic and natural end-member or nearly end-member silicate garnets were investigated in the past via adiabatic calorimetry and more recently and extensively with the relaxation method. First C_p and $S°$ results have been obtained on spessartine ($Mn_3Al_2Si_3O_{12}$) and reinvestigations on pyrope ($Mg_3Al_2Si_3O_{12}$), almandine ($Fe_3Al_2Si_3O_{12}$), grossular ($Ca_3Al_2Si_3O_{12}$) and andradite ($Ca_3Al_2Si_3O_{12}$), often on multiple samples, have resolved uncertainties and certain problems with published data. $S°$ can be affected by low temperature phenomena, such as magnetic phase transitions or Schottky anomalies at $T <$ 15 K, which were not fully described in some older calorimetric studies. Small differences in the thermodynamic behavior between natural and synthetic silicates may exist as demonstrated by extensive work on grossular.

The C_p behavior and $S°$ values for the five common garnets are analyzed and the latter are compared to the "best fit or optimized" $S°$ values given in various internally consistent thermodynamic databases. Conclusions are drawn on what types and directions of calorimetric study are required in order to obtain better thermodynamic property determinations of minerals.

Formation environment reconstruction and petrography of Praid salt rocks (Transylvania)

[1]Orsolya Gelencsér[#] and [1]Csaba Szabó

[1] Eötvös University, Faculty of Science, Lithosphere Fluid Research Lab, Pazmany P. setany 1/C, H-1117 Budapest, Hungary [#]gecso@caesar.elte.hu

Key words: salt deposit, evaporite texture, Transylvanian Basin

In the Central-European region there are several saline formations formed during the Miocene. A large deposit can be found in the Transylvanian Basin (TB). The majority of the papers, related to this deposit, focus on the tectonics, stratigraphy, palynology of salt deposits, whereas the salt petrography has received less attention. Therefore, our study applies detailed petrographic observation to reconstruct the formation environment of the salt in TB.

Evaporites are sediments, which require particular environments to form. The icehouse-greenhouse changes are in a remarkable effect of the salt formations (Warren 2006). The Middle Miocene climate optimum (arid event) is followed by the formation of evaporites in the Paratethys region. The salt was buried after the late Miocene tectonic event (e.g., subsiding basin and volcanic material production in TB) connected to the Carpathian orogen (Szakács and Krézsek 2006).

Sample was collected form Praid salt mine, where we observed two types of salt rock. One is greyish coarse grained massive halite, and the other has laminated structures, suggesting different formation environments.

To determine evaporitic textures, thin sections were made with dry procedure. The samples were examined under polarizing microscope. There is no petrographic terminology applied to primary and secondary features. Our applied textural classifications of Hardie et al. (1983) and Kátai (2017) is based on grain size and morphology of halite crystals. Two types of textures can be distinguished: inequigranular sutured mosaic and inequigranular polygonal mosaic textures. Both of them related to the salt-tectonics. Although the salt formation in the TB underwent a large-scale diapirism and salt has mostly secondary mosaic structure, the primary features are rarely preserved as relicts. The fluid inclusions trapped in halite can be identified such as primary and secondary generation based on the distribution, size, ratio and number phases (liquid and vapour), provides information about the temperature and chemical composition of the paleo-seawater. Beside fluid inclusions, solid inclusions also can be find in the salt which are mainly authigenic sulphates and carbonates. Rounded quartz and clay minerals supposed to be detrital origin.

Summarizing our work, we identified shallow marine and deep water depositional signatures. The formation environment, in turn, constrains the texture of the salt. The shallow samples stemming from massive grey salt contains chevron structure growth align crystals with primary fluid inclusions, playing important role in the environment reconstruction. The deep water deposition consists of white and grey laminates as results of a long term sinking of continuously precipitating halite crystals. In these layers, only secondary generations of fluid inclusions can be observed.

Acknowledgment: We are grateful to Dr. Zoltán Unger for organizing the sample collection. Thanks to the members of the Lithosphere Fluid Research Lab for their support.

REFERENCES

Warren J.K. (2006): Evaporites: Sediments, Resources and Hydrocarbons. Springer.

Szakács S. and Krézsek Cs. (2006): J Vol Geotherm Res 158:6–20.

Hardie L.A. et al. (1983): Sixth International Symposium of Salt. Salt Institute Publisher.

Kátai O. (2017): Textural and fluid inclusion study on Praid salt rocks. MSc Thesis.

Rock fulgurites and their mineralogical secrets

[1]Reto Gieré[#]

[1] University of Pennsylvania, Department of Earth and Environmental Science, 240 S. 33rd Street, 19146 Philadelphia, USA [#]giere@sas.upenn.edu

Key words: lightning, impact, cristobalite, high-T metamorphism, high-P metamorphism

Lightning is an electric discharge occurring within a thundercloud, between clouds, or between a cloud and the ground. It is estimated that, on average, nearly 1.4 billion lightning discharges occur annually around the globe, equivalent to 44 ± 5 lightning flashes per second, of which approximately 10% are ground strikes. Cloud-to-ground lightning strikes are highly energetic and very short events with peak lightning currents that are typically on the order of tens of kA, but may exceed 200 kA. During such lightning strikes, the target rock surface can be heated to over 2000 K within tens of microseconds, followed by quenching. These very fast and pronounced changes in temperature result in the formation of a so-called rock fulgurite, which appears as a distinctive, thin, garbled coating composed of glassy to fine-grained porous material. A fairly wide range of minerals has been observed in rock fulgurites formed on granite, including quartz, cristobalite, albite, iron oxides, ilmenite, rutile, epidote, and barite. These minerals are embedded in a highly porous amorphous matrix, which may also include burned organic material present on the rock surface before the lightning impact.

The lightning strike also generates a strong shock wave in the vicinity of the strike point, as evidenced by the presence of shock lamellae in crystalline quartz, which have been shown to occur in the target rock underneath the fulgurite layer. Shock lamellae are typically associated with meteorite impacts, but a recent model has shown that lightning impacts may produce shock pressures between 7 and 21 GPa, i.e. similar to those generated during a meteorite impact.

Lightning affects a significant portion of the rocks exposed at the Earth's surface. Since glass is geologically susceptible to alteration, the predicted large areas covered by rock fulgurites produced every year may potentially weather more rapidly than the non-affected rocks. Lightning thus, can be considered a force that actively participates in shaping the Earth's surface.

Sc distribution in minerals of the Cínovec-south deposit

[1]Sebastián Hreus[#], [1,2]Jakub Výravský, [1]Jan Cempírek

[1] Masaryk University, Faculty of Science, Department of Geological Sciences, Kotlářská 267/2, 611 37 Brno, Czech Republic [#]sebastian.hreus@mail.muni.cz
[2] TESCAN Brno, s.r.o, Libušina třída 1, 623 00 Brno, Czech Republic

Key words: Greisen, Geochemical analyses, Electron Microprobe, Zircon, Ixiolite

INTRODUCTION

Greisen deposits in Krušné Hory/Erzgebirge area are well known for their Sn, W and Li resources. Worldwide, scandium occurs in greisens in relatively small quantities and its contents were discussed in detail in few publications only (e. g. Kempe and Wolf 2006, Wise et al. 1998). On the other hand, Sc amounts of several tens of ppm in bulk could be, in some cases, sufficient amount for its production during mining of other commodities, due to high Sc fractionation in ore minerals.

Cínovec-Zinnwald is famous historically mined deposit. The A-type Cínovec granite cupola penetrates the Teplice rhyolite; numerous ore bodies represented by massive greisens and quartz vein stockwork with greisen envelopes with Li, Sn, W, Nb, Ta, Sc, REE mineralization are spatially distributed in its apical parts. In general, greisenisation degree of the granite is significantly variable. Different type of mineralisation is represented by younger hydrothermal veins with common sulphides (typically sphalerite and galena) which locally cuts greisens.

Tin ores were mined in Cínovec from 14th to 19th century. Production of W ore commenced in 19th century, and both Sn and W ores were systematically mined during 20th century until the mine closure in 1990. For a short period in 1950's, Sc from the wolframite was extracted (Petrů et al. 1956).

RECENT EXPLORATION ACTIVITIES AT CÍNOVEC

Cínovec-south deposit is currently examined by Geomet, s.r.o., part of European Metals Holdings Ltd., for its remarkable resources of Li, W and Sn; potential by-products include e.g. Nb, Ta, Rb, Cs and Sc. The company runs a comprehensive drilling program and kindly provided samples for this study.

INVESTIGATED MINERALS

Several distinct rock types (granites, greisenized granites, greisens and hydrothermal veins; in total 23 samples) were studied in order to characterize the Sc mineralisation in the Cínovec-south deposit.

Cassiterite occurs as an accessory ore mineral and forms predominantly subhedral, fresh aggregates with variable porosity (fig. 1). Concentrations of Sc (0-0.007 apfu; 0-0.317 wt.% Sc_2O_3) are usually close to the detection limit of electron microprobe; average amount of Sc in cassiterite is 0.07 apfu.

The Nb-rutile has been found in only 3 samples (greisen, greisenized porphyry granite and albite granite). It forms either irregular grains up to ca. 50 μm enclosed in zinnwaldite (fig. 4) or occurs as substantially larger grains (ca. 200 μm) showing very complicated internal zoning and locally also contains inclusions of Sc-rich columbite. The amount of Sc ranges from zero to 0.28 wt. % Sc_2O_3 (0-0.004 apfu), with the average of 0.16 wt. % Sc_2O_3.

The W-Nb-Sc ixiolite-like phase is quite rare and in significant amount occurs only in 2 samples (quartz vein with wolframite and greisen). According to textural relations, the ixiolites are always associated with Nb-Sc-rich wolframites and appear to be of secondary origin (fig. 5). The ixiolites contain highest amounts of Sc from all the investigated phases; their Sc content is up to 4.87 wt. % Sc_2O_3 (0.19 apfu), with average of 2.24 wt. % Sc_2O_3

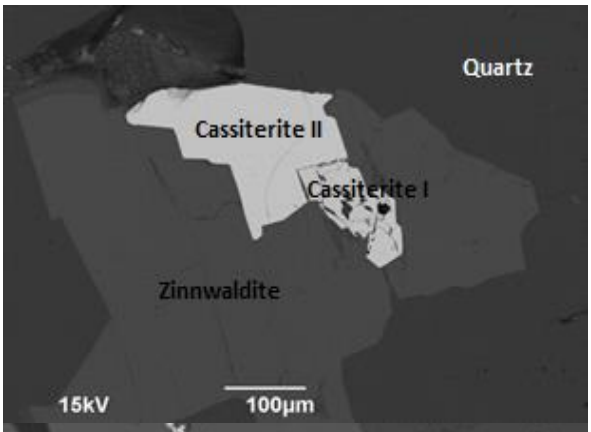

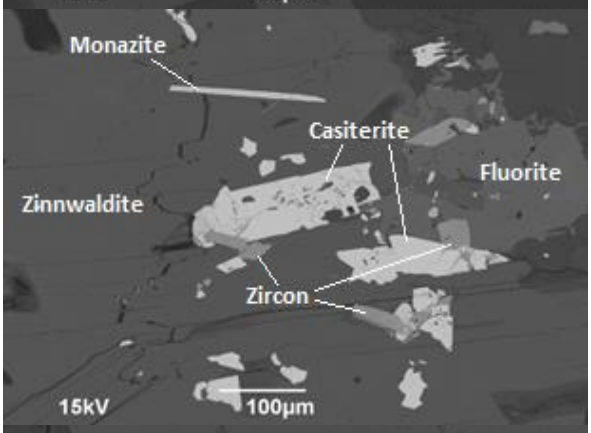

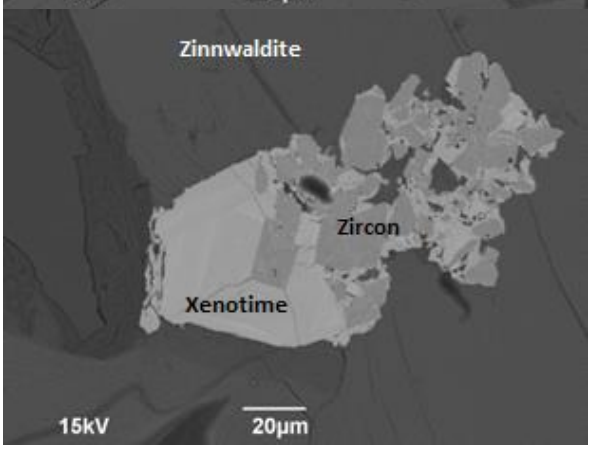

Fig. 1: (left, on the top): Aggregate of fractured porous cassiterite I overgrown by homogeneous cassiterite II. Cassiterite is enclosed in zinnwaldite; greisen.
Fig. 2: (left, in the middle): Unusually high inclusions amount in zinnwaldite; greisen.
Fig. 3: (left, down): Zircon aggregates are overgrown by younger zonal xenotime. Both minerals are enclosed in foliated zinnwaldite; greisen.

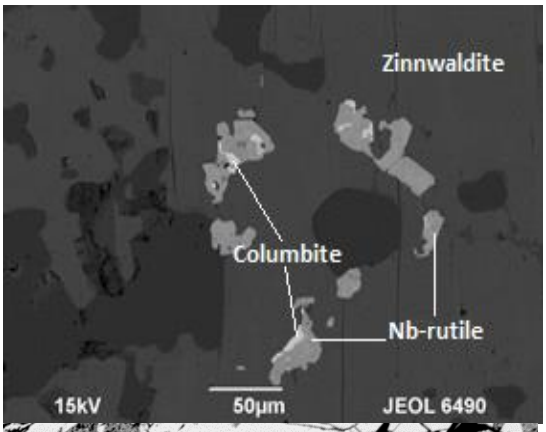

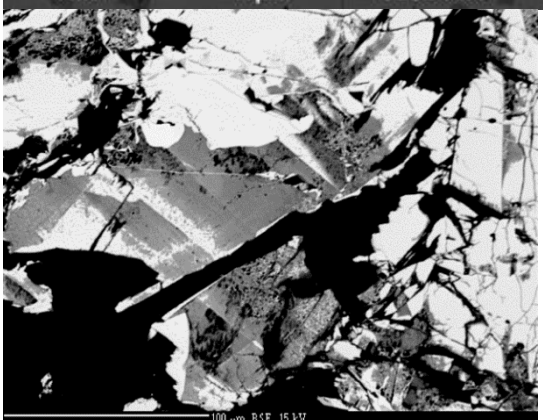

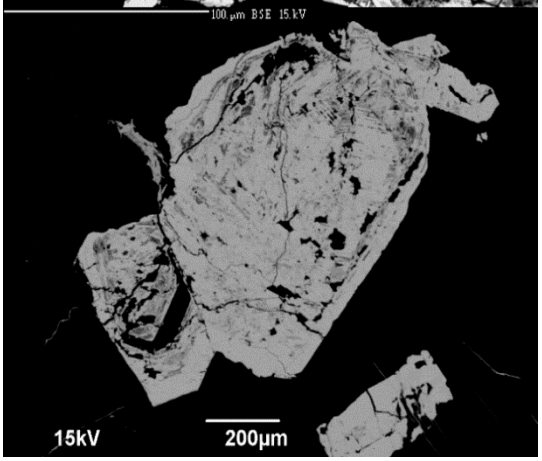

Fig. 4: (right, on the top): Nb-rutile with columbite inclusions in zinnwaldite; albitized granite.
Fig. 5: (right, in the middle): porous, darker Sc-rich ixiolite replacing older bright wolframite; hydrothermal vein.
Fig. 6: (right, down): Zonal wolframite (bright) with newly formed ixiolite inside (grey colored parts); greisen.

Wolframite (Fig. 6) was found in hydrothermal quartz veins and greisens (6 samples). Mineral shows high variation in Sc (and other impurities) content, both between different samples and in a single sample. Average Sc content for bulk wolframites is 0.01 apfu (0.24 wt. % Sc_2O_3), but those from sample of altered granite with sulphides contain only 0.003 apfu (0.06 wt. % Sc_2O_3) and the rest 0.016 apfu (0.39 wt. % Sc_2O_3). Scandium shows very strong positive correlation with Nb (R=0.93), indicating that Sc enters the structure of wolframite via coupled substitution $Fe^{2+} + W^{6+} = Sc^{3+} + Nb^{5+}$.

Columbite is a ubiquitous accessory mineral at Cínovec and has been found in most of the samples. Principally, it occurs either in zinnwaldite as disseminated grains (ca 5-20 µm) or clusters of grains, commonly associated or directly intergrowing with zircons or it forms slightly bigger individual grains (ca. 10-100 µm) in other minerals, again commonly intergrown with zircons. Only rarely the size of columbite grains exceeds 100 µm and the largest reach ca 400 µm in length. Columbite Sc content varies between 0.006-0.165 apfu (0.12-3.04 wt. % Sc_2O_3) with avg. value of 1.35 wt. % Sc_2O_3 and 0.07 apfu.

Zircon occurs frequently in all types of studied rocks, except the samples with sulphide mineralisation. Zircon typically forms euhedral crystals. It is often enclosed in zinnwaldite (fig 3). Most significant substituents in zircons include Hf (0.013-0.114 apfu), Y (0-0.139 apfu), and Sc (0-2.5 wt.%; 0-0.086 apfu Sc). Zircon has highly variable Sc contents; average Sc content is 0.02 apfu and its content increases with zircon fractionation (fig. 7).

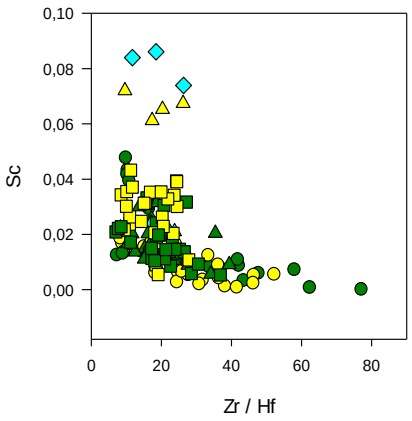

Fig. 7: Correlation between Zr/Hf fractionation and Sc contents in zircon.

The mica group minerals are present in all types of studied rocks, but only in greisens and partly also in greisenized granites micas belong among the main rock forming minerals. Dominant zinnwaldite is, in some cases (mostly in granite), the main mineral that encloses accessory inclusions of columbite, zircon or xenotime (fig. 2). Muscovite was observed as a younger zinnwaldite alteration product. Sc was detected only in several analyses (13), highest Sc content is 0.083 wt.%, 0,0012 apfu.

CONCLUSIONS

Sc content in investigated minerals of Cínovec-South deposit shows significant variation (fig. 8). Among the investigated minerals, Li-micas have relatively low Sc content, but they could be interesting Sc-bearing minerals due to their large amounts at the deposit. Noticeably high Sc content was detected in zircon, wolframite, columbite and especially in later stage W-mineral – ixiolite. Production of Sc from the above-mentioned minerals is theoretical only, as some problematic ore properties (e.g., very small grain size of zircon and columbite, problems with mineral separation and metallurgy) can become limiting aspects.

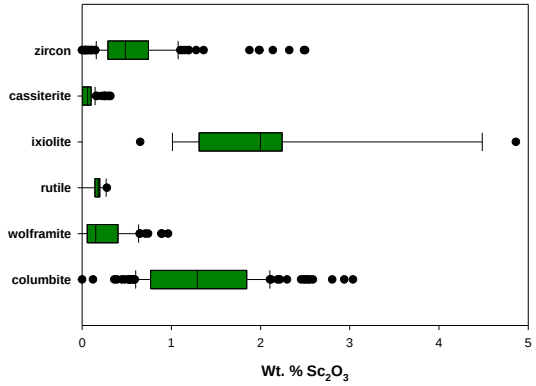

Fig. 8: Concentrations of Sc in minerals of the Cínovec-south deposit.

Acknowledgment: This research was supported by grant MUNI/A/1088/2017. We thank P. Reichl and V. Šešulka (Geomet, s.r.o.) for allowing access to samples and their expertise in data processing and sampling.

REFERENCES

Kempe U. and Wolf D. (2006): Ore Geol Rev 28:103–122.
Wise M.A. et al. (1998): Can Min 36:673–680.
Petrů F. (1956): Chem Listy 50:1696.

Pyrochlore-supergroup minerals in granitic pegmatites from Maršíkov area, Czech Republic: crystal chemistry an genetic relations

[1]Štěpán Chládek[#], [1]Pavel Uher, [2]Milan Novák and [3]Tomáš Opletal

[1] Comenius University, Faculty of Natural Sciences, Department of Mineralogy and Petrology, Ilkovičova 6, 842 15 Bratislava, Slovakia [#]st.chladek@seznam.cz
[2] Masaryk University, Faculty of Natural Sciences, Department of Geological Sciences, Kotlářská 267/2, 311 37 Brno, Czech Republic
[3] Palacký University, Faculty of Natural Sciences, Department of Analytical Chemistry, tr. 17. listopadu 12, 771 46 Olomouc, Czech Republic

Key words: beryl-columbite pegmatite, pyrochlore group, microlite group, compositional variations, uranium valence state

Metasedimentary and metavolcanic complex of Silesicum Unit, Bohemian Massif (Czech Republic) hosts frequent rare-element Variscan granitic pegmatites of beryl-columbite subtype with numerous Nb-Ta oxide minerals. Here, we describe the pyrochlore-supergroup minerals (PSGM) from the Maršíkov area in southern part of the Silesicum Unit.

Investigated pegmatites (Lysá Hora, Scheibengraben, Schinderhübel I, and Bienergraben) contain PSGM in association with columbite-group minerals (CGM), predominantly in blocky K-feldspar, quartz core and late metasomatic sacharoidal albite. The PSGM occur along the cracks and rims of magmatic CGM crystals. Consequently, PSGM represent products of CGM alteration due to interaction with the late-magmatic to hydrothermal fluids.

Three genetic types of U-rich pyrochore members (still IMA unapproved) occur in the Lysá Hora pegmatite: (i) early subsolidus homogeneous relics of "oxyuranopyrochlore", which frequently contain almost 56 wt.% UO_2 (1.6 *apfu* U^{4+}), (ii) "oxykenopyrochlore" or "kenopyrochlore", showing high vacances in *A* position and a half contents of U, Na, and Ca, compared to (i) type. The X-ray photoelectron spectroscopy (XPS) reveal 77.5 at.% U^{4+} and 22.5 at.% U^{6+} in this pyrochlore. The presence of U^{6+} is probably a result of partial oxidation of U, connected with radiation damage of the mineral. This phenomenon is also contributed by higher Si and P contents of radiation damaged domains of pyrochlore (ii). The micro-Raman spectroscopy (μRS) does not verify any presence of structural $(OH)^-$ and molecular H_2O in pyrochlore (ii), therefore the anion *Y*-site position is vacant. Very rare late irregulary zoned rims of "oxy/kenopyrochlore" (iii) show a lower content of Ca and Na and similar U content to type (ii).

In other three pegmatite occurrences, electron-microprobe (EMPA) and μRS documented also oscillatorily zonal hydroxycalciomicrolite (≤1.7 *apfu* Ca^{2+}) as the latest (iv) but dominant PSGM, locally in association with fersmite. Entry of other elements into the microlite lattice is possible *via* following substitutions:

$2Ca^{2+} \leftrightarrow U^{4+} + {}^{\square}A$;

$Na^{+} + Ca^{2+} + F^{-} \leftrightarrow U^{4+} + {}^{\square}A + O^{2-}$.

The origin of PSGM indicates the *P-T* disequilibrium between crystallizing pegmatite melt and late autometasomatic fluids rich in Na, Ca, U and F. Alteration of U-rich PSGM (i) leads to more vacant compositions (ii; iii), and whole alteration including the radiation damage leads to a formation of the latest Ta-rich PSGM, hydroxycalciomicrolite (iv).

Acknowledgment: This research was supported by APVV-14-0278 and APVV-15-0050 projects, and MŠMT of Slovak Republic due to the projects VEGA-1/0499/16 a VEGA-1/007915.

New data on chemical composition of Au-Ag-S system minerals in precious and base metal deposit Hodruša – Hámre

[1,2]Stanislav Jeleň, [3]Sergiy Kurylo, [4]Vladimir A. Kovalenker, [2]Jarmila Luptáková, [1]Ľuboš Polák and [1]Renáta Durajová

[1] Matej Bel University, Faculty of Natural Sciences, Department of Geography and Geology, Tajovského 40, 974 01 Banská Bystrica, Slovak Republic #stanislav.jelen@umb.sk
[2] Earth Science Institute, Slovak Academy of Sciences, branch: Ďumbierska 1, 974 11 Banská Bystrica, Slovak Republic
[3] M.P. Semenenko Institute of Geochemistry, Mineralogy and Ore Formation National Academy of Sciences of Ukraine, Palladina av. 34, 03680 Kiev-142, Ukraine
[4] Institute of Geology of Ore Deposits, Petrography, Mineralogy and Geochemistry, Russian Academy of Sciences, Staromonetny per. 35, Moscow, Russian Federation

Key words: Hodruša-Hámre, Rozália mine, Au-Ag-S system, petrovskaite, uytenbogaardtite

The epithermal precious and base metal mineralization of intermediate-sulphidation type at the Rozália mine is located in the Central Zone of the Štiavnica Stratovolcano. It occurs in pre-caldera andesite, predominantly hosted by shallow-dipping structures of a shear-zone (Kubač et al. 2018). During a detailed investigation of Natália vein on XIII level of Rozália (ca. 300 m from the surface), were found minerals, unusual for their optical properties and chemical composition. Those are similar to uytenbogaardite and petrovskaite, and associate with gold of higher fineness (817-844), quartz, galena, sphalerite, pyrite, chalcopyrite, hessite and petzite. They form separate isometric and irregular grains intergrowing with gold, in sulphides, also thin reaction rims (thickness up to 10 μm) on the border of the gold grains, respectively on their contact with quartz and/or small grains of galena. They also form irregular aggregates (up to 100 μm in size) in central part of the gold grains. In reflected light they have intensive white-yellow to yellow colour. For this reason, they are difficult to distinguish from the gold. After oxidation in air they have light to dark grey colour, with pink, blue or yellow shades, depending on their chemical composition. The SEM images shows that in the most grains can be observed non-homogeneous surface structure, similar to exsolutions of solid solutions disintegration. Irregularly growing domains up to 1 μm in size have different Au and Ag ratios. It also documents the variable chemical composition of the investigated phases. Gold content ranges is from 48.98 to 80.66 wt.%, Ag from 17.68 to 49.29 wt.% and S from 1.97 to 7.09 wt.%. Content of other elements is weak (Te to 0.6; Se and Cu to 0.2 wt.%). Wide range of changes in composition of natural Au and Ag sulphides from Ag_3AuS_2 to AgAuS was found by several authors (e.g. Paľyanova et al. 2011). The calculated formula corresponds to petrovskaite $(Au_{1.60}Ag_{0.89})_{\sum 2.49}(S_{0.50}Se_{0.01})_{\sum 0.51}$.

Chovan et al. (2016) found in the products of ore processing similar AgAuS phases by QEMSCAN. Their chemical composition resemble uytenbogaardtite (Ag_3AuS_2), or unknown suloteluride AuAgSTe. Interrelationships of precious metal minerals in aggregates indicate the probable activity of late fluid (higher sulphur activity and oxidation potential) from which studied Au and Ag sulphides could be originate.

Acknowledgment: This contribution was supported by Slovak Research and Development Agency (No. APVV-15-0083), and Research Agency of the Ministry of Education, Science, Research and Sport of Slovak Republic (No. VEGA 1/0560/15) and by project: RFBR 16-05-00622.

REFERENCES

Chovan M. et al. (2016): Acta Geol Slov 8:203–216.

Kubač A. et al. (2018): Min Petrol 1–27.

Paľyanova et al. (2011): Russian Geol Geophys 52:443–449.

Metallic phases in historical copper slags form Lower Silesia, Poland: An overview of diversity and weathering resistance

[1]Katarzyna Kądziołka[#]

[1] University of Wroclaw, Faculty of Earth Sciences and Environmental Management, Department of Geological Sciences, pl. Maksa Borna 9, 50-205 Wrocław, Poland
[#]katarzyna.kadziolka2@uwr.edu.pl

Key words: metallic phases, sulphides, copper slags, weathering resistance, historical metal smelting

INTRODUCTION

Slags, as a waste product of metal smelting, often comprise numerous metallic phases which usually are a basic reason of slag environmental threat. Upon weathering, many potentially toxic elements can be released and cause contamination in the area of storage. As such, metallic phases are most often considered in the matter of their environmental impact. Nevertheless, their strong differentiation within one slag sample or a single phase provides an interesting field for mineralogical considerations. This study considers preferred sulphide assemblages, their dependence on slag chemistry and phase composition, factors causing variability, as well as sulphides weathering resistance.

GEOLOGICAL AND HISTORICAL SETTING

Lower Silesia is located in south-western Poland, Europe. Leszczyna and Kondratów are two villages in Kaczawskie Foothills, south-eastern part of North-Sudetic Basin known also as an Old Copper Basin (Fig. 1). Copper deposits are genetically connected with those of New Copper Basin (Fore-Sudetic Monocline) in Poland where current copper exploitation is carried out. Deposits occur within Permian sedimentary rocks, mostly shales, marls, limestones and dolomites. The rocks had formed since Lower Permian until Cretaceous with recurrent Zechstein Sea transgressions and regressions as the studied area was on the edge of the maximal sea range. The main mineralisation appears in the Upper Permian shales and is related to the Zechstein Kupferschiefer formation (Sawlowicz 1992). Copper mineralisation is epigenetic and related to the activity of two brines with different chemical and physical parameters (Kucha and Pawlikowski 2006).

First attempts of mining and metal smelting in the area are dated back to the 13th century AD. Exploitation of copper ore shale and marl of Zechstein Kupferschiefer formation lasted for several centuries but until 18th (Kondratów) and 19th (Leszczyna) century was conducted only on a small scale. Production flourished with "Silent Luck" mine and smelter in Leszczyna and resulted in extensive slag discharge.

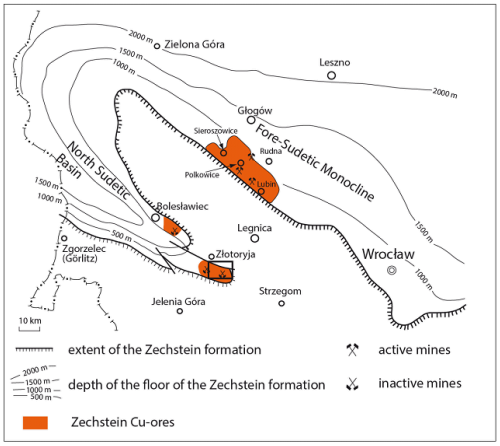

Fig. 1: North-Sudetic Basin and Fore-Sudetic Monocline (Stolarczyk et al. 2015).

METHODOLOGY

29 slag and 6 rock (ore) samples from two sites of historical copper smelting were chosen for this study. We conducted petrographic observations of slag texture and mineralogy, focusing mostly on metallic phases and their secondary transformations. The research was carried using polarizing microscopes: Leica

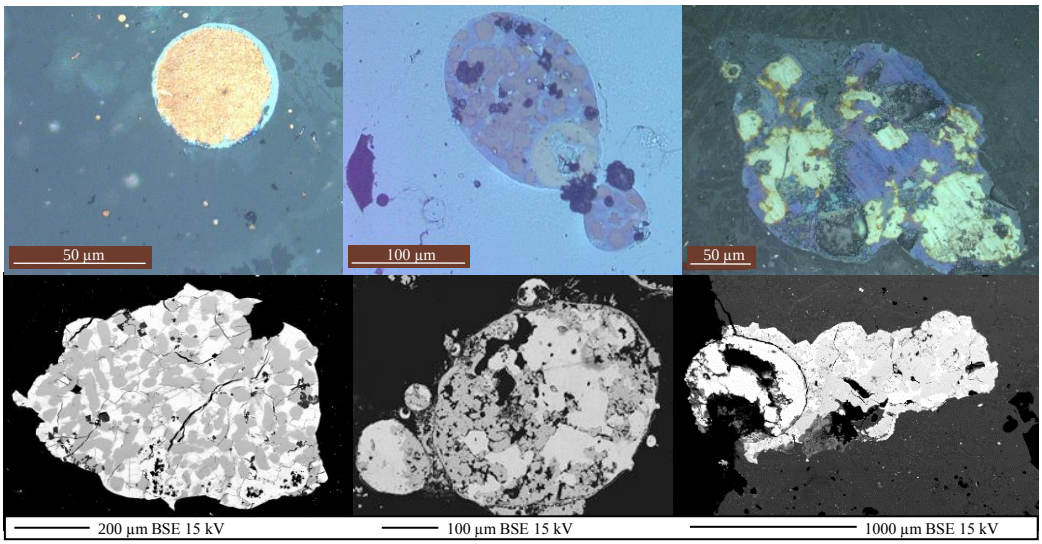

Fig. 2: Metallic phases in reflected light and SEM microphotographs. Strong diversity in shape, size and composition is noticeable. Top left: Cu droplet, bornite with digenite and chalcopyrite, secondary cuprite replacing chalcopyrite. Bottom left: multi-composition phase of bornite-pyrrhotite alloy, sulphide oxidation, iron droplet with continuous iron depletion (98-14 wt. %).

DM2500P and Zeiss Axiolab in transmitted and reflected light. Observations in greater magnifications were carried with JSM-IT100 Scanning Electron Microscope with Oxford Instruments x-act EDS. Phase chemical composition was determined using Cameca SX 100 electron microprobe. X-ray powder diffraction with Siemens D-5005 and Co X-ray source was also applied for confirming slag phase composition. Results were analysed with 2.0 PANalytical X'Pert HighScore with JCPDS PDF-2 database.

SLAGS PHASE AND CHEMICAL COMPOSITION

Two general textures were distinguished – glassy and crystalline slags. Within second type leucite, various clinopyroxenes and anorthite constitute the most common phases.
An average chemical composition is presented in Table 1. Slags are mainly composed of SiO_2 (42.5-49.8 wt. %), CaO (12.6-27.4 wt. %), Al_2O_3 (9.6-18.9 wt. %) with various amounts of Fe_2O_3 (2.3-23.1 wt. %). High K_2O (3.41-6.7 wt. %) content was also observed. Within metals, especially elevated amounts of Cu (0.15-4.4 wt. %) and Zn (52-1305 mg/kg) were recognised. Total sulphur content is low (0.05-1.12 wt. %) with 0.29 wt. % on average in all 29 samples.

METALLIC PHASES

The chemical composition of sulphides is dominated by S-Cu-Fe assemblage. Within broadly appearing primary phases bornite (29 %), Cu metal (22 %) pyrrhotite (17 wt. %), and chalcocite (10 %) were distinguished. Fe_4P (4.8 %), digenite (4%) and Fe metal (0.4 %) are less common but present in slags from both localities. Higher Fe content is usually associated with elevated P amount (circa 1 up to 11.8 wt. %). Zn appears in both metallic phases and glass but Mn and Mg content was detected only in the glass and crystalline phases and was not incorporated in the sulphides. Metallic phases appear in the general forms of (1) separated metal droplets (round, 1 up to 300 µm in diameter) composed of pure metal, usually Cu (also Fe and Pb) (Fig. 2), (2) sulphides in various shapes, sizes and compositions (commonly round or edgy, reaching up to over 1000 µm) tied up within

Table 1: Average chemical composition of slags from two localities

		wt. %								mg/kg			
	n samples	SiO_2	Al_2O_3	Fe_2O_3	MgO	CaO	Na_2O	K_2O	TiO_2	Co	Cu	Pb	Zn
Leszczyna	14	45.9	17.4	3.6	2.7	21.2	0.2	6.1	0.8	44.5	3733	53.7	249.6
Kondratów	15	47.0	13.2	11.6	2.3	18.2	0.2	4.8	0.6	95.6	12074	66.0	392.6

matte droplets and (3) small, a few micrometer inclusions concentrating in glass between the phases of crystalline samples. No significant chemical difference between sulphides from crystalline and amorphous slag was observed, but within the amorphous type almost only separated, round metal droplets are present.
With BSE imaging strong differentiation within phases is observable. Heterogeneous composition of three different minerals (pyrrhotite – bornite - Cu metal) can be discovered within numerous phases (Fig. 3) and appears in chaotic distribution or gradual replacement. This variation is most probably a result of high susceptibility to re-equilibration during slag cooling. During the transition from the above- to below-solvus conditions Cu and Fe are distributed accordingly to structural metal vacancies that differ strongly in the mentioned minerals leading to the phase inhomogeneity. With following cooling, exsolution texture appears on a various scale (Grguric and Putnis 1999).

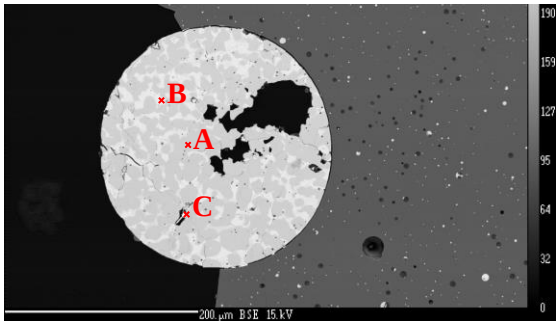

Fig. 3: Mixed pyrrhotite-bornite-Cu metal texture

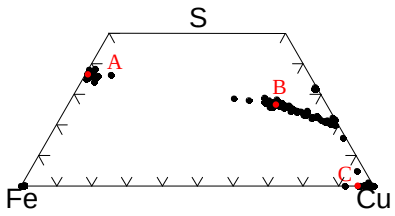

Fig. 4: The chemical composition of sulphides, metallic droplets and metallic inclusions. Diagram based on 201 EMPA analysis with highlighted A, B and C points.

Response to weathering processes vary with different chemical composition and slag texture. Phases tied up within glassy slag leach less metallic elements compared to the crystalline slags according to performed laboratory experiments. Reactivity is elevated on the surface of the thin sections where continuous weathering occurs but within phases is usually limited to cracks and vines. Cu droplets present strongest signs of oxidation and are partially replaced with secondary cuprite.

CONCLUSIONS

Slags of similar chemical composition contain various metallic phases. Cu metal and sulphides with high Cu amount are most common (bornite, pyrrhotite, chalcocite) and frequently are non-homogenous within one grain (Fig. 3). We observed that the slag texture does not influence the metal phase composition but different type of cooling might cause different appearance of a sulphide and different weathering susceptibility.

Acknowledgement: I would like to thank my co-workers, especially prof. Jakub Kierczak for scientific advisement and guidance with SEM observations. Tomasz Stolarczyk is acknowledged for his archaeological impact as well as prof. Jacek Puziewicz for allowing to use the laboratory and microscopes. I would like to also thank prof. Juraj Majzlan for revising and improving this text.

This research was supported by Polish Ministry of Sciences and Higher Education within grant: Diamond (Diamentowy) Grant (decision: DI2015 023345).

REFERENCES

Kucha H. and Pawlikowski M. (2010): Geologia 36:513–538.
Grguric B.A. and Putnis A. (1999): Min Mag 63:1–12.
Sawlowicz Z. (1992): Applied Earth Sci 101:B1–B8.
Stolarczyk T. et al. (2015): Fund Archeolog Archeo, Radziechów.

First results of the archaeometrical investigation of Neolithic amphibolite polished stone tools from Herman Ottó Museum (Miskolc, Hungary)

[1]Erika Kereskényi[#], [2]György Szakmány, [1]Béla Fehér and [3]Zsolt Kasztovszky

[1] Herman Ottó Museum, Department of Mineralogy, Kossuth street 13, 3525 Miskolc, Hungary
[#]kereskenyierika@yahoo.com
[2] Eötvös Loránd University, Department of Petrology and Geochemistry, Pázmány Péter street 1/A, 1117 Budapest, Hungary
[3] Centre for Energy Research, Hungarian Academy of Sciences, Konkoly Thege M. street 29-33. 1121 Budapest, Hungary

Key words: amphibolite, polished stone tools, archaeometry

Approximately 500 Neolithic polished stone tools, representing various lithotypes, are possessed by Herman Ottó Museum. Recently 12 stone axes coming from different localities of Borsod-Abaúj-Zemplén County are proved to be amphibolite by EDS/SEM. Macroscopically the axes are fine-grained, compact textured, the most of the retrograde amphibolite axes are foliated. Their colours are grey, greyish black and dark brown. Green and brown patches and bands can be recognized on their surfaces by naked eye. The mean value of magnetic susceptibility is 8.82×10^{-3} SI. Regarding their archaeological typology most of them are flat axes, two tools have shoe-last form and one axe is shaft hole-drilled.

Amphiboles were named following the classification of Hawthorne et al. (2012). Fe^{3+}/Fe^{2+} ratio was calculated with the ACES Excel spreadsheet (Locock, 2014). Two groups were distinguished by the chemical composition of amphiboles and feldspars and their textural positions.

1. Prograde amphibolite stone tools

Magnesio-hornblende is contained in all six samples. In 53.160.11 and D08 samples magnesio-ferri-hornblende is also recorded. In 53.160.11 sample pargasite is detected on the edge of magnesio-hornblende. In 53.160.150 sample magnesio-hornblende is recorded on the edge of actinolite. In D06 sample on the edge of actinolite winchite is detected, furthermore on the edge of magnesio-hornblende ferri-winchite can be studied. In D08 sample the prograde metamorphosis is shown by the appearance of ferri-tschermakite and ferro-ferri-tschermakite. In B12 sample pargasite and ferro-pargasite is detected on the edge of sadanagaite and actinolite. Sadanagaite and ferrosadanagaite are detected on the edge of actinolite only in B12 sample.

2. Retrograde amphibolite stone tools

The elongated magnesio-hornblende is contained in all six samples. Actinolite typically situated on the edge of magnesio-hornblende referring to retrograde metamorphism. In the B05 sample besides actinolite, ferri-actinolite is also observed. Potassic-feldspar is detected in the B04, B05 and D09 retrograde samples.

Plagioclases show various chemical composition from albite to bytownite in each type of amphibolites. Bulk elemental composition of 5 polished stone tools has been determined by prompt-gamma activation analysis (PGAA). Representing data on TAS diagram: 2 samples plot in the basaltic andesite field while the other samples meet trachybasalt, basaltic trachyandesite and basalt fields referring to the protoliths.

Presently the possible provenience of amphibolite raw materials has not been located since there are numerous occurrences around the Carpathian Basin (e.g. Little Carpathians, Danube-, Váh-, Nitra-riverbeds; sporadically in Gemericum, Veporicum, Slovakia; Transylvanian Mid-Mountains, Romania; Kutná Horá, Jihlava-riverbed; Czech Republic) (Přichystal 2013).

REFERENCES

Hawthorne F.C. et al. (2012): Am Min 97:2031–2048.

Locock A. (2014): Comp Sci 62:1–11.

Přichystal A. (2013): Lithic raw materials in prehistoric times of Eastern Central Europe. Masaryk University.

Joint 5th Central-European Mineralogical Conference and
7th Mineral Sciences in the Carpathians Conference
Banská Štiavnica 2018

Tourmaline evolution in the Nedvědice orthogneiss, Svratka Unit, Bohemian Massif

[1]Ján Kliština[#] and [1]Jan Cempírek

[1] Masaryk University, Faculty of Science, Department of Geological Science, Kotlářská 2, CZ-611 37, Czech Republic [#]jan.klistinec@gmail.com

Key words: orthogneiss, tourmaline, metamorphic overprint, hydrothermal veins, chemical composition.

The studied area is located near Nedvědice, west Moravia (Bohemian massif, Czech Republic), in the southern part of the Svratka Unit near its border with the Polička crystalline complex and the Moravian Dome. Typical rocks for this region are medium- to coarse-grained mica schist, two mica paragneiss, migmatites, F-,Sn-,B-rich orthogneiss, amphibolites, rare marbles, Fe-skarns, and tourmalinites (Novák et al. 1998; Čopjaková et al. 2009). Tourmaline is common in the area.

The Nedvědice orthogneiss is characterized by high contents of F, and B_2O_3, manifested by the presence of F-rich muscovite, F-rich tourmaline, and rare fluorite-tourmaline layers. Tourmaline forms subhedral grains in the orthogneiss up to 3,5 cm long prismatic crystals in muscovite and fluorite-tourmaline layers in the orthogneiss. Tourmaline is also present as fine-grained layers in the muscovite layers. Novák et al. (1998) ascribed origin of the orthogneiss schorl assemblage to crystallization from a highly evolved B- and F-rich granitic melt; heterogeneous schorl-dravite from mica schist with high F-content probably formed by reaction of metapelite envelope with B-, F-rich fluids released from the granite. Novák et al. (1998) reported that medium-grade regional metamorphism probably did not change the primary composition of the tourmaline.

In our study, two types of tourmaline zoning were distinguished in the four types of studied rocks. More common type with Fe-rich cores, present in migmatitic orthogneiss and mica layers, is a multi-generation tourmaline with brecciated and corroded pre-metamorphic fluor-schorl core (enriched in Na, OH and Fe, and poor in X-site vacancy and Ca) and fluor-dravite to fluor-schorl rims with slightly higher Ca and enriched in F and Mg compared to the tourmaline core. On the other hand, the tourmaline found in the fluorite and coarse-grained quartz + tourmaline layer has Mg-rich pre-metamorphic core. The core is dominated by Na, enriched in F and has Mg/Fe around 1 (fluor-dravite – fluor-schorl), whereas the crystal rims (fluor-schorl) are enriched in Fe and also slightly in OH.

So far, our results show a significant change of tourmaline composition during metamorphic recrystallization and confirm earlier analytical results except high K_2O contents in Tur cores.

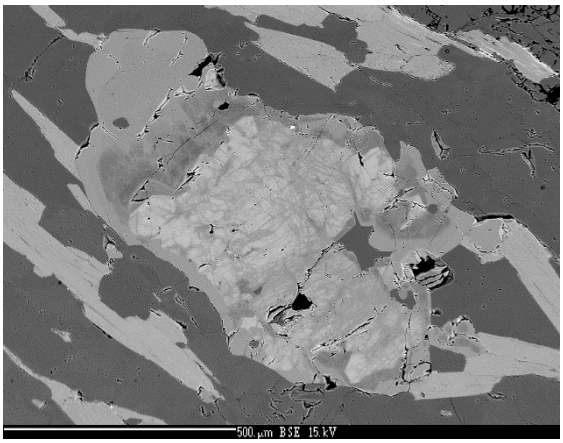

Fig. 1: Zoned grain of tourmaline, with bright magmatic core and grey metamorphic rims.

Acknowledgment: This work was supported by the Masaryk University grant MUNI/A/1088/2017.

References

Novák M. et al. (1998): J Geosci 43:37–44.

Čopjaková R. et al. (2009): J Geosci 54:221–243.

Joint 5th Central-European Mineralogical Conference and
7th Mineral Sciences in the Carpathians Conference
Banská Štiavnica 2018

Microbial sulfidogenesis of As in wetlands

[1]Magdaléna Knappová[#], [1]Petr Drahota, [2]Vít Penížek, [3]Mariana Klementová, [4]František Veselovský and [5]Martin Racek

[1] Charles University, Faculty of Science, Institute of Geochemistry, Mineralogy and Mineral Resources, Albertov 6, 128 43 Prague 2, Czech Republic, [#]magda.pp@volny.cz
[2] Department of Soil Science and Soil Protection, Faculty of Agrobiology, Food and Natural Resources, Czech University of Life Sciences Prague, Kamýcka 129, Praha 6, Czech Republic
[3] Institute of Inorganic Chemistry of the CAS, v.v.i., 250 68 Husinec-Řež, Czech Republic
[4] Czech Geological Survey, Geologická 6, 152 00 Prague 2, Czech Republic
[5] Charles University, Faculty of Science, Institute of Petrology and Structural Geology, Albertov 6, 128 43 Prague 2, Czech Republic

Key words: wetland soil, arsenic, realgar, framboidal pyrite, microbes

Wetland soils have been recognized as important sinks for As; yet the sources and immobilization mechanisms of As often vary in these environments. Here, we examine Fe-As-S mineralization in naturally As-enriched wetland soils located at Smolotely (Czech Republic). In our previous study (Drahota et al., 2018), we identified an interesting assemblage of As-hosted phases in oxic soils (As-bearing Fe (hydr)oxides, arseniosiderite, bariopharmacosiderite, yukonite); however, dominant As solid-speciation in the slightly reducing wetland soil remained unrevealed for us.

Herein, we characterised two wetland soil profiles by geochemical (bulk soil, pore water, selective chemical extractions), mineralogical (XRD, TEM, SEM/EDX) and S isotope analyses to determine the distribution and speciation of As as a function of soil depth.

Mineralogical research of the oxic zone of wetland soil profiles (<30 cm) revealed that As is mostly sequestered by Fe (hydr)oxides (up to 10 wt.% of As). Bulk-soil analyses show significant correlation between contents of As, S and TOC in anoxic zone of the profiles (>70 cm), caused by strong accumulation of As (19.3 wt.%), Fe (4.7 wt.%) and S (11.9 wt.%) in most fragments of buried natural organic matter (NOM). Detailed mineralogical investigations of these NOM fragments revealed assemblage of nanocrystalline realgar (As_4S_4), As-bearing framboidal pyrite (~1 wt.% of As), and As-bearing Fe monosulphide (~2 wt.% of As). It should be also noted that trace amounts of As-bearing Fe (hydr)oxides have been also detected in the anoxic zone of the soil, with association of As-bearing sulphides.

Based on preliminary results of S isotope study As-bearing sulphides are depleted in the $\delta^{34}S$ by 11.6 ‰ relative to aqueous sulphate supplied to the soil, implying biologically induced formation of the sulphide phases.

We propose that the realgar and As-bearing Fe sulphides were generated by in-situ microbial reduction of aqueous sulphate in the strongly reducing microenvironments. The sulphides are associated with particulate organic matter probably acting as a C source for sulphate reducers. The formation of realgar has been identified a prominent As sequestration pathway in the naturally As-enriched wetland at the Smolotely geochemical anomaly.

Acknowledgment: This study has been supported by Grant GACR 16-09352S from the Czech Science Foundation and Center for Geosphere Dynamics (UNCE/SCI/006).

REFERENCES

Drahota P. et al. (2018): Appl Geochem 89:243–254.

Joint 5th Central-European Mineralogical Conference and
7th Mineral Sciences in the Carpathians Conference

Characteristics and metallogeny of epithermal mineralisation in the Central Slovakia Volcanic Field

[1]Peter Koděra[#] and [2]Jaroslav Lexa

[1] Comenius University, Faculty of Natural Sciences, Department of Geology of Mineral Deposits, Ilkovičova 6, 842 15 Bratislava, Slovakia [#]kodera1@uniba.sk
[2] Earth Science Institute of the Slovak Academy of Sciences, Dúbravská cesta 9, 840 05 Bratislava, Slovakia

Key words: epithermal vein, mineralogy, metallogeny, gold, silver

INTRODUCTION

The Central Slovakia Volcanic Field hosts famous mining regions with historical and recent exploitation of precious metal epithermal ores, including Banská Štiavnica and Kremnica deposits. The major ore districts in this field are hosted by large Neogene andesite stratovolcanoes, involving extensive subvolcanic intrusive complexes and complexes of differentiated rocks, as well as volcanotectonic depressions and resurgent horsts, related to back-arc extension processes. There occur three separate ore districts: Banská Štiavnica – Hodruša ore district in the central zone of the Štiavnica stratovolcano, Nová Baňa – Pukanec and Prochoť districts in the western flanks of the Štiavnica stratovolcano, and the Kremnica district in the Kremnické vrchy Mts. Each of these districts contains various vein systems with different characteristics, including base and precious metals contents, Au-Ag ratio and sulfidation state ranging from intermediate to low sulfidation types (Table 1). During the recent years, a significant progress was achieved in understanding of mineralogy and genesis of these epithermal systems, including their link to geological and tectonic evolution of the hosting stratovolcanoes and volcano-tectonic fault systems. This contribution aims to summarise the current level of knowledge.

CENTRAL ZONE OF THE ŠTIAVNICA STRATOVOLCANO

The largest Banská Štiavnica-Hodruša district is hosted by a major resurgent horst in the caldera centre of the Štiavnica stratovolcano and contains four distinct vein systems.

The earliest vein system (~13.0 Ma) consists of precious and base metal veins of intermediate sulfidation type, currently mined at the Rozália mine in Hodruša. This deposit represents an unusual subhorizontal multi-stage vein system, related to processes of underground cauldron subsidence and a quick exhumation of a subvolcanic granodiorite pluton. Veins are developed in a low-angle normal shear zone (LANF), possibly representing base of a sector collapse of the hosting stratovolcano. The subhorizontal vein system occurs in 400–650 m depth, near to the flat roof of the pre-mineralisation subvolcanic granodiorite pluton. The deposit consists of two parts, separated by a thick sill of post-mineralisation quartz-diorite porphyry. The epithermal vein mineralization developed during 5 stages, while the major productive stage corresponds to a stockwork with quartz, rhodonite, rhodochrosite, sphalerite, galena, chalcopyrite, gold and rare Ag-Au tellurides. The ore mineralisation has a high Au:Ag ratio (1:1 to 1:10) and it is accompanied by strong adularisation, while illite dominates along the upper plane of the shear zone. Palaeofluids were of low salinity (~1-3 wt% NaCl eq,) and high to moderate temperature (~250–310°C) and have experienced boiling. The magmatic component in the fluids came from a shallow, differentiated andesitic magma chamber, which was later also responsible for the emplacement of quartz-diorite porphyries.

The later three extensive vein systems of low to intermediate sulfidation types correspond to hydrothermal activity during the long-lasting uplift of the resurgent horst in the centre of the caldera (12.0-10.7 Ma). They are localized at steep extension faults of the horst,

related to NW-SE extension of the regional stress field and rhyolite volcanic activity. Veins occur in a zonal arrangement: sulphide-rich base metal veins in the east/central part of the horst (Banská Štiavnica area), Ag-rich veins in the central/western part of the horst (Hodruša area) and Au-Ag veins hosted by marginal faults of the horst (Banská Belá, Kopanice, Vyhne). The central Ag-rich and sulphide-rich veins are probably the oldest veins, while the marginal Au-Ag veins are the youngest. Vein systems show a large variability in mineral content with numerous stages and substages and Au:Ag ratios (1:1 to 1:100, see details in Table 1). Fluid properties have generally changed from more saline (>10 wt% NaCl eq.) and rather hot (>300°C) towards less saline (<3 wt% NaCl eq.) and moderate temperate (<260°C) with evidence for boiling and mixing. The zonal arrangement of vein systems probably results from continuous, long-lasting uplift of the horst with subsequent transfer of hydrothermal activity from the centre to the margins of the horst, accompanied by changing metal-endowment of hydrothermal fluids corresponding to evolution of the parental magma chamber. Very different vertical extent of the individual vein systems (central sulphide-rich <1000 m, Ag-rich 200 – 500 m, marginal Au-Ag < 300 m) with only a sparse presence of base metals in deepest parts of the Ag-rich and Au-rich vein systems indicate, that differences in erosion level of the vein systems had only a minor influence on the zonal arrangement of veins observed today.

WESTERN FLANKS OF THE ŠTIAVNICA STRATOVOLCANO

The Prochot district is located about 10 km NW from the margin of the central zone of the Štiavnica stratovolcano. This small gold-rich vein system of intermediate to low sulphidation type is hosted by a steep regional NW-SE trending fault, accompanied by extensive brecciation and alteration in zonal arrangement (distal steam-heated and proximal adularia-rich zones). Quartz-carbonate veins with native gold, tetrahedrite and pyrite have high Au:Ag ratio (1:1 to 1:10). The vein system evolved during the pre-caldera stage of the stratovolcano, i.e. it is similar in age to the Rozália mine precious and base metal deposit. The source of ore-bearing fluids was related either to the magma chamber below the central zone of the stratovolcano or to a local dioritic magma chamber below the Prochot Intrusive Complex.

The Nová Baňa - Pukanec ore district includes three small vein systems of low- to intermediate sulfidation type, located on local horsts: Nová Baňa, Pukanec and Rudno nad Hronom – Brehy. The vein systems occur on steep N-S oriented faults that gradually divide local horst from the relatively subsided parts in their vicinity. Some of these faults were also used for emplacement of the late stage rhyolite bodies. All of these systems are rich in precious metals (especially electrum and Ag-sulphosalts) with variable Au:Ag ratios (1:10 to 1:70), minor base metal sulphides in quartz or quartz-carbonate gangue. Specifically, Pukanec is rich in Mn-bearing minerals (rhodochrosite, Mn-carbonates and their weathering products). Fluids had similar properties as the horst-related Ag-rich and Au-Ag veins in the central zone of the Štiavnica stratovolcano (<5 wt% NaCl eq., <260°C), and have experienced boiling.

KREMNICKÉ VRCHY MTS.

The Kremnica ore district is located in the northern part of the Central Slovakia Volcanic Field. It is situated at centre of the Kremnica graben, on eastern marginal faults of a major resurgent horst, which uplift was contemporaneous with the epithermal system and rhyolite volcanism (12.1 – 11.1 Ma). The mostly N-S trending system of faults corresponds to the regional stress field with a strong NW-SE extension. The extensive system of epithermal gold veins of low sulfidation type consist of "1st vein system", hosted by a major transtension fault and complementary anthitetic veins, and "2nd vein system", located in the hanging wall of the major fault. The epithermal veins mostly contain electrum, gold, pyrite or marcasite in quartz gangue, while the Au:Ag ratio is about 1:10). Fluids were of low salinity (<2 wt% NaCl eq.), with apparent decrease in temperature along the system from N to S (270–140°C), which is related to a decrease in erosion level from c. 500 m to c. 50 m.

CONCLUSIONS

The early vein systems in the Central Slovakia Volcanic Field are closely related to a

Table 1. Basic characteristics of epithermal vein mineralization in the Central Slovakia Volcanic Field. Ages of volcanic rocks and mineralisation are from Lexa and Pécskay (2010, 2013), Chernyshev et al. (2013), and from unpublished data (Pukanec and Rudno nad Hronom).

Regional setting	**Central zone of the Štiavnica stratovolcano – major resurgent horst**				**Western flanks of the Štiavnica stratovolcano**				**Kremnické vrchy Mts**
Ore district	**Banská Štiavnica – Hodruša**				**Prochot**	**Nová Baňa – Pukanec**			**Kremnica**
Deposit or vein system	**Rozália mine**	**Banská Štiavnica**	**Hodruša**	**Banská Belá, Kopanice, Vyhne**	**Prochot-Lazy**	**Nová Baňa**	**Pukanec**	**Rudno nad Hronom, Brehy**	**Kremnica**
Location	W central part - underground only	E, SE and central part of the horst	Central, W, NW parts of the horst	Marginal parts of the horst (E, W, S)	NW of the central zone	Local horst WSW of the central zone	Local horst, SW of the central zone	Local horst, SW of the central zone	Major resurgent horst
Main metals	Au-Ag-Pb-Zn-Cu	Pb-Zn-Cu ± Au-Ag	Ag ± Au-Pb-Zn	Au-Ag ± Pb-Zn-Cu	Au-Ag	Au-Ag ± Pb-Zn-Cu	Au-Ag ± Pb-Zn-Cu	Au-Ag ± Pb-Zn-Cu	Au-Ag ± Pb-Zn-Cu
Genetically related volcanics, their age	Qtz-diorite porphyry, 13.1 – 12.7 Ma	Rhyolite, 12.2 – 11.4 Ma	Rhyolite, 12.2 – 11.4 Ma	Rhyolite, 12.2 – 11.4 Ma	Diorite?, 13.5–12.7 Ma	Rhyolite, 12.3 – 12.0 Ma	Rhyolite, ~12.6 Ma	Rhyolite, ~12.6 Ma	Rhyolite 12.4 – 11.6 Ma
Age of mineralisation	~13.0 Ma	12.0 – 10.7 Ma	12.0 – 10.7 Ma	12.0 – 10.7 Ma	Not defined	12.1 – 11.8 Ma	~12.0 – 11.8 Ma	~12.0 – 11.8 Ma	12.1 – 11.1 Ma
Sulfidation state	Intermediate	Intermediate	Interm. to low	Low	Interm. to low	Interm. to low	Interm. to low	Interm. to low	Low
Major ore minerals	Gold, El, Sph, Ga, Ccp, Ag-Au tellurides	Ga, Sph, Ccp, Py ± Ac, Ag, Ag-sulfosalts, El	Prg-Prs, Pol-Prc, Ste ± El, Ag, Ga, Sph, Ccp, Py	Ag-sulfosalts, El ± Ag, Ccp, Ga, Sph, Py/Mc	Gold, Ttd, Py	El, Ag-Ttd, Ac, Pol-Prc, Prg-Prs ± Ag, Py, Sph, Ga	El, Ag-sulfosalts, Ga, Sph, Ccp	Ag-sulfosalts, El ± Ga, Sph, Ccp	El, Gold, Py/Mc, Asp ± Sph, Ga, Ccp, Ttd, Prs, Prg, Pol-Prc, Ag-sufosalts
Major gangue minerals	Qtz, Mn-Car, Rhd	Qtz, Mn-Car, Rhd	Car, Qtz	Qtz, Car	Qtz, Car (incl. Mn)	Qtz	Qtz, Mn-Car, Rhd	Qtz, Car	Qtz
Ag-Au ratio of ores	1:1 to 10:1	10:1 to 20:1	100:1	1:1 to 10:1	1:1 to 6:1	10:1 to 70 :1	30:1	40:1	10:1
Alteration	Illite, Ad, Qtz	Illite, Qtz, Ad	Illite, I/S, Ad, Qtz	Qtz, Ad, I, I-S	Qtz, Ad, Py	Qtz, Ad, I-S	Qtz, Ser, Ad	Ad	Illite, I-S, Ad
Fluids properties (salinity in NaCl eq.)	< 3 wt% 280-330 °C boiling	< 11 wt% <100-380 °C, mixing, boiling	< 6 wt% 200-300 °C boiling	< 3 wt% 220-260 °C boiling	Not defined	< 5 wt% 190-260 ºC, boiling	< 3 wt% 200-260 °C	Not defined	< 2 wt% 150-260 °C boiling
Main references	Maťo et al. 1996, Koděra et al. 2005; Kubač et al. 2018	Koděra 1963; Kovalenker et al. 1991, 2006	Onačila et al. 1993; Majzlan 2009, Majzlan et al. 2016	Lexa et al. 1997; Berkh et al. 2014	Koděra et al. 2016	Lexa et al. 2000; Majzlan et al. 2018	Bahna and Chovan 2001; Lexa and Smolka 2002	Lexa and Smolka 2002	Böhmer 1966; Maťo 1997; Koděra et al. 2014

Mineral abbreviations: El = electrum, Ag = native silver, Sph = sphalerite, Ga = galena, Ccp = chalcopyrite, Py = pyrite, Mc = marcasite, Asp = arsenopyrite, Ttd = tetrahedrite, Ac = acanthite, Pol = polybasite, Prc = pearceite, Prg = pyrargyrite, Prs = proustite, Ste = stephanite, Qtz = quartz, Car = carbonate, Rhd = rodonite, I-S = illite-smectite, Ad = adularia, Ser = sericite

low-angle normal shear zone (Rozália mine) or a regional fault (Prochot), with the source of magmatic component in the fluid coming from the andesitic/dioritic magma chamber(s).

The later vein systems are controlled by the horst-graben extension tectonics and rhyolite volcanic activity that was predominantly related to crustal anatexis. Similar ages of rhyolite volcanism in the entire volcanic field indicate a common, spatially extensive source of rhyolite magma. During this long-lasting stage, the vein systems changed from early intermediate sulfidation sulphide-rich towards low sulfidation gold-rich, most likely due to evolution of the parental magma chamber and increasing meteoric water component in the hydrothermal fluids.

Acknowledgments: This study was supported by the Slovak Research and Development Agency, contract No. 15-0083 and by the VEGA grant 1/0560/1.

REFERENCES

Bahna B. and Chovan M. (2001): Geolines 13:11–17.

Berkh K. et al. (2014): Neues Jb Min Abh 191:237–256.

Böhmer M. (1966): Acta Geol Geogr Univ Comen 11:5–123.

Chernyshev I.V. et al. (2013): Geol Carpath 64:327–351.

Koděra P. et al. (2005): Min Deposita 39:921–943.

Koděra, M. (1963): Geol Surv Czech Rep, Prague 1:184–189 (In German).

Koděra P. et al. M. (2016): AGEOS 8:149–163.

Koděra P. et al. (2014): In: Garofalo P.S. & Ridley J.R. (eds) Geolog Soc, London, Spec Publ 402:177–206.

Lexa J. and Pécskay Z. (2010): In: Kohút M. (ed) Dating 2010: State Geol Inst D Štúr, 21–22.

Lexa J. and Pecskay Z. (2013): Abstracts book Geol evol W Carpathians. Geol Inst Slovak Acad Scien, Bratislava, 80–81.

Kovalenker V.A. (1991): Geol Carpath 42:291–302.

Kovalenker V.A. (2006): Geochem Int 44:118–136.

Kubač, A. (2018): Min Petrol https://doi.org/10.1007/s00710-018-0558-y

Lexa J. and Smolka J. (2002): Archive State Geol Inst D Štúr, Bratislava (In Slovak).

Lexa J. et al. (1997): Open file report, Archive State Geol Inst D Štúr, Bratislava (in Slovak).

Lexa J. et al. (2000): Open file report, Archive State Geol Inst D Štúr, Bratislava (In Slovak).

Majzlan J. (2009): Min Slov 41:45–54.

Majzlan J. et al. (2016): AGEOS 8:199–213.

Majzlan, J. et al. (2018): Min Petrol 112:1–23.

Maťo Ľ. (1997): Open file report, Archive State Geol Inst D Štúr, Bratislava (In Slovak).

Maťo Ľ. Et al. (1996): Min Slov 28:455–490 (In Slovak).

Onačila D. et al. (1993): Open file report, Archive State Geol Inst D Štúr (In Slovak).

Joint 5th Central-European Mineralogical Conference and
7th Mineral Sciences in the Carpathians Conference

The mineralogy and petrology of the Carpathian obsidians

[1]Milan Kohút [#], [2]Viera Kollárová, [3]Tomáš Mikuš, [2]Patrik Konečný, [3]Juraj Šurka, [3]Stanislava Milovská, [2]Ivan Holický and [4]Pavel Bačo

[1] Earth Science Institute, Slovak Academy of Sciences, Dúbravská cesta 9, 840 05 Bratislava, Slovakia [#]milan.kohut@savba.sk
[2] Dionýz Štúr State Institute of Geology, Mlynská dolina 1, 817 04 Bratislava, Slovakia
[3] Earth Science Institute, Slovak Academy of Sciences, Ďumbierska 1, 974 01 Banská Bystrica, SK
[4] Dionýz Štúr State Institute of Geology, Jesenského 8, 040 01 Košice, Slovakia

Key words: Carpathians obsidian, mineralogy, geochemistry, provenance, genesis

INTRODUCTION

Obsidian is quickly solidified (quenched) igneous – volcanic rock, originated mainly from the acid rhyolitic (rarely basic basaltic) melt, often referred to as "natural glass" with typical glassy lustre and usually dark jet-black, grey or brown colour. Generally, it is dominantly composed of amorphous, dark (opaque) volcanic glass (≥ 95 volume %), with addition of various minerals like biotite, plagioclase, alkali feldspar, quartz, pyroxenes, amphibole, magnetite, Fe-Ti oxides, pyrrhotite, pyrite, olivine, zircon, apatite, monazite, uraninite, ilmenite, and garnet. Obsidian was widely used for tool-making (stone industry) during prehistoric times, and played significant role in the humanity evolution and civilization. Volcanic glass was geologically known since the end of the 18th Century, and it was archeologically documented in the 19th Century in the Zemplín – Tokaj area (on the both sides of present boundary between SE Slovakia and NE Hungary), the only natural volcanic glass region in Central Europe (see review: Biró 2006).

GEOLOGICAL SETTING

The Carpathian obsidians from the studied Zemplín-Tokaj area belong to the Eastern Slovakian Neovolcanic Field (ESNF) in the SE Slovakia/NE Hungary, where the isolated Sarmatian volcanoes penetrate the Miocene strata and pre-Cainozoic basement. Geological setting of the Zemplínske vrchy Mts. (ZVM) and their surrounding is complicated. It includes the evolution from the Paleozoic up to recent. The ZVM form typical tectonic horst surrounded by the East Slovakian Basin with several elevated volcanic bodies. Present architecture is a consequence of the back-arc extension, associated with the asthenosphere updoming accompanied by calc-alkaline volcanism and pull-apart opening during the Miocene, followed by the Pannonian to Quaternary late stage regional uplift and erosion. The Paleozoic basement rock sequences encompass various sedimentary and volcanic rocks of the Carboniferous to Permian age, whereas the high-grade metamorphic rocks (gneisses, amphibolites, and metagranites) can be found in deeper horizon. The Mesozoic cover is composed of conglomerates, sandstones, calcareous shales, dolomites, rarely with the evaporate intercalations of the Lower Triassic in age. The Middle Triassic is formed mainly by carbonates (limestones and dolomites). The oldest Cainozoic sediments in the studied area are the Lower Miocene – Karpatian in age (claystones and of sandstones), followed by the Badenian basal conglomerates, sandstones, and grey calcareous claystones, that were overlaid by extrusive rhyodacite lava flow bodies and their tuffites and tuffs of the Upper Badenian age. The Lower – Middle Sarmatian rhyolite tuffs and tuffites are intercalated by clays and sandy claystones. The Middle – Upper Sarmatian rhyolite volcanism is represented by the dyke bodies, and an extrusion body with associated volcanoclastics in the Viničky broader area. The margins of the bodies are formed by perlitized obsidian, often in breccia development. The Upper Sarmatian is formed by calcareous sands and sandstones with interbeds of clays, tuffitic clays and tuffites.

The sequence finished by the Pannonian lacustrine and river clays, silts with intercalations of sands, river gravels (Kobulský et al. 2011).

MINERALOGY

Although the obsidians are dominated by the amorphous volcanic glass an important role play the rock-forming and accessory minerals from genetic point of view. The Carpathian obsidians consist of a broad association of minerals like plagioclase, biotite, alkali feldspar, quartz, pyroxenes, amphiboles, magnetite, Fe-Ti oxides, pyrrhotite, pyrite, olivine, zircon, apatite, monazite, uraninite, ilmenite, and garnet that are observable mainly under the microscope. These minerals can be present in the form of phenocrysts (having size 100 ~ 1000 μm), microlites (10 ~ 50 μm), and hair like trichites. Beside the autolithic origin of these minerals, sporadic xenoliths from the source and/or assimilated rocks can be also present. Commonly observed banded texture or alternation of dark and pale stripes is caused by minute microlites and trichites oriented in the direction of the melt flow. Although, the majority of described minerals have the primary magmatic origin, not all of them reflect their crystallization from a parent rhyolite melt. Plagioclases – most of the grains are subhedral microlites, although the phenocrysts in the size up to 450 μm are present locally as well. Generally, they are zoned with broad chemical composition (andesine – bytownite An_{33-89}) in the cores, whereas more acid oligoclase (An_{19-31}) and scarcely albite compositions were identified in the rime. K-fs's – are less frequent than Pl; sporadic anhedral grains up to 100 μm are mainly anortoclases, while high-temperature sanidines were found as well as. Biotites – form mainly larger laths 100 ~ 850 μm in size, and/or smaller oval/anhedral flakes having brown pleochroic colour. Typical primary magmatic Fe-biotites have annite composition with $mg^{\#}$ = 0.32 ~ 0.43 and/or high TiO_2 content 3.2 ~ 4.6 wt. % indicating high-temperature origin. Elevated Fe content together with moderate Mg and Al contents show their peraluminous character influenced partly by calc-alkaline source. Generally, the low Fe^{3+} (ca 7 % from FeO^t) suggests for their crystallization at QFM buffer. Pyroxenes – form essentially euhedral and subhedral microlites and trichites, and locally anhedral grains in aggregates. Commonly, all of them belong to Ca-Fe-Mg group of pyroxenes. Pyroxenes are dominantly orthopyroxenes; clinopyroxenes are rare. Opx's are of enstatite compositon ($mg^{\#}$ = 0.55 ~ 0.76), some of them have pigeonite and ferrosilite composition ($mg^{\#}$ = 0.29 ~ 0.35). Cpx's have augitic composition ($mg^{\#}$ = 0.60 ~ 0.68). Amphiboles – were identified as subhedral microlites, and/or anhedral grains in aggregates. They fit in to Mg-Fe-Mn group of amphiboles of grunerite and/or commingtonite composition ($Si_{(apfu)}$ = 7.02 ~ 7.64; and $Mg^{\#}$ = 0.31 ~ 0.58). Magnetite – form mostly small anhedral grains and trichites, and/or subhedral/anhedral xenocrystic grains up to 45 μm with typical ilmenite lamellas in a few cases. Olivines – were locally found with pyroxene in xenocrystic aggregates as anhedral grains 5 ~ 100 μm of forsterite composition ($mg^{\#}$ = 0.55 ~ 0.68, and $fe^{\#}$ = 0.32 ~ 0.49), having tholeiitic character. Zircon – form euhedral quadrate and prismatic grains 10 ~ 50 μm in size with low HfO_2 = 1.33 ~ 1.88 wt. % and low Th/U = 0.11 ~ 0.46 distinctive for felsic fractionated igneous rocks. Apatites – form mainly euhedral and subhedral prismatic microlites in size of 20 ~ 55 μm. Typical fluor-apatites with increased fluorine content F = 2.02 ~ 4.41 wt. % indicate igneous origin from fractionated melt. Monazites – were commonly found as subhedral grains 15 ~ 100 μm in size and/or oval grains with sign of magmatic corrosion. Studied monazites are commonly enriched in Th ($ThO_2 \leq 10.63$ wt. %) and depleted in uranium ($UO_2 \leq 0.75$ wt. %) or Si ($SiO_2 \leq 2.65$ wt. %) with both cheralite and huttonite substitutions. Primary magmatic monazites (Ce) yield normally the Cainozoic – Miocene ages (CHIME), although the Variscan restite ones with the age 330 Ma were identified as well as.

GEOCHEMISTRY

Geochemically studied samples of the Carpathian obsidians from ZVM belong to the volcanic peraluminous rocks, high potassium calc-alkaline rhyolite series (ASI = 1.05 ~ 1.15). Their SiO_2 content varies in narrow interval from 76.4 to 77.5 wt. % reflecting their fractionated nature. Relatively elevated FeO^t values with simultaneous declination in MgO (wt. %) indicate their overall ferroan

character. The Rb/Sr ratio = 2.13 ~ 3.46 points to the distinct differentiation of these volcanic rocks, however this does not appear in most of the surrounding rocks. Based on the classical I/S-typology for felsic magmatic rocks, studied obsidians belong to typical mixed (hybrid) I/S-type igneous rocks. Normalized REE patterns show uniform distribution trend with a pronounced negative Eu anomaly, La_N/Yb_N = 3.43 ~ 7.17 and partially elevated HREE values compared to surrounding rhyolite and dacite rocks. Their C1 chondrite normalized REE patterns are falling on the boundary between "hot-dry-reduced" and "cold-wet-oxidized" magmas (Bachmann and Bergantz 2008) reflecting genesis of magma from mantle and crust sources. The binary diagrams of CaO/Na_2O vs. Al_2O_3/TiO_2 respectively Rb/Ba vs. Rb/Sr for the mixing of mantle and crustal magmas estimation, clearly indicate that our samples fit the mixing trajectories with dominant crustal magma proportion and weak (30 ~ 10 %) contribution from mantle component. The Carpathian obsidians and their host rhyolite and dacite rocks represent a typical magmatic analogue of volcanic arc products from the geotectonic point of view (Kohút et al. 2016, 2017).

The pioneer work of Williams-Thorpe et al. (1984) brought the first provenance study of the Carpathian obsidians from archeological point of view. The authors recognized major source zones for obsidian samples from the Zemplín – Tokaj area of Central Europe, using the INAA analyses, and graphically displayed in the diagrams such as: "Carpathian-1" originating from the Viničky and Malá Tŕňa localities; "Carpathian-2a" form the occurrences at Csepegő Forrás, Tolcsva, Olaszliszka and Erdőbénye located in the southern Hungarian sector; and "Carpathian-2b" representing redeposited obsidians from Erdőbénye. The statistical dispersion of our samples falls within the Carpathian-1 and Carpathian-2 interface, following the trend of data by Williams-Thorpe et al. (1984) with a slight decrease on the y-axis in the diagram. We tested the revised provenance diagrams for the Carpathian obsidians suggested by Rosania et al. (2008) in a similar way. The authors used trace elements in two Harker diagrams of Sr vs. Zr and U vs. Rb for discrimination only. However, our data demonstrated the compatibility of analytical determinations only for strontium, rubidium and zirconium, whereas uranium and thorium analytical determinations by XRF or INAA were not optimal, and ICP MS analysis (alike we done) are recommended today. Hence, our data do not show any difference in composition of our obsidians, and indicate common provenance Carpathian-1 for Viničky and Cejkov locality as well in the frame of Rosania's discrimination (Kohút et al. 2016).

CONCLUSION

It is obvious that the Carpathian obsidians show lot of contradictory features in their genesis, from above mentioned. The genesis of the Carpathians obsidians was a consequence of the multi-step complicated processes with the primary mantle basaltic magma at the beginning, followed by melting of the lower crustal source on the mantle/crust boundary, formation of a melt reservoir in the middle crust, accompanied by secondary melting of the surrounding rocks, and/or repeated process of assimilation and fractionation, consequently producing set of various rocks from basalt to rhyolites and also obsidians, what is in line with the idea of Kohút et al. (2012, 2016).

Acknowledgment: Support from the Slovak Research and Development Agency: Grant APVV-0549-07, APVV-14-278, and VEGA 0084/17 are greatly appreciated.

REFERENCES

Bachmann O. and Bergantz G.W. (2008): J Petrol 49:2277–228.

Biró K.T. (2006): Proceedings of the 34th Intern. Symp. on Archaeometry, 3-7 May 2004, (Zaragoza, Spain), Institución Fernando el Católico (C.S.I.C.). 267–278.

Kobulský et al. (2011): Open file report. Archive ŠGÚDŠ, 143 pp.

Kohút M. et al. (2012): Proceedings of the GEOCHÉMIA 2012; Conferences, Symposia & Seminars ŠGÚDŠ Bratislava, 71–75.

Kohút M. et al. (2016): Proceedings of the GEOCHÉMIA 2016; Conferences, Symposia & Seminars ŠGÚDŠ Bratislava, 78–81.

Kohút M. et al. (2017): Proceedings of the GEOCHÉMIA 2017; Conferences, Symposia & Seminars ŠGÚDŠ Bratislava, 79–82.

Rosania C.N. et al. (2008): Antiquity 82:318–320.

Williams-Thorpe O. et al. (1984): J Archaeol Sci 11:183–212.

Joint 5th Central-European Mineralogical Conference and
7th Mineral Sciences in the Carpathians Conference

Mineralogy of "eye-like" opals from Nová Ves near Oslavany (Moldanubian zone, Bohemian Massif)

[1]Šárka Koníčková[#], [1]Zdeněk Losos, [2]Vladimír Hrazdil, [2]Stanislav Houzar and [1]Dalibor Všianský

[1] Masaryk University, Faculty of Science, Department of Geological Sciences, Kotlářská 2, 611 37, Brno, Czech Republic;[#]327669@mail.muni.cz
[2] Moravian Museum, Department of Mineralogy and Petrography, Zelný trh 6, 659 37 Brno, Czech Republic

Key words: eye-like concentric opal, quartz, mineralogy, weathering, serpentinite

The "eye-like" opals from Nová Ves have been recognized by collectors for more than 100 years, but their mineralogy and especially the genesis are almost unknown. The aim of the research is to supplement existing information of these unique opals with the results of study by modern methods and explain their conditions of their origin.

The locality Nová Ves near Oslavany, situated in Moldanubian zone of western Moravia, represents the only known occurrence of zonal "eye-like" (concentric) opals in Bohemian Massif. This specific type of opal is characterized by a concentric zonal texture with white core ("eye"), brown massive translucent inner rim and locally also white porous outer rim. These opals occur in residual sediments in a small area along the contact of serpentinized peridotite and granulite.

Optical microscopy, Raman spectroscopy, X-ray powder diffraction and electron microprobe analysis of these individual zones showed that white and grey "eye" and brown inner zone contains mainly opal-CT. Quartz and moganite are present in part in white aggregates of the "eye" only. White outer rim of opals is composed of calcite with disseminated opal relics and this zone is younger as core and inner rim (calcite replaces opal). X-ray powder diffraction analyses proved presence of sepiolite admixture in brown part and accessory amount of sepiolite and chlorite in white rim.

Origin of "eye-like" opals from Nová Ves is not a typical product of serpentinite weathering, but it is the result of multistage weathering process on the boundary between peridotite and granulite. Source of younger calcification of opals remains unknown.

Acknowledgment: The research was supported by the Ministry of Culture as part of the institutional funding for long-term strategic development research organization Moravian Museum (DKRVO, MK000094862).

Analytical work was financially supported by means of specific research of the Department of Geological Sciences, Masaryk University.

REFERENCES

Graetsch, H. (1994): Min Soc Amer, Washington, D.C. 209–232.
Kettner R. (1919): Čas Morav zem muzea 17–19:169–177.
Kovář, O. et al. (2008): Acta Mus Morav Sci. Geol 93:19–35.
Medaris G. et al. (2005): Lithos 82:1–23.
Moxon T. (2002): Eur J Min 14:1109–1118.

Joint 5th Central-European Mineralogical Conference and
7th Mineral Sciences in the Carpathians Conference
Banská Štiavnica 2018

Chemistry and provenance of tourmaline from Albian sands of southern Poland

[1]Jakub Kotowski, [1]Krzysztof Nejbert and [1]Danuta Olszewska-Nejbert

[1] University of Warsaw, Faculty of Geology, Al. Żwirki i Wigury 93, 02-089 Warszawa, Poland
[#]jb.kotowski@gmail.com

Key words: tourmaline, mineral chemistry, provenance, Albian sands, southern Poland

The transgressive Albian deposits in extra-Carpathian outcrops are developed as quartz sands and sandstones. In the NW-SE elongated basin called Mid-Polish through the Albian deposits exceed the thickness more than 100 m and now are used as valuable raw material for glass industry. The area studied here includes seven isolated outcrops situated between Kraków and Radomsko in southern Poland. In these localities were the Albian sands sampled: Korzkiew, Glanów, Przychody, Lelów, Mokrzesz, Bolmin and Chełmo Mount. The investigated material consists of quartz sand/rarely sandstone with various admixture of glauconite, muscovite (Si 3.082-3.389 apfu), feldspars, and heavy minerals. The heavy minerals include tourmaline, rutile, garnet ($Alm_{30.97-85.03}Prp_{5.11-52.96}Grs_{0-28.29}$), staurolite (Mg# 0.09-0.25), ilmenite, titanite, zircon, monazite, kyanite, and gahnite. The other minerals, especially those containing Fe and Ti (e.g. amphibole, magnetite and biotite) are subordinate.

Tourmaline is in the detrital heavy mineral assemblages of the examined material the dominant mineral. Members of the turmaline supergroup are treated as very useful for the provenance analysis. Over 520 tourmalines were analysed using EPMA. The majority of these grains belong to the alkali tourmaline group, in which the *X* site is dominated by Na (Henry et al. 2011). Sodium is the most abundant cation ranging from 0.4 to 0.9 apfu while K amounts are very low (usually below detection limit). *X*-site vacancies range from 0.02 to 0.6 apfu, but usually are below 0.3 apfu. The fluorine content varies from concentrations below detection limit to 0.7 apfu, but in the most analysed tourmaline grains it is not significant. Other *Y*-site cations (such as Ti, Mn, V, Zn, Cr) rarely exceed 0.1 apfu. The detrital tourmalines are represented mainly by schorl and dravite with avg. X_{Mg} values >0.6. Such chemical compositions indicate that the alimentation area was probably located in the eastern part of the Bohemian Massif (see Čopáková et al. 2009). The chemical composition of our studied tourmalines is similar to the composition of detrital tourmaline from numerous localites located in southern Poland, e.g. from epicontinental carbonates of Middle Triassic age (Kowal-Linka and Stawikowski 2013), from the Jurassic pre-Callovian palaeokarst infill (Salata 2013), from Ropianka (Upper Cretaceous) and Menilite (Oligocene) formations, Carpathians (Salata 2014). There is evidence that the suggested alimentation area was eroded almost throughout the Mesozoic and Paleogene time, or that material from this area was recycled during the sedimentary processes.

Acknowledgments: This work was funded by University of Warsaw (DSM grant no. 115611; grant no. BOB-661-300/17 and BSt grant no. 180302).

References

Čopjaková R. et al. (2009): J Geosci 54:221–243.
Henry D.J. and Guidotti C.V. (1985): Am Min 70:1–15.
Henry D.J. et al. (2011): Am Min 96:895–913.
Kowal-Linka M. and Stawikowski W. (2013): Sed Geol 291:27–47.
Salata D. (2013): Geol Quarterly 57:537–550.
Salata D. (2014): Geol Quarterly 58:19–30.

Mechanical and alkali activation of perlite (Pálháza), pumicite (Erdőbénye) and zeolitic tuff (Rátka) from NE-Hungary: role of mineralogy

[1]Ferenc Kristály[#], [2]Gábor Mucsi, [2]Katalin Bohács, [1]Ferenc Móricz and [2]Roland Szabó

[1] University of Miskolc, Faculty of Earth Science and Engineering, Institute of Mineralogy and Geology, Egyetem Street No. 1, 3515 Miskolc, Hungary [#]askkf@uni-miskolc.hu
[2] University of Miskolc, Faculty of Earth Science and Engineering, Institute of Raw Material Preparation and Environmental Processing, Egyetem Street No. 1, 3515 Miskolc, Hungary

Key words: Rietveld refinement, amorphisation, volcanic glass, glass activation

In NE-Hungary the Tokaj-Eperjes and Zemplén Mts. have been important sources for decades of rhyolite volcanism related non-metallic industrial minerals, like kaoline, smectites, zeolites, perlite, diatomite and pumicite. However at the end of 20th century most of these resources lost importance and mining was ceased or drastically reduced for perlite, zeolite and diatomite (not considered in this study). However, classical uses constantly need to be revised and new applications developed for a sustainable resources management. In recent experiments mechanical (ultrafine grinding) and alkali (geopolymerisation) activation was tested for several raw materials. The present study focuses on detailed description of initial mineralogy and mineralogical changes by activation experiments. Possible application include green cement, geopolymer, ionic and molecular adsorption aiding agents or agricultural additives.

The samples were investigated by X-ray powder diffraction (XRD) and attenuated total reflectance Fourier-transformed infrared spectroscopy (ATR-FTIR). Additionally, X-ray fluorescence spectrometry (XRF), scanning electron microscopy with energy dispersive spectrometry (SEM+EDS) and petrographic microscopy when required. After grinding in high energy ball mill at various frequency for various periods, XRD and ATR-FTIR were repeated. Particle size analysis was conducted on laser diffraction system (LPSA). Of particular interest is the development and evolution of nanocrystalline phases, together with amorphous material. Mechanical activation is important for alkali activation efficiency, but also the adsorption properties were tested with lime adsorption capacity and methylene blue adsorption.

Depending on mineralogy of raw materials, several transformation were deduced and characterized. Using Rietveld refinement on XRD results, combined with ATR-FTIR, we observed that the type (composition and structural character) of amorphous materials can be distinguished for each material.

A peculiar feature of mechanical activation of perlite and pumicite is the alteration of volcanic glass, into a more active glassy phase, as observed by the alkali activation efficiency of grinded materials. By alkali activation a hydrous phyllosilicate type gel is developed.

Crystalline components are severely amorphised even after 30 min of grinding, in parallel with crystallite size reduction. The destruction of crystal lattices is also evidenced by ATR-FTIR, while adsorption bands assigned to the naturally contained amorphous material are shifted and distorted.

The combination of LPSA, ATR-FTIR and XRD indicate, that amorphisation proceeds via crystallite erosion combined with intra-grain structure destruction by strain accumulation. Application of Rietveld refinement proved to be an extremely useful method for tracing the nanocrystalline and amorphous material changes.

Acknowledgment: The described work/article was carried out as part of the „Sustainable Raw Material Management Thematic Network – RING 2017", EFOP-3.6.2-16-2017-00010 project in the framework of the Széchenyi2020 Program. The realization of this project is supported by the European Union, co-financed by the European Social Fund.

The Erdőbénye-Ligetmajor (NE-Hungary) diatomite deposit

[1] Ferenc Kristály[#], [2]Nóra Halyag and [1]János Földessy

[1] University of Miskolc, Faculty of Earth Science and Engineering, Institute of Mineralogy and Geology, Egyetem Street No. 1, 3515 Miskolc, Hungary [#]askkf@uni-miskolc.hu
[2] University of Miskolc, Faculty of Earth Science and Engineering, Institute of Raw Material Preparation and Environmental Processing, Egyetem Street No. 1, 3515 Miskolc, Hungary

Key words: perlite sand, montmorillonite

The Ligetmajor diatomite deposit is set in the Tokaj Mts, at the locality of Erdőbénye. The open pit mining is operated since several decades with fluctuating production. The deposit is an alternating lacustrine accumulation from coarse to fine sand layers (0.1 to 10 cm), smectite (1 to 20 cm) rich layers and diatomite beds (0.1 to 0.5 m). High occurrence of plant fossils is characteristic, seasonal or some larger period variations are marked by millimetric organic material laminas. The formation was generated during and after the Sarmatian rhyolitic-andesitic volcanism. Our aim was a reinvestigation of mineralogy and performing dye adsorption tests. Samples were collected from the > 1 cm layers along a 5 m column. Average samples of several meters were also investigated.

The samples were investigated by optical microscopy. Texture related chemical investigations were obtained by X-ray mapping with scanning electron microscopy and energy dispersive spectrometry (SEM+EDS). Bulk mineralogy was determined by X-ray powder diffraction (XRD). For an in-depth characterization, diagnostic clay mineral investigation was performed on oriented clay specimens with XRD. Specific surface area was tested with BET. Dye adsorption tests were carried out with methylene blue adsorption tests with UV-spectroscopy (Spectronic 20D+).

Optical microscopy revealed the presence of volcanic glass and perlite grains and shards as the dominant phase of sand layers. Crystal relicts and clasts are mainly intermediary plagioclase in the 0.5 to 1 mm size range. XRD results helped to clearly distinguish between different layers and beds. Sand layer is mainly perlite type amorphous material, while diatomite layers are of opal-A type silica. Smectite rich layers contain calcite and the clay mineral is montmorillonite according to diagnostic tests and K-exchange experiments. XRD and SME+EDS allowed to observe a large variety of feldspar clasts, ranging from orthoclase to anorthite. This indicates the origin of sediment from multiple volcanic stages and/or sources. Pumice fragments observed by SEM confirm the contribution of explosive rhyolitic volcanism also. Beyond ilmenite no other heavy minerals was detected.

SSA varies according to lithology. For samples of perlite shard rich sands the BET multipoint values are < 5 m^2/g. The other samples are in the 10 to 13 m^2/g for the rest of the samples. Methylene blues adsorption revealed a 30% dye removal capacity even for the fine sand material. Diatomite samples produced >80% removal capacity, while samples of montmorillonite+diatomite showed 100% removal values.

The alternating layers in the deposit can be grouped in five different petrographic types: 1) the coarse sand is perlite dominated, 2) fine sand is mainly feldspar and perlite built, 3) smectite rich layers are montmorillonite < diatomite +/- magnesian calcite, 4) diatomite layers have some minor montmorillonite content, 5) black lamina is decayed organic matter. Mg observed in the composition of montmorillonite and calcite is derived from lacustrine infiltrations, since no Mg-bearing mineral or glass material was observed in the beds.

Average samples showed that the combination of fine sand with the smectite and diatomite layers retain the dye removal capacity of the material. It was also determined, that on average samples discrimination between volcanic glass and diatomite is possible by XRD, even with limited quantification of the two materials.

Mineral textures of olivine minette from Horní Kožlí (the Moldanubian Zone of the Bohemian Massif) and their implication for understanding of crystallization history of the rock

[1]Šárka Kubínová[#] and [1]Shah Wali Faryad

[1] Charles University, Faculty of Science, Institute of Petrology and Structural Geology, Albertov 6, 128 43 Prague 2, Czech Republic [#]sarka.kubinova@natur.cuni.cz

Key words: ultrapotassic magmatism, dyke swarm, Bohemian Massif

The ultrapotassic dykes (minettes, vaugnerites and melasyenite to melagranite porphyries) of late-Variscan age are widespread in the Moldanubian Zone at contact to the Teplá-Barrandian Unit. Based on modal and mineral compositions and bulk-rock geochemistry, the dykes show close relations to the ultrapotassic plutonic bodies, the so called durbachite, in the Moldanubian Zone (e. g. Holub 1997, 1999, Kubínová et al. 2017).

A W–E trending dyke of olivine minette from Horní Kožlí (near Prachatice) penetrates biotite migmatites in the western part of the Moldanubian Zone. The olivine minette has a porphyric texture represented by phenocrysts of olivine, clinopyroxene and biotite. Olivine is mostly replaced by talc. Rarely, larger grains of quartz with clinopyroxene rims occur. The fine-grained matrix consists of K-feldspar, biotite, clinopyroxene and minor plagioclase and quartz. Accessory minerals are apatite, Cr-rich spinel and iron sulphides.

The pale pink olivine phenocrysts have high Mg content (77.82–90.55% forsterite) and show a compositional zoning with decrease of Mg and increase of Fe and Mn contents from the core to the rim. The pale yellow-brown to green talc in the pseudomorphs after olivine has optical orientation in one direction suggesting topotactic replacement along the crystal shape. The pseudomorphs have corona composed by two zones - talc-rich inner zone and biotite-rich outer zone. These two zones are also observed around olivine phenocrysts.

Biotite is brown to brown-orange. Based on Mg and Fe ratios, the phenocrysts are phlogopite in composition (XMg = Mg/(Mg + Fe) = 0.57–0.80), small grains in matrix correspond to biotite (XMg = 0.53–0.59) and that in the corona around olivine phenocrysts and olivine pseudomorphs show a wide compositional variation from biotite to phlogopite (XMg = 0.59–0.93).

The colourless clinopyroxene is augite to diopside in composition with magnesium number (Mg# = 100 Mg/(Mg + Fe)) 55.94–85.33. It forms phenocrysts with oscillatory zoning that reflects the rimwards changes of Mg, Cr, Ti, Fe, Mn, Ca and Na contents. The fine grains in the matrix have a wide compositional variation with Mg# = 51.25–81.54 and show composition of augite to diopside. Rare orthopyroxene (~ 84 mol. % enstatite) forms relicts of primary phenocrysts that are overgrown or replaced by clinopyroxene (augite to diopside in composition with Mg# = 52.83–83.48).

Rarely, large oval quartz grains with reaction rims, formed by fine columnar clinopyroxene (augite in composition with Mg# = 76.81–80.86) and K-feldspar, are also present. The clinopyroxene grows mostly perpendicular to the quartz rim and radially penetrate to the quartz crystal. In case of small quartz grains, the quartz is present only in the central part or it is totally overgrown by clinopyroxene.

Acknowledgment: This study is supported by the Czech Science Foundation (project 18-03160S).

References

Holub F.V. (1997): Sb Geol Věd, Lož Geol Min 31:5–26.

Holub F.V. (1999): Geolines 8: 28.

Kubínová Š. et al. (2017): Lithos 272–273:205–221.

Mass balance and major and trace element zoning in atoll garnet from eclogite facies rocks

[1]Jan Kulhánek[#], [1]Shah Wali Faryad, [1]Radim Jedlička and [2]Martin Svojtka

[1]Charles University, Faculty of Science, Institute of Petrology and Structural Geology, Albertov 6, 128 43 Prague 2, Czech Republic [#]jan.kulhanek@natur.cuni.cz
[2]Institute of Geology of the Czech Academy of Sciences, Rozvojová 269, 160 00 Prague 6, Czech Republic

Key words: atoll garnet, compositional zoning, trace elements, eclogite

Eclogite from this study comes from central part of the Krušné hory Mountains (Saxothuringian Zone, Bohemian Massif). The estimated PT conditions are about 26 kbar and 650-700 °C (Klápová et al. 1998; Faryad et al. 2010; Collett et al. 2017). The main minerals present in the rock are omphacite, garnet, quartz and amphibole which replaces omphacite. Minor rutile, +/- phengite, paragonite, apatite, ilmenite and retrograde chlorite are also present. Garnet contains inclusions of quartz, clinopyroxene, rutile, apatite and zircon. Amphibole, chlorite and plagioclase can be also present in the garnet. Idioblastic crystals of garnets are mostly fractured. In many cases, they form atoll garnet textures where central parts of garnet grains are filled by other minerals (quartz, amphibole, clinopyroxene and chlorite).

By using compositional mapping and profiles of garnets we distinguished two, older (I) and younger garnets (II), respectively. Garnet I, occurring in the core and at the mantle parts of grains, has higher contents of Ca and Mn and lower amounts of Mg and Fe then garnet II, which grows on the most rims of garnet or replaces garnet I in the central part. Younger garnet II in the central parts or that at the rims are similar in composition. Garnet I preserves prograde zoning with decreasing Ca and/or Mn from core to the rims with garnet II.

According to Faryad et al. (2010) the atoll garnets formed during fluid infiltration and element exchange between older garnets and matrix during prograde stage of eclogite facies metamorphism. Garnet II should be then formed not only by the exchange of elements with the matrix, but also by dissolution of older garnet I. To verify this idea, trace elements (especially Y and HREE), which have very slow distribution coefficients and they are highly compatible in garnet (Spear and Kohn, 1996; Carlson, et al. 2014) were analysed. Using LA-ICP-MS, the trace element concentrations (including Y+REE) were obtained for separate zone recognized by the major element distributions.

The central parts of garnet I are rich in Y and HREE (Lu, Yb, Tm, Er) with elevated MREE (Ho, Dy, Tb, Gd) contents. Based on the compositional profiles, they show zoning with decrease towards the rims of garnet I. The contents of Y and HREE are high in garnet II at the rims, but mostly oscillate due to continuous dissolving and variable influx of elements from garnet I. It was shown that the early garnet I cores were the main source to provide the Y+HREE budget into garnet II.

To discover possible effect of other minerals in the reactions, Y+REE distribution in omphacite was also investigated. Omphacite shows well developed zoning of LREE and +/- Y and MREE.

Acknowledgment: This study is supported by the Charles University (project GAUK 243 250 373) and Czech Science Foundation (project. 18-03160S).

References

Carlson W.D. et al. (2014): Am Min 99:1022–1034.
Collett S. et al. (2017): J Met Geol 35:253–280.
Faryad S.W. et al. (2010): Min Mag 74:111–126.
Klápová H. et al. (1998): J Geol Soc 155:567–583.
Spear F.S. and Kohn M.J. (1996): Geology 24:1099–1102.

Joint 5th Central-European Mineralogical Conference and
7th Mineral Sciences in the Carpathians Conference

Parasymplesite - annabergite solid solution from Dobšiná (Slovakia)

[1]Klaudia Lásková[#], [1]Daniel Ozdín and [1]Peter Cibula

[1] Comenius University, Faculty of Natural Sciences, Department of Mineralogy and Petrology, Ilkovičova 6, 84215 Bratislava, Slovakia [#]klaudia.laskova@gmail.com

Key words: Parasymplesite, annabergite, solid solution, Dobšiná, crystal chemistry

INTRODUCTION

Dobšiná is a historic mining district in Slovakia, well known for the mineral extraction of Co-Ni ore minerals. There have been described various arsenate and phosphate minerals from this locality: annabergite $Ni_3(AsO_4)_2 \cdot 8H_2O$, erythrite $Co_3(AsO_4)_2 \cdot 8H_2O$, vivianite $Fe^{2+}{}_3(PO_4)_2 \cdot 8H_2O$, scorodite $Fe^{3+}(AsO_4) \cdot 2H_2O$ and hörnesite $Mg_3(AsO_4)_2 \cdot 8H_2O$ (Cotta and Fellenberg 1862, Kúšik 2010, Ozdín et al. 2017, Peterec and Ďuďa 1993, Zepharovich 1859). Parasymplesite $Fe^{2+}{}_3(AsO_4)_2 \cdot 8H_2O$ is a monoclinic arsenate crystallising in the space group *C*2/*m*. Its unit cell parameters are: $a = 10.349$ Å, $b = 13.525$ Å, $c = 4.789$ Å, $\beta = 104.92°$ and $V = 647.72$ Å^3 (Mori & Ito, 1950).

The chemical composition of Zn-free parasymplesite was studied by Mori & Ito (1950) and the solid solution formed by köttigite and parasymplesite was described by Yoshiasa et al. (2016). The structure of vivianite and parasymplesite was first described by the authors (Mori and Ito 1950). The structure of vivianite was later defined by Fejdi et al. (1980), while there is no actual description of the mineral structure of parasymplesite (Yoshiasa et al. 2016). Important knowledge which refers to crystal chemistry discovery is the description of the substitution of $Fe^{2+} + H_2O \leftrightarrow Fe^{3+} + (OH)^-$ between vivianite and metavivianite (Yoshiasa et al., 2016), which could also occur in parasymplesite. Parasymplesite is a rare supergene mineral occurring in oxide zones of arsenic rich hydrothermal base-metal deposits. Dimorphism occurs in parasymplesite which includes symplesite and forms series with köttigite (Anthony et al., 2000).

Parasymplesite is the supergene mineral, which belongs to the arsenate of the vivianite group defined by the general formula $M^{2+}{}_3(XO_4)_2 \cdot 8H_2O$. Its chemical composition is formed by the octahedral sites M_3 of Fe^{2+}, which may be substituted by the elements as Zn, Ni, Co, Mg, Mn, Pb, Cu. At position *X* enters As^{5+}, which can be replaced in homovalent substitutions by P^{5+}, V^{5+} and in heterovalent substitutions by S^{6+}, Si^{4+}. Between separate members of the vivianite group is an extensive isomorphism, but parasymplesite associates in solid solution forms only with köttigite $Zn_{3-x}Fe_x(AsO_4)_2 \cdot 8H_2O$ (Yoshiasa et al. 2016; Plášil et al. 2017, Jambor and Dutrizac 1995).

EXPERIMENTS

Powder X-ray diffractometer was used to identify individual supergene arsenate as well as other supporting phases.

X-ray powder diffraction data of the supergene phases were obtained using a Bruker D8 Advance powder diffractometer (Faculty of Natural Sciences of the Comenius university in Bratislava) with a semiconductor position sensitive LynxEye detector using CuKa radiation under the following conditions: 40 kV, 40 mA, step 0.01 ° 20, time 3-5 s / step. The prepared single-phase powder formulations were applied to a support made from a mono crystalline Si to reduce the recording background in an acetone suspension. The obtained diffraction data was evaluated using the BrukerDIFFRACplus EVA software (DIFFRACplusEVA). The lattice parameters of the studied phases were calculated and specified by the Rietveld method using the BrukerDIFFRACplus TOPAS program (DIFFRACplusTOPAS) using the Pearson VII profile function. Formats from the AMCSD (Downs and Hall-Wallace, 2003).

Electron microprobe analysis (EMPA - WDS) to be used for studying the chemical

composition of supergene phases (EDS, WDS) as well as documentation of their relations supergene minerals mode backscattered electrons (BSE).

Quantitative (WDS) analysis of the minerals in polished sections have been drawn using an electron microanalyzer Cameca SX 100 (Faculty of Science, Masaryk University, Brno). Measuring conditions were as follows: accelerating voltage 15 kV, sample current of 2-10 nA electron beam diameter of 5-20 μm, standards and spectral lines: lammerite (As Lα), sanidine (Si Kα), Mg_2SiO_4 (Mg Kα), fluorapatite (P Kα), vanadinite (Cl Kα), almandine (Fe Kα) , Ni_2SiO_4 (Ni Kα), Co (Co Kα), gahnite (Zn Kα), $ScVO_4$ (V Kα), spessartine (Mn Kα), topas (F Kα), $SrSO_4$ (S Kα), Bi (Bi Mβ), Sb (Sb Lβ). The contents of the measured elements that are not listed in the tables, were below the detection limit of the device. Empirical formulations of individual mineral phases have always been calculated on 5 cations. H_2O content was calculated based on theoretical content.

Results And Discussion

In the future work we are prepared to deal with previously unknown solid solution between parasymplesite and annabergite $Fe^{2+}{}_{3x}Ni_x(AsO_4)_2{\cdot}8H_2O$. The solid solution which occurred in the samples from Dobšiná, was described by EMPA and powder X-ray diffraction methods. Analyzed samples with parasymplesite were collected at heaps and in mine of Dobšiná and form dark green beads aggregates composed of needle crystals up to 0.3 mm in size (Fig. 1).

The most important contribution by our research is the discovery of solid solution parasymplesite with annabergite. There has been described only a solid solution of parasymplesite with köttigite (Fejdi et al. 1980) and erythrite with annabergite (Wildner et al. 1996) so far.

Empirical formula for parasymplesite from Dobšiná is $(Fe^{2+}{}_{1.84}Ni_{0.92}Mg_{0.11}Mn_{0.07}Co_{0.01}Cu_{0.01}Na_{0.01})(As^{5+}{}_{1.98}S^{6+}{}_{0.02}O_4){\cdot}8H_2O$. By analyzing the chemical composition we found that it entered the octahedral position on average 1.84 *apfu* Fe^{2+}, Ni in proportion 0.92 *apfu* and 0.11 *apfu* Mg. To this position also entered trace amounts of Mn, Co, Cu, Ca, Mg, Na and Al. Tetrahedral sites mostly occupied As^{5+} an average of 1.98 *apfu* and trace amounts of S^{6+}, Si^{4+}. The ratio $Fe^{2+}+Al^{3+}$/Ni+Co+Mg+Mn+Ca in octahedral site suggests to considerable inversely proportional dependence. The structure of these minerals is composed of octahedron $M(1)O_2(H_2O)_4$ and pairs octahedron $M(2)_2O_6(H_2O)_4$, which are linked through tetrahedrons XO_4 and hydrogen bonds into layers parallel to the direction (010), and the individual layers are joined solely by hydrogen bonds (Wildner et al. 1996). It is known that in a solid solution between köttigite and parasymplesite is preferred a smaller ion Zn^{2+} entry into a larger position *M*(1) (Yoshiasa et al. 2016), while in our case even smaller Ni^{2+} ion and larger ion Fe^{2+} enter a smaller position *M*(2). This unique preference cations entering into these positions causes the reduction of structural deformations (Yoshiasa et al. 2016). In erythrite and annabergite is shown that Ni^{2+} preferably occupies the octahedral position *M*(1), while Co^{2+} position *M*(2), Mg^{2+} and Fe^{2+} show preference to enter position *M*(2) (Wildner et al. 1996). The unit cell parameters for the analyzed parasymplesite from Dobšiná is: $a = 10.141(5)$, $b = 13.261(4)$, $c = 4.725(2)$ Å, $\beta = 104.98(4)°$, $V = 613.94(54)$ Å^3. This unit cell parameters for parasymplesite from Dobšiná are significantly lower as published data. Due to the unusual entry of individual elements into the octahedral position, this phenomenon occurs probably due to the entry of cations with a smaller ionic radius Ni^{2+} (Co, Zn, Mg) into a larger position and the entry of a larger Fe^{2+} cation into a smaller position (Shannon 1976).

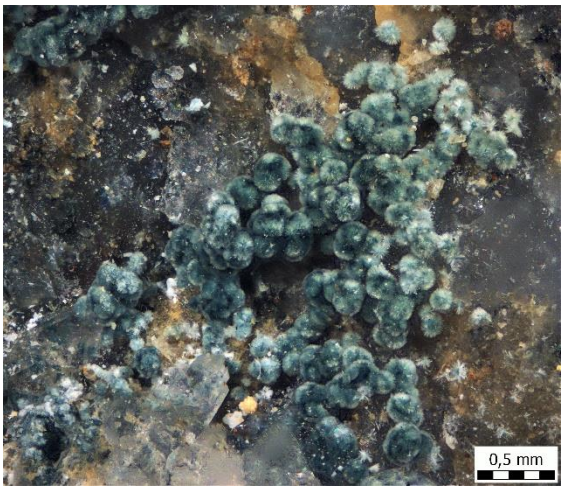

Fig. 1: green-blue crystals of parasymplesite from Dobšiná (max 0.3 mm).

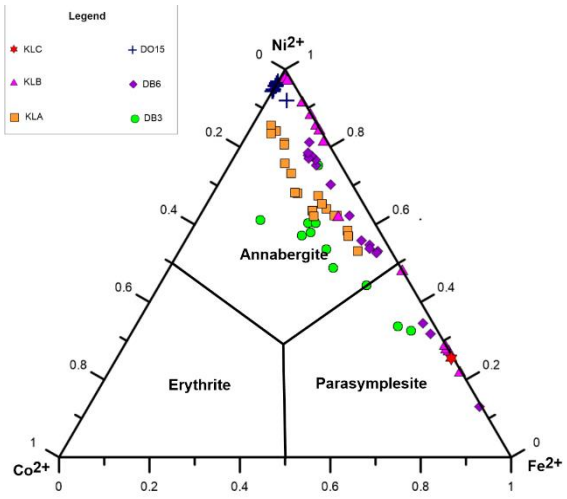

Fig. 2: The ternary diagram from parasymplesite – annabergite solid solution from Dobšiná.

CONCLUSION

In our research from Dobšiná we described parasymplesite which was discovered for the first time in Slovakia. Its chemical composition is: $(Fe^{2+}_{1.84}Ni_{0.92}Mg_{0.11}Mn_{0.07}Co_{0.01}Cu_{0.01}Na_{0.01})(As^{5+}_{1.98}S^{6+}_{0.02}O_4)\cdot 8H_2O$. Characteristic is its chemical composition, which ranges from parasymplesite to annabergite. In the structure of parasymplesite, we found a significant deformation in the octahedral position, possibly caused by the entry of a cation with a smaller ionic radius Ni^{2+} to a larger position and the entry of the larger cation of Fe^{2+} into a smaller position. In order to clarify the iron input into individual cationic positions in the parasymplesite structure, Mössbauer spectroscopy will be used in further research.

Acknowledgment: This work was supported by the Slovak Research and Development Agency Contracts no. APVV-0375-12, APVV-15-0050 Serpentinites and rodingites of metaperidotites from accretionary complexes of the Inner Western Carpathians and eastern Austro-Alpine margin: petrology and genetic aspects VEGA 1/0079/15 and Comenius University grant No. G-18-215-00.

REFERENCES

Anthony J.W. et al. (2000): Handbook of Mineralogy. IV. Arsenates, Phosphates, Vanadates. Mineral Data Publishing.

Cotta B. and Fellenberg E. (1862): Die erzlagerstätten Ungarns und Siebenbürgens. Freiberg.

DIFFRACplusEVA. (30th March 2017). (*http://www.brukeraxs.com/eva.html.*

DIFFRACplusTOPAS. (30th March 2017). *(http://www.brukeraxs.de/topas.html.*

Downs R.T. and Hall-Wallace M. (2003): Am. Min 88:247–250.

Fejdi P. et al. (1980): Bull. Minéral. 103:135–138.

Jambor J.L. and Dutrizac J.E. (1995): Can Min 33:1063–1071.

Kúšik D. (2010): Minerál 18:360–362.

Mori H. and Ito T. (1950): Acta Crystallogr. 3: 1-6.

Ozdín D. et al. (2017): Mineralogicko-petrologická konferencia Petros 2017. Univerzita Komenského v Bratislave, 39–40.

Peterec D. and Ďuďa R. (1993): Minerál 1:30–31.

Plášil J. et al. (2017): J. Geosci. 62:261–270.

Shannon R.D. (1976): Acta Cryst A32:751–767.

Yoshiasa A. et al. (2016): J Min Petrol Sci 111:363–369.

Wildner M. et al. (1996): Eur. J. Min. 8:187–192.

Zepharovich V. (1859): Mineralogisches Lexicon für das Kaisserthum Österreich. I. Wilhem Braumüller, Wien.

Joint 5th Central-European Mineralogical Conference and
7th Mineral Sciences in the Carpathians Conference
Banská Štiavnica 2018

Crystal structure study of thalhammerite ($Pd_9Ag_2Bi_2S_4$) and laflammeite ($Pd_3Pb_2S_2$)

[1]František Laufek[#], [1]Anna Vymazalová, [2]Sergei F. Sluzhenikin, [3]Vladimir V. Kozlov, [4]Jakub Plášil, [5]Federica Zaccarini and [5]Giorgio Garuti

[1] Czech Geological Survey, Geologická 6, 152 00 Prague 5, Czech Republic
[#]frantisek.laufek@geology.cz
[2] Institute of Geology of Ore Deposits, Mineralogy, Petrography and Geochemistry RAS, Staromonetnyi per. 12, Moscow 119017, Russia
[3] Oxford Instruments (Moscow Office), 26, Denisovskii Pereulok, Moscow, 105005, Russia
[4] Institute of Physics, AS CR v.v.i. Na Slovance 2, 182 21, Prague 8, Czech Republic
[5] University of Leoben, P.Turner Str. 5, A-8700 Leoben, Austria

Key words: platinum-group minerals, crystal structure, new minerals

Laflammeite ($Pd_3Pb_2S_2$) was described as a new mineral by Barkov et al. (2002) from the Kirakkajuppura platinum-deposit, Penikat layered complex, Finland. Barkov et al. (2002) provided chemical and physical characterisation of this mineral, however its detailed crystal structural analysis has been lacking. The phase $Pd_9Ag_2Bi_2S_4$ was reported in millerite-pyrite-chalcopyrite vein-disseminated ore from ore from the Komsomolsky mine in the Talnakh deposit, Russia (Sluzhenikin and Mokhov, 2015). Subsequently, this phase was described as a new mineral thalhammerite. Crystal structures of both minerals and relevant crystal-chemical implications will be discussed.

Thalhammerite occurs as tiny inclusions (from few μm up to about 40-50 μm) in galena, chalcopyrite and also in bornite, where it forms intergrowns with other Pd-bearing minerals. Laflammeite occurs as subhedral platelets up to 150 μm, however the crystals are finely twinned and consequently unsuitable for crystal structure study (Barkov et al. 2002). Therefore, both minerals were synthetized by silica glass tube technique by heating from stoichiometric mixture of elements. The prepared synthetic analogues of laflammeite and thalhammerite were used for a structure study. The structural identity between natural and synthetic materials was confirmed by electron-backscattered diffraction, Raman spectroscopy and optical study.

Laflammeite, $Pd_3Pb_2S_2$, crystalizes in *Pmmn* space group (a = 5.78, b = 8.18, c = 5.96 Å) and Z = 2. Its crystal structure is strongly related to that of shandite ($Ni_3Pb_2S_2$, $R\bar{3}m$), parkerite ($Ni_3Bi_2S_2$, $C2/m$) and vymazálovaite ($Pd_3Bi_2S_2$, $I213$). Crystal structure of all these minerals show a common structure motive: a pseudocubic subcell CsCl-type composed of Bi(Pb) and S atoms. A half of available octahedral voids is occupied by Ni or Pd atoms. The distribution of Ni(Pd) atoms (i.e. the ordering scheme) determines the structure type. In this context, all these minerals can be considered as half-ordered antiperovskites.

Thalhammerite, $Pd_9Ag_2Bi_2S_4$ shows $I4/mmm$ symmetry (a = 8.02, c = 9.15 Å) and Z = 2. Its unique crystal structure is based on a three-dimensional framework which consists of two types of blocks of polyhedra that interpenetrate and support each other. The first type consists of corner-sharing [PdS_4] and [$PdBi_2S_2$] squares. The second is formed by flattened tetrahedra [$PdBi_2S_2$]. Ag atoms occupy channels running along the c direction. Thalhammerite crystal structure merges metallic building blocks with structure motives typical for polar sulphides.

Acknowledgment:

REFERENCES

Barkov, Y.A. et al. (2002): Can Min 40:671–678.

Sluzhenikin, S.F. and Mokhov, A.V. (2015): Min Deposita 50:465-492.

Joint 5th Central-European Mineralogical Conference and
7th Mineral Sciences in the Carpathians Conference

Mineralogical investigation of the Serra das Tulhas Fe-Mn mine (Cercal do Alentejo, Portugal): salvage in the last moment

[1]Máté Zs. Leskó[#], [1]Richárd Z. Papp, [1]Ferenc Kristály, [2]Iuliu Bobos, [2]Alexandra Guedes and [1]Norbert Zajzon

[1] University of Miskolc, Institute of Mineralogy and Geology, Miskolc-Egyetemvaros H-3515, Miskolc, Hungary [#]askmate@uni-miskolc.hu

[2] University of Porto, Institute of Earth Sciences-Porto, Rua do Campo Alegre 687, P-4169-007, Porto, Portugal

Key words: Iberian Pyrite Belt, manganese, ore deposit, archive samples

The mining history of Europe is widespread. From the early history until nowadays every region of Europe had or have different areas, which were/are worldwide significant. There are some old traditional mining districts, like Banská Štiavnica, where the documentation and available samples from the closed mines are abundant. But there are some regions, where after the end of mining documentation and samples are limited or not available.

The Iberian Pyrite Belt has more active world class Volcanogenic Massive Sulphide (VMS) deposits (like Neves Corvo in Portugal), which have serious influence to the world raw material supply. But unfortunately there are many other little VMS and other ore related mines in this area, which were closed few decades ago sometimes with no documentation and no preserved samples at all, completely lost for the science.

However the Serra das Tulhas Fe-Mn mine (Cercal do Alentejo, Portugal) was operated for decades in the second half of the 20th century and was closed in the middle of 1980s, there was not any scientific investigation before, during or after the mining operation.

This research is focused on this little known Serra das Tulhas Mn-Fe mine mineralogy: our sampling was the last moment to save any data remained from the mining.

The samples were investigated at the first with optical microscope, X-ray powder diffraction, X-ray fluorescence spectroscopy, and scanning electron microscopy.

Some different Fe-oxides (goethite, maghemite, hematite, magnetite,) and some Mn-oxides (todorokite, ramsdellite, pyrolusite, cryptomelane, and hollandite) with heterogeneous chemical composition and different textures were identified until now. Back-scattering electron microscopy (BSEM) identified primary texture of precipitated minerals directly from VMS related hydrothermal fluids and also recrystallized textures. The textural features of the different Fe-oxides and Mn-oxides are well preserved. Major chemical elements correspond to SiO_2 (8–85 wt%), Fe_2O_3 (10–80 wt%) and MnO (0.10–0.40 wt%). Trace elements are represented by Cu (20–1600 ppm), Zn (60–3000 ppm) and Pb (10–950 ppm).

The results support that the mineralogy is in line with a mid-ocean ridge related deposit, where certain samples reflect autigenous alteration.

Acknowledgment: This work was partially financed by the Bilateral Scientific and Technological Collaboration between Hungary (TÉT_16-1-2016-0074) and Portugal (Fundação para a Ciência e a Tecnologia – Lisboa). The described study was carried out as part of the EFOP-3.6.1-16-2016-00011 "Younger and Renewing University – Innovative Knowledge City – institutional development of the University of Miskolc aiming at intelligent specialisation" project implemented in the framework of the Széchenyi 2020 program. The realization of this project is supported by the EU, co-financed by the European Social Fund.

REFERENCES

Barriga F. (1990) In: Dallmeyer R.D. and Martinez García E. (Eds.) Pre-Mesozoic geology of Iberia, 369–379.

Neogene evolution of the lithospheric mantle beneath the Nógrád-Gömör Volcanic Field

[1,2]Nóra Liptai, [1]Levente Patkó, [1]László E. Aradi, [3]István J. Kovács, [4]Károly Hidas, [2]Suzanne Y. O'Reilly, [2]William L. Griffin and [1]Csaba Szabó[#]

1 Lithosphere Fluid Research Laboratory, Eötvös University, PázmányPétersétány 1/C, H-1117, Budapest, Hungary [#]cszabo@elte.hu
2 ARC Centre of Excellence for Core to Crust Fluid Systems and GEMOC, Macquarie University, North Ryde, 2109, Sydney, Australia
3 Geodetic and Geophysical Institute, MTA Research Centre for Astronomy and Earth Sciences, Sopron, H-9400, Hungary
4 Instituto Andaluz de Ciencias de la Tierra, CSIC & UGR, Avenida de las Palmeras 4, E-18100 Armilla (Granada), Spain

Key words: xenolith, lithospheric mantle, Pannonian Basin, metasomatism, annealing

The Nógrád-Gömör Volcanic Field (NGVF), located in the northern part of the Pannonian Basin, is one of the five key localities in the Carpathian-Pannonian region, where mantle xenoliths are hosted in late Miocene – Pleistocene alkali basalts. In recent years, over 200 spinel peridotite xenoliths were collected and examined from all xenolith-bearing localities within the volcanic field.

The xenoliths can be divided into a lherzolitic and a wehrlitic suite based on their modal and mineral compositions and textural characteristics. The lherzolitic suite bears evidence of multiple metasomatic events (Liptai et al. 2017). The last of these processes resulted in an increase in Fe-, Mn-, Ti- and LREE-content, a feature which is characteristic for the wehrlite suite as well. Wehrlitic xenoliths, present only in the central part of the NGVF, contain max. 0.5 % orthopyroxene, and consist of clinopyroxene-rich and olivine-rich parts. The wehrlitic suite is considered to be the product of an interaction between a mafic melt and the lherzolitic wallrock (Patkó et al. 2013). This process resulted in the formation of clinopyroxene at the expense of orthopyroxene. The reacting melt is most likely of asthenospheric origin, and similar in composition to the host basalt. Recent magnetotelluric measurements revealed a low resistivity body (Novák et al 2014) which suggests the presence of this melt under the central region of the NGVF.

The percolating melts had further physical effects on the upper mantle beneath the NGVF. First, it resulted in annealing, which is reflected in the microstructures of most of the lherzolite xenoliths. These features are overprinting earlier deformation events having taken place in a transpressional regime, which can be linked to recent convergent tectonics between Adria and Europe. Seismic properties of the xenoliths suggest that deformed layers are present even below the lithosphere-asthenosphere boundary.

The annealing effect of the percolating melts may also be at least partially responsible for the extremely low amount of incorporated 'water' in the nominally anhydrous mineral constituents. Olivine and both pyroxenes have undergone water loss to a degree, which is uncommon for mantle xenoliths worldwide. Such phenomenon may be caused by elevated temperatures at depth, or by rapid hydrogen diffusion (e.g., Ingrin and Blanchard 2006) during ascent or cooling on the surface. In case of the NGVF, the latter option is more likely, because xenoliths hosted in pyroclastic rocks have higher amount of incorporated 'water' compared to those hosted in basaltic lava flows.

REFERENCES

Ingrin J. and Blanchard M. (2006): Rev Min Geochem 62:291–320.
Liptai N. et al. (2017): J Petrol 58:1107–1144.
Novák A. et al. (2014): 22nd Induction Workshop Extended Abstracts: 1–4.
Patkó L. et al. (2013): Goldschmidt 2013 Conference Abstracts Min Mag 77:1934.

Garnet (almandine−pyrope series) from the Svecofennian migmatised gneiss schists (Nynäshamn, Bergslagen, Sweden)

[1]Łukasz Maciąg[#] and [2]Rafał Wróbel

[1] University of Szczecin, Faculty of Geosciences, Institute of Marine and Coastal Sciences, Marine Geology Unit, Mickiewicza 16A, 70-383 Szczecin, Poland [#]lukasz.maciag@usz.edu.pl
[2] West Pomeranian University of Technology, Faculty of Chemical Technology and Engineering, Piastów 42, 71-065 Szczecin, Poland

Key words: garnet, almandine−pyrope, gneiss, Svecofennian, Nynäshamn

INTRODUCTION

Garnets are commonly found minerals, being important indicators of regional and local metamorphism and P-T conditions. Their zonal structure and mixed chemical composition, represented mainly by almandine, pyrope, grossular, spessartine end-members, are useful tools for geothermobarometric considerations.

The almandine-pyrope is considered one of the most important geothermometers, mainly due to practically undisturbed Fe and Mg partitioning between garnets and other minerals, like biotite and pyroxenes (Koziol and Bohlen 1992).

The crystalline bedrock of central Sweden was formed in the Svecofennian (Svecokarelian) orogenic phase, under conditions of active continental margin subduction zone. Its age is Orosirian, estimated locally on 1.96-1.75 Ga. Main geological division is here the Bergslagen lithotectonic unit, composed of large variety of metamorphic and magmatic rocks. Several metasedimentary and metavolcanic types had been here distinguished (Bergman et al. 2012).

Nynäshamn is partially located on the bedrock consisting of migmatised "older granitoids", syenites of age 1.89-1.85 Ga and complex of metagreywackes, mica schists, graphite-sulphide-bearing schists, paragneiss, migmatites, quartzites and amphibolites (Bergman et al. 2012).

The regional metamorphism conditions were recognized as a low pressure and high temperature, in facies of kyanite-andalusite-syllimanite, with T=400 to 700°C and P in range of 100-500 MPa (Sjöström and Bergman 1998). Region is known also of rich skarn ore deposits (Allen et al. 2013).

MATERIAL AND METHODS

The gneiss samples containing garnets were collected in 2009 in the city of Nynäshamn, Sweden, located on the Baltic Sea coast, about 60 kilometres SW from Stockholm (Fig. 1), within house excavation nearby the city centre.

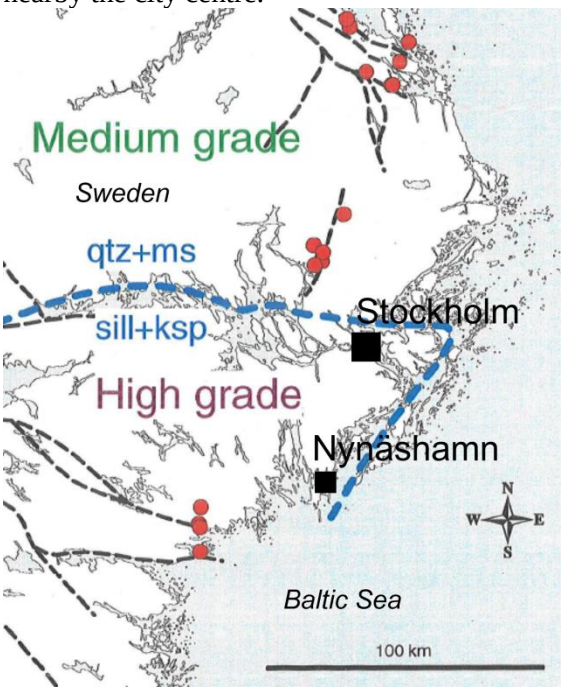

Fig. 1: The location of Nynäshamn, Sweden, Baltic coast. Blue line shows range of medium/high temperature metamorphism zone, affecting bedrock formation during Orosirian (Sjöström and Bergman 1998).

The thin and polished sections were prepared for binocular and polarising microscope observations (Zeiss AXIO Lab.A1 with digital camera) at the Faculty of Geosciences, University of Szczecin, Poland.

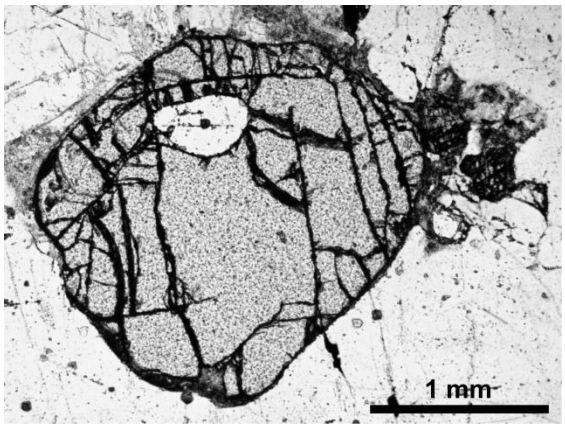

Fig. 2: The representative garnet xenomorph from Nynäshamn. In the upper part of the photo visible cracks with quartz? inclusion (1xP).

The preliminary chemical analyses were carried out at the Faculty of Chemical Technology and Engineering, West Pomeranian University of Technology, Szczecin, Poland, using cold emission SEM Hitachi SU 8070 with EDS Thermo Scientific Fisher NORAN 7. Analysis was prepared basing on two samples containing garnets.

Results of chemical microanalysis were normalized to 12 oxygens, with garnet end-members distinguished basing on a mol % cation ratio of Fe^{2+}.

The preliminary thermodynamic calculations were conducted using PT Quick Software.

RESULTS

The rock samples, containing previously non-described garnets, were identified as a migmatised gneiss schists. Some of them were recognised also as a highly homogenised, showing non-directional, medium to coarse texture. Mineralogical composition of both textural groups was however the same. Melanosome was dominated by medium to coarse biotite, distributed in 10-15 mm thick schlieren. Thicker leucosome (10-30 mm) was composed mainly of medium to coarse crystalline feldspar and quartz.

The quartz was mainly xenomorphic, in some cases with domain-like assemblages. Few myrmeckite forms were also identified.

The feldspars were represented mainly by plagioclase, with less microcline and some pertites. According to the extinction light angles (~20-45°) (compare Barker 2014), they represent series of anorthite-bytownite-oligoclase, showing typical lamellae intergrowths zonation.

The biotite was also xenomorphic, strongly pleochroic, brown- to greenish, showing traces of thermal alteration.

The other identified accessory minerals were syllimanite, kyanite, cordierite, zircon, monazite and probably some opaque ilmenite. Biotite was showing often some association with sillimanite and kyanite.

The identified garnet phenocrystals were xenomorphic, rounded and crushed, filled by feldspar-quartz and biotite, with traces of syllimanite and kyanite. Their dimensions were varying from 1 to 20 mm, however larger clusters had been revealed. Some opaque inclusions were also recognized (Fig. 2).

The representative thin section analysis is presented in Table 1.

According to the chemical analysis data, garnet end-members are major of almandine-pyrope composition, with minor spessartine and grossular admixtures. Calculated mean garnet is $Alm_{63.8}Pyr_{30.6}Grs_{3.3}Sps_{2.3}$. Only in one sample larger amount of grossular was detected (19.31 mol %).

Most garnets were showing weak zoning, with domination of pyrope in core to almandine in rim parts. In some cases reversed zoning was observed, with garnets progressively enriched with pyrope towards the rim (Tab. 2).

The decrease of the Fe and Mn contents towards the rim may reflect higher than usual diffusion at low or intermediate temperatures. However, these variations may be attributed to the post-peak metamorphic exchange between garnet and biotite (compare Sjöström and Bergman 1998).

Tab. 1: The mineral composition of migmatised gneiss from Nynäshamn basing on a thin section analysis of the NYN-1 sample.

Sample NYN-1 mineralogical composition [%]						
quartz	plagioclase	pertite	biotite	garnet	other*	total
41.47	31.78	10.07	9.69	1.17	5.81	100.00

* sillimanite, kyanite, cordierite, zircon, monazite and opaque minerals (probably ilmenite)

Tab. 2: The representative chemical data of garnet end-members from Nynäshamn, Sweden.

id	Na_2O	MgO	Al_2O_3	SiO_2	Cl	K_2O	CaO	TiO_2	MnO	FeO	Total	Spess	Gross	Pyr	Alm	zone
Nyn1_1	0.00	8.52	30.57	49.18	0.00	0.00	0.43	0.00	0.39	10.89	99.98	1.46	2.04	56.20	40.30	rim
Nyn1_2	0.00	8.88	25.60	39.28	0.00	1.44	0.45	0.00	0.84	23.47	99.96	2.09	1.42	38.87	57.63	core
Nyn1_3	0.00	6.38	26.76	45.19	0.00	0.00	0.52	0.00	0.64	20.49	99.98	1.95	2.01	34.28	61.76	core
Nyn1_4	0.00	6.15	28.53	48.72	0.00	0.00	0.34	0.00	0.63	15.60	99.97	2.31	1.58	39.67	56.45	core
Nyn1_5	0.00	9.00	25.31	42.73	0.00	0.28	0.48	0.00	0.74	21.44	99.98	1.93	1.58	41.30	55.19	core
Nyn1_6	0.00	2.23	21.27	36.85	0.00	0.00	0.67	0.00	1.36	37.60	99.98	3.14	1.96	9.07	85.82	core
Nyn1_7	6.07	7.56	20.18	50.47	1.01	0.94	0.46	0.19	0.43	12.64	99.95	4.90	2.10	47.99	45.01	rim
Nyn2_1	5.27	4.27	22.34	37.84	0.00	0.25	0.86	0.00	0.93	28.24	100.00	2.49	2.91	20.09	74.52	rim
Nyn2_2	0.56	3.26	21.70	40.96	0.00	0.62	0.87	0.00	1.07	30.96	100.00	2.78	2.86	14.91	79.45	core
Nyn2_3	0.16	5.23	26.33	45.10	0.00	0.00	0.68	0.00	0.63	21.88	100.00	1.95	2.66	28.50	66.89	core
Nyn2_4	0.40	7.12	23.00	41.63	0.00	0.00	0.70	0.00	0.77	26.38	100.00	1.91	2.20	31.15	64.74	core
Nyn2_5	0.30	4.82	24.28	43.03	0.00	0.13	0.78	0.00	0.86	25.79	100.00	2.40	2.76	23.70	71.48	rim
Nyn2_6	0.00	4.75	23.30	41.84	0.00	0.00	0.87	0.00	0.96	28.27	100.00	2.50	2.87	21.81	72.82	rim
Nyn2_7	0.00	3.43	22.35	35.63	0.00	3.86	6.43	0.00	0.74	27.55	100.00	1.76	19.31	14.35	64.55	core
Nyn2_8	0.87	7.29	24.69	42.39	0.00	0.13	0.75	0.00	0.83	23.07	100.00	2.22	2.54	34.32	60.92	core
Nyn2_9	0.16	7.28	25.52	41.25	0.00	0.14	0.65	0.00	0.60	24.42	100.00	1.56	2.14	33.41	62.88	rim
mean	0.86	6.01	24.48	42.63	0.06	0.49	1.00	0.01	0.78	23.67	99.99	2.33	3.31	30.60	63.78	
st. dev.	1.84	2.03	2.67	4.16	0.24	0.96	1.41	0.05	0.23	6.55	0.02	0.79	4.16	12.43	11.40	

The preliminary results of T-P modelling confirmed garnets formation in pressure of the range of 100-300 MPa and, however with in higher temperatures than reported before, even above 800°C.

REFERENCES

Allen R. et al. (2013): 12th Biennial SGA Meeting. Uppsala, Sweden.

Barker A. (2014): A Key for Identification of Rock-forming Minerals in Thin Section. CRC Press.

Bergman S. et al. (2012): Sveriges berggrund, skala 1:1 miljon. Sveriges geologiska undersökning, K423.

Koziol A.M. and Bohlen S.R. (1992): Am Min 77:765−773.

Sjöström H. and Bergman S. (1998): Svecofennian Metamorphic and Tectonic Evolution of Central Sweden. Uppsala.

Corrensite, tosudite and vermiculite in the hydrothermally altered andesite of Csákta- and Homorú-hill (Karancs Mts, N-Hungary)

[1]Ferenc Mádai[#], [1]Ferenc Kristály, [1]Tamás Kaszás and [1]Ferenc Móricz

[1] University of Miskolc, Faculty of Earth Science and Engineering, Institute of Mineralogy and Geology, Egyetem Street No. 1, 3515 Miskolc, Hungary [#]askmf@uni-miskolc.hu

Key words: K-alteration, propylitization, interstratified clay minerals

Karancs Mts is located on the Hungarian-Slovakian border, norther Hungary. The geology of the area is dominated by sedimentary formations, sandstone and marl beds of lower Miocene to Oligocene age. Subvolcanic andesite bodies were emplaced cca. 15 million years ago, creating contact aureole with the sedimentary formations and also undergoing a strong hydrothermal alteration. Three petrographic types are distinguished in the laccolith: amphibole andesite, hypersthene andesite and dacite, all garnet-bearing. The extensive hydrothermal alteration (K-metasomatism, propylitization, argillic alteration) were noticed earlier and tested for Pb-Zn and Au-Ag mineralization. Clay minerals, however, were studied to a lesser extent. In our work the hydrothermally generated clay mineral assemblages are investigated in relation to andesite durability quality properties. Although the overall clay mineral content of the samples is < 5 wt%, some special features require their detailed investigation.

Diagnostic clay mineral investigation shows the presence of clinochlore and vermiculite as main clay minerals, with subordinate illite (trioctahedral), smectite and kaolinite. Corrensite and tosudite were identified as minor phases.

The rock samples were described with detailed optical microscopy observations. Texture related chemical characterization was obtained by X-ray mapping with scanning electron microscopy and energy dispersive spectrometry (SEM+EDS). Bulk mineralogy was determined by X-ray powder diffraction (XRD), while bulk rock chemistry was obtained with X-ray fluorescence spectrometry (XRF). For an in-depth characterization, diagnostic clay mineral investigation was performed on oriented clay specimens with XRD.

Optical microscopy revealed the strong K-alteration with significant microcline developed in the groundmass and on the expense of neutral plagioclases. Sericitization of feldspars is significant. A three-step alteration of mafic minerals was observed. The original andesite-related mafic component was mostly hornblende. The potassic alteration generated a biotitization of hornblende, which underwent into chloritisation during the propylitic stage. These relicts have developed well-distinguished opaque aureole with magnetite and undistinguished clay mineral mixture.

SEM+EDS X-ray mapping proved K-alteration and the existence of hornblende-biotite-chlorite +/- clay mineral alteration sequences. Chemical point analysis by EDS returned a biotite-related altered clay mineral phase beyond chlorite. Magmatic feldspars were identified as zoned phenocrysts from anorthite to andesine, with some oligoclase and albite as hydrothermal phases.

XRD bulk analysis showed significant amount of quartz and microcline in the samples, as well as plagioclase with composition varying from An 50% to An 65% and subordinate An >90% presence. Traces of pyroxenes and amphiboles were also observed, with clinochlore and biotite.

XRF measurements also revealed the elevated silica content (> 50 wt%), but Mg, Ca and Fe concentrations indicate a calc-alkaline basaltic andesite nature for the intrusive phase.

According to our observations, vermiculite was formed on the expense of K-alteration derived biotite, leading to corrensite and tosudite formation in the argillic alteration stage.

Joint 5th Central-European Mineralogical Conference and
7th Mineral Sciences in the Carpathians Conference

Graphite in black schists from Dédestapolcsány (Uppony Mts.), Gadna and Szendrőlád (Szendrő Mts.) in NE-Hungary

[1]Lívia Majoros[#], [1]Ferenc Kristály and [1]Sándor Szakáll

[1] University of Miskolc, Faculty of Earth Science and Engineering, Department of Mineralogy and Petrology, Miskolc-Egyetemváros, 3515, Hungary [#]majoros.livia@gmail.com

Key words: graphitisation, graphite categorization, shear zone, black schist

Graphite is a polymorphic form of carbon crystallized in hexagonal symmetry (Dill 2010). From the 20th century, thanks to its particular chemical and physical properties graphite has become one of the most important industrial minerals. In the last decade it is included on the EU critical raw materials list. Thus, it is important to be aware of graphite occurrences and types also in Hungary.

Therefore, our aim was to examine in detail three Hungarian occurrences for graphite content, and to place them into the international industrial and geological categorizations. Moreover, we compare them with Slovak examples in order to find their analogues.

At the first occurrence (Rágyincs Valley, Dédestapolcsány in Uppony Mts) the graphite bearing rock is siliceous black shale, member of Tapolcsány Formation (Silurian, deep sea facies). At the second occurrence (Gadna, Szendrő Mts) graphite bearing rock is black phyllite, the member of the Irota Formation (Devonian, deep sea facies). The third occurrence (Szendrőlád, Szendrő Mts.) the graphite bearing rock is black phyllite (Devonian, deep sea facies).

The samples were investigated with polarizing microscopy, scanning electron microscopy (SEM-EDS) and with X-ray powder diffraction (XRD). In addition, we carried out a structural geology survey in the Dédestapolcsány area, by which in light of the mineral associations, we tried to draw conclusions regarding the origin and evolution of graphitic material.

According to our results, two types of graphite can be distinguished in the samples from Dédestapolcsány: the first one is 1-20 μm sized flaky graphite scattered in the matrix, the second one is 100-300 μm sized flaky graphite, as well, found nearby the polycrystalline quartz veins and structural elements. S content of graphite and V content of sericite indicate the organic material origin of carbon.

The sample from Gadna contains one type of graphite, 5-8 μm sized flaky form scattered between the mica plates (biotite >> muscovite). Probably, these graphite flakes are only detrital remains. The amount of graphite in the sample is negligible. Neither S, nor V was detected in the sample.

From Szendrőlád samples of a drill core were investigated, from 270-291 m depth. Graphite is present as 30-50 μm sized flakes arranged in > 300 μm lenticular and lamellar aggregates. In contrast to the first two occurrences, important calcite, clinochlore and kaolinite content is observed. Chalcopyrite and other sulphides may show hydrothermal influences.

Graphite from Dédestapolcsány was formed through low grade regional metamorphism by organic material graphitization. Formation of graphite is epigenetic and generally related to shear zones. At Szendrőlád we found also epigenetic, low grade metamorphic graphite. In contrast, graphite from Gadna is only detrital, relicts in the phyllite. However, a connection may be established, as the Darnó Zone runs through these areas.

Acknowledgment: Special thanks are due to Dr. Norbert Németh for his help in the field survey.

REFERENCES

Dill H.G. (2010): Earth Sci Rev 100:347–351.

Joint 5th Central-European Mineralogical Conference and
7th Mineral Sciences in the Carpathians Conference

Lost areas as a consequence of past mining: Case studies from Poproč, Slovakia, and Kutná Hora, Czech Republic

[1]Juraj Majzlan, [2]Petr Drahota and [3]Ľubomír Jurkovič

[1] Institute of Geosciences, University of Jena, Burgweg 11, D-07749, Jena, Germany
[#]juraj.majzlan@uni-jena.de
[2] Institute of Geochemistry, Mineralogy and Mineral Resources, Faculty of Science, Charles University, Albertov 6, 128 43 Prague 2, Czech Republic
[3] Comenius University, Faculty of Natural Sciences, Department of Geochemistry, Mlynská dolina, Ilkovičova 6, 842 15 Bratislava, Slovakia

Key words: mining waste, arsenic, antimony, environment, remediation

Mining activities produced and keep producing large amount of waste around the world. Mining industry is becoming increasingly cautious of the impact of its activity and implements new technologies. The environmental impact of mining, however, is inevitable, as long as the general population desires to possess the usual goods.

'Lost areas' are regions, be they small or larger, that are polluted to the extent that their remediation is unrealistic. Limited measures can be taken to alleviate the impact of the pollution or the best action could be defined as 'no action'. In this contribution, we present two case studies on such lost areas, with additional examples from elsewhere. One of the goals of our work is to develop a knowledge base that the current and future mining activities do not generate new lost areas.

At Kutná Hora in Czech Republic, mining for silver continued since Medieval ages until mid-20th century. Many dumps were deposited in the soft, flat relief around the city, creating a belt of fine-grained, often earthy material, particularly rich in arsenic. This material is well known for its eye-catching mineralogy, including the arsenates bukovskýite, kaňkite, zýkaite, scorodite and parascorodite. Arsenic is also stored in iron oxides and to a smaller extent in jarosite. Sequential extractions show the largest release of arsenic in the NH_4-oxalate solution (reacted with the samples in dark), confirming the association of arsenic with poorly-crystalline iron oxides and reactive arsenates. The thermodynamic analysis of the pore-water compositions shows clearly that the solubility of arsenic is controlled by iron oxides, not by the conspicuous arsenates. Hydrogeological research (Čížek et al. 2012) shows that the flat underground reservoirs are locally extremely polluted (with 1440 mg As/L) and transport this element to an unknown destination.

At Poproč in Slovakia, ores of antimony were mined between 17th and 20th century. In the modern times, the ores were processed by flotation and the flotation waste deposited in depressions along the local stream, without any barriers to the surface or underground water. The discharge from the old mines and release of Sb and As from the tailings pollute the local water to the extent that it can be used neither for drinking nor for agricultural purposes (As up to 0.1 mg/L, Sb up to 0.37 mg/L). Contaminated soils and sediments contain iron oxides (ferrihydrite and goethite), tripuhyite, and rarely other Sb-bearing minerals. Sequential extractions show that Sb remains mostly in the 'insoluble' fraction, perhaps in the form of nanocrystalline tripuhyite. At this site, we are observing natural attenuation of Sb and As. This attenuation, however, is not sufficient to retain the toxic elements and, in addition, creates secondary pollution anomalies.

References

Čížek J. (2012): Technical Report, Geofond 1236/2011. (in Czech).

Joint 5th Central-European Mineralogical Conference and
7th Mineral Sciences in the Carpathians Conference

Optical absorption spectrum of Cr^{3+} in spinel

[1]Iveta Malíčková, [1,2]Peter Bačík, [1]Jana Fridrichová, [3]Stanislava Milovská, [4]Radek Škoda, [5]Ľudmila Illášová and [5]Ján Štubňa

[1] Comenius University, Faculty of Natural Sciences, Department of Mineralogy and Petrology, Ilkovičova 6, 842 15 Bratislava, Slovakia #malickova3@uniba.sk
[2] Earth Science Institute of the Slovak Academy of Science, Dúbravska cesta 9, 840 05, Bratislava, Slovakia
[3] Earth Science Institute of the Slovak Academy of Science, Geological Division, 974 01 Ďumbierska 1, Banská Bystrica, Slovakia
[4] Masaryk University, Faculty of Science, Department of Geological Science, Kotlářská 267/2, 611 37 Brno, Czech Republic
[5] Constantine the Philosopher University in Nitra, Faculty of Natural Science, Gemological Institute, Nábrežie mládeže 91, 949 74 Nitra, Slovakia

Key words: optical spectroscopy, spinel, chrome, Raman spectroscopy, Tanabe-Sugano diagrams

INTRODUCTION

Spinel ($MgAl_2O_4$) contains various concentrations of Cr^{3+} ions in the octahedral coordination. Spinel belongs to the cubic space group O_h^7 with eight formula units per cell and two sites for metal ions. The *A* site (Mg) has the tetrahedral coordination with T_d symmetry and the *B* site (Al, Cr) is six-fold distorted with octahedral coordination in D_{3d} point group (Wood and Imbusch, 1968).

We studied one crystal fragment of natural spinel from Mogok. In this study, we would like to emphasize the role of 3*d* elements and their crystal field energy on the absorption of visible light induced by the electron transitions on the example of Cr-bearing spinel.

METHODS

Raman spectroscopy was performed by LabRAM-HR Evolution (Horiba Jobin-Yvon) spectrometer system with a Peltier cooled CCD detector and Olympus BX-41 microscope (Masaryk University, Department of Geological Sciences). Raman spectra were excited by 473 nm frequency-doubled diode laser and a 520.6 cm^{-1} silicon wafer enabled spectral calibration. Spectra ranged from 100 to 10 000 cm^{-1} with acquisition time of 10 s per frame and 2 accumulations.

Optical absorption spectra of samples in the region (400–750 nm) were measured with the GL Gem SpectrometerTM at room temperature in the Gemological Institute of Constantine the Philosopher University, Nitra.

Chemical composition was determined by micro X-ray fluorescence spectroscopy (micro-XRF) using an instrument M4 TORNADO, Bruker (Earth Science Institute of the Slovak Academy of Science, Banská Bystrica). Incident X-ray beam (Rh anode) was focused by polycapillary optics to 25-micron spot, interaction depth was ca. 10-1000 µm, excitation current 600 µA at 50 kV. Analyses were acquired at 20 mbar vacuum. A silicon drift detector (SDD) collecting the fluorescence signal has an active area 30 mm^2 and spectral resolution 145 e. Measuring time of point analyses was 70 s, live time 60 s, energy range of 0.25-20 keV. Element concentrations were computed by fundamental parameters method.

RESULTS

Results obtained from XRF analysis (Table 1) were not converted to crystal-chemical formula, but are reported in wt. % because the measured data did not have sufficient precision to calculate the stoichiometric formula. Spinel (SPM-1) was measured on two spots, and the highest content of Al and Mg corresponds to the composition of the spinel; it is also enriched in Cr, V, Fe. On the basis of the measurements, we can claim that this is Cr-enriched spinel (Fig. 1).

Raman bands (Fig. 2) were assigned according to Slotznick and Shim (2008); 307

and 662 cm^{-1} to T_{2g} symmetry, 403 cm^{-1} to E_g and 763 cm^{-1} to A_{1g}.

Fig. 1: Red Cr-enriched spinel SPM-1.

The optical absorption spectrum of spinel has broad band in range of 400 – 600 nm with maxima at 454 and 551 nm (Fig. 3). Significant absorption is in ultraviolet, yellow-green region, weak transmission is observed in the green and significant transmission in the red region. The resulting colour of the spinel is red.

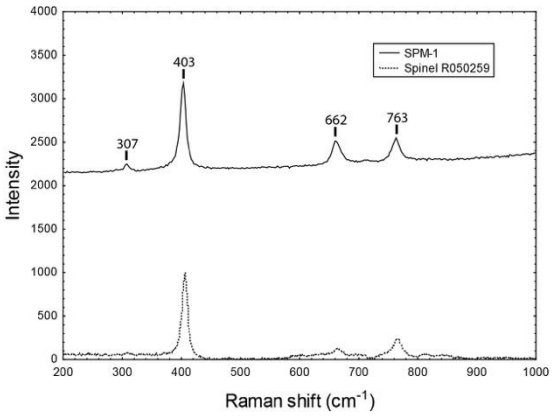

Fig. 2: Raman spectrum of spinel SPM-1, compared to RRUFF database (dashed line).

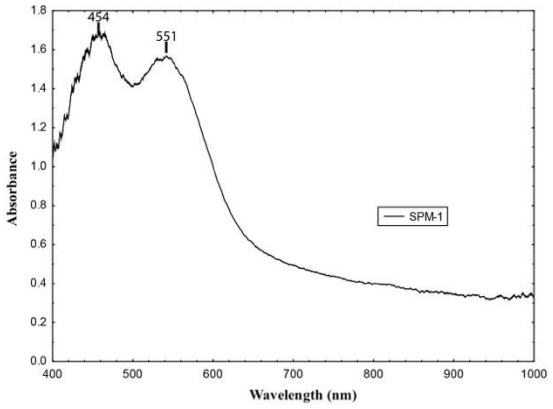

Fig. 3: Optical spectrum of the studied spinel SPM-1.

Table 1: Chemical composition of spinel SPM-1.

	SPM-1 1 (wt. %)	SPM-1 2 (wt. %)
SiO_2	0.79	0.76
TiO_2	0.07	0.07
Al_2O_3	68.36	68.39
Cr_2O_3	3.96	3.96
V_2O_3	0.63	0.62
FeO	0.15	0.15
MnO	0.02	0.02
MgO	24.23	24.26
CoO	0.00	0.00
NiO	0.01	0.01
SrO	0.02	0.02
CaO	0.50	0.48

DISCUSSION

In general, spinel colour can be caused by e.g. Cr^{3+}, Fe^{2+}, Fe^{3+} and Co^{2+}. The red colour is due to Cr^{3+} at the octahedral site (Fritsch & Rossman, 1988). According to Wood and Imbrusch (1968) our maxima at 454 nm and 551 nm can be assigned to Cr^{3+}, and spin-allowed transitions $^4A_{2g} \Rightarrow {}^4T_{2g}$, $^4A_{2g} \Rightarrow {}^4T_{1g}$.

Once the photons of radiation are absorbed in the ultraviolet and visible regions of the electromagnetic spectrum, the electron configuration changes (Kováč et al., 1987). The electronic configuration for Cr^{3+} is [Ar]3d^3. The content of vanadium was very low compared to chromium. We can assume that vanadium has only minor influence on the crystal field energy. Chromium in an octahedral coordination has t_{2g}^3 configuration in the ground state, which gives rise to $^4A_{2g}$, ^2E_g, $^2T_{1g}$ a $^2T_{2g}$ states. The $^4A_{2g}$ state is the ground state for the chromium ions. The $t_{2g}^2e_g$ excited configuration, gives rise to $^4T_{2g}$, $^4T_{1g}$ states (Lakshman & Reddy, 1974). The spin-allowed $^4A_{2g} \rightarrow {}^4T_{1g}$ transition corresponds to the absorption band at 454 nm (22,026 cm^{-1}), and $^4A_{2g} \rightarrow {}^4T_{2g}$ corresponds to the absorption band at 551 nm (18,148 cm^{-1}) (Fig. 4). The extent of the *d* orbital scattering is defined by Δ_o (crystal field parameter), which indicates the crystal field energy (Housecroft & Sharpe, 2005). The ratio of the absorption bands is 1.2. In the Tanabe-Sugano diagram, the same ratio of allowed transitions is Δ_o/B =50.93. First

transition at this Δ_o/B corresponds to E/B (ν_1/B) energy of 50.93. Second transition corresponds to E/B (ν_2/B) of 62.09. Resulting Racah parameter B is 356.3 cm^{-1}.

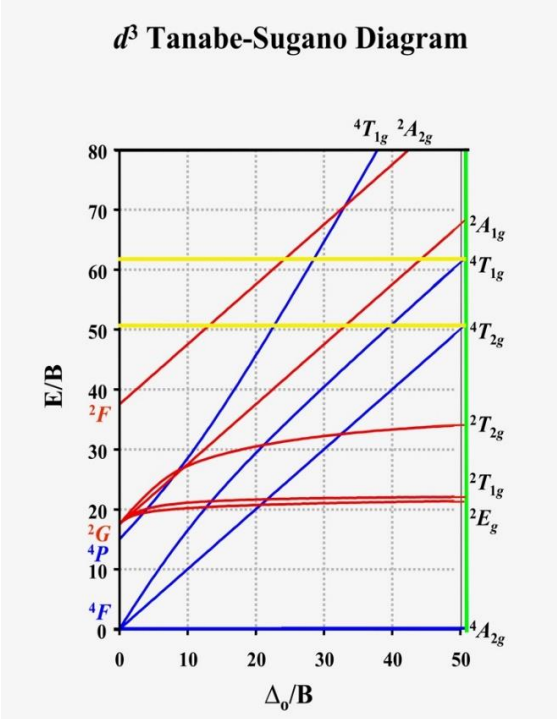

Fig. 4: Tanabe Sugano diagram of d^3 configuration with Δ_o/B of spinel SPM-1 (https://chem.libretexts.org, modified).

Trivalent central atom has 40-80% greater crystal field energy than divalent cation (Housecroft & Sharpe, 2005). Crystal field energy is: Δ_o/B = 50.93, Δ_o = B*50.93 = 356.3 * 50.93 = 18,148 cm^{-1}.

The ruby has Δ_o around 18,000 cm^{-1}, which is lower than the studied spinel. Stronger crystal field is probably caused by the presence of divalent neighbours (Mg^{2+}) instead trivalent ones as in the case of ruby (Al^{3+}) or Y-Al garnet (Y^{3+}, Al^{3+}) (Wood and Imbusch, 1968).

Conclusion

We measured two absorption bands at 454 nm and 551 nm. We calculated the crystal field energy, Δ_o/B = 18,148 cm^{-1}. The spin-allowed transitions $^4A_{2g} \rightarrow {}^4T_{2g}$ are associated with a configuration change $t_{2g}^3 \rightarrow t_{2g}^2$, which leads to the excitation of many vibrations and results in a broad band in the optical spectrum. On the other hand, the spin-forbidden transitions are $^4A_{2g} \rightarrow {}^2E_g$ and $^4A_{2g} \rightarrow {}^2T_{1g}$ based on the configuration t_{2g}^3. The energies of the intra-configurational spin-forbidden are not dependent upon $10D_q$ (Δ_o).

References

Fritsch E. and Rossman G. (1988): Gems & Gemology 24:81–102.

Housecroft C.E. and Sharpe A.G. (2005): Inorganic Chemistry, Pearson Prentice Hall.

Kováč Š. et al. (1987): Methods of Technological Process Control: Spectral Methods in Organic Chemistry and Technology. Alfa, Bratislava.

Lakshman S.V.J. and Reddy B.J. (1974): Physica 71:197–203.

Rossman G.R. (2018): Min Spec Server. http://minerals.gps.caltech.edu/. [20.3. 2018].

Slotznick S.P. and Shim S.H. (2008): Am Min 93:470–476.

Wood D.L. and Imbrusch G.F. (1968) J Chem Phys 48:5255–5263.

https://chem.libretexts.org/Core/Inorganic_Chemistry/Crystal_Field_Theory/Tanabe-Sugano_Diagrams [16.04.2018; 10.05]

Joint 5th Central-European Mineralogical Conference and
7th Mineral Sciences in the Carpathians Conference
Banská Štiavnica 2018

Bi-sulphosalts from the Mazhiq, Stan Terg area, Kosovo

[1]Sławomir Mederski[#], [1]Jaroslav Pršek, [2]Burim Asllani and [1]Gabriela Kozub-Budzyń

[1] AGH University of Science and Technology, Faculty of Geology, Geophysics and Environmental Protection, Department of Economic Geology, al. A. Mickiewicza 30, 30-059 Kraków, Poland
[#]mederski@agh.edu.pl
[2] E&E Experts LLC, 10000, Prishtina, Republic of Kosovo

Key words: Bi-sulphosalts, Mazhiq, cosalite, krupkaite, bismuthinite

Mazhiq occurrence is located in the northern part of Kosovo, 2 km east of Stan Terg Pb-Zn(-Ag-Bi) deposit within Vardar Zone. The area is composed of Tertiary volcanic and pyroclastic rocks of andesite, trachyte and latite composition. The polymetallic mineralization is related to the Oligocene – Miocene magmatic activity. Within the Trepça Mineral Belt Bi-sulphosalts were previously described only at the Stan Terg deposit by Terzić et al. (1974) and Kołodziejczyk et al. (2015; 2017). The objective of this study was compare new occurrence of these minerals in Stan Terg area with previous works.

Several chalcopyrite veinlets up to 10 cm wide are observed within the pyroclastic rocks in Mazhiq area. Moreover, numerous mineralized boulders with galena, arsenopyrite, sphalerite, Bi-sulphosalts, Mn-oxides, quartz and Mn-carbonates were found. Bismuth sulphosalts occur in needle like form up to 1 cm long. The bismuth sulphosalts were investigated by reflected light and EPMA analyses.

Bi-sulphosalts are present as polymineral aggregates composed of intergrowth of three main mineral phases together with pyrite and chalcopyrite. Additionally tiny monomineral idiomorphic crystals are observed in the samples. Cosalite and members of the bismuthinite – aikinite series (krupkaite, bismuthinite and pekoite) were recognized.

Cosalite with approximate formula $(Cu_{0.74}Ag_{0.28})_{\Sigma\ 1.03}(Fe_{0.04}Pb_{7.51})_{\Sigma\ 7.55}(Bi_{8.38}Sb_{0.1})_{\Sigma\ 8.48}Se_{0.01}S_{19.99}$ (calculated cf. Topa & Makovicky 2010) is characterized by homogenous chemical composition. Cosalite crystals from Mazhiq have high content of Cu (0.6–1 apfu), low content of Fe (0–0.2 apfu) and Sb (approx. 0.1 apfu) compared to cosalite from Stan Terg deposit (Cu approx. 0.19 apfu; Fe 0.14–0.4 apfu; Sb up to 3.9 apfu) (Kołodziejczyk et al. 2017). In addition cosalite has high Pb content (approx. 7.5 apfu).

Minerals from bismuthinite – aikinite series are represented by krupkaite (n_{aik}=48.8-49.4), bismuthinite (n_{aik}=3.01-11.46) and pekoite (n_{aik}=18.95).

Krupkaite crystals are characterized by homogenous chemical composition and occurs as irregular crystals at the contact between cosalite and bismuthinite crystals.

The content of Sb in bismuthinite varies from 0.02-1 wt. % at, but content of Pb varies from 1.9-3.7 wt. %. Bismuthinite from Mazhiq is characterized by higher Cu content (1 wt. %) than bismuthinite from Stan Terg deposit (0.01 wt. %) (Kołodziejczyk et al. 2015). One analyse occurs above bismuthinite field (n_{aik}=11.46) (cf. Topa et al. 2002) and has the highest Cu and Pb content (Cu - 1.5 wt. %, Pb - 6.3 wt. %). Another analyse occurs above pekoite field (n_{aik}=18.95) and has high Cu and Pb content (Cu - 2.6 wt. %; Pb - 4.2 wt. %). The association of the Bi-sulphosalts show potential for occurrence of other Bi-sulphosalts and the deposit could be compare rather to the Romanian skarns (Ocna de Fier, Baita Bihorului) than Stan Terg deposit.

REFERENCES

Kołodziejczyk J. et al. (2015): Neues Jahrb Min Abh 192:317–333.

Kołodziejczyk J. et al. (2017): Geol Carpath 68:366–381.

Terzić S.B. et al. (1974): Schweiz Min Petrog Mitt 54:209–211.

Topa D. et al. (2002): Can Min 40:849–869.

Topa D. and Makovicky E. (2010): Can Min 48:1081–1107.

Joint 5th Central-European Mineralogical Conference and
7th Mineral Sciences in the Carpathians Conference
Banská Štiavnica 2018

W-(V, Cr, Fe) bearing rutile from the Ochtiná W-Mo deposit, Slovakia (preliminary study)

[1]Tomáš Mikuš[#], [2]František Bakos, [1]Stanislava Milovská, [3]Peter Koděra, [4]Juraj Majzlan, [5]Martin Števko, [2]Maroš Sýkora and [3]Jozef Majtán

[1] Earth Science Institute, Slovak Academy of Sciences, Ďumbierska 1, Banská Bystrica, Slovakia
[#]mikus@savbb.sk
[2] GREEN VIEW, s.r.o., Nevädzová 5, 821 01 Bratislava, Slovakia
[3] Comenius University, Faculty of Natural Sciences, Department of Economic Geology, Ilkovičova 6, Mlynská dolina, 842 15 Bratislava, Slovakia
[4] Institute of Geosciences, University of Jena, Burgweg 11, D-07749, Jena, Germany
[5] Department of Mineralogy and Petrology, National Museum, Cirkusová 1740, 193 00 Prague 9, Czech Republic

Key words: rutile, substitutions, tungsten, geochemistry, Ochtiná

Rutile is a widely distributed mineral in alteration haloes associated with a variety of hydrothermal and metamorphosed ore deposits, and although poorly studied, anomalous rutile compositions appear to reflect significant metal concentrations in many types of orebodies.

Ochtiná W-Mo deposit represents vein-stockwork and disseminated tungsten mineralization with quartz, pyrite, scheelite, wolframite and molybdenite as dominant minerals. Mineralization is developed in the contact zone of two major tectonic units: Gemeric and Veporic, predominantly in the rocks belonging to the Ochtiná formation (represented by basic volcanics, shales and sandstones metamorphosed in green schist facies).

Rutile is a common accessory phase at the Ochtiná deposit, spatially closely related to W mineralization. It forms euhedral to anhedral grains up to first hundreds of μm enclosed in quartz together with mica and molybdenite. Typical features of the studied rutile are sector or oscillatory growth chemical zoning with preserved homogenous cores. Rutile shows a rather unique chemical composition; especially interesting is content of tungsten, which can reach up to 0.14 apfu of W and had not been detected in rutile before. Beside tungsten, rutile has elevated contents of Fe (up to 0.1 apfu), Cr (up to 0.18 apfu) and V (up to 0.10 apfu). In all its substitutive variations, rutile was confirmed by micro Raman spectroscopy as the only present TiO_2 polymorph.

Isomorphic capacity or compatibility of rutile with trace elements and therefore their content in rutile depends on many factors, such as valence and effective ionic radii of the octahedrally coordinated trace elements, genetic type of host rock and its concentration of trace elements. Incorporation of cations with a valence higher or lower than 4 into the structure of rutile requires charge compensation. The charge balance mechanisms and coupled cation compensation substitutions derived from the correlation ratios are considered: R^{3+}(Fe, V, Al) + R^{5+}(Nb, Ta, Sb) → $2Ti^{4+}$, $2R^{3+}$ + R^{6+}(W) → $3Ti^{4+}$, R^{2+}(Ca, Sr, Mg) + $2R^{5+}$ → $3Ti^{4+}$ and so on (e.g. Rice et al. 1998; Scott and Radford, 2007). In general, coupled cation substitutions should satisfy the condition $2R^{2+} + R^{3+} = R^{5+} + 2R^{6+}$.

Acknowledgment: This work was financially supported by the VEGA project (2/0023/17).

REFERENCES

Rice C.M. et al. (1998): Min Mag 62:421–429.
Scott K.M. and Radford N.W. (2007): Expl Env Anal 7:353–361.

Authigenic vivianite in glacial sediments of Batizovské pleso, Tatra Mts., Slovakia

[1]Stanislava Milovská[#], [1]Adrián Biroň, [1]Radovan Pipík, [1]Juraj Šurka, [2]Dušan Starek, [3]Peter Uhlík, [1]Tomáš Mikuš, [1]Jana Rigová, [1]Lucia Žatková and [1]Marina Vidhya

1 Earth Sciences Institute of the Slovak Academy of Sciences, Ďumbierska 1, Banská Bystrica, Slovakia [#]milovska@savbb.sk
2 Earth Sciences Institute of the Slovak Academy of Sciences, Dúbravská cesta 9, Bratislava, Slovakia
3 Comenius University, Faculty of Natural Sciences, Department of Economic Geology, Ilkovičova 6, Mlynská dolina, 84215, Bratislava, Slovakia

Key words: phosphate, vivianite, lake sediments, deglaciation, High Tatra Mts.

The Batizovské pleso is a glacial mountain lake, located in Batizovská dolina (Tatra Mts.) at an altitude 1884 m a.s.l., with surface area of 3 ha. Lake is dammed by granitoid bedrock, recharged by underground flow through blocky moraines and discharged by one surface stream. Two sediment cores were taken by percussion corer in 2016.

Microchemical scanning by X-ray fluorescence (XRF) revealed distinct phosphate enrichment in some laminae, rare dark blue drusy aggregates of vivianite $Fe^{2+}_3(PO_4)_2 \cdot 8H_2O$ are bound to these layers, of size up to 18 mm. Vivianite concretions are buried in the depth of 315 cm within finely laminated, organic-poor sequence presumably deposited in periglacial conditions. Sediment is composed of quartz, plagioclase, K-feldspar, muscovite, illite/smectite, chlorite, kaolinite and biotite, grain-size fraction <0.06 mm dominates. Alternating dark- and light grey laminae have thickness ca. 0.5 – 2 mm, dark laminae are enriched in iron and fine grained organic matter.

Vivianite was identified by means of XRPD analysis and Raman spectroscopy. Its structure was described using Pawley refinement. A monoclinic cell with a = 10.009(12), b = 13.416(7), c = 4.706(5) Å, β = 102.53(5) ° and space group I2/m could be used to fit its structure. The basic features in Raman spectra correspond to vivianite, with lattice modes below 360 cm^{-1}, internal modes at 454, 540, 835, 950, 1054 cm^{-1}, and vibrations of molecular water at frequencies 3100 – 3500 cm^{-1}. The structure of vivianite partially degrades under oxidative conditions, resulting in decay of spectra. XRF analyses show enrichment in Mn.

Vivianite nodules form postdepositionally in lake sediments, when Fe^{III} oxyhydroxides dissolve under reducing conditions in absence of sulfur. Released Fe^{II} and sorbed P reprecipitates in form of Fe^{II} phosphates. Source of phosphorus is an open question – organic-bound phosphorus or weathering of accessory phosphates in granitoids come under consideration.

Acknowledgment: This work was supported by the project APVV-15-0292.

Metamorphism of the Western Hindukush based on the crustal xenoliths in metaigneous rocks

[1]Hezbullah Moiny[#] and [1]Shah Wali Faryad

[1]Charles University, Faculty of Science, Institute of Petrology and Structural Geology, Albertov 6, 128 43 Prague 2, Czech Republic [#]moinyhe@natur.cuni.cz

Key words: crustal xenoliths, metamorphism, Western Hindu Kush

The Western Hindu Kush refers to a ca 220 km long segment of nearly east–west trending high mountains which continue eastward through the Central and Eastern Hindu Kush to the Karakoram. It is bounded by the Panjshir fault in the east and the Bamiyan–Shibar fault in the west. The rocks exposed on the surface are interpreted as Paleoproterozoic and Paleozoic basement that show various degrees of metamorphism and intruded by Triassic to Paleogene granite–granodiorite plutons (Vallbrecher 1973; Bouline 1991; Faryad et al. 2013).

We examined xenoliths of crustal rocks within amphibolite facies metgranodiorite exposed at the triple points of two crustal blocks (Kabul and Nuristan) with the Western Hindu Kush. The xenoliths are represented by calc-silicate rocks and mafic granulite. In addition to almost monomineralic clinopyroxene and garnet-scapolite-bearing calc-silicate an orthopyroxene-bearing granulite was also selected for detailed study. It was aimed to analyse, whether the xenoliths derived from the surrounding basement units or from the high-grade Kabul Block, which is pushed beneath the Western Hindu Kush. Various thermo-barometric methods and pseudosection technique were applied both to xenoliths, host metagranite and surrounding basements rocks.

The results show that the surrounding basement rocks, previously assumed as medium-grade metamorphosed volcano-sedimentary sequence, preserve relicts an earlier granulite facies minerals. In addition to K-feldspar and sillimanite in metapelite, the mafic rocks contain clinopyroxene, anorthite-rich plagioclase and rarely spinel. They are strongly retrogressed and together with the Cretaceous granodiorite affected by the Eocene amphibolite facies metamorphism (Faryad et al. 2013). In addition to thermal effects by granite intrusion and subsequent amphibolite facies metamorphism, the granulite facies xenolith still contains equilibrium assemblage of plagioclase + orthopyroxene + quartz + cummingtonite + ilmenite. The results show low-to medium-pressure granulite facies conditions for the xenoliths and for the surrounding basement rocks. The calculated PT conditions for this high-grade are similar to those estimated for the Archaen-Paleoproterozoic orthogneiss exposed in the central part of the Kabul Block (Faryad et al. 2016).

Acknowledgment: This study is supported by the Charles University (project GAUK 243 250 373) and Czech Science Foundation (project. 18-03160S).

References

Boulin J. (1991): Tectonophysics 196:211–268.
Collett S. et al. (2017): J Met Geol 35:253–280.
Faryad S.W. (2013): Lithos 175:302–314.
Faryad S.W. (2016): Gond Res 34:221–240.
Wallbrecher E. (1974): PhD thesis, Freien Universität Berlin, pp. 150.

Garnet from Julianna Pegmatite System, Sudetes – record of magmatic to hydrothermal evolution

[1]Krzysztof Nejbert[#], [1]Sławomir Ilnicki, [2]Adam Pieczka, [3]Eligiusz Szełęg, [4]Adam Szuszkiewicz and [4]Krzysztof Turniak

[1] University of Warsaw, Faculty of Geology, Al. Żwirki i Wigury 93, 02-089 Warszawa, Poland [#]knejbert@uw.edu.pl
[2] AGH – University of Science and Technology, Department of Mineralogy, Petrography and Geochemistry, Mickiewicza 30, 30-059 Kraków, Poland
[3] University of Silesia, Faculty of Earth Sciences, Department of Geochemistry, Mineralogy and Petrography, Będzińska 60, 41-200 Sosnowiec, Poland
[4] University of Wrocław, Institute of Geological Sciences, Cybulskiego 30, 50-205 Wrocław, Poland

Key words: garnet, Sc minerals, Ca-REE metasomatism, Julianna Pegmatite System, Sudetes

The Julianna Pegmatite System discovered within migmatites, amphibolites, and retrogressed eclogites at Piława Górna, Góry Sowie Block represents mixed NYF+LCT anatectic pegmatite type. Its origin is related with tectonic exhumation of the Góry Sowie Block that undergone polymetamorphic evolution ca. 370–385 Ma, finally under amphibolite facies metamorphism. Pegmatite bodies distributed at all levels of the mine, are represented by (I) numerous thin primitive anatectic pegmatites with a thickness range from a few cm up to 0.5 m, and (II) not very common highly fractionated pegmatite veins (up to 6 m in thickness), characterized by well developed zoning, typical for granitoid pegmatites. Relations between individual pegmatite veins are difficult to trace, mainly due to a sudden change in the thickness of pegmatite bodies.

Garnet occurs in various amounts both in thin, primitive pegmatite veins (I type) and in the highly fractionated pegmatites (II type). It is therefore a universal tool to track the genetic relationships of individual pegmatite veins. In highly fractionated pegmatites (II type), garnet is present: in graphic intergrowths zone, sometimes in paragenesis with biotite; occur in the blocky feldspar zone, where coexist with muscovite and tourmaline; and less frequently in the quartz core. Garnet commonly forms euhedral crystals (up to 6 cm in diameter), and a spectacular skeletal garnet intergrowths with quartz, feldspar, or muscovite, up to 20 cm in diameter.

Garnet in all pegmatites is represented by spessartine-almandine, with Mn/(Fe+Mn) ratio varying from 0.41 (most primitive - 0.02 at TRIO) to 0.98 (most Mn enriched, in the Jan pegmatite vein, LCT pegmatite type). The most spessartine enriched garnet were found as small euhedral inclusions within spodumene (up to 99.55 % of spessartine) that crystallized contemporaneously with the host mineral. The progressive change from almandine/spessartine garnet to spessartine dominated reflect fractionation of pegmatitic melts during magmatic evolution stage of the Julianna Pegmatite System. Garnets crystallized from weakly fractionated melts show enhanced concentration of Y_2O_3 (up to 1.11 wt.%) and Sc_2O_3 up to 0.23 wt%). In one pegmatite vein, with light pink quartz core, almandine-spessartine garnets contains numerous inclusions of thortveitite (Sc/Y ~1.37-0.85).

Garnet from hydrothermal/metasomatic stage is characterized by an increased content of CaO (up to 36,38 % of grossular end-member). Texture is a main criterion for distinguishing these generations of garnet. Secondary generations of garnet form characteristic network replacment along cracks within primary garnet, or crystallize as anhedral grains, arranged along the fractures or cleavage planes, together with a fine-grained muscovite.

Acknowledgment: The NCN grant No 2015/19/B/ST10/01809 supported the study.

Fenitization in the Eastern part of the Bükk Mts, NE Hungary

[1]Norbert Németh[#], [2]Ferenc Kristály and [2] Ferenc Móricz

[1] University of Miskolc, Faculty of Earth Science and Engineering, Department of Geology and Mineral Deposits, Miskolc-Egyetemváros, 3515 Miskolc, Hungary [#]foldnn@uni-miskolc.hu
[2] University of Miskolc, Faculty of Earth Science and Engineering, Department of Mineralogy and Petrology, Miskolc-Egyetemváros, 3515 Miskolc, Hungary

Key words: metasomatic alteration, HFSE, Bükk Mts

Geochemical sampling and assaying in 2014 revealed the existence of a hitherto unknown alteration paragenesis in the Permo-Triassic successions of the Bükk Mts (Németh et al. 2016). The characteristic geochemical feature is the significant enrichment (5-10 times compared to the upper crust and the host rock average) of several high field strength elements: Nb, Ta, Th, Zr and rare earth elements except Eu, together with enrichment of potassium. Host rocks are either metavolcanic layers or siliciclastic beds embedded in limestone with a thickness of some meters or decimeters. The limestone country rock bears no signs of any effects of the alteration even in the direct contact with the altered beds.

Common minerals of the alteration paragenesis are monazite-(Ce), zircon and niobian rutile. Monazite and zircon grains are typically smaller than 10 μm. Monazite occurs disseminated or in small nests, together with potassic feldspars usually. Zircon tends to concentrate in cleavage domains or veinlets crosscutting the cleavage together with phyllosilicates, or as replacement together with niobian rutile. The rutile forms grains or groups of 10-100 μm size. Further minerals found mainly in sedimentary samples are parisite-(Ce), bastnäsite and nioboaeschynite-(Y). Potassic feldspars and phyllosilicates were also formed, while other minerals of the host rocks were altered or replaced. Affected metavolcanics were found depleted in Ba, Fe, Mn, Mg, Na and P indicating the destruction of chlorite and albite. Pyrite was oxidized with the formation of a characteristic coating containing also Si and Al.

Local enrichments and minerals of the HFSE were also found in albitized metavolcanics, associated to quartz-albite veins crosscutting the cleavage (Zajzon et al. 2014). The main REE bearing phase of the albitized rocks is allanite-(Ce) as an alteration product of epidote.

The paragenesis corresponds to a low-temperature fenitization caused by alkaline fluids. The mineralization overprints the fabric of the host rocks, so it has to be a later metasomatic event than the regional metamorphism and synmetamorphic ductile deformation known in this part of the Bükk Mts. Altered bodies are located in two major fault zones bordering different tectofacies units, which may have been the structural control of the mineralization. However, there is no known possible magmatic source for the fluids.

References

Németh N. et al. (2016): Földtani Közlöny 146:11–26.

Zajzon N. et al. (2014): CriticEl Monography Series 5:91–108.

Joint 5th Central-European Mineralogical Conference and
7th Mineral Sciences in the Carpathians Conference

Ore-mineral textures of Cu-bearing marls from the North Sudetic Synclinorium, SW Poland

[1]Izabella Nowak and [2]Krzysztof Nejbert

[1] KGHM Cuprum Ltd Research and Development Centre, ul. Gen. Wł. Sikorskiego 2-8, 53-659 Wrocław, Poland #inowak@cuprum.wroc.pl
[2] University of Warsaw, Faculty of Geology, Al. Żwirki i Wigury 93, 02-089 Warszawa, Poland

Key words: Cu-Ag mineralization, Cu-bearing marls, North Sudetic Synclinorium, Poland

Ore mineralogy in the North Sudetic Synclinorium (NSS) in SW Poland, as in the Pre-Sudetic Monocline (PSM), is dominated by chalcocite group minerals (CGM), yarrowite, covellite, bornite, chalcopyrite, and pyrite. Galena, sphalerite, tennnatite-tetrahedrite, silver, stromeyerite, and eugenite are commonly observed (Konstantynowicz 1965; Kucha 2007). The five-stage genesis of the Cu-Ag mineralization observed in these areas is related with late-diagenetic and low-temperature hydrothermal processes (Wodzicki, Piestrzyński 1994).

In the NSS the largest quantities of the Cu-sulphides are observed in Cu-bearing marls from Leszczyna area and underground Konrad Mine. Bornite, Zn-tennnatite and chalcopyrite are subordinate. Optical properties, textures, as well as Cu/S ratios of the CGM are varied. The Cu/S ratios fill range from 0.02 to 2 that is interpreted as presence of chalcocite, djurleite, anilite, spionkopite, geerite, roxbyite, yarrowite, and covellite.

Two textural types (I and II) of CGM are found in the Cu-bearing marls. The type of I consist of chalcocite and djurleite forming large aggregates and co-occurring with a Zn-tennantite, bornite and chalcopyrite. Small amounts of unknown $ZnAs_2$ phase (~ 30.8% wt.% Zn and ~ 69.4 wt.% As) are found in association with the Zn-tennantite. Inside the textural generation of type I, cuprite and cerussite pseudomorphs after Cu, Pb minerals belonging to the early stage of the mineralization, are also observed. Numerous small Ag-native inclusions in cuprite and neighboring chalcocite or djurleite are present. In addition, the CGM with cuprite intergrowth have relatively high values of Ag (from 2.44 to 7.45 wt.%), while average of all chalcocite analyses was close to 0.67 wt.%.

The textural CGM of type II is represented by anilite, spionkopite, geerite, roxbyite, yarrowite, and covellite. The Cu-sulphides have low Ag content, rarely exceed 0.3 wt.% and form single grains or small intergrowths dispersed regularly in the matrix of the rocks.

Textural relations of ore-minerals in the Cu-bearing marls of the NSS indicate the record of at least two stages of ore mineralization. Hydrothermal solutions, from which generation CGM of the I textural type crystallized, affected previously existing Cu-S sulfides. During these interactions, existing chalcocite and djurleite were transformed under the influence of acidic sulphate solutions into anilite, geerite, roxbyite, spionkopite, yarrowite, and covellite (II textural type). The conditions and course of these processes may have been carried out in accordance with the model described by Whiteside et al. (1986) and Large et al. (1995).

Acknowledgment: The study was supported by KGHM Cuprum – Research and Development Centre as part of the project: "Integrated geochemical and mineralogical research as a method of exploration of Cu-Ag-Pb-Zn mineralization".

REFERENCES

Konstantynowicz E. (1965): Prace Geol 28: 1–109.

Kucha H. (2007): Biul PIG 423:77–94.

Large D.J. et al. (1995): Econ Geol 90:2143–2155.

Whiteside L.S. and Goble R.J. (1986): Can Min 24:247–258.

Wodzicki A. and Piestrzyński A. (1994): Min Deposita 29:30-43.

Galena alteration to cerussite and phosphohedyphane by carbonated fluids in Permian aplite (Western Carpathians, Slovakia)

[1]Martin Ondrejka[#], [2]Tomáš Mikuš, [1]Peter Bačík, [1]Marián Putiš, [1]Pavel Uher and [2]Jarmila Luptáková

[1] Comenius University, Faculty of Natural Sciences, Department of Mineralogy and Petrology, Ilkovičova 6, Mlynská dolina, 84215 Bratislava, Slovakia [#]martin.ondrejka@uniba.sk
[2] Slovak Academy of Sciences, Earth Science Institute, Ďumbierska 1, 97401 Banská Bystrica, Slovakia

Key words: phosphohedyphane, cerussite, galena, fluid-rock interaction, alteration

A unique assemblage of Ca-Pb phosphates belonging to the apatite supergroup (ASM), namely phosphohedyphane $Ca_2Pb_3(PO_4)Cl$ and "hydroxylphosphohedyphane" $Ca_2Pb_3(PO_4)OH$ in association with cerussite $PbCO_3$, calcite and rarely also *REE* carbonates [bastnäsite $Ce(CO_3)F$ to synchysite $CaCe(CO_3)_2F$)] where identified in the Permian aplite dykes crosscutting the orthogneisses from the pre-Alpine basement in the Veľký Zelený Potok Valley - VZP (the Veporic Unit, Western Carpathians, central Slovakia). The chemical composition of these ASM suggest the presence of Pb, Ca, P and Cl being the dominant constituents and $Pb^{2+}\leftrightarrow Ca^{2+}$ being the dominant homovalent substitution at the non-equivalent large cation *M*1 and *M*2 crystallographic sites. However, some minor isomorphic substitutions at *T* and *X* sites including $P^{5+}\leftrightarrow As^{5+}$, $P^{5+}\leftrightarrow(CO_3)^{2-}$ and $Cl^{-}\leftrightarrow OH^{-}$ were also reported. X-ray compositional mapping and microRaman spectra suggest the systematic presence of $(CO_3)^{2-}$ anion group in ASM and it is the first time reported carbonate-bearing phosphohedyphane in nature.

Chlorine-dominant ASM from VZP are even more widespread phases; however some analyses show a systematic Cl+F deficiency which may correspond to the OH analogue of phosphohedyphane and most probably represents the new mineral species "hydroxylphosphohedyphane".

The fluid-assisted decomposition of galena to secondary cerussite and carbonate-bearing ASM represents another "piece of puzzle" to a complex tectonothermal history of Veporic crystalline basement in the Western Carpathians. The carbonate-rich mineral assemblage described herein suggests the post-Permian CO_2-rich fluid activity (Ondrejka et al. 2012; 2016). These fluids were also likely responsible for the formation of secondary *REE* carbonates (bastnäsite to synchysite) and calcite in adjacent orthogneisses and in felsic volcanites, microgranites and pegmatites-aplites as well (Ondrejka et al. 2012). The dissolution-reprecipitation reactions and alterations are connected with a Late Cretaceous collision metamorphic event. This evolved, late-metamorphic fluid phase with increased CO_2 most likely derived from metamorphosed carbonates at shallower exhumation level.

Acknowledgment: This work was supported by the Slovak Research and Development Agency under contract No. APVV-14-0278, APVV-15-0050 and VEGA Agency 1/0079/15, 1/0193/13.

References

Ondrejka M. et al. (2012): Lithos 142–143: 245–255.

Ondrejka M. et al. (2016): Min Petrol 110: 561–580.

Joint 5th Central-European Mineralogical Conference and
7th Mineral Sciences in the Carpathians Conference
Banská Štiavnica 2018

Classification of Alpine-type veins in the Western Carpathians

[1]Daniel Ozdín[#] and [1]Gabriela Kučerová

[1] Comenius University, Faculty of Natural Sciences, Department of Mineralogy and Petrology, Ilkovičova 6, Mlynská dolina, 84215 Bratislava, Slovakia [#]daniel.ozdin@gmail.com

Key words: classification, Alpine-type veins, Western Carpathians, Slovakia

INTRODUCTION

Alpine veins are a characteristic type of mineralization, especially in the orogenic regions of Europe, Asia, North Africa and the western part of the American continent.

Minerals of the Alpine assemblages form characteristic types of mineral associations that crystallize in cavities and cracks of various rocks. Fluids which generated the mineralization are genetically related to the interactions of mineral associations in the host rocks with aqueous solutions in the presence of various components including CO_2, methane, Cl at temperatures up to ~ 350°C and pressures that corresponds to the depth of the formation of these rocks in the earth's crust (Fišera 2000).

Despite the frequent occurrence of the Alpine paragenesis, the classification thereof is only developed in the Swiss Alps (Stalder et al. 1973) and the Czech Republic (Bernard ed. 1981; Fišera 2000).

ALPINE VEINS IN SLOVAKIA

Alpine-type veins have been known for a long time in Slovakia especially from the Veporic Unit crystalline basement and the siderite-quartz-sulphide hydrothermal veins of Tatric, Veporic and Gemericum Unit. In addition, several other types of hydrothermal veins and various types of mineralization have been known. However, their relationship to Alpine type veins was not known. Based mainly on mineral associations, host rocks, texture and genetic data, we classify alpine-type veins in the Western Carpathians into the following groups:

1. Minerals of Alpine-type veins in acidic rocks with the following mineral assemblages:
1A. Quartz (milky quartz, smoky quartz, rutile, anatase, brookite, orthoclase, albite, tourmaline, calcite, titanite, muscovite, epidote, clinochlore, ilmenite, hydrobiotite etc.); in Palaeozoic granitoids and gneisses (e.g. Čierny Balog, Hriňová, Látky, Klenovec, Veľký Klíž, Revúca, Drábsko, Malá Ida)

1B. Lazulite (lazulite, baryte, cinnabar, fluorapatite, svanbergite, gorceixite, hematite); in Triassic quartzites (e.g. Skýcov, Kostoľany pod Tribečom, Bádice, Jelenec)
1C. Epidote (epidote, quartz); in Carboniferous granitoids (e.g. Bratislava, Višňové, Vysoké Tatry)
1D. Andalusite (andalusite, quartz, fluorapatite, muscovite); in Palaeozoic gneisses (e.g. Pezinok – Pezinská Baba)
1E. Fluorite (fluorite, quartz, calcite); in Carboniferous granodiorites to tonalites (Višňové)
1F. Zeolite (stilbite-(Ca), chabazite-(Ca), calcite, pyrite); in Carboniferous granitoids (e.g. Višňové, Kežmarský peak, Vysoké Tatry)

2. Minerals of Alpine-type veins in basic and ultrabasic rocks with the following mineral assemblages:
2A. Axinite (axinite-(Fe), axinite-(Mn), actinolite, calcite, albite, titanite etc.); in Palaeozoic basic rocks (e.g. Gemerská Poloma, Limbach, Grexa, Jasenie)

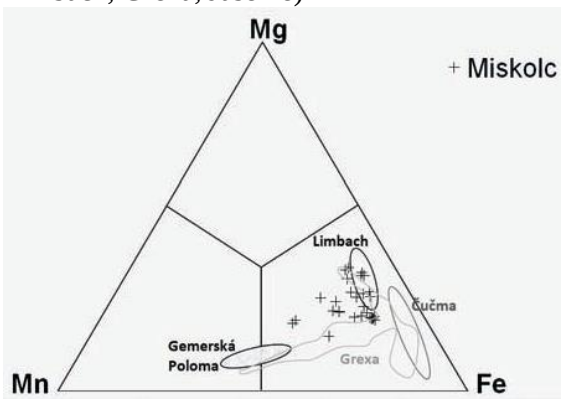

Fig. 1: Chemical composition of axinites from Western Carpathians and Miskolc in Hungary (Ozdín and Szakáll 2014).

2B. Epidote-calcite (epidote, calcite, prehnite, pumpellyite, hematite, magnetite); in Permian paleobasalts or Palaeozoic metabasites (e.g. Sološnica, Lošonec, Šalková, Hranovnica, Limbach)

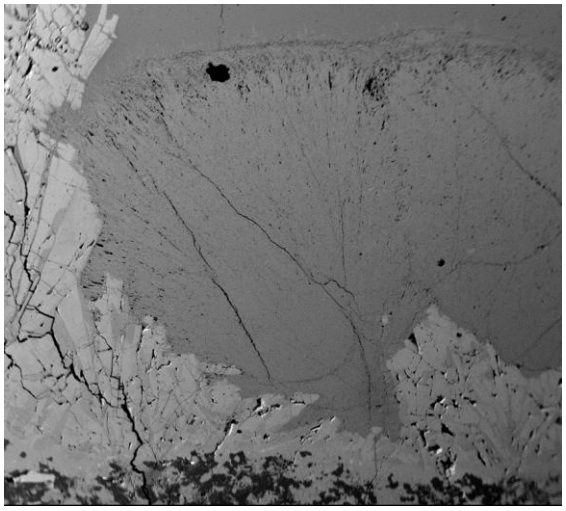

Fig. 3: Radial aggregates of pumpellyite (grey) growing on epidote (light grey). Above it is calcite (dark grey) and the bottom is a matrix of Permian basalt. Locality: Sološnica, field of view 2 mm.

2C. Quartz-calcite (quartz var. chalcedony, agate or jasper, opal, calcite, hematite); in metaperidotites (Dobšiná) and Permian paleobasalts (e.g. Sološnica, Lošonec, Poprad). These minerals occur in veins or tectonic faults (not like a filling of hollow).
2D. Talc (talc, dolomite, hydroxylapatite, clinochlore, magnetite); in Palaeozoic ultrabasic rocks, rarely in gneisses (e.g. Muránska Dlhá Lúka)
2E. Zeolite (natrolite, analcime, calcite, pyrite); in Palaeozoic actinolite schists (e.g. Pezinok)

3. Minerals of Alpine-type veins in carbonate rocks with the following mineral assemblage:
3A. Quartz-calcite (quartz, calcite, albite, dolomite); in Triassic to Jurassic limestones and dolomites (e.g. Stupava, Borinka)

4. Minerals of Alpine-type veins in hydrothermal carbonate-quartz-sulphidic veins with the following mineral assemblages:
4A. Tourmaline (schorl, dravite, albite, quartz, orthoclase; e.g. Ľubietová, Brezno – Koleso, Jedľové Kostoľany, Hnúšťa, Rudňany, Mlynky)
4B. Phosphate (fluorapatite, monazite-(Ce), xenotime-(Y), zircon, titanite, rutile, ilmenite; e.g. Ľubietová, Hnúšťa, Jedľové Kostoľany, Čierny Balog, Medzibrod, Špania Dolina)
4C. Hematite (hematite var. specularite, magnetite; e.g. Brezno – Koleso, Brezno – Mlynná dolina, Rudňany, Jasenie)
4D. Chlorite (chamosite, clinochlore ± quartz; e.g. Brezno – Koleso, Slovinky, Rožňava)
4E. Muscovite (muscovite; e.g. Brezno – Koleso, Jedľové Kostoľany, Slovinky, Rožňava)

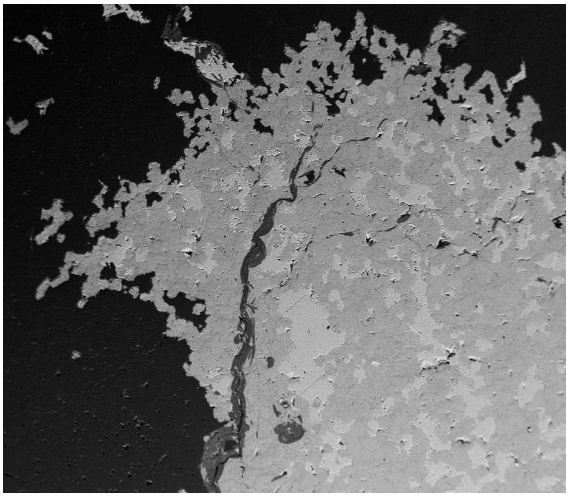

Fig. 3: Part of chamosite vein (grey) with siderite relicts (light grey). Thin dark grey veinlet cutting of chamosite is muscovite. Locality Brezno – Koleso in the Nízke Tatry Mts. BSE, field of view 1.8 cm.

The mineral paragenesis 4A-4E are hosted by Palaeozoic metamorphic rocks.

The homogenization temperatures of fluid inclusions in smoky quartz from 1A group is 230-250 °C (Hurai and Streško 1987). More data on fluid inclusions of quartz and orthoclase from Alpine fissures of Veporic Unit are published by Hurai (1983) and Hurai et al. (1991). The average of homogenization temperatures of fluid inclusions from tourmaline is 184 °C (Ľubietová). The average salinity of fluid inclusions was 10.2 wt. % NaCl eq. (calculated from the ice-melting temperature; Michňová et al. 2008).

Minerals Alpine type paragenesis from all groups in the Western Carpathians are Alpine age, although the presence of this type of mineralization of Variscan age in Slovakia cannot be exactly excluded. For the time being well determined only the Model age 1A, 4B and 4E subgroups. K/Ar dating gave following model ages of orthoclase var. adular (Hurai et al. 1991): the older generation 79.6 ± 1.7 Ma

(Klenovec) and 71.1 ± 1.1 Ma (Skorušiná), the younger generation 79.4 ± 1.6 Ma (Klenovec) and 89.8 ± 1.8 Ma (Skorušiná). Based on the monazite dating, the age of hydrothermal monazite from 4B subgroup is 92 ± 11 Ma (Ľubietová – Svätodušná (Ozdín, 2015)), 97 ± 9.2 Ma (Ľubietová – Podlipa (Ozdín et al. 2016)) and 83 ± 9 Ma (Jedľové Kostoľany – Brezov štál Ozdín (2010)). The youngest Alpine paragenesis in Slovakia is from the locality Ľubietová - Jamešná, where muscovite veins with rutile, zircon and xenotime-(Y) intersect opal, which is the product of Miocene volcanic activity. This means that this Alpine paragenesis is younger than 12 Ma. This age proves the continuing metallogenetic-tectonic events in the very near geological past, which are likely to continue today (Ozdín 2015).

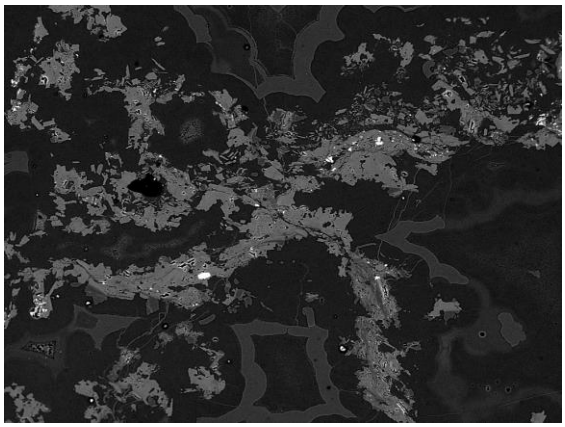

Fig. 4: Genetically younger muscovite veins (light grey) with zircon, rutile and xenotime-(Y) (all white) cutting opal (dark grey to black) from the Ľubietová – Jamešná. Probably the youngest Alpine paragenesis in Carpathians. Field of view 0.6 mm.

The age of the hydrothermal muscovite from Jedľová Kostoľany - Brezov, with subgroups 4E based on Ar/Ar dating is 75.1 ± 1 Ma and 75.4 ± 2 Ma (Ozdín 2010). At least two generations of Alpine paragenesis are documented from Hnúšťa where second one are formed by fluorapatite, dolomite, talc, quartz and pyrite (Ozdín and Sečkár, 2016). This is in line with the published 2 metamorphic events on the Hnúšťa – Mútnik deposit (Radvanec et al. 2010; Koděra a Radvanec 2002).

Acknowledgment: This work was supported by the Slovak Research and Development Agency under the contract No. APVV-15-0050 and APVV-0375-12.

REFERENCES

Bernard J.H. ed. (1981): Mineralogie Československa. Academia, Praha.
Fišera M. (2000): Bull mineral-petrolog Odd Nár Muz 8:23–40.
Hurai V. (1983): Min Slov 15:243–260.
Hurai et al. (1991): Min Slov 23:133–144.
Hurai V. and Streško V. (1987): Chem Geol 61:225–239.
Koděra P. and Radvanec M. (2002): Bol Paranaense Geoci 50:131–150.
Michňová et al. (2008): Bull mineral-petrolog Odd Nár Muz 16:100–108.
Ozdín D. (2010): Acta Min-Petrograph Abstr Ser 6:240.
Ozdín D. (2015): Esemestník 4:37–38.
Ozdín et al. (2016): Nerastné suroviny v 21. storočí. Banská Štiavnica.
Ozdín D. and Sečkár P. (2016): Esemestník 5:27–30.
Ozdín D. and Szakáll S. (2014): Herman Ottó Múzeum és Magyar Minerofil Társaság, Miskolc, 203–217.
Radvanec M. et al. (2010): Magnesite and talc in Slovakia – genetic and geoenvironmental models. ŠGÚDŠ, Bratislava.
Stalder H.A. et al. (1973): Die Mineralfunde der Schweiz. Basel.

Water content of nominally anhydrous minerals in Northern Hungarian middle Miocene volcanic chain

[1]Zsófia Pálos[#], [2]István Kovács, [1]Dávid Karátson, [1]Tamás Biró, [3]Judit Sándor-Kovács, [4]Dóra Kesjár, [1]Mátyás Hencz, [5]Éva Bertalan, [5]Anikó Besnyi, [5]György Falus, [5]Tamás Fancsik and [2]Viktor Wesztergom

[1] Eötvös Loránd University, Faculty of Science, Pázmány Péter street 1/C 1117, Budapest, Hungary [#]paloszsofia@gmail.com
[2] Kövesligethy Radó Seismological Observatory Geodetic and Geophysical Institute Research Centre for Astronomy and Earth Sciences Hungarian Academy of Sciences, Meredek street 18. 1112 Budapest, Hungary
[3] Hungarian Institute of Forensic Sciences, Mosonyi street 9, 1087, Budapest, Hungary
[4] Institute for Geological and Geochemical Research, Budaörsi street45, Budapest, Hungary
[5] Mining and Geological Survey of Hungary, Columbus street 17-23, 1145, Budapest, Hungary

Key words: micro-FTIR, NAM, plagioclase, clinopyroxene, structural hydroxyl

Water is one of the major magmatic volatile, which enhances the rheology, even the eruptive behaviour. The accurate measurement of magmatic water concentration is challenging in some cases, when magmas are more evolved and there is limited chance to measure primary silicate melt inclusions in primitive phenocrysts. Structural hydroxyl content of nominally anhydrous minerals (NAMs e.g. clinopyroxenes and feldspars) is proportional to the magmatic water content, consequently, several studies have been completed in this field in past decade (Wade et al. 2008; Turner et al. 2017 etc.). Many of them applied Fourier-transform infrared spectroscopy (micro-FTIR) which is a sensitive instrument for detecting small amounts of hydroxyl. FTIR studies apply mostly polarized infrared radiation along principal crystallographic section. The preparation of such samples is often challenging, if not impossible, for volcanic phenocrysts. Sambridge et al. (2007) and Kovács et al. (2008) provided theoretical and empirical evidence that measurements with unpolarized infrared radiation still give reasonable accuracy on the structural hydroxyl content of NAMs, when about 10 unoriented phenocrysts' absorbance is averaged by the measurements of doubly polished approximately 200 μm thick sections. Our goals are to determine the structural hydroxyl contents of NAMs from the middle Miocene volcanites of Carpathian-Pannonian Region's "western segment" in Northern Hungary, which help to estimate systematic trends in magmatic water contents, and systematic trends in syn- and post-eruptive processes, that can affect the data obtained from the phenocrysts. Samples were collected in Visegrád, Börzsöny and Mátra Mts., published by Karátson et al. (2001; 2007) and Karátson (2007). The bulk rock geochemistry of samples represent a subduction-related signature, there is no unambiguous evidence for contemporaneous subduction during volcanism, so mantle source could have been previously enriched one (Kovács and Szabó 2008). Thus, this study aims to explore whether such trends are also present in the structural hydroxyl contents of NAMs.

References

Karátson D. et al. (2000): Geol Carpath 51:325–343.
Karátson D. et al. (2007): Geol Carpath 58:541–563.
Karátson D. ed. (2007): A Börzsönytől a Hargitáig. Budapest Typotex.
Kovács I. et al. (2008): Am Min 93:765–778.
Kovács I. and Szabó Cs. (2008): J Geodyn 45: 1–17.
Sambridge M. et al. (2008): Am Min 93:751–764.
Turner M. et al. (2017): Chem Geol 466:436–445
Wade J.A. et al. (2008): Geology 36:799–802.

Joint 5th Central-European Mineralogical Conference and
7th Mineral Sciences in the Carpathians Conference
Banská Štiavnica 2018

Study on andorite IV and andorite VI from Meleg-hill, Velence Mts., and Mátraszentimre, Mátra Mts., Hungary

[1]Richárd Z. Papp [#] and [1]Norbert Zajzon

[1] University of Miskolc, Faculty of Earth Science and Engineering, Department of Mineralogy and Geology, Miskolc, Egyetemváros, H-3515, Hungary [#]askprz@uni-miskolc.hu

Key words: andorite, sulfosalt, mineral chemistry

INTRODUCTION

The aim of our work was to study the andorites of the Meleg-hill and Mátraszentimre locations at Hungary.

In the last few years numerous ore samples were collected from the deposits and were studied with X-ray Diffraction, Scanning Electron Microscopy and Electron microprobe analysis at the University of Miskolc, but previously the andorite was not specified in details and the andorite IV (quatrandorite) and andorite VI (senandorite) was not distinguished.

GEOLOGY

The Meleg-hill is located at Western Hungary in the Velence mountains. It is a Paleogene andesite stratovolcanic unit which is located above a subvolcanic diorite intrusion lying on the dominant Variscian granite of the VelenceMts..In this area a massive epithermal-hydrothermal system (Oligocene) created several different alteration zones (argillic, illite-sericite, pyrophyllite alterations) related to the formation of the andesite. (Szakáll et. al. 2016)

Mátraszentimre is a distal part of the Gyöngyösoroszi hydrothermal lead-zinc ore deposit. In this location Miocene cherty andesite and cherty andesite-tuff contain high amount of sulphide minerals in several different zones. The antimony concentration increased in the coolest – at near-surface – zone. Due to this antimonite and boulangerite appeared as also other Sb minerals. (Szakáll et. al. 2016)

ANALYTICAL METHODS

The analytical measurements (XRD, SEM and EMPA) were made at the Department of Mineralogy and Geology at the University of Miskolc.

The electron microprobe measurements were performed on a JEOL JXA-8600 Superprobe with upgraded SAMX software, 15–20 kV acceleration voltage and 10–20 nA beam current. The Table 1. contains the used analyser crystals and standard materials what were used during theWDX measurements.

Table 1: The used crystals and standards for the measured elements.

Element	Anal. crystal	Standard
As Lα	TAP	GaAs
Ag Lα	PET	Ag
S Kα	PET	MnS_2
Cu Kα	TAP	Cu_3Se_2
Sb Lα	PET	Sb_2S_3
Bi Mα	PET	Bi
Fe Kα	LDE	$FeTiO_3$
Cd Lα	PET	CdTe
Pb Mα	PET	PbS
Zn Kα	TAP	Zn

The X-ray powder diffraction measurements were carried out on a Bruker D8 Advance diffractometer (CuKα X-ray tube, 40 kV accelerating voltage, 40 mA tube current, parallel beam reflection geometry Göbel mirror, Vantec-1 position-sensitive detector with 1°slit and 0.007° 2θ / 14 sec goniometer running speed).

ANDORITE IV – VI DIFFERENTIATION

Andorite is one of the end member of the andorite-fizelyite series. These minerals are the Sb-rich members of the lillianite hometypic series and they are usually crystallized in the

final stage after the precipitation of stibnite (Ozdín and Sejkora 2009; Pršek et al. 2009). For our calculations we used as an analogy the work of Makovicky and Karup-Moller (1977) about the classification of the lillianite series which is based on the lillianite homologoue, the molar fraction and the substitution percentage of the phases.

The andorite homologue (N) was calculated with the next equation:

$$N = -1 + \frac{1}{Sbi + \frac{Pbi}{2} - \frac{1}{2}}$$

where Sbi = Sb/(Ag+Sb+Pb) Pbi = Pb/(Ag+Sb+Pb); Sb = Sb+Bi+As; Ag = Ag+Cu and Pb = Pb+Zn+Hg+Cd (Moëlo *et al.*, 1984).

The molar fraction (mol%) of the Ag-Sb and member of the andorite is equal to

$$mol\% = 1 - \frac{2Sbi - Pbi - 1}{6\left(Bi + \frac{Pbi}{2} - \frac{5}{6}\right)} * 100$$

and the substitution parameter is:

$$x = \frac{mol\% * (N - 2)}{200}$$

The equations were calculated to the ideal end member of andorite series ($PbAgSb_3S_6$).

The andorite series comprise only a few well defined minerals with limited composition ranges and uptake of specific minor elements. The composition range of the roshchinite is $And_{\sim 118.75}$, the andorite IV is $And_{93.75}$–And_{99}; the andorite VI is And_{102}–$And_{\sim 110}$, the fizelyite $And_{\sim 62.5}$ and the range of the ramdohrite is $And_{\sim 68.75}$ (Moëlo et al. 2008).

Based on Moëlo et al. (1984) and Makovicky et al. (2018) the substitution parameters were calculated for selected members of the andorite homologous series from different location (Table 2.).

Table 2: Substitution parameters (x) and andorite homologue (N) of the roshchinite ([1]Fersman Mineralogical Museum, Russian Academy of Sciences, senandorite (andorite VI)([2]Oruro, Bolivia (?) [3]San José, Bolivia), quatrandorite (andorite IV) ([4]Oruro, Bolivia (?)), fizelyite ([5]Baita, Mures, Romania) and ramdohrite ([6]Colorado Veine, Potosí, Bolivia) minerals.

Mineral	x	N
roshchinite[1]	119.80	3.84
senandorite[2]	103.43	3.86
senandorite[3]	109.93	3.68
quatrandorite[4]	95.33	3.93
fizelyite[5]	62.78	4.13
ramdohrite[6]	69.62	4.33

RESULTS

The andorite minerals usually occurs as 5–50 µm big crystals with varying chemical composition (Table 3. 1–11.) at the Meleg-hill. Single andorite crystals cannot be found in the samples, it is crystallized together with different As-Ag-Sb-Pb sulfosalts (enargite, plagionite, sorbyite, veenite and zinkenite) and sulphides (antimonite, galena, pyrite, sphalerite and chalcopyrite).

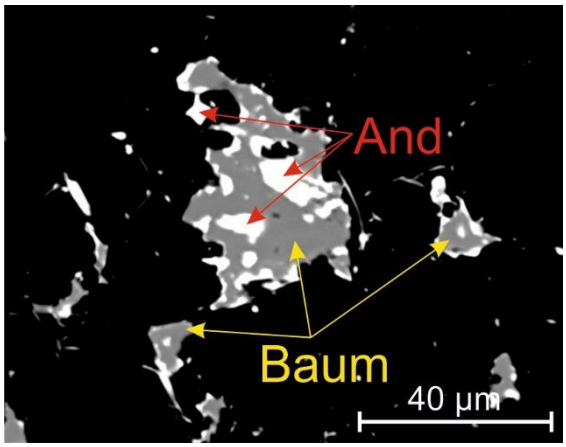

Fig. 1: Back scattered image of andorite grains from Meleg-hegy
(And – andorite; Baum – baumstarkite)

In the samples from Mátraszentimre the grain size was usually less than 5 µm and the chemical composition was also varying (Table 2. 12–19.). The paragenesis is less diverse, boulangerit was found as sulfosalt and pyrite, antimonite, cinnabar, galena, pyrite and sphalerite was found in our samples.

Due to the very small amount of andorite crystals only the major phases in the samples were identified with X-ray diffraction method.

Table 3: Results of the chemical analysis and calculations of the samples from the Meleg-hill (1–11) and Mátraszentimre (12–19)

	As	Ag	S	Cu	Sb	Bi	Pb	N	x
				[At%]					
1	3.5	9.07	54.31	n.a	24.26	1.31	7.55	3.57	115.62
2	2.77	8.73	54.87	n.a	24.23	1.58	7.81	3.55	113.78
3	2.77	9.09	54.77	n.a	23.99	1.53	7.86	3.71	110.58
4	3.17	8.89	54.68	n.a	24	1.61	7.65	3.56	114.82
5	3.27	8.67	54.8	n.a	24.02	1.58	7.67	3.48	116.30
6	2.96	9.32	54.34	n.a	24.07	1.64	7.67	3.72	112.05
7	2.95	9.55	54.16	n.a	24.02	2.19	7.13	3.68	116.29
8	2.42	9.7	54.1	n.a	24.37	1.95	7.46	3.82	111.88
9	2.66	9.76	54.79	n.a	23.77	2.19	6.82	3.79	115.43
10	2.9	9.51	54.39	n.a	24.24	1.65	7.31	3.73	113.96
11	3.05	11.02	54.55	n.a	21.94	3.16	5.94	4.27	113.52
12	2.53	10.53	55.37	1.30	22.98	0.10	7.19	5.48	98.75
13	2.52	10.94	53.60	1.17	24.00	0.12	7.64	5.39	98.48
14	2.99	11.11	54.93	0.57	23.14	0.09	7.17	5.20	100.43
15	2.80	9.32	55.61	0.99	24.00	0.14	7.14	4.34	106.04
16	3.27	9.27	54.95	0.48	24.16	0.10	7.76	4.07	106.15
17	3.15	10.04	54.08	0.89	24.11	0.10	7.63	4.59	102.75
18	2.78	9.41	54.95	1.23	24.42	0.10	7.12	4.41	106.03
19	2.72	10.11	55.32	0.61	23.59	0.11	7.54	4.69	101.47

CONCLUSIONS

The members of andorite series from the two investigated localities can be separated by chemistry. The range of the substitution parameter is 110.58–116.29 at the Meleg-hill, which is higher than theoretical range of the andorite IV or VI (And_{94}–And_{110}), in contrast the samples from Mátraszentimre shown a range between 98.48–106.15.

SUMMARY

With EMPA measurement the exact chemical composition were defined of the andorite crystals at the Meleg-hill and Mátraszentimre locations. The andorite homologue (N), the molar fraction (mol%) and the substitution parameters (x) were calculated from the given data and three types of andorite were distinguished.

In Mátraszentimre andorite IV (x = 98.48 – 98.75; $As_{0.27–0.28}Ag_{1.14–1.22}Cu_{0.14–0.13}Sb_{2.49–2.69}Bi_{0.01}Pb_{0.78–0.86}S_6$) and andorite VI (x = 100.43 – 106.03; $As_{0.30–0.36}Ag_{1.01–1.11}Cu_{0.05–0.13}Sb_{2.53–2.67}Bi_{0.01–0.02}Pb_{0.77–0.85}S_6$) also were identified. Due to the very small grain size, the measurements can contain error so to prove the presence of the andorite IV further measurements are required. At the Meleg-hill andorite VI or roshchinite were found with high substitution parameter (x = 110.58 – 116.29) and a very diverse chemical composition ($Ag_{1.03-1.14}As_{0.31-0.33}Sb_{2.48-2.63}Bi_{0.22-0.36}Pb_{0.67-0.79}S_6$).

REFERENCES

Makovicky, E. and Kraup-Moller S. (1977): Neues Jb Min Abh 130:264–287.

Makovicky E. et al. (2018): Z Kristallogr 233:255–267.

Moëlo Y. et. al. (1984): Neues Jb Min Mh 4:175–182.

Moëlo Y. et. al. (2008): Eur J Min 20:7–46.

Ozdín D. and Sejkora J. (2009): Bull mineral -petrolog Odd Nár Muz 17:65–68.

Pršek J. et al. (2009): Min Slov 41:183–190.

Szakáll, S. et al. (2016): Minerals of Hungary, GeoLitera, Szeged (in Hungarian).

Geological and geophysical sensors of the UX-1 autonomous underwater robot (UNEXMIN)

[1]Richárd Z. Papp[#], [2]Máté Koba, [2]Márton L. Kiss and [1]Norbert Zajzon

[1] University of Miskolc, Faculty of Earth Science and Engineering, Department of Mineralogy and Geology, Miskolc, Egyetemváros, H-3515, Hungary [#]askprz@uni-miskolc.hu
[2] University of Miskolc, Faculty of Mechanical Engineering and Informatics, Institute of Automation and Infocommunication, Miskolc, Egyetemváros, H-3515, Hungary

Key words: UNEXMIN, in-situ measurement, autonomous underwater vehicle

UX-1 is an autonomous underwater robot which was developed as a part of the UNEXMIN –an EU founded Horizon 2020 – project (www.unexmin.eu; Lopes et al. 2017 a,b, Zajzon et al. this volume). This vehicle capable of explore the underwater environment in flooded underground mines. This project is operated by an international consortium with 12 members all over Europe and the main task for the team of the University of Miskolc was to develop different instruments and sensors to deliver geological and geophysical information as much as possible.

During the development the team have to remain within the predefined limitations of the environment, the robot and the project: the devices have to be operate up to 500 m water depth (50 bar), everything should fit into a 60 cm diameter sphere, all of the methods have to be non-destructive, cannot contact to the wall and should be energy effective and light weight within the budget.

Considering the possibilities in the last few years 8 different devices were developed. These analytical techniques were classified into three groups:

1. techniques providing geological-mineralogical information,
2. geophysical methods and
3. measurements of mine-water parameters.

The selected instruments are the following:

- for collecting geological and mineralogical data a fluorescent imaging module (UV: 365 nm) and a multispectral unit (long UV – visible light – NIR in 14 different wavelengths between 400–850 nm) were made,
- for geophysical measurements total natural gamma-ray counting, sub-bottom sonar and magnetic field measuring unit (orientation and size of the local magnetic vector) were developed,
- to measure the mine-water chemistry electrical conductivity (EC) and pH units and a water sampling unit were developed.

The given information are going to be integrated with the data of the navigational sensors of the robot (supplying also temperature, pressure data) – which will deliver high resolution 3D maps from the environment. During the next 1.5 year total of three robots are going to be built which share the above sensors.

After the laboratory measurements, calibrations and setup phases, the UX-1 is going to be tested at Finland in the Kaatiala mine under real life conditions in June, 2018. Following the Finnish dive three other test site will be visited: the Idrija mercury mine in Slovenia, the Urgeiriça uranium mine in Portugal and the final demonstration will occur in the UK with the resurveying of the entire flooded section of the Ecton Cu-(Zn-Pb) mine that nobody has seen for over 150 years.

Acknowledgment: This project has received funding from the European Union's Horizon 2020 research and innovation programme under grant agreement No. 690008.

REFERENCES

Lopes L. et al. (2017a): Energy Proc 125:41–49.
Lopes L. et al. (2017b): Eur Geol 44:54–57.
Zajzon N. et al. (this volume)

Joint 5th Central-European Mineralogical Conference and
7th Mineral Sciences in the Carpathians Conference
Banská Štiavnica 2018

Extremely Mn,Be,Na,Cs-rich cordierite from the Szklary pegmatite, Lower Silesia, Poland

[1]Adam Pieczka[#], [2]Eligiusz Szełęg, [3]Adam Szuszkiewicz and [4]Petr Gadas

[1] AGH University of Science and Technology, Faculty of Geology, Geophysics and Environmental Protection, Department of Mineralogy, Petrography and Geochemistry 30-059 Kraków, Mickiewicza 30, Poland [#]pieczka@agh.edu.pl
[2] University of Silesia, Faculty of Earth Sciences, Department of Geochemistry, Mineralogy and Petrography, 41-200 Sosnowiec, Będzińska 60, Poland
[3] University of Wrocław, Institute of Geological Sciences, 50-204 Wrocław, pl. M. Borna 9, Poland
[4] Masaryk University, Department of Geological Sciences, Kotlářská 2, 611 37 Brno, Czech Republic

Key words: cordierite group, Mn,Be,Na,Cs enrichment, Szklary pegmatite, Poland

Cordierite, $Mg_2[Al_4Si_5O_{18}]$, and sekaninaite $Fe^{2+}{}_2[Al_4Si_5O_{18}]$, are two members of the cordierite group distinct by the dominant Mg or Fe. Due to diverse substitutions, the minerals usually show a broad range of compositions, which may be expressed by the general formula $^{Ch}(Na,K,Cs,Ca)_{0\text{-}1}{}^{VI}(Mg,Fe^{2+},Mn,Li)_2[^{IV}Al_3{}^{IV}(Al,Be,Mg,Fe^{2+},Fe^{3+})_{\Sigma 1}{}^{IV}Si_5O_{18}] \cdot x\ ^{Ch}(H_2O,CO_2,CH_4,N_2,\ldots)$, where 'Ch' denotes channel positions. Cordierite is a common rock-forming mineral in medium and high-grade aluminous rocks of the amphibolite and granulite facies and in associated pegmatites, whereas sekaninaite is typically related to felsic magmatic rocks and their pegmatites. The naturally occurring Mn-dominant analogue of the two minerals is still not known, and the highest Mn contents observed to date in cordierite does not exceed 2 wt.% MnO. However, in the Szklary pegmatite we found relics of exceptionally Mn-rich (Be,Na,Cs)-bearing cordierite.

The beryl–columbite–phosphate pegmatite of the *REL*-Li class from Szklary crops out in the northern part of the Szklary serpentinite massif, ~60 km south of Wrocław, SW Poland. It forms a NNE-SSW elongated lens or a boudin, ~4×1 m large in planar section, adjoined to aplitic gneiss to the SE and surrounded by tectonized serpentinite. A vermiculite-talc-chlorite zone is present along the pegmatite-serpentinite contact. The age of the pegmatite (383±2 Ma) is contemporaneous to pegmatite-forming anatectic event in the neighboring Góry Sowie metamorphic unit and suggests that the pegmatite formed from anatectic melts that intruded into the Szklary serpentinites.

The (Mn,Be,Na,Cs)-bearing cordierite occurs as a component of well-defined assemblage composed of quartz, albite, Cs,Mg-bearing beryl, dravite, epidote-allanite, zircon, xenotime-(Y), (Ta,Nb)-eriched rutile, ilmenite grading to pyrophanite, Cs-bearing muscovite, phlogopite and annite, paragonite, clinochlore and chamosite, harmotome, vermiculite, smectites, hematite, schafarzikite and other unrecognized Mn-Fe-As-Sb oxides, native Sb and Bi. Textural evidence (altered relics of the mafic rocks replaced finally by vermiculite and smectites) indicates that the mineral formed during reactions of the mafic host rocks with a highly evolved LCT-type melt.

The Szklary cordierites exhibit three distinct stages of Mn- and Fe-enrichment with increasing Mn content from ~3.7 MnO wt.% (0.33 Mn apfu) through 5.1 MnO wt.% (0.46 Mn apfu), up to ~6.7 MnO wt.% (0.61 Mn apfu), and FeO from 5.7–5.9 up to 7.3 FeO wt.% (0.50–0.53 up to 0.65 Fe apfu, respectively). They additionally have high Na and Be contents, reaching ~1.8–2.0 Na_2O wt.% (~0.37–0.40 Na apfu) and 1.7–1.8 BeO wt.% (0.45–0.47 Be apfu), at simultaneously high Cs_2O contents up to 0.8–1.0 wt.% (0.04–0.05 Cs apfu). These compositions place the Szklary cordierite among the most (Na+Cs)- and Be-rich cordierites worldwide and the observed Mn concentrations are the highest ever noted .

Acknowledgment: The studies were supported by the National Science Centre (Poland) grant 2015/19/B/ST10/01809 to AP.

Joint 5th Central-European Mineralogical Conference and
7th Mineral Sciences in the Carpathians Conference

A new data on ore minerals from Sn-bearing schists of the Krobica-Gierczyn area, Sudetes

[1]Alicja Pietrzela[#] and [1]Krzysztof Nejbert[#]

[1] University of Warsaw, Faculty of Geology, Żwirki i Wigury 93, 02-089 Warsaw, Poland
[#]a.pietrzela@student.uw.edu.pl, [#]knejbert@uw.edu.pl

Key words: Sn-Co-Bi mineralization, mineral chemistry, Stara Kamienica range, West Sudetes

In the northern and eastern metamorphic envelope of the Karkonosze Granitoid Massif (KGM) numerous polymetallic deposits were exploited in past times. The Krobica-Gierczyn-Przecznica area located in the northern surroundings of the KGM is known for the occurrence of Sn and Co mineralization, which were mined from the 16th to the first half of the 19th century. In the eastern metamorphic envelope of the KGM, polymetallic ore deposits and ore minerals occurrences are found in the area of Miedzianka-Ciechanowice, Radzimowice, Wieściszowice, Rędziny, Czarnów, and Kowary (Osika 1990). These polymetallic ores are of contact-metasomatic and/or hydrothermal genesis, related to the evolution of the KMG (Mochnacka et al. 2015).

The Krobica-Gierczyn area is characterized by a strong geochemical diversity related to increased concentration of Cu, Zn, Sn Co, Ni, Bi, As, Sb, Ag, and Se. This is reflected by rich inventory of ore minerals such as: pyrrhotite, chalcopyrite, sphalerite, arsenopyrite, löllingite, glaucodot, gersdorffite, galena, nickeline, cobaltite, native bismuth, stannite, cassiterite, ilmenite and rutile (Wiszniewska 1984; Cook and Dudek 1994). During the study, majority of these minerals were identified and their chemical composition was determined by electron microprobe.

Previous geochemical studies of polymetallic ores from the Gierczyn-Krobica area showed increased concentrations of In, reaching up to 404 ppm (Wagner 2016). Indium belongs to the group of critical metals, which is used in the most modern technologies (Schwarz-Schampera and Herzig 2002). During the study no In-bearing phases have been found so far, however, indium is commonly present as a structural admixtures in sphalerite (up to 0.11 wt.% of In) and in cassiterite (from 0.07 to 0.33 wt.%. of In_2O_3)

Cobalt, which also has a great economic importance, constitutes cobaltite and occurs as admixtures in the structure of arsenopyrite, löllingite, and glaucodot. Co concentrations in these minerals were in the ranges 0.01-7.65 wt.%, 5.10-8.68 wt.%, and 25.75-29.01 wt.%, respectively.

Bismuth was found mainly in the form of native bismuth, sulphides and sulphosalts. Increased Bi concentrations (up to 1.19 wt.%) were found also in galena. Minerals enriched in Ag were galena (up to 0.36 wt.%) and giessenite (up to 0.94 wt.%).

Chemical composition of the examined ores support genetic relationship between ore mineralization and the KGM. Increased concentrations of In and Ta in the cassiterite confirm its hydrothermal origin, despite petrographic data documenting the episodes of metamorphic recrystallization of cassiterite grains. Nowadays, polymetallic mineralization in the Gierczyn-Krobica region is considered as cut-off grade, however documented increased concentrations of In may be the basis for a reassessment of the economic value of these deposits.

References

Cook N.J. and Dudek K. (1994): Chemie der Erde 54:1–32.

Mochnacka K. et al. (2015): Ore Geol Rev 64:215–238.

Osika R. (1990): Geology of Poland. Mineral deposits. Wydawnictwa Geologiczne.

Schwarz-Schampera U. and Herzig P.M. (2002): Indium. Geology, Mineralogy and Economics. Springer.

Wagner J. (2016): MSc Thesis. Archiwum IGMiP.

Wiszniewska J. (1984): Archiwum Mineralogiczne 40:115–187.

Mineralogy of Ľubietová-Jamešná deposit, Slovak Republic

[1]Ľuboš Polák[#] and [1]Stanislav Jeleň

[1] Matej Bel University, Faculty of Natural Sciences, Department of Geography and Geology, Tajovského 40, 974 01, Banská Bystrica, Slovak Republic [#]silur.devon7@gmail.com

Key words: iron ores, manganese minerals, chemical composition, Ľubietová-Jamešná, North Veporic Unit

Mineralogical research of iron ores on the Ľubietova-Jamešná deposit has been attended by several authors in recent years (e.g. Ozdín 2015; Polák and Jeleň 2017; Polák et al. 2017). In addition to iron ores, opal mineralization along with manganese mineralization is also of interest to researchers (e.g. Ozdín 2015, 2016; Polák and Jeleň 2017; Števko 2017).

The aim of this paper is to present new and currently known information on the mineralogical proportions of the deposit with chemical analysis of iron ores, directly from the underground spaces of the deposit.

Ľubietová-Jamešná is the most important Fe deposit in the North Veporic Unit. It is located in the tectonic zone of NE-SW direction, between Middle Triassic dolomites and Lower to Middle Sarmatian andesite volcanites (Slavkay et al. 2004).

From a mineralogical point of view, iron ore was the main subject of mining which specifically represent: goethite, hematite and limonite, less siderite and ankerite (Bergfest 1951).

From the SiO_2 mass, chalcedony, hyalite, ferric and milky opal have been found so far. Furthermore, pyrite and crandallite were also identified on the deposit (Bergfest 1951; Ozdín 2016).

Manganese minerals are present to a lesser extent in the form of prismatic crystals (pyrolusite) at the heaps of the adit no. 2, as well as in mining spaces. In addition, yet Števko (2017) also mentions an unknown mineral from the hollandite subgroup.

New chemical analyses (by ICP-ES/ICPMS; Bureau veritas mineral laboratories, Vancouver, Canada) of goethite, which was collected from ore nests in Bieliska adit point to the interesting quality of the mined iron ores. In particular, the iron content of the studied ore is more than 40 wt. %, Mn is 0.5 wt. %, P 0.07 wt. % and V is 0.05 wt. %.

From the clay minerals were found nontronite to a large extent within the underground spaces of deposit. It was identified by XRD and infrared spectroscopy.

More recently, cryptomelane was identified from manganese minerals by XRD and Raman spcestroscopy study, and manganite by Raman spectroscopy study. Coronadite (?) (Polák and Jeleň 2017) so far remains unidentified.

Acknowledgment: This study was supported by projects: APVV 15-0050, VEGA 1/0650/15.

References

Bergfest A. (1951): The mining in Ľubietová on iron ores. The II. part history of mining in Ľubietová. (in Slovak)

Ozdín D. (2015): Esemestník 4:37–38. (in Slovak).

Ozdín D. (2016): Minerals and Mineralogy in the 21st Century, International scientific symposium, Jáchymov, 71–74. (in Slovak)

Polák Ľ. and Jeleň S. (2017): Mente et Malleo 3 (in Slovak)

Polák Ľ. et al. (2017): Mineral 25:554–559 (in Slovak).

Slavkay M. et al. (2004): Mineral deposits of the Slovak Ore Mountains, Vol. 2. (in Slovak)

Števko M. (2017): Esemestník 6:106 (in Slovak).

Joint 5th Central-European Mineralogical Conference and
7th Mineral Sciences in the Carpathians Conference
Banská Štiavnica 2018

Crystallization of pyromorphite on the surface of iron oxyhydroxides

[1]Grzegorz Rzepa[#], [1]Maciej Manecki and [1]Marcelina Radlińska

[1] AGH University of Science and Technology, Faculty of Geology, Geophysics and Environmental Protection, Department of Mineralogy, Petrography and Geochemistry, al. Mickiewicza 30, 30-059 Kraków, Poland [#]gprzepa@cyf-kr.edu.pl

Key words: lead phosphate, goethite, ferrihydrite, akaganéite, in-situ remediation

INTRODUCTION

In situ immobilization of toxic metals and metalloids by the formation of virtually insoluble minerals like phosphates and arsenates is a widely-discussed method for remediation of polluted soils and sediments (Raicevic et al. 2005; Bajda et al. 2011). This process usually takes place in the presence of various iron (oxyhydr)oxides which are widespread in polluted media. Synthetic goethite has been often used in the model experiments (Zhang et al. 1997; Kleszczewska-Zębala et al. 2016). However, the goethite applied in the majority of the studies was relatively well-crystalline whereas natural soil goethites are usually poorly-crystalline. Moreover, in many soils and sediments goethite co-occurs with other iron (oxyhydr)oxides, like ferrihydrite, hematite, lepidocrocite, akaganéite etc., that possess different affinities to lead and phosphate that goethite does. Therefore the nucleation and crystallization of insoluble phosphates might proceed differently in other Fe-(oxyhydr)oxide systems. In this work we have verified a hypothesis that mineralogy and crystallinity of iron oxyhydroxide affect nucleation and growth of pyromorphite $Pb_5(PO_4)_3Cl$ (virtually insoluble lead apatite used in remediation procedures) and hence alter the effectiveness of in-situ lead immobilization.

MATERIALS AND METHODS

Batch experiments were carried out using various substrates, including synthetic iron oxyhydroxides: well-crystalline goethite (Gt-W), poorly-crystalline goethite (Gt-P), Al-goethite (Gt-Al), ferrihydrite (Fh), Si-ferrihydrite (Fh-Si) and akaganéite (Ak). Additionally, natural bog iron ore (BIO), rich in iron oxyhydroxides (including ferrihydrite and goethite) and a water treatment plant sludge (WTS) which is particularly rich in ferrihydrite, were used for comparison with synthetic phases. Two experimental setups were applied: 1) a P-Pb system in which phosphate was sorbed on the substrate and then phosphate-loaded substrates were reacted with aqueous Pb(II) or 2) a Pb-P system in which lead-loaded minerals were reacted with aqueous phosphate. In both setups, 20 mM PO_4 or Pb solution in NH_4Cl matrix was used as reactant. The efficiency of lead or phosphate immobilization was assessed by the analysis of the solution (AAS and UV-Vis spectroscopies) whereas the solids were characterized using XRD and SEM-EDS.

RESULTS

The results of batch experiments show that the efficiency of lead and phosphate removal by iron oxyhydroxides depends on the mineral surface area and surface chemistry. Regardless the adsorbate, the ferrihydrites and Fh-rich sediments possess higher sorption capacities than all goethites and akaganéite (Table 1).

Table 1: Comparison of BET surface areas [m^2/g] and adsorption capacities [mg/g] in P-Pb and Pb-P systems.

	BET	**Pb**		**PO_4**	
		Pb-P	P-Pb	P-Pb	Pb-P
Gt-W	27	4.4	28.7	15.0	24.2
Gt-P	60	11.9	36.5	32.1	34.6
Gt-Al	23	0.4	30.2	20.4	15.1
Ak	71	0.1	19.2	17.8	21.9
Fh	277	57.0	38.4	66.2	53.9
Fh-Si	310	44.7	30.5	43.0	92.7
WTS	170	202.1	189.6	94.2	94.1
BIO	170	77.3	42.9	53.2	69.8

These capacities were, however, affected by Pb or PO_4 pretreatment. Lead immobilization was distinctly more effective by PO_4-loaded goethites and akaganéite but not by PO_4-loaded ferrihydrites when compared to unloaded samples. Phosphate behavior is more complex but again Pb-loaded goethites and akaganéite remove PO_4 more effectively than unloaded minerals (Table 1). This enhanced PO_4 or Pb efficiency is chiefly related to the formation of pyromorphite. Its presence was proved by X-ray diffraction patterns and SEM images (Fig. 1,2). In contrast to the previous works (Manecki et al. 2006), relatively low amount of large pyromorphite crystals emerged indicating precipitation from only slightly oversaturated solution.

Due to higher phosphate than lead sorption efficiency, more pyromorphite crystals were formed onto all the goethites when phosphate had been added first to the system (Fig. 1a–c). The crystals from P-Pb system were also usually larger. The differences between the goethites result from different sorption capacities.

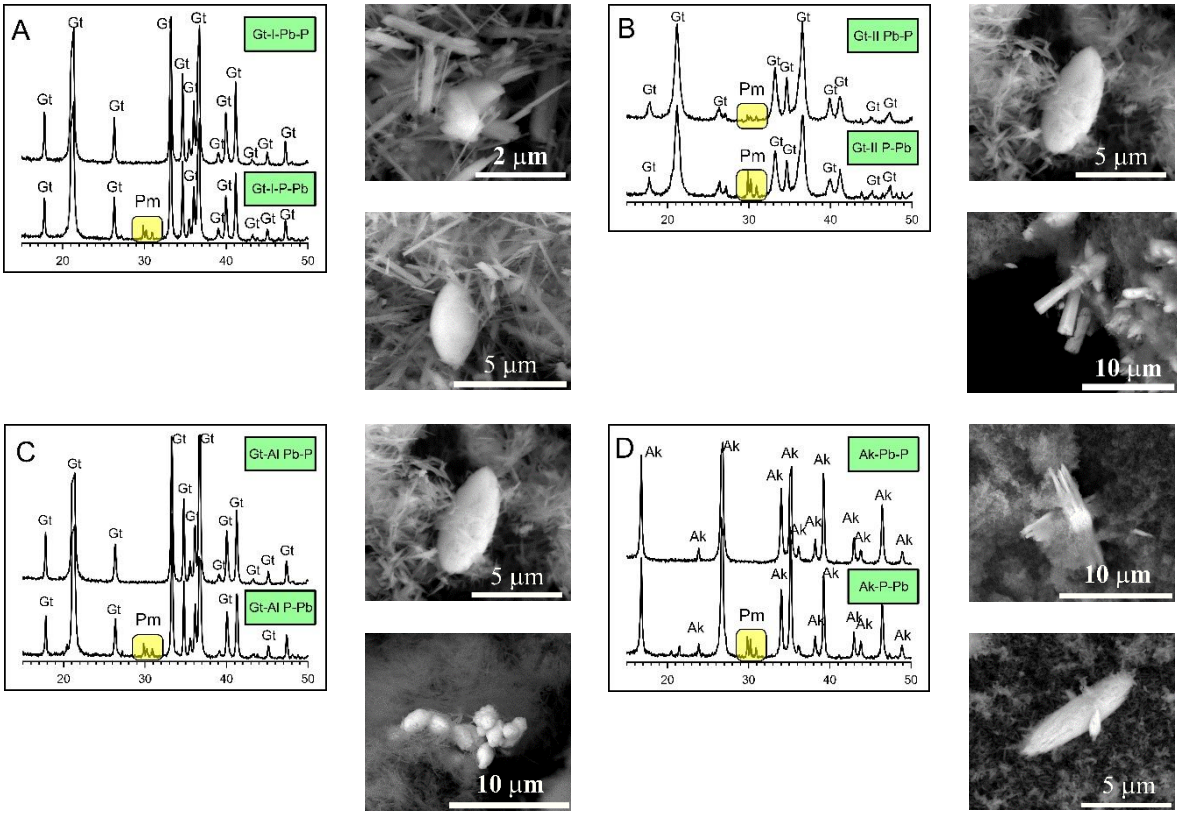

Fig. 1: X-ray diffraction patterns of well-crystalline goethite (a), poorly-crystalline goethite (b), Al-goethite (c) and akaganéite (d) after the experiments in Pb-P (upper patterns) and P-Pb systems (lower patterns) and exemplary SEM images of pyromorphite formed. Pm – pyromorphite, Gt – goethite, Ak – akaganéite.

Similarly to the goethites, more pyromorphite crystals precipitated on akaganéite when phosphate had been added first (Fig. 1d). The emergence of some pyromorphite when no chloride was present in the system might suggest that chloride anions from akaganéite tunnels took a part in the reaction. On the other hand, strongly adsorbed phosphate on ferrihydrite surface appeared to be virtually unavailable for pyromorphite formation and therefore hardly any pyromorphite crystals formed on both ferrihydrite and Si-ferrihydrite (Fig. 2a,b). Some lead chlorides emerged instead. Hence surface ternary adsorption was probably the most important mechanism of lead immobilization rather than surface precipitation of lead phosphate. Higher amounts of pyromorphite were observed when lead had been added first to the system. Here, a wide range of pyromorphite habits was observed.

For natural polymineral samples (BIO and WTS) rich in ferrihydrite and goethite, again more pyromorphite formed when Pb-loaded sediments reacted with aqueous phosphate.

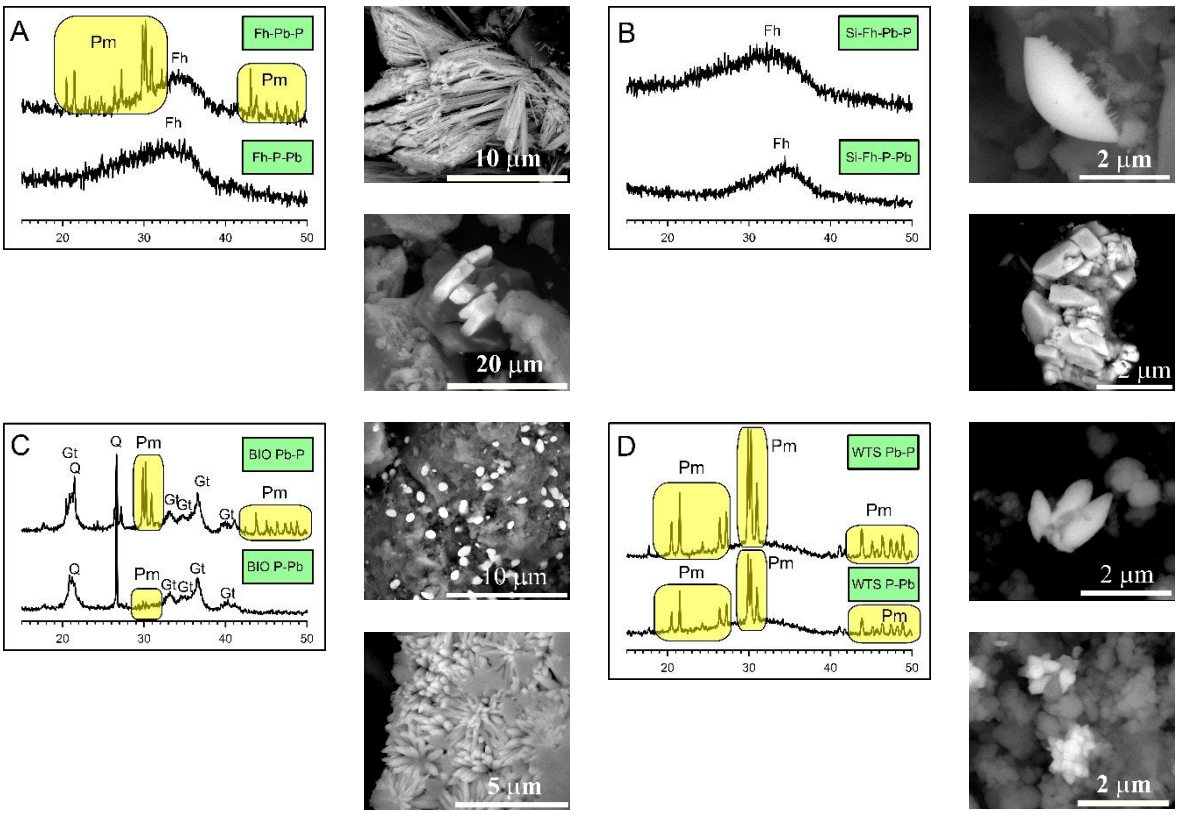

Fig. 2: X-ray diffraction patterns of ferrihydrite (a), Si-ferrihydrite (b), bog iron ore (c) and water treatment sludge (d) after the experiments in Pb-P (upper patterns) and P-Pb systems (lower patterns) and exemplary SEM images of secondary phases formed. Note that in the case of ferrihydrite and Si-ferrihydrite lead chloride crystallized instead of pyromorphite in P-Pb system. Pm – pyromorphite, Gt – goethite, Fh – ferrihydrite, Q - quartz.

Some pyromorphite precipitated also when lead solution reacted with non-Pb-loaded materials which was a result of a reaction with phosphate naturally adsorbed onto Fe oxyhydroxides.

SUMMARY AND CONCLUSIONS

The results revealed that the mineralogy and surface chemistry of Fe phases and Fe-rich sediments highly affect the effectiveness and the mechanism of Pb removal, the amount of pyromorphite formed as well as its habit and size. These are related mainly to the different sorption capacities of individual Fe oxyhydroxides and different strength of the bonds between the mineral and lead or phosphate. Moreover, since these properties depend also on an oxyhydroxide crystallinity and surface chemistry, the efficiency of heavy metal removal via pyromorphite crystallization appears to be much harder to predict than it has been thought so far.

Acknowledgment: This work was supported by AGH-UST statutory grant 11.11.140.158.

REFERENCES

Bajda T. et al. (2011): Mineralogia 42:75–91.
Kleszczewska-Zębala A. et al. (2016): Microsc Microanal 22:698–705.
Manecki M. et al. (2006): Environ Chem Lett 3:178–181.
Rajcevic S. et al. (2005): J Hazard Mater 117:41–53.
Zhang P. and Ryan L. (1997): Environ Sci Technol 31:2673–2678.

Joint 5th Central-European Mineralogical Conference and
7th Mineral Sciences in the Carpathians Conference
Banská Štiavnica 2018

Waste magnesite as potential SO_2 sorbents

[1]Magdalena Sęk[#] and [1]Elżbieta Hycnar

[1] AGH University of Science and Technology, Department of Mineralogy, Petrography and Geochemistry, Al. Mickiewicza 30, 30-059 Cracow, Poland, [#]mmsek@agh.edu.pl

Key words: magnesite, sorbents, SO_2, sorption, magnesium sulfate

Burning of solid fuels and biomass causes the emission of SO_2 with flue gases, as a result of the oxidation of sulphur contained in the organic and mineral matter. The uses of low-emission burners and fluid boilers resulted in the development of dry methods of desulfurization. The basic SO_2 sorbents are high-quality limestone, less often products of their processing (CaO, $Ca(OH)_2$) or other sorbents such as dolostones, magnesites. In the dry desulfurization technology, the mechanism of SO_2 binding from the flue gas is based on the sorption on highly reactive and porous products of carbonates calcination process and leads to the formation of stable sulfates (e.g. Kaljuvee 2005, Antony 1995). The desulfurization efficiency in dry technologies essentially depends on the development of porosity (the size of the pores) and specific surface area during calcination.

The waste magnesites from Wiry and Szklary deposits (SW Poland) were examined as a potential material showing good sorption properties toward SO_2 under conditions corresponding to the dry methods of desulfurization in the power plants. The waste magnesite was examined by physicochemical and mineralogical methods, including XRD, DTA, TG, SEM/EDX, ICP-MS, and ASA. In order to determine sorption efficiency towards SO_2, experiments at a laboratory scale were performed in accordance with the methodology developed by the Ahlstrom Pyropower Development Laboratory (1995). Analyses of the waste magnesite and products of reactions were carried out using XRD, SEM/EDS. Magnesite is the predominant mineral component in the samples from Wiry as well as from Szklary. Moreover, dolomite and quartz were noticed. In case of samples from Wiry, the average MgO and CaO contents are 36.3 wt.% and 1.43 wt.%, respectively. The samples from Szklary contained also calcite, minerals of the serpentine subgroup (antigorite, chrysotile), clay minerals of the smectite group (montmorillonite) and talc. Therefore, the average content of MgO is lower (30.77 wt.%) and that of CaO higher (2.72 wt.%). Both magnesites show some degree of Fe^{2+} substitution, confirmed by diffraction and thermogravimetric data. The reactivity with SO_2 documents excellent sorption properties of magnesite from Wiry (ca. 122 g S/1 kg of sorbent). These results are comparable with the data of the currently used limestone sorbents (ca. 126 g S/kg). Waste magnesite from Szklary has worse, but still satisfactory sorption properties (an average of 100 g S/kg). The XRD analysis of the product of sulphation confirmed the formation of $MgSO_4$ and additionally $CaMg_3(SO_4)_4$ under the above experimental conditions.

Preliminary results suggest the possibility of using waste magnesite as a sorbent in dry desulfurization processes. It is predicted that different range of thermal decomposition of magnesite and calcite may account for a multistage calcination process. It may contribute to more effective porosity development and additional participation of MgO in the sorption of SO_2 that may increase the effectiveness of this process.

Acknowledgment: Studies have been done using Center of Energy AGH infrastructure and 11.11.140.158.

REFERENCES

Alsthrom Pyropower Reactivity index (1995): Alsthrom Pyropower.

Anthony E.J. (1995): Prog Energy Combust Sci 21:239–268.

Kaljuvee T. et al. (2005): J Therm Anal Calorim 80:591–597.

Joint 5th Central-European Mineralogical Conference and
7th Mineral Sciences in the Carpathians Conference

Metamorphic tourmalines of the Wołowa Góra region, Eastern Karkonosze

[1]Mateusz Przemysław Sęk[#] and [1]Adam Pieczka

[1] AGH University of Science and Technology, Department of Mineralogy, Petrography and Geochemistry, Mickiewicza 30, 30-059 Cracow, Poland; [#]msek@agh.edu.pl

Key words: tourmaline, contact metamorphism, Bohemian Massif, Karkonosze-Izera Massif

Tourmaline-supergroup minerals are common accessories in a wide range of magmatic and metamorphic rocks. Due to diverse chemical compositions, generalized by the formula $XY_3Z_6(BO_3)_3(T_6O_{18})(OH)_3(OH,F,O)$, minerals of the supergroup are valuable petrological indicators.

In the eastern metamorphic cover of the Karkonosze granite in Lower Silesia, SW Poland, tourmalines are accessories rarely found in granitic gneisses, mica schists, hornfelses, and in host-cutting quartz veins. The rocks formed from mixed magmatic-sedimentary protoliths of ~490 Ma age underwent regional metamorphism under MP-MT conditions and were modified by contact metamorphism induced by the Karkonosze granite pluton intrusion. Tourmalines in the area represent schorl and dravite as the most common members, partially evolving to oxy-dravite and uvite-type tourmalines. The Wołowa Góra and Budniki area, close to the Kowary town, is a region where the metamorphic tourmalines are common and occur in the form of relatively large crystals (even several centimetres). They were an object of detailed mineralogical studies.

Chemical compositions of zoned tourmaline crystals, occurring in quartz veins on a pass between Wołowa Góra Mt. and Czoło Mt. in the eastern part of the Karkonosze range, were analyzed using a Cameca SX 100 electron microprobe. Chemical formulae of the tourmalines were normalized on the basis of Y+Z+T = 15 (apfu) or of Y+Z = 9 apfu in case of the too high content of Si (> 6 apfu), with B_2O_3 and H_2O calculated from stoichiometry.

Due to the dominancy of Na at the X site and monovalent anions at the W site, the tourmalines belong to the alkaline group and hydroxy-fluor series, with partly increasing oxy-species contents. The yellowish Mg-rich tourmaline from axial parts of a quartz vein displays the dominance of oxy-species, although $^{W}(OH+F)^{-} > {}^{W}O^{2-}$. In external zones of the vein, it evolves towards a composition richer in Fe with decreasing contents of oxy-tourmaline members and distinct dominancy of OH over F.

The Y and Z structural sites in this tourmaline are mainly occupied by Mg and Al, and subordinately by Fe and Ti. The content of ^{Y+Z}Al reaches the highest value of ~6.9 apfu in internal parts of the tourmaline crystals. In the intermediate zone, Al decreases from 6.7 to 5.7 apfu, and in the rim of this tourmaline, a sudden increase up to 6.2 Al apfu takes place. The tourmalines are also characterized by the variable Mg content with Mg/(Mg+Fe) ratio of 0.52–0.89 in the rim and 0.91–0.99 in the middle part of the intermediate zone. A significant increase in Fe and Ti (up to 7.82 wt.% FeO and 1.08 wt.% TiO_2) is visible in the crystal rim and fracture fillings.

The formation of oxy-dravite as the first-generation tourmaline is interpreted as a result of (regional) metamorphism of metasomatically altered prior-protolith represented by Al- and Mg-rich sediments, basalts and basaltic tuffs of the pre-Variscian bimodal volcanism. The schorl/dravite evolving to fluor-schorl/fluor-dravite of the second generation is related to later stages of regional metamorphism or contact metamorphism induced by the granite intrusion. The increase in Fe, Ca and Ti in these tourmalines is related to partial dissolution and recrystallization of amphiboles, plagioclases and Ti-oxides in the stage.

Acknowledgment: The study was supported by the the National Science Centre (Poland) grant 2017/27/N/ST10/01579 to M.S.

Joint 5th Central-European Mineralogical Conference and
7th Mineral Sciences in the Carpathians Conference

Fractionation of tourmaline in the Lhenice lepidolite pegmatite

[1]Lenka Skřápková and [1]Jan Cempírek[#]

[1] Department of Geological Sciences, Faculty of Science, Masaryk University, Kotlářská 2, 611 37 Brno [#]jcemp@sci.muni.cz

Key words: tourmaline, pegmatite, lithium, compositional evolution, fractionation

INTRODUCTION

The lepidolite-subtype pegmatite at Lhenice is a member of the South-Bohemian pegmatite field (Novák & Cempírek, 2010); the nearest rare-element pegmatites include Lhenice II, Nová Ves and Chvalovice I and II. All pegmatites are characterized by high Li and P contents and similar mineral composition (elbaite, schorl, biotite, K-feldspar, lepidolite). The Lhenice pegmatite is moderate-sized and highly fractionated, with abundant lepidolite, elbaite, amblygonite and cassiterite. It was found in 2003 and the research material has not been studied yet. Tourmaline samples were analysed using EMPA and LA-ICP-MS.

The area which surrounds the pegmatite belongs to Moldanubian Zone and is characterised by high-grade metamorphic rock like gneisses, granulites and serpentinites.

PEGMATITE STRUCTURE

The pegmatite dike forms flat-laying tabular body, ca. 4 m thick and 20 m long in its most fractionated part. The dike has concentric zoning (from border to center): graphic zone (needles and grains of fine-grained black tourmaline in K-feldspar and quartz; minor biotite), granitic zone (thick prismatic black tourmaline in quartz; minor garnet, albite, muscovite), Qtz-Ms-Ab zone (black and green tourmaline in quartz; minor amblygonite, albite, muscovite) and Ab-Lpd zone (pink and white prismatic and pink fibrous tourmaline in quartz or lepidolite; minor albite).

METHODS

Tourmaline samples were analysed using EMPA (Cameca SX100 electron microprobe; Department of Geological Sciences, MU) and part of them also using LA-ICP-MS (a laser ablation system Analyte G2 connected to a sector field ICP-MS spectrometer Element 2; Department of Chemistry, MU).

TOURMALINE COMPOSITION

The tourmaline evolved in several generations through the pegmatite.

The crystallization of primary generation starts with the most primitive tourmaline of Mg-bearing foitite to Al-rich schorl composition in the graphic zone. Then continues with tourmaline of foitite to schorl composition in the granitic zone and F-rich schorl in the Qtz-Ms-Ab zone. These three zones represent outer part of the pegmatite that crystallized from the original potassic-sodic pegmatitic melt (Fig. 1).

The final stage of the primary crystallization took place in the inner, most fractionated part of the pegmatite, from a residual Li-rich albitic melt. The primary tourmaline in the Ab-Lpd zone slightly changed its composition during the crystallization from its core to rims (i.e., three "generations" of primary tourmaline evolved here). First crystallized Ca-bearing fluor-elbaite followed by Mn-bearing darrellhenryite and fluor-elbaite as the last (Fig. 1).

Metasomatic tourmaline evolved mainly on the rims and along fractures of the primary tourmaline but in some cases replaced it completely – the original primary tourmaline was fractured by later movements during the pegmatite evolution and fluids could fill this fractures or altered the primary tourmaline along them. Its composition is quite similar through the zones: Li-rich schorl → fluor-elbaite → fluor-elbaite → Fe-bearing fluor-elbaite. In each zone, its composition was either affected by composition of the replaced tourmaline (however, to much lesser extent than the replacing tourmaline below), or the compositional change represents gradual

evolution of single metasomatic fluid during its propagation along fractures in solidified pegmatite.

The recrystallized tourmaline represents the combination of the primary and metasomatic tourmaline composition, and usually forms zones between the two. The compositional sequence of the recrystallized tourmaline from the graphic to Ab-Lpd zone follows further (mixing) trend: Al-rich schorl → fluor-schorl to fluor-elbaite → Fe-rich fluor-elbaite → Fe-bearing fluor-elbaite.

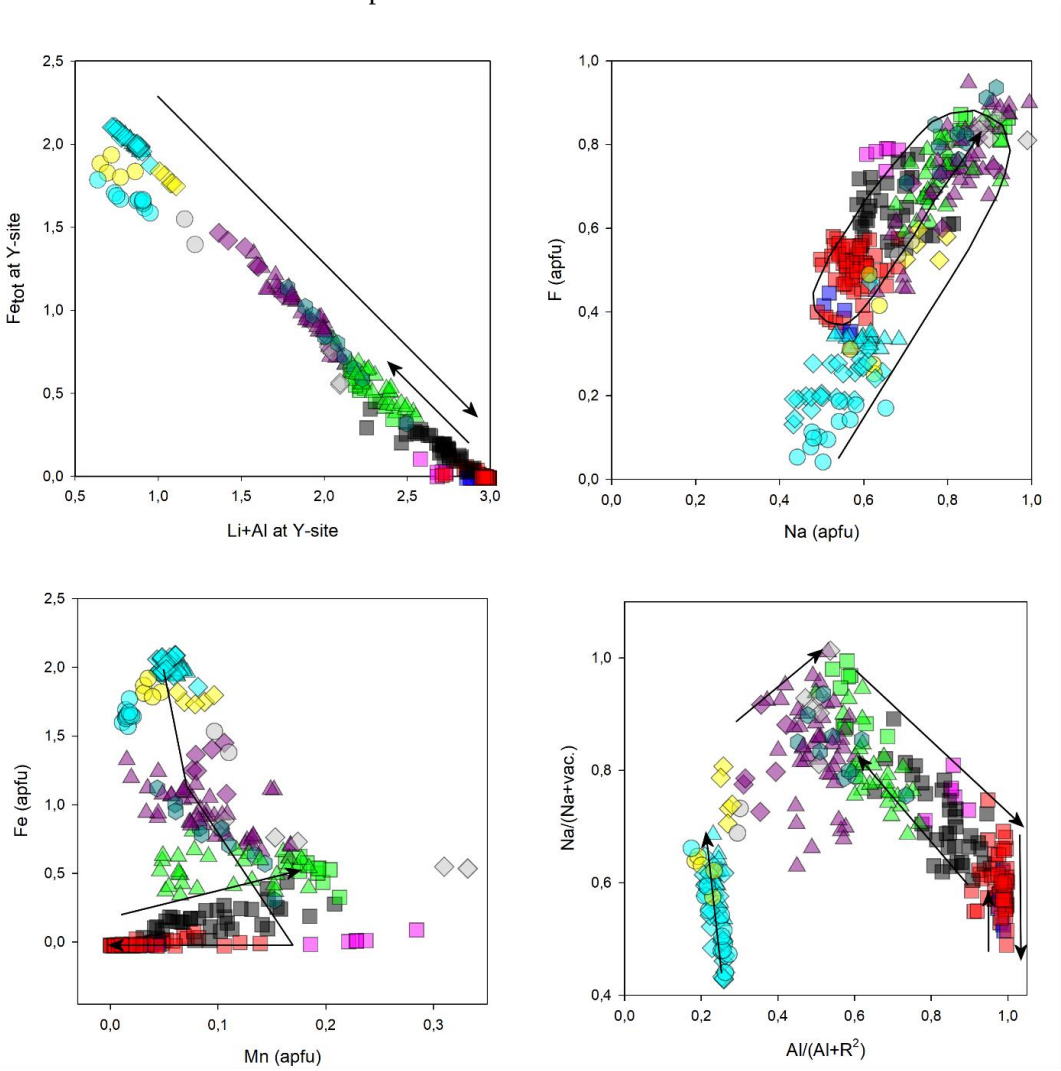

Fig. 1: The crystallization sequence of the primary tourmaline: ● – graphic zone, ● - granitic zone, ▲ – Qtz-Ms-Ab zone, ■ – Ab-Lpd zone (core); ■ – Ab-Lpd zone (darrellhenryite); ■ – Ab-Lpd zone (crystal rims); the metasomatic tourmaline: ● – graphic zone, ♦ - granitic zone, ▲ – Qtz-Ms-Ab zone, ■ – Ab-Lpd zone (M-Tur I), ■ – Ab-Lpd zone (M-Tur II); and recrystallized tourmaline: ● – graphic zone, ♦ - granitic zone (R-Tur I), ♦ - granitic zone (R-Tur II), ▲ – Qtz-Ms-Ab zone.

TOURMALINE EVOLUTION

The primary tourmaline in the graphic zone represents the most primitive zone encountered in the pegmatite; the primary tourmaline is quite enriched in Mg in contrast to the other zones. Increased content of Mg during crystallization of the graphic zone is also demonstrated by the presence of biotite. The Mg in the tourmaline and biotite of the graphic zone is the last occurrence of Mg in the pegmatite crystallization – the primary tourmaline generation in the granitic and blocky zones do not contain magnesium. This might suggest high initial fractionation of the pegmatite melt; however, the question will need to be resolved later after study of all pegmatite assemblages.

The primary tourmaline in the granitic zone is associated with Fe-rich spessartine. Compared to the black tourmaline from the graphic zone is slightly enriched by MnO, the

content of Na is basically the same, but the value of F slightly increased. The increase of Mn and F in tourmaline (as well as presence of garnet) documents the gradual increase of melt fractionation.

The blocky zone and its altered relics in the Qtz-Ms-Ab zone contain black primary magmatic tourmaline cores, replaced on their rims by metasomatic tourmaline. The primary tourmaline (F-rich schorl) documents further increase of Na and F in the melt, as their amounts reach the maximum values of those in the granitic zone whereas Mn contents are similar.

Compared to earlier primary tourmalines (crystallized from potassic melt) the first primary tourmaline in the Ab-Lpd zone has similar amounts of Na but significantly higher F, Al, Li, and slightly higher Ca and Mn contents (Fig. 1). The dramatic change in tourmaline chemistry reflects the difference in the source melt composition as the Al-Lpd zone crystallized from an albitic Li- and F-rich melt.

The crystallization of metasomatic generation in the graphic zone is characterized by increase in Na, F and Li+Al but it was not enough to reach the elbaite composition in contrast to the other zones.

The metasomatic generation in the granitic zone was formed on the rims of the primary tourmaline and in contrast to the graphic zone contains less Fe and more Li. The recrystallized zones document increased intensity of corrosive effect of metasomatic fluids on primary magmatic tourmaline; in contrast to the graphic zone, two different recrystallized zones of tourmaline formed here. The zone R-Tur I (fluor-schorl) represents recrystallization of the primary tourmaline with small addition of the metasomatic component (F, Na and Li) whereas the zone R-Tur II (fluor-schorl to fluor-elbaite) is rather a contamination of the metasomatic tourmaline by the primary component. The R-Tur I is very similar to the recrystallized tourmaline in the graphic zone; on the other hand, the R-Tur II is very similar to that from the Qtz-Ms-Ab zone (both in composition and diffuse oscillatory zoning).

The metasomatic and recrystallized tourmaline in the Qtz-Ms-Ab zone is developed mainly on the rims of the primary tourmaline or along its fractures; similarly to metasomatic tourmaline from other zones, it is slightly enriched in Mn. The metasomatic generation, identical in composition and zoning to that from rims and fractures, also forms separate green diffuse- or oscillatory-zoned crystals often associated with muscovite. The oscillatory zoning represents repeated increase in Li and decrease in Fe in the system.

Compositionally the same metasomatic generation is present also in the Ab-Lpd zone. The virtual identity of main compositional features of all metasomatic tourmalines (elevated Na, F, Li, Mn) indicates common fluid source and a fluid flow between the inner and outer zones of the pegmatite. Main differences among the metasomatic tourmalines are decrease in Li and increase in Fe contents from core zone to the pegmatite border; this can be affected by the transport distance and degree of reaction with the primary Fe-tourmalines. Since the metasomatic tourmaline is enclosed in other minerals (muscovite, quartz) crystallization from albitic melt enriched in Fe from dissolved primary schorl is more likely than hydrothermal origin.

Later metasomatic (hydrothermal) tourmaline stage (M-Tur II) in the Ab-Lpd zone have much higher Na and F contents than the earlier metasomatic tourmaline. Its texture (acicular overgrowths or fracture-fillings) and association with late K-feldspar in pockets and fractures indicate hydrothermal origin (e.g. Dutrow & Henry, 2016).

Acknowledgments: This research was supported by grants MUNI/A/1088/2017 and GA17-17276S.

REFERENCES

Dutrow B.L. and Henry D.J. (2016): Can Min 54:311–335.

Novák M. and Cempírek J. (2010): Acta Min-Petrograph 6:1–56.

Novák M. et al. (2013): Am Min 98:1886–1892.

Joint 5th Central-European Mineralogical Conference and
7th Mineral Sciences in the Carpathians Conference
Banská Štiavnica 2018

Monazite-(Ce) and xenotime-(Y) in A-type granites from Velence Hills, Hungary: Variations in composition and in situ chemical dating

[1]Tomáš Sobocký[#], [1]Martin Ondrejka and [1]Pavel Uher

[1] Comenius University, Faculty of Natural Sciences, Department of Mineralogy and Petrology, Ilkovičova 6, Mlynská dolina, 84215, Bratislava, Slovakia [#]tomas.sobocky@gmail.com

Key words: A-type granites, monazite-(Ce), xenotime-(Y), U-Th-Pb dating, Velence

Accessory REE phosphates are generally used as petrogenetic indicators during the evolution of igneous rocks, because of their physical-chemical resistance. In general, they are isomorphic solid solutions with a general formula AXO_4, where the A crystallographic site is occupied by the rare earth elements REE (mostly Ce^{3+}, La^{3+}, Nd^{3+}, Sm^{3+}) + Y^{3+}, Ca^{2+}, Th^{4+}, U^{4+} and X crystallographic site is occupied by P^{5+}, As^{5+}, Si^{4+}, S^{6+}.

Accessory monazite-(Ce) and xenotime-(Y) are relatively rare mineral species in granitic rocks from the Velence Hills, Hungary and they occur together with allanite-(Ce), zircon, rarely apatite and Fe-Ti oxides. The xenotime-(Y) forms unusually large (>500 μm) subhedral to anhedral crystals. The monazite-(Ce) forms mostly anhedral crystals (>200 μm) and occasionally zonal, which is a result of variable REE and Ca, Th contents. The chemical composition of the monazite-(Ce) indicates the predominance of the $CePO_4$ end-member [X_{mnz} (62 – 98)], with a lower content of huttonite ($ThSiO_4$) [X_{hutt} (0.5 – 5.0)] and cheralite ($Ca_{0.5}Th_{0.5}PO_4$) [X_{chrl} (0.7 – 47)] components. Some crystals show the systematic enrichment in La (3.13 – 17.08 wt. % La_2O_3; 0.044 – 0.251 apfu La and Nd (8.09 – 13.80 wt. % Nd_2O_3; 0.105 – 0.187 apfu Nd) as well. The most monazite analyses show the substitution mechanism along the huttonite line, with exception of some analyses in which the increased Ca concentration indicates a cheralite substitution mechanism. Monazites with a very low Ca content are a characteristic feature of a specific A-type granitoid chemistry, as there is a Ca deficiency compared to other chemical elements in the overall chemical composition. On the other hand, the cheralite end-member was confirmed in A-type granites of the Velence Hills. The xenotimes represent almost pure end member of YPO_4 (37.17 – 46.62 wt. % Y_2O_3; 0.699 – 0.803 apfu Y) and locally with an increased U content (0.15 – 1.98 wt. % UO_2; 0.001 – 0.015 apfu U). The change in chemical composition is controlled in particular by the thorite substitution mechanism.

Monazite dating was performed on 44 analyses with calculated Lower Permian age 292 ± 9.5 Ma (Cisuralian). These age data approximate to the data from Horváth et al. 2004, which published Upper Carboniferous (Pennsylvanian) to Lower Permian (Cisuralian) ages 271 – 291 Ma. They have used K/Ar, Rb/Sr dating on biotites. A surprising result was done by the xenotime dating (26 analyses), which showed Permian age 265 ± 9.3 Ma (Guadalupian). The xenotime-(Y) age is compatible to ages known from the A-types in central Western Carpathians. A significantly wide age range of monazites vs xenotimes may indicate a different time of crystallization of the accessory phosphates under magmatic conditions where the monazite is apparently the early-magmatic phase, whereas xenotime crystallized in late-magmatic stage of plutonite evolution. On the other hand, it may also suggests different degree of stability of monazite and xenotime.

Acknowledgment

Research have been financed from project APVV-15-0050, VEGA 1/0079/15 and UK/253/2018.

References

Broska I. and Williams C.T. (2003): J Czech Geol Soc 482:27.

Stern R.A. and Berman R.G. (2001): Chem Geol 172:113–130.

Gyalog L. and Horváth I. (eds) (2004): Geology of the Velence Hills and the Balatonfő. Geological Institute of Hungary. 1–316.

Joint 5th Central-European Mineralogical Conference and
7th Mineral Sciences in the Carpathians Conference
Banská Štiavnica 2018

New data on adelite and olivenite group minerals from Drienok deposit near Poniky, Slovakia

[1,2]Martin Števko[#], [1]Jiří Sejkora and [3]Štefan Súľovec

[1] Department of Mineralogy and Petrology, National Museum, Cirkusová 1740, 193 00 Praha 9 - Horní Počernice, Czech Republic [#]msminerals@gmail.com
[2] UK Mining Ventures Ltd., No. 1, The Old Coach Yard, East Coker; Somerset, BA22 9HY; Great Britain
[3] Stará dedina 40/37, 951 05 Veľký Cetín, Slovak Republic

Key words: conichalcite-duftite series, olivenite, zincolivenite, Drienok, Slovakia

An interesting associations of supergene minerals including minerals of the adelite and olivenite group were recently identified at the abandoned Drienok base-metal deposit near Poniky, Banská Bystrica Region, Slovakia.

Minerals of the adelite group (conichalcite-duftite series) forms pale-green, apple-green to yellowish-green crystalline aggregates, crusts or coatings, covering areas up to 6 cm^2 on the fissures and cavities of the mineralized limestone. Aggregates of the adelite group minerals consists of individual, well developed pseudorhombohedral crystals up to 50 μm in size. Typical associated supergene minerals are mimetite, azurite, malachite, calcite, aragonite, cerussite and zincolivenite. Paramorphoses of adelite group minerals after mimetite crystals were occasionally also observed.

Minerals of the adelite group from the Drienok deposit shows strong oscillatory chemical zoning in BSE, which is caused by an extensive Pb↔Ca substitution. Rather wide compositional range from duftite with up to 0.3 *apfu* Ca to conichalcite with up to 0.2 *apfu* Pb was observed. The *B* site is predominantly occupied by Cu with only minor amounts of Zn (up to 0.14 *apfu*) and Al (up to 0.10 *apfu*). Except of dominant content of As minor Si (up to 0.14 *apfu*) and P (up to 0.02 *apfu*) contents are also present. The average (n = 36) empirical formula of the adelite group minerals from the Drienok deposit, based on As+P+Si = 1 is $(Pb_{0.57}Ca_{0.47})_{1.04}(Cu_{1.07}Zn_{0.07}Al_{0.01})_{1.15}[(AsO_4)_{0.99}(SiO_4)_{0.01}]_{1.00}(OH)_{1.03}$.

Two different genetic types of the olivenite group minerals were discovered at the Drienok deposit. The first type was formed by the weathering of tennantite in supergene zone *in-situ* and it occurs as olive- to bright-green crystalline aggregates and crusts, which consists of prismatic crystals up to 0.7 mm in size. It is associated with azurite, malachite, conichalcite-duftite and calcite. The second type is represented by (sub)recently formed (around 400-500 years period) olive to greenish-white crystalline crusts or radial aggregates, which consists of short-prismatic to acicular crystals up to 1.5 mm in size. This type occurs solely on the surface of the weathered ore fragments in the backfill of the abandoned medieval tunnels. Associated minerals are gypsum, strashimirite, brochantite, devilline, langite, linarite and Co- and Cu-rich köttigite to Zn- and Cu-rich erythrite.

The both observed genetic types of olivenite group minerals from the Drienok deposit have elevated, but distinct content of Zn. The first type originating from the supergene zone *in-situ*, with Zn content ranging from 0.42 up to 0.71 *apfu*, is representing zincolivenite to Zn-rich olivenite compositions with an average (n = 14) empirical formula $(Cu_{1.38}Zn_{0.61})_{1.99}(AsO_4)_{1.00}(OH)_{1.01}$ based on As+P+Si+S = 1. The second, (sub)recently formed phase has comparably lower contents of Zn, ranging from 0.00 up to 0.22 *apfu* with an average (n = 28) empirical formula $(Cu_{1.94}Zn_{0.05}Pb_{0.02}Fe_{0.01})_{2.02}[(AsO_4)_{0.99}(SO_4)_{0.01}]_{1.00}(OH)_{1.04}$ based on As+P+Si+S = 1. Minor contents of S (up to 0.03 *apfu*) are also typical for this type of olivenite.

Acknowledgment: This research was financially supported by Czech Science Foundation (project GACR 17-09161S).

Joint 5th Central-European Mineralogical Conference and
7th Mineral Sciences in the Carpathians Conference

New Slovak gemstones

[1]Ján Štubňa[#], [2]Jana Fridrichová, [1]Ľudmila Illášová, [2]Peter Bačík, [3]Zuzana Pulišová and [4]Radek Hanus

[1] Constantine the Philosopher University in Nitra, Faculty of Natural Sciences, Gemmological Institute, Nábrežie mládeže 91, 949 74 Nitra, Slovakia [#]janstubna@gmail.com
[2] Comenius University in Bratislava, Faculty of Natural Sciences, Department of Mineralogy and Petrology, Ilkovičova 6, Mlynská dolina, 842 15 Bratislava, Slovakia
[3] Slovak Academy of Sciences, Geological Institute, Ďumbierska 1, Banská Bystrica, Slovakia
[4] Gemmological Laboratory of e-gems.cz, Prague, Czech Republic

Key words: gemstone, jewellery, deposit, gemmology

INTRODUCTION

The geological structure of Slovakia does not provide the prerequisite for gemstone minerals such as e.g. diamond, corundum (var. ruby), gem variety of beryl (excluding aquamarine), chysoberyl var. alexandrite.

As precious stones, rocks from Slovakia, where industrial mining can be applied, are more suitable. Limnosilicities are suitable for grinding as a cabochon (Illášová et al., 2013). Obsidian can be grinded as a cabochon or as a facetted stone (Illášová and Turnovec, 2003; Illášová and Spišiak, 2010; Hovorka and Illášová, 2010). Travertine, known as "Golden onyx" is also suitable for jewellery (Illášová and Spišiak, 2010).

However, several surveys have been carried out to evaluate potential raw materials for jewellery. The most famous gemstone from Slovakia is the precious opal. It is the famous European deposits of precious opal occur in the eastern range of the West Carpathian Mountains, east of Prešov and Košice. Opal has been traced further southward along Slanski Ridge as far as Tokai, Hungary, and opal has presumably been mined on the slopes of the Šimonka and Libanka Mountains near Dubník and Červenica since ancient times (Leechman, 1961; Ďuďa and Molnár, 1992; Kievlenko, 2003).

Some other gemstones were sometimes used. They were obtained during the exploitation of polymetallic raw materials in Štiavnické vrchy Mts. and Kremnické vrchy Mts. (quartz var. amethyst, chalcedony and jasper) (Herčko, 1987). We have reports about garnets from High Tatras, which have been termed Carbuncles in the past. Most of the precious stones regarded as (and named) carbuncles were ruby, spinel and garnet. Ruby and spinel do not occur in the High Tatras, therefore it must be garnet var. almandine only (Papp, 2007). Czirbesz (1772) assumed, that adding if one dig deeper in the rock, one would possibly find purer and harder garnets, which, consequently, would be more suitable to cut and polish. This assumption has not yet been confirmed.

Local citizens gathered and sold as a jewellery raw material garnet from the site between Hrb and Tri vody in Ľubietová in Slovenské Rudohorie Mts. (Zypharovich, 1859).

The possibility of processing some attractive raw materials from the territory of Slovakia for jewellery and decorative objects was solved by a state task. The research was conducted in the years 1980-1985 and 1986-1990 under the direction of R. Ďuďa (1990). In the first phase, the archive processing of about 600 localities of minerals and rocks. They are used as precious or decorative stones in the world. In the second phase, about 100 localities were documented. Samples were technologically processed in Turnov (Czech Republic). They were made of jewellery after processing. Gem quality minerals were found in 72 localities. Six minerals (quartz var. amethyst, quartz var. smoky quartz, sphalerite, pyrite, garnet var. almandine, and hematite) were faceted. The other samples were grinded to cabochons, tumbler stones, glyptics, cameo stones, planar grinding and decorative objects.

Natural crystals were also used for jewellery manufacture.

At the turn of the millennium, Barok and Tichý (2002) sought to confirm previous research. In papers and publications (Barok, Beličáková, 2001; Barok, 1999; Barok, Molnár, 2001) they confirmed the accuracy of previous research.

The aim of the paper is to familiarize acquainted with the newly discovered gem quality minerals that were discovered after 2000. There have been gemmological and spectroscopic studies of minerals such as quartz var. smoky quartz (Fridrichová et al. 2016) and sphalerite (Fridrichová et al. 2017), carried out and published in the past. These minerals have been described as minerals of gem quality in research in the 1980s.

List of gem quality minerals (garnet, rhodonite, chalcedony, wood opal, quartz var. amethyst, quartz var. rock crystal, quartz var. smoky quartz, pyrite, opal, fuchsite) have been extended to new localities.

The original list was extended by facet grinding (quartz var. rock crystal (e.g. Ozdín, 2017), wood opal and chalcedony).

We have discovered new gem quality minerals such as lazulite form locality Žirany and Bádice in Tríbeč hills and epidote from locality Skýcov in Tríbeč hills (Illášová, 2006; Illášová, Spišiak, 2010). We treated these minerals in the cabochons and tumbler stones. These minerals to be up to standard the parameters of Jewellery – industrial stone, which is possible, make cabochons (Kievlenko, 2003).

The new gem quality minerals such as, corundum var. sapphire from Gemerský Jablonec, Gortva and Hajnáčka in Cerová Highlands (Ozdín, 2017), garnet var. demantoid from Dobšiná in Slovenské Rudohorie Mts. (fig. 1a), hydroxylapatite from Muránska Dlhá Lúka in Stolické vrchy Mts. (a potential gemmological assessment was suggested by the authors Bancík et al. 2014) (fig. 1b), spinel var. pleonaste form Hodruša-Hámre in Štiavnické vrchy Mts. (fig. 1c), euchroite from Ľubietová in Slovenské Rudohorie Mts. (fig. 2a), libethenite from Ľubietová in Slovenské Rudohorie Mts. (fig. 2b) and fluorite from Gemerská Poloma in Slovenské Rudohorie Mts. (fig. 2c), are suitable for faceting. Jewellery stones is only corundum var. blue sapphire (1st class) and garnet var. demantoid (2nd class) (Kievlenko, 2003). Others faceting stones are interesting only for collectors.

a) b) c)

Fig. 1: The 0,11 ct garnet var. demantoid from Dobšiná (a), the 0,68 ct hydroxylapatite from Muránska Dlhá Lúka (b), the 2,61 ct spinel var. pleonaste from Hodruša Hámre(c)

a) b) c)

Fig. 2: The 1,35 ct euchroite from Ľubietová (a), the 0,04 ct libethenite from Ľubietová (b), the 0,85 ct fluorite from Gemerská Poloma (c)

Acknowledgment: This present research was supported by the Ministry of Education of Slovak Republic Grant Agency under the contracts KEGA 062UKF-4/2016.

REFERENCES

Bancík T. et al. (2014) : Minerál 6:522–526.
Barok M. and Tichý V. (2002): Drahé a ozdobné kamene Slovenskej republiky. GEMGEO Bojnice.
Barok M. and Beličáková S. (2001): The Slovaks precious stones – the unfamiliar world. www.geology.cz.
Barok M. (1999): Acta Mont Slov 1:80–82.
Barok M. and Molnár J. (2001): Minerál 4:300–303.
Czirbesz J.A. (1772): Königlich allergnädigst privilegirte Anzeigen 2:285–288.
Ďuďa R. and Molnár J. (1992): Lapis 92:23–28.
Ďuďa R. (1990): Šperkařství 3:21–30.
Fridrichová J. et al. (2016): Vibr Spectr 7:71–78.
Fridrichová J. et al. (2017): Esemestník 1:6–9.
Herčko I. (1987): Geol průzkum 11:330–331.
Hovorka D. and Illášová Ľ. (2010): Proceedings if the XIX CBGA Congress: 385–390.
Illášová Ľ. and Turnovec I. (2003): Bull. mineral.-petrolog. Odd. Nár. Muz 11:150–152.
Illášová Ľ. (2006): Gemologický spravodajca 2:21–23.
Illášová Ľ. and Spišiak J. (2010): Geol Balcan 164–165.
Illášová Ľ. et al. (2013): Min Slov 45:201–212.
Kievlenko E.Y. (2003): Geology of gems. Ocean Pictures Ltd.
Leechman F. (1961): The opal book a complete guide to the famous gemstone. Lansdowne Press.
Ozdín D. (2017): Montanarevue 3:24.
Ozdín D. (2017): Montanarevue 3:27.
Papp G. (2007): Prvenstvá nerastnej ríše Slovenska: 46–50.
Zypharovich V. (1859): Mineralogisches Lexicon für das Keisserthum Österreich. Wilhelm Braumüller.

Joint 5th Central-European Mineralogical Conference and
7th Mineral Sciences in the Carpathians Conference
Banská Štiavnica 2018

Zinc in Piława Górna pegmatitic system, Góry Sowie Block, SW Poland

[1]Eligiusz Szełęg[#], [2]Adam Pieczka and [3]Adam Szuszkiewicz

[1] University of Silesia in Katowice, Faculty of Earth Sciences, Będzińska 60, 41-200 Sosnowiec, Poland [#] eligiusz.szeleg@us.edu.pl
[2] AGH University of Science and Technology, Department of Geochemistry, Mineralogy and Petrography, Mickiewicza 30, 30-059 Kraków, Poland
[3] University of Wrocław, Institute of Geological Sciences, Borna 9, 50-204 Wrocław, Poland

Key words: Zinc, granitic pegmatite, Góry Sowie Block, Piława, Sudetes

The Julianna pegmatitic system at Piława is the largest pegmatitic occurrence in the Góry Sowie Block at the NE margin of the Variscan Bohemian Massif. As a whole, Julianna represents the NYF (Nb–Y–F) + LCT (Li–Cs–Ta) mixed pegmatite family of anatectic origin. Zinc-rich minerals of the system represent (1) oxides, (2) silicates and (3) sulphides.

(1) Oxides: Zinc-bearing ilmenite-pyrophanite series minerals are found sporadically in the weakly to moderately evolved Jul4+5 (NYF/LCT) dyke. The enrichment in Zn (up to 10.05 wt.% of ZnO) has a local character. However, most of the ilmenite-pyrophanite grains are Zn-poor.

Compositionally heterogeneous crystals of gahnite are found in the Jul4+5 (NYF/LCT), Subtrio (NYF/LCT) and Blue Beryl (LCT) dykes. The compositions can be presented as complex solid solutions: ($Ghn_{0.67–0.84}Hc_{0.14–0.30}Glx_{0.01-0.02}Frk_{0.00–0.02}Spl_{0.00–0.01}Mgn_{0.00–0.01}$), ($Ghn_{0.74–0.82}Hc_{0.16–0.23}Glx_{0.00–0.01}Frk_{0.00–0.01}Spl_{0.00-0.01}$), ($Ghn_{0.69–0.90}Hc_{0.08–0.26}Glx_{0.01–0.02}Frk_{0.00–0.02}Spl_{0.00–0.01}Mgn_{0.00–0.01}$) and ($Ghn_{0.95–0.99}Hc_{0.00–0.04}Glx_{0.00–0.01}Frk_{0.00–0.02}Spl_{0.00–0.01}Mgn_{0.00–0.01}$), respectively, where the abbreviations denote end-members gahnite, hercynite, galaxite, franklinite, spinel and magnetite. In the Blue Beryl dyke, the gahnite is associated with a Zn-rich tourmaline.

Nigerite-group minerals are found only in the cassiterite-rich Blue Beryl dyke. Typically, the minerals are dominated by Al_2O_3 (50.72–53.84 wt.%) with varying SnO_2 (12.97–20.87 wt.%) and negligible TiO_2 (0.09–0.65 wt.%) and SiO_2 (0.08–0.74 wt.%). ZnO ranges from 7.71 wt.% in ferronigerite to 23.18 wt.% in zinconigerite, whereas the total content of $FeO+Fe_2O_3$ reaches 13.39 wt.% and 3.52 wt.%, respectively. MnO varies in the range of 0.28–1.01 wt.%. Trace amounts of ≤0.13 wt.% MgO, ≤0.17 wt.% CaO and up to 0.19 wt.% Cr_2O_3 are also present.

(2) Silicates: Zn-rich tourmalines (Zn-rich fluor-elbaite and elbaite with up to ~7.5 wt.% ZnO) occur only in the Blue Beryl dyke, as products of a late (Na,Li,B,F)-metasomatism of gahnite. They occur only in the thin ~100 μm wide zone around partly dissolved gahnite. Lower enrichment in Zn, up to 3.12 wt.% ZnO, is observed in schorl also associated with gahnite in the same dyke.

Helvine-group minerals are found in the Blue Beryl and high evolved Jul4+5 dykes. Genthelvite with 43.11-45.56 ZnO wt.% occurs as discontinuous overgrowths on gahnite in the Blue Beryl dyke. Helvine, containing 1.88-2.31 ZnO wt.%, is found in the high evolved Jul4+5 dyke.

(3) Sulphides: Sphalerite, ZnS, and greenockite or hawleite, (Cd,Zn)S, are accessory components mainly of pegmatites with prevailing LCT characteristics.

The primary source of Zn in the pegmatite-forming anatectic melts of the GSB unit were geosynclinic sandstone-mudstone and greywacke series of the Neoproterosoic–Cambrian flysch with inclusions of basic to acidic lavas and associated tuffs metamorphosed and partly migmatized to various gneisses and amphibolites. Melting of the migmatitic biotite, other mafic components and sulphides (mainly sphalerite) of the amphibolites, could have supplied Zn into the pegmatite-forming anatectic melts.

Acknowledgment: The studies were supported by the National Science Centre (NCN) grant 2015/19/B/ST10/01809 to AP.

Joint 5th Central-European Mineralogical Conference and
7th Mineral Sciences in the Carpathians Conference

Caesium and rubidium in minerals from the Julianna pegmatites, Sudetes, SW Poland

[1]Adam Szuszkiewicz[#], [2]Adam Pieczka and [3]Eligiusz Szełęg

[1] University of Wrocław, Institute of Geological Sciences, 50-204 Wrocław, pl. M. Borna 9, Poland
[#]adam.szuszkiewicz@uwr.edu.pl
[2] AGH University of Science and Technology, Department of Mineralogy, Petrography and Geochemistry 30-059 Kraków, Mickiewicza 30, Poland
[3] University of Silesia, Department of Geochemistry, Mineralogy and Petrography, 41-200 Sosnowiec, Będzińska 60, Poland

Key words: caesium, pollucite, granitic pegmatites, Sudetes

The Julianna rare-element pegmatites are exposed near Piława Górna, SW Poland, in partly migmatized gneisses and amphibolites of the Góry Sowie Block at the NE margin of the Bohemian Massif. The pegmatites, up to ~7 m thick, vary from primitive and NYF-affiliated moderately evolved simply-zoned bodies to highly fractionated dikes that contain lithium mica–cleavelandite–quartz zone and a spodumene-lepidolite core with LCT characteristics, located centrally instead of a usual quartz core. Saccharoidal albite and fine-grained K-mica built replacement units.

With increasing fractionation, Cs and Rb substitute K attaining typically up to 0.31 wt% Cs_2O and 0.53 wt% Rb_2O in K-feldspar and up to 1.12 wt% Cs_2O and 0.84 wt% Rb_2O in primary white mica. Concentrations of Cs and Rb in common dark mica are typically below detection limits of electron microprobe. Volumetrically insignificant Cs-rich beryl and pezzottaite with up to 16.56 wt% Cs_2O are also present. Metasomatic alterations in the most evolved dikes result in the local increase up to 4.21 wt% of Cs_2O in white micas and up to 1.91 wt.% Cs_2O and 0.45 wt.% Rb_2O in biotite.

In Fe-rich tourmaline that formed as a result of tourmalinization of biotite, inclusions of secondary dark micas contain up to 3.26 wt.% Cs_2O and 0.61 wt.% Rb_2O, and some of them accumulate as much as 16.28 wt.% Cs_2O (0.67 apfu) and 0.73 wt.% Rb_2O (0.04 apfu). Because Cs >> K, Fe+Mg > Li+Al and Fe > Mg, this mica could be considered as a Cs-analogue of annite. The same mica with up to 18.71 wt.% Cs_2O (0.76 apfu) and 0.49 wt.% Rb_2O (0.03 apfu) was found in another dyke with hybrid NYF+LCT characteristics. Sokolovaite, the Cs-dominant light Li-bearing mica with up to 26.80 wt.% Cs_2O (0.96 Cs apfu) and ≤0.09 wt.% Rb_2O was found as inclusions in lithiophilite in phosphate nodules close to the spodumene–lepidolite core.

Pollucite, $Cs[AlSi_2O_6]\ nH_2O$, was found in the graphic intermediate zone partly replaced by secondary albite near the LCT-affiliated central units of the largest and most fractionated dike. It occurs as up to mm-sized oval crystals in ovoid white to brownish-orange nodular pockets, up to 30 cm large, and as small grains interstitially scattered in the vicinity of the pockets. The pockets contain also Ca-zeolite, Li-poor sometimes Fe-rich muscovite and smectites. The replacement of pollucite by clay minerals is widespread. The pollucite (Poll) contains 14.67–16.45 SiO_2, 38.65–47.62 Al_2O_3, 30.96–41.73 Cs_2O and 0.54–2.37 Na_2O as well as <0.27 of Rb_2O and <0.22 CaO (in wt%). Several compositional types are distinguished basing on %CRK [$100\cdot(Cs+Rb+K)/\Sigma M^{1+}$ cations]: (1) primary Poll with 77.9–81.4, (2) secondary veinlets cutting the primary Poll with 81.7–84.3, (3) secondary rims around the primary Poll with 85.7–93.6 and (4) replacement veinlets with 74.4–76.5. Types 2-3 formed due to re-equilibration with the evolving fluid and type 4 represents incipient alteration to clay minerals.

We tentatively attribute the formation of Cs- and Rb-enriched micas and pollucite in the Julianna system to the action of fluids emanating from the most evolved pegmatitic zones with pronounced LCT characteristics.

Acknowledgment: The study was financed by the University of Wrocław grant 0401/0156/18 to AS and National Science Centre grant 2015/19/B/ST10/01809 to AP.

Joint 5th Central-European Mineralogical Conference and
7th Mineral Sciences in the Carpathians Conference
Banská Štiavnica 2018

Phosphates in the Julianna pegmatitic system at Piława Górna, Góry Sowie Block

[1]Diana Twardak[#] and [1]Adam Pieczka

[1] AGH University of Science and Technology, Faculty of Geology, Geophysics and Environmental Protection, Department of Mineralogy, Petrography and Geochemistry, 30-059 Kraków, Mickiewicza 30, Poland [#]twardak@agh.edu.pl

Key words: phosphate mineralization, anatectic pegmatites, Julianna system, Piława Górna

The Julianna pegmatitic system consists of coeval and cogenetic pegmatites exposed in 2007 during mining works in the migmatite-amphibolite quarry at Piława Górna in the Góry Sowie Block, Lower Silesia, SW Poland. Up to 2011 the pegmatites, along with the host migmatites and amphibolites, were intensively exploited for crushed stones. Since then the quarry exploits the deposit part poor in pegmatite mineralization.

Pegmatites of the system formed from anatectic melts generated by partial melting of the metasedimentary–metavolcanic sequence and were intruded during decompression, ~380–370 Ma, into tectonized amphibolite as a network of dikes and apophyses varying in size, internal structure, and degree of geochemical fractionation. They display NYF (Nb–Y–F) or mixed NYF ± LCT (Li–Cs–Ta) signature, ranging from homogeneous and relatively primitive dikes through simply zoned, weakly to moderately evolved NYF-affiliated bodies, to highly fractionated LCT pods, up to several meters in diameter, in central parts of swellings at intersections of larger pegmatitic dikes. Typical zoning pattern comprises border unit + graphic intermediate unit + blocky feldspar intermediate unit + quartz core in less evolved bodies, and + saccharoidal albite unit + lithium-mica–cleavelandite–quartz unit + spodumene–lepidolite core in the LCT pods.

Pegmatites of the system represent various types and subtypes of the REL-REE and REL-Li subclasses of the rare-element pegmatitic class, in which phosphate minerals are common accessories. Xenotime-(Y), monazite-(Ce), and fluorapatite with slightly elevated REE ± Mn are the only phosphates in the moderately-evolved NYF-affiliated bodies mainly of the euxenite type with yellowish-green beryl and black tourmaline, [Mn/(Mn+Fe) ratio in garnet ~0.63; in primary Nb-Ta oxides ~0.56]. In the more evolved dyke(s) with blue beryl and rare fluor-elbaite [Mn/(Mn+Fe) ratio in garnet ~0.66; in primary Nb-Ta oxides ~0.95], phosphates are very rare and represented only by Fe-bearing lithiophilite and its alteration products sicklerite + alluaudite (all with the ratio 0.58) + secondary mitridatite (0.12) + unrecognized secondary phosphates (0.11–0.58).

The most abundant phosphate assemblage occurring in the form of small nodules was encountered at contacts of the lithium-mica–cleavelandite–quartz unit with the spodumene–lepidolite core in the Li-Cs-bearing pods. All Mn-Fe phosphates of the assemblage reveal extremely high Mn-Fe fractionation [Mn/(Mn+Fe)>0.995]. They are associated with spessartine garnet (0.95–0.99) and primary Nb-Ta oxides (0.95–0.99). Lithiophilite, evolving in places to natrophilite, and Mn- and/or Sr-bearing fluorapatite are the main components of the nodules. They are associated by inclusions of triploidite, triplite and plausibly joosteite in the lithiophilite–natrophilite matrix. Mn-bearing hydroxylapatite, chlorapatite and pieczkaite occur as accessories in fluorapatite. Purpurite and serrabrancaite are the main secondary phosphates in lithiophilite interior of the nodules, whereas hureaulite (locally enriched in Ca), fairfieldite and pararobertsite, appear more closely to the fluorapatite rim. Tiny inclusions of ximengite, U-bearing phosphates close to lermontovite and vyacheslavite, Ca-bearing Mn oxide (ranciéite) and light Cs-Li-bearing mica (sokolovaite) could be occasionally found as accessories.

Acknowledgment: The study was supported by the National Science Centre (Poland) grant 2015/19/B/ST10/01809 to AP.

Joint 5th Central-European Mineralogical Conference and
7th Mineral Sciences in the Carpathians Conference
Banská Štiavnica 2018

Elbaite-bearing, Nb-Ta-rich granitic pegmatite from Dobšiná, Gemeric Unit, Eastern Slovakia: the first documented occurrence in the Western Carpathians

[1]Pavel Uher[#], [1]Peter Bačík, [2]Martin Števko, [1]Štěpán Chládek and [1]Jana Fridrichová

[1] Comenius University, Faculty of Natural Sciences, Department of Mineralogy and Petrology, Ilkovičova 6, 842 15 Bratislava, Slovakia [#]pavel.uher@uniba.sk
[2] Department of Mineralogy and Petrology, National Museum, Cirkusová 1740, 193 00 Prague 9, Czech Republic

Key words: elbaite, schorl, columbite, fersmite, granitic pegmatite

Granitic pegmatites are relatively common rocks in pre-Alpine (Paleozoic) crystalline basement of the Tatric and Veporic Units of the Western Carpathians. They are genetically connected with orogen-related Variscan granitic rocks of S- or I-type affinity. The most evolved West-Carpathian pegmatites contain beryl and/or Nb-Ta oxide minerals (columbite-tantalite, rarely tapiolite-, wodginite- and pyrochlore/microlite-groups, Nb-Ta rutile, and fersmite) and they belong to beryl-columbite subtype of rare-element class and LCT-family. However, all these pegmatites are poor in Li and without Li-minerals. Moreover, granitic pegmatites were not known in the Gemeric Unit of the Western Carpathians.

Here, we describe the first occurrence of granitic pegmatite in the Gemeric Unit and the first documented rare-element, Nb-Ta-rich granitic pegmatite with frequent Li-mineral (elbaite-schorl) in the whole Western Carpathians. The pegmatite forms 2–3 m thick dike in host gneisses and amphibolites of the Klátov Group, situated in Malá Vlčia Valley near Dobšiná town in the NW part of the Gemeric Unit. The pegmatite shows K-feldspar-quartz graphic to blocky feldspar zone, coarse-grained K-feldspar-albite-quartz-muscovite unit and quartz core.

Tourmaline forms long prismatic crystals and fan-shaped crystal aggregates (up to 3 cm long) in quartz and albite. Electron-microprobe (EPMA) and LA-ICP-MS analyses of tourmaline reveal intermediate schorl to elbaite composition with presence of dominant schorl, fluor-schorl, elbaite and fluor-elbaite members. Lithium content in tourmaline attains 0.6–1.2 wt.% Li_2O (0.40–0.76 apfu Li), ≤54 mol.% of (fluor-)elbaite. The tourmaline contains 6.1–10.5 wt.% FeO (0.82–1.47 apfu Fe) and 1.5–2.4 wt.% MnO (0.21–0.33 apfu Mn); Mn/(Mn+Fe) = 0.14–0.27. Content of Ca is very low (≤0.2 wt.% CaO; ≤0.03 apfu Ca), Ti and Mg are usually under EPMA detection limit. The X-site vacancy is generally low (0.02–0.14 apfu), F concentration attains 0.8–1.2 wt.% (0.44–0.63 apfu).

Columbite-(Mn) [$Mn/(Mn+Fe^{2+})$ = 0.94-0.98; Ta/(Ta+Nb) = 0.31–0.48] forms subhedral crystals with irregular zoning and partial replacement by hydroxycalciomicrolite and hydroxycalciopyrochlore to hydrokeno-pyrochlore. Fersmite [Ta/(Ta+Nb) = 0.08–0.16] associates with Sn-rich hydroxy-calciomicrolite (≤6 wt.% SnO; ≤0.23 apfu Sn). Other accessory minerals comprise Mn-rich almandine (≤46 mol.% spessartine), zircon (≤8.5 wt.% HfO_2; ≤0.08 apfu Zr), fluorapatite, monazite-(Ce), xenotime-(Y), thorite/huttonite, cassiterite, magnetite/hematite, and sphalerite.

The Dobšiná pegmatite shows affinity to the LCT-family with distinct enrichment in B, Li, Sn, Nb, and Ta. This geochemical feature is typical for Permian tin-bearing, specialized S-type granites of the Gemeric Unit (e.g., Hnilec, Dlhá Valley, Betliar occurrences). Consequently, we assume a genetic relationship between the Gemeric granites and the Dobšiná pegmatite. Moreover, the pegmatite shows a distinct Alpine tectono-metamorphic overprint connected with formation of secondary mineral assemblage: mosaic quartz, Ca-rich almandine (14–35 mol.% grossular), chamosite, part of Nb-Ta phases (?), and dravite fissure-fillings in schorl-elbaite.

The Velká Bíteš pegmatite field: new rare-element pegmatite occurrences at the eastern margin of the Moldanubian Zone, Czech Republic

[1]Scarlett Urbanová[#] and [1]Jan Cempírek

[1] Masaryk University, Faculty of Science, Department of Geological Sciences, Kotlářská 2, 611 37 Brno, Czech Republic [#]394715@mail.muni.cz

Key words: pegmatite, tourmaline, columbite, topaz, zircon, cassiterite, fluorapatite

Mineralogy of 8 localities (Osová Bítýška, Vlkov, Křižínkov I-V, and Křoví) from the newly-discovered Velká Bíteš rare-element pegmatite field (Czech Republic) was studied in order to determine their degree of fractionation and type of their rare-element mineralization (Urbanová 2017).

The studied granitic pegmatites are situated in the easternmost part of the Moldanubian Zone, characterized by presence of S-type granites and leucogranites in the thermal aureole of the A-type Třebíč durbachite pluton, and various metamorphosed, strongly migmatized paragneiss to migmatites of the Gföhl Unit, Moldanubian Zone of the Bohemian massif.

Elevated contents of F, Li, Rb, Cs, Sn, Ta, and W were found at most localities. The pegmatite at Osová Bítýška is isolated from the rest of the field. It has a small core with Li-mineralization (green and pink tourmaline, lepidolite) and high contents of F, Rb, Cs and elevated Sn. Accessory minerals include lacroixite topaz, zircon, cassiterite and fluorapatite. Pegmatite at Vlkov is chemically primitive, it contains only elevated Nb (oxides) and F (tourmaline). The Křižínkov I pegmatite is well fractionated, contains elevated Li, F, Sn, and W (tourmaline – elbaite, cassiterite, wodginite, ixiolite); similar fractionation degree is in the adjacent pegmatite at Křoví (with common cassiterite, ixiolite, rutile and fluorapatite). The Křižínkov II pegmatite is relatively primitive, deformed, and contains elevated REE and Zr [zircon, monazite-(Ce), cheralite, xenotime-(Y)] and increased contents of Nb and F (columbite, tourmaline). Elevated fractionation in the Křižínkov III dike is indicated by presence of topaz and minor elbaite, whereas Křižínkov IV is a large and rather primitive dike. The Křižínkov V pegmatite with common NbTa-oxides and elbaite (columbite, fluor-elbaite) is the most fractionated dike from the Křižínkov group.

The observed degree of tourmaline fractionation correlates well with the observed amount and type of rare-metal mineralization, especially Sn, and to a lesser degree also Nb and Ta (Fig. 1). Despite their subeconomic character, the Velká Bíteš pegmatite field is a good example of unexpected occurrence of rare-element mineralization (Li, Rb, Cs, Sn, Ta, and W) generated from apparently small volumes of S-type granitic melts.

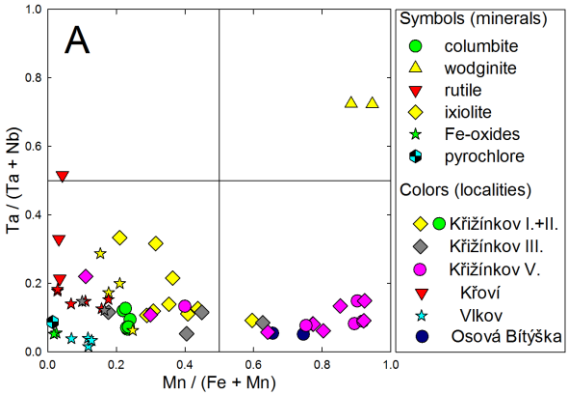

Fig. 1: Chemical composition of Nb,Ta,Sn,W,Fe,Mn-oxide minerals in the columbite quadrilateral diagram.

Acknowledgment: This work was supported by the Masaryk University grant MUNI/A/1088/2017.

References

Urbanová, S. (2017): Rare-element pegmatites in SE part of the Strážek Moldanubicum. MSc. Thesis, Masaryk University, Brno, 95 p.

Joint 5th Central-European Mineralogical Conference and
7th Mineral Sciences in the Carpathians Conference

Sulfide mineralization in Ediacaran black shales of the Teplá-Barrandian unit (central Bohemia, Czech Republic)

[1]František Veselovský[#], [1]Jan Pašava, [1]Ondřej Pour, [1]Tomáš Magna, [1]Petr Dobeš, [2]Lukáš Ackerman, [2]Martin Svojtka, [3]Jiří Žák and [3]Jaroslava Hajná

[1] Czech Geological Survey, Klárov 3, 118 21 Prague, Czech Republic [#]frantisek.veselovsky@geology.cz
[2] Institute of Geology of the Czech Academy of Sciences, Rozvojová 269, 165 00 Prague, Czech Republic
[3] Institute of Geology and Paleontology, Faculty of Science, Charles University, Albertov 6, 128 43 Prague, Czech Republic

Key words: Žloukovice, black shales, pyrite, weathering

The Ediacaran black shales at Žloukovice section crop out in the lithologically monotonous Zbiroh–Šárka belt (dominated by meta-graywackes, meta-siltstones, slates and cherts of unknown origin without the presence of any volcanic rocks) of the Blovice complex, a Cadomian accretionary wedge exposed in the central Bohemian Massif. The maximum depositional age of the greywackes–shales was determined at 571 ± 3 Ma (U–Pb dating on zircon) and the mineral assemblages suggest their subsequent low-grade, up to lower greenschist facies metamorphic overprint.

Sulfides are irregularly disseminated in black shales and pyrite is the main sulfide. It forms small grains, larger aggregates and thin layers or veinlets. Pyrite forming often folded layers is of synsedimentary origin. The centre of these layers is formed by a mixture of organic matter and silicate matrix, indicating sulfidation/pyritization process of organic matter. Some larger isolated pyrite grains are inhomogenous and show zonality caused by substitution of S by As. Lighter zones are characterized by higher As contents (up to 4 wt.%) while darker parts are As-poor (As = up to 0.5 wt.%) and contain up to 0.X wt.% Co and Sb. Outer zone in these pyrite grains contains the lowest As content which is most likely related to partial dissolution which was not observed in inner parts of pyrite grains. This is a clear evidence that this zonality is not related to weathering of pyrite which resulted in the formation of jarosite and Fe-oxyhydroxides.

Some grains of pyrite contain inclusions of sphalerite, chalcopyrite, and galena up to 2 μm, exceptionally up to 5 μm. As to higher solubility of these sulfides than that of pyrite, small open cavities originated in pyrite grains. These cavities were locally filled in anglesite.

Rather rare isolated grains of arsenopyrite and unidentified phase (Fe, Ni)-Co-As-S up to 4 μm in size were observed in the shale. Marcasite forms sharp crystals forming rosette aggregates up to several mm. Marcasite was later partially substituted by pyrite.

The analyses of major and trace elements in 18 samples revealed presence of two types of shales. Normal black shales are, compared to Au-enriched facies, characterized by lower average values of SiO_2 (63 wt.%), Fe_2O_3 (1.73 wt.%), S (0.06 wt.%), TOC (0.2 wt%), As (16 ppm), Sb (6 ppm), V (126 ppm) and low average SiO_2/Al_2O_3 (3.9) and K_2O/Na_2O (1). They, however, contain higher average values of Co (17 ppm), Ni (58 ppm), Cu (48 ppm), Zn (87 ppm) and ΣREE (146 ppm). Geochemical characteristics and Li isotopic compositions indicate that these facies contain chemically immature crustal material originated in an active continental margin/continental island arc. Conversely, Au-enriched facies are strongly silicified and typical for significantly higher average values of SiO_2 (74 wt.%), S (0.31 wt.%), Fe_2O_3 (2.13 wt.%), TOC (0.6 wt.%), As (61 ppm), Sb (60 ppm), V (202 ppm) but lower average Co (3 ppm), Ni (21 ppm) , Cu (20 ppm) Zn (27 ppm) and ΣREE (107 ppm). Geochemical signatures indicate their origin at a passive margin, in a basin developed on continental crust.

Acknowledgment: This study is a contribution to the GAČR project 17-15700S.

Geochemistry and geochronology of calc-alkaline lamprophyres, Central Slovakia/ Western Carpathians

[1]Lucia Vetráková[#] and [1]Ján Spišiak

[1] Matej Bel University, Faculty of Natural Sciences, Department of Geography and Geology, Tajovského 40, 97401, Slovak republic [#] lucia.vetrakova@umb.sk

Key words: geochemistry, geochronology, calc-alkaline lamprophyres, Nízke Tatry Mts.

Calc-alkaline lamprophyres in Western Carpathians are not common. They were described from only a few core mountains (Nízke Tatry Mts., Malá Fatra Mts. and Považský Inovec Mts.). We studied lamprophyres from Jarabá area (Hovorka 1967; Kamenický 1962; Krist 1967). They crop out as dikes cutting the gneisses of the Tatric Paleozoic crystalline complexes and are of 5-20 m thick.

The studied lamprophyres from Jarabá area are dark-green colour with abundant phenocrysts of clinopyroxene, biotite and amphibole and in the matrix there are plagioclases, quartz and alkaline feldspars. Clinopyroxene correspond to augite (Morimoto et al. 1988). Biotite and amphibole are younger than clinopyroxene. Plagioclases are zonal with An_{36-55} in core and An_{18} in rims. Apatite is the main accessory. According to their texture and modal composition, these rocks can be classified as kersantite to spessartite.

In the classification diagram of the lamprophyre rocks (Rock 1991), they lie in the field of calc - alkaline lamprophyres. The calc - alkaline and geotectonic character of the studied lamprophyres is documented in other discrimination diagrams (Meschede 1986; Pearce and Cann 1973 and others). In the chondrite normalized REE pattern, the studied lamprophyres present enrichment of LREE relative to HREE with slight Eu-anomaly. Trace element diagram normalized to primitive mantle shows lower content of Nb and Sr, and higher contents of Cs. The isotope ratios ($^{87}Sr/^{86}Sri$ = 0,709-0,723, $^{143}Nd/^{144}Ndi$ = 0,5120-0,5121, $^{176}Lu/^{177}Hf$ = 0,012-0,014, $^{176}Hf/^{177}Hf$ = 0,282) indicate the crustal material input during magma generation.

The age of studied lamprophyres has not been determined. Tera-Wasserburg concordia plots for LA-ICP-MS U-Pb apatite (Trinity College, Dublin) analyses from Jarabá area documented age 259,0 ± 2.8 Ma. This age corresponds to their tectonic position.

Acknowledgment: This study represents a partial output of the grants: APVV-15-0050 VEGA 1/0650/15 and VEGA 1/0237/18.

REFERENCES

Hovorka D. (1967): Záp Karp 8:51–78.
Kamenický J. (1962): Geol. práce, Zprávy 24:135–141.
Krist E. (1967): Acta Geol Geogr Univ Com Geol. 12:63–73.
Meschede M. (1986): Chem Geol 56:207–218.
Morimoto N. et al. (1988): Am Min 73:1123–1133.
Pearce J. and Cann J.R. (1973): Earth Planet Sci Lett 19:290–300.
Rock N.M.S. (1991): Lamprophyres. Blackie and Son Ltd. 285.

Joint 5th Central-European Mineralogical Conference and
7th Mineral Sciences in the Carpathians Conference

An interesting secondary phosphates association with allanpringite from abandoned iron deposit Krušná Hora near Beroun, Czech Republic

[1,2]Luboš Vrtiška[#], [2]Jiří Sejkora and [2]Radana Malíková

[1] Masaryk University, Faculty of Science, Department of Geological Sciences, Kotlářská 2, 611 37 Brno, Czech Republic [#]lubos_vrtiska@nm.cz
[2] National Museum, Department of Mineralogy and Petrology, Cirkusová 1740, 193 00 Prague-Horní Počernice, Czech Republic

Key words: secondary phosphates, allanpringite, Al-rich beraunite, Krušná Hora, Czech Republic

During the revision of old localities represented by historical samples in the mineralogical collection of the National Museum in Prague an interesting association of phosphate minerals in iron ores from abandoned iron deposit Krušná Hora in Central Bohemia was discovered. The locality Krušná Hora is situated about 12 km NW of Beroun (30 km WSW of Prague) in an area of the Ordovician sedimentary rocks of the Teplá-Barrandian unit. The locality itself and its geology and mineralogical composition were described e.g. by Bořický (1869) or Vtělenský (1959) etc.

Phosphates are bound to cracks and cavities in iron ores (mainly hematite). Most frequently observed phosphate minerals are: variscite and strengite, which occurs there as a white to transparent concentric aggregates up to 2 mm in size; fluorwavellite which forms white needle crystals up to 4 mm, with content of F^- up to 1.33 apfu and yellow to orange cacoxenite which occurs there as radial and concentric aggregates up to 1.5 mm in size with content of Al up to 5.80 apfu. Rarer phosphosiderite forms white to creamy altered radial aggregates up to 15 mm in size and spherical aggregates up to 1 mm in size, with content of Al (metavariscite component) up to 0.19 apfu. Very interesting is occurrence of extremely rare allanpringite, Fe phosphate with ideal formula $Fe_3(PO_4)_2(OH)_3 \cdot 5H_2O$ firstly described from Grube Mark near Essershausen, Germany (Kolitsch et al. 2006). Allanpringite from Krušná Hora forms yellow powder and earthy aggregates in association with needles of fluorwavellite; its empirical formula is $Fe_{2.80}Al_{0.08}(PO_4)_2(OH)_{2.67} \cdot 5H_2O$ and refined unit-cell parameters are a 9.778(2), b 7.352(3), c 17.883(4) Å, β 92.17(4)° and V 1281.1(7) $Å^3$ Also a member of beraunite-tvrdýite solid solution was found. This mineral forms green to yellow-green radial aggregates up to 4 mm in size; its empirical formula is $Fe^{2+}_{1.11}(Fe^{3+}_{2.86}Al^{3+}_{2.14})_{\sum 5.00}[(SiO_4)_{0.06}(PO_4)_{3.93}(SO_4)_{0.01}]_{\sum 4.00}(OH)_{5.31} \cdot 6H_2O$ and was found in association with younger earthy yellow-orange jarosite.

Phosphate minerals assemblage in the iron sedimentary deposit Krušná Hora near Beroun is unique especially in occurrence of mineral allanpringite, which is the first occurrence in the Czech Republic and the second described occurrence in the world. The increased Al contents unusual for phosphate minerals from iron deposits are also remarkable.

Acknowledgment: This research was financially supported by Ministry of Culture of the Czech Republic (long-term project DKRVO 2018/02; National Museum, 00023272)

References

Bořický E. (1869): Akad Wissen Math 59:589–620.

Kolitsch U. et al. (2006): Eur J Min 18:793–801.

Vtělenský J. (1959): Geotechnica 26:1–71.

Joint 5th Central-European Mineralogical Conference and
7th Mineral Sciences in the Carpathians Conference

The crystal chemistry of the triphylite-ferrisicklerite-heterosite phases in granitic pegmatites from Poland

[1]Adam Włodek[#], [1]Sylwia Zelek-Pogudz, [2]Katarzyna Stadnicka and [1]Adam Pieczka

[1] AGH University of Science and Technology, Faculty of Geology, Geophysics and Environmental Protection, Department of Mineralogy, Petrography and Geochemistry, al. Mickiewicza 30, 30-059 Kraków, Poland [#]wlodek@agh.edu.pl

[2] Jagiellonian University, Faculty of Chemistry, Department of Crystal Chemistry and Crystal Physics, Gronostajowa 2, 30-387 Kraków, Poland

Key words: olivine-type phosphates, granitic pegmatites, Lutomia, single-crystal XRD, EPMA

INTRODUCTION

Triphylite $LiFe^{2+}PO_4$ forms solid-solution series with lithiophilite $LiMn^{2+}PO_4$. These minerals occur in evolved LCT-type granitic pegmatites enriched in phosphate minerals. Both triphylite and lithiophilite are primary phases and generally are associated with manganese-rich garnet or other primary phosphates such as graftonite-group minerals or sarcopside. Due to topotactic oxidation, lithiophilite and triphylite can be transformed into sicklerite $Li_{1-x}Mn^{2+}_{1-x}Fe^{3+}_xPO_4$ and ferrisicklerite $Li_{1-x}Fe^{3+}_xFe^{2+}_{1-x}PO_4$ and next to the Li-free phases: heterosite $Fe^{3+}PO_4$ and purpurite $Mn^{3+}PO_4$. In polish Sudetes, triphylite and lithiophilite were found in granitic pegmatites at Lutomia, Michałkowa and Piława Górna (for mineralogical details and geological settings see Grochowina et al. 2017; Pieczka et al. 2015; Włodek et al. 2015). Previous crystal-chemical studies of olivine structural type phosphates were based on structural variations in the lithiophilite-triphylite series (Losey et al. 2004) or lithiophilite and oxidation products (Hatert et al. 2012).

In this paper we present crystal-chemical data obtained for natural triphylite, ferrisicklerite and heterosite crystals from granitic pegmatite at Lutomia.

ANALYTICAL METHODS

Natural crystals of triphylite, ferrisicklerite and heterosite were separated from phosphate nodules. These nodules were composed mainly of graftonite-group minerals, sarcopside and triphylite (or its transformation products – ferrisicklerite and heterosite) (Fig. 1). The single-crystal X-ray diffraction experiment was carried out using graphite-monochromated Mo Kα radiation (λ = 0.71073 Å). The experimental data were collected using a diffractometer Bruker Nonius KappaCCD for triphylite single crystal and SuperNova Rigaku Oxford Diffraction for ferrisicklerite and heterosite single crystals. The details of data collection are summarized in Table 1. Afterwards, crystals were investigated by electron microprobe JEOL-JXA 8230 at the following conditions: acceleration voltage 15kV, probe current 20nA and defocused probe with diameters up to 5μm. Following micro-analysis standards were used: albite (for Na and Si), diopside (Mg, Ca), YPO_4 (P), fayalite (Fe), rhodonite (Mn), willemite (Zn).

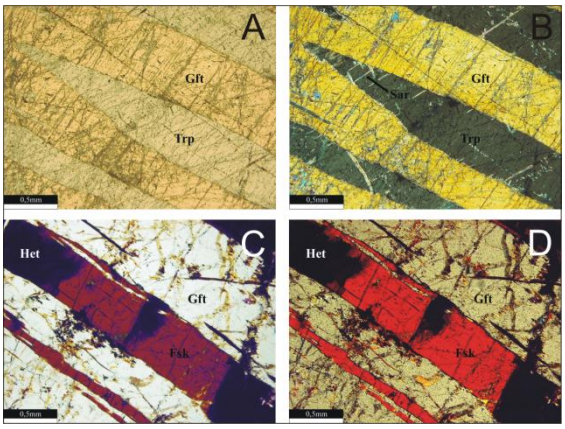

Fig. 1: Photomicrographs showing triphylite, ferrisicklerite and heterosite crystals intergrown with graftonite and sarcopside. Lutomia pegmatite. A,B – "fresh" sample, C, D-hydrothermally changed sample.

Table 1. Data collection details of single-crystal XRD measurements.

	Data collection		
	Triphylite	**Ferrisicklerite**	**Heterosite**
Diffractometer	Bruker Nonius KappaCCD	SuperNova Rigaku Oxford Diffraction	
Temperature (K)		293	
Wavelength (Å)		0.71073 (MoKα)	
θ Range (º)	3.94 – 30.14	4.07-31.86	4.1 – 31.74
hkl ranges	h: -14, 14; k:-8, 8; l:-6, 6	h: -14, 14; k:-8, 8; l:-7, 6	h: -14, 14; k:-8, 8; l:-7, 7
Reflections collected	756	3969	7990
Absorption corrections		multi-scan	

CRYSTAL STRUCTURE AND REFINEMENT

The structures were solved and refined in space group *Pnma* using two different software packages: Superflip (Palatinus and Chapuis, 2007) and Jana2006 (Petricek et al. 2014). For calculations it was assumed that *M1* position could be occupied by Li^+ or stays vacant and *M2* position is occupied by Fe. The final conventional R1 factors (for $F^2>2\sigma(F^2)$) reach values: 0.0210 for triphylite, 0.0211 for ferrisicklerite and 0.0224 for heterosite. Crystal data and refinement conditions were listed in Table 2.

ELECTRON MICROPROBE RESULTS

Chemical analyses of investigated crystals of triphylite (Trp), ferrisicklerite (Fsk) and heterosite (Het) show their weak chemical diversity, characterized by similar contents of major elements: 43.14 (Trp) to 47.57 (Fsk) P_2O_5, 29.76 (Het) to 32.55 (Trp) FeO, 10.46 (Trp) to 13.71 (Fsk) MnO and 2.33 (Fsk) to 2.82 (Trp) MgO. The major issue of chemical data obtained by EPMA is the unknown Li^+ content and Fe^{2+}/Fe^{3+} and Mn^{2+}/Mn^{3+} ratios. To solve this problem, for calculation of the Li^+ content we used an equation (in *apfu*):

$$Li = Mg + Ca + Mn^{2+} + Fe^{2+} - (Si + Na)$$

Fe^{3+} and Mn^{3+} contents were calculated to obtain a sum of analysis equal 100.00 wt%.

Recalculated chemical compositions of investigated crystals were listed in Table 3.

Table 2: Crystal data and refinement data for single crystals of phosphates from Lutomia pegmatite.

Chemical formula	$Fe_{0.922}Li_{0.970}PO_4$	$Fe_{0.912}Li_{0.268}PO_4$	$Fe_{0.920}Li_{0.166}PO_4$
Crystal system		Orthorhombic	
Space group		P n m a (no. 62)	
Unit cell dimensions (Å)	10.3430(8); 6.0170(10); 4.7000(13)	10.0103(7); 5.9086(3); 4.8005(3)	9.9339(3); 5.8892(2); 4.7932(13)
V (Mg/m^3)	292.499	283.9345	280.4153
Refinement			
R1/ wR2 / S for $F^2> 2\sigma(F^2)$	2.10/3.10/1.86	2.11/2.55/1.59	2.24/2.88/1.89
R1 / wR2 (F^2) / S (all reflections)	2.34/3.14/1.81	2.83/2.62/1.50	2.87/2.91/1.80

Table 3: Chemical compositions of investigated phosphate crystals.

	Trp (n = 18)	Fsk (n = 5)	Het (n = 8)
Li_2O*	9.22	2.14	1.76
Na_2O	0.00	0.00	0.02
MgO	2.82	2.33	2.45
SiO_2	1.50	0.04	0.04
P_2O_5	43.14	47.58	47.08
CaO	0.00	0.09	0.15
MnO	10.46	4.97	3.02
Mn_2O_3	0.00	9.73	11.77
FeO	29.62	0.00	0.00
Fe_2O_3	3.26	33.07	33.75
ZnO	0.00	0.06	0.00
Σ	100.01	100.00	100.03
	apfu (P + Si = 1.00)		
Li^+*	0.96	0.19	0.16
Na^+	0.00	0.00	0.00
Mg^{2+}	0.11	0.09	0.09
Si^{4+}	0.04	0.00	0.00
P^{5+}	0.96	1.00	1.00
Ca^{2+}	0.00	0.00	0.00
Mn^{2+}	0.23	0.10	0.06
Mn^{3+}	0.00	0.18	0.22
Fe^{2+}	0.65	0.00	0.00
Fe^{3+}	0.06	0.62	0.64
Zn^{2+}	0.00	0.00	0.00
Li^+**	0.97	0.27	0.17

*Li^+ content calculated at the basis of EPMA analysis, **Li^+ content calculated at the basis of single-crystal XRD.

Acknowledgment: This work was financially supported by National Science Centre of Poland (NCN) grant 2015/17/N/ST10/02666.

REFERENCES

Grochowina et al. (2017): Mineralogia – Spec Pap 47:48–49.

Hatert et al. (2012): Can Min 50:843–854.

Losey et al. (2004): Can Min 42:1105–1115.

Palatinus L. and Chapuis G. (2007): J Appl Cryst 40:786–790

Petricek et al. (2014): Z Kristallogr 229:345–352.

Pieczka et al. (2015): 7th international symposium on Granitic Pegmatites: Book of abstracts.

Włodek et al. (2015): J Geosci 60:45–72.

int 5th Central-European Mineralogical Conference and
7th Mineral Sciences in the Carpathians Conference

Beryllium minerals from NYF intragranitic pegmatites of the ultrapotassic Třebíč Pluton, Czech Republic

[1]Adam Zachař[#] and [1]Milan Novák

[1] Masaryk University, Faculty of Science, Department of Geological Sciences, Kotlářská 2, 611 37 Brno, Czech Republic [#]adamzachar@seznam.cz

Key words: intragranitic pegmatites, Na-Mg-beryl, bazzite, milarite, alterations

Intragranitic NYF granitic pegmatites of Variscan, high Mg-K-syenogranitic Třebíč Pluton (Moldanubian Unit, Bohemian Massif), contain Be-minerals, which part of them show unusual chemical features and reports several different alteration processes.

The intragranitic, well-zoned euxenite pegmatites contain Be-minerals, "amazonite", aeschynite- and euxenite- group minerals, Sc-enriched columbite, cassiterite and Ca-Ti-dravite/schorl.

The Be-minerals from the Číměř, Kožichovice I-III and Pozďátky pegmatites were studied by EMPA, and LA-ICP-MS (beside Číměř; Novák and Filip 2010). Three main assemblages can be distinguished: I) beryl I,II (brl I,II) + bavenite (bvn) + bazzite (bz) + smectite (sm); ii) brl I+bvn+bz+ milarite I (mil I) + phenakite II (phk II); iii) phenakite I (phk I) +bvn+milarite II (mil II) +brl II. Primary minerals include Na-Mg-rich brl I and phk I. Phk I was found only in the Číměř locality. Brl I shows unusual enrichment in Na (0.20-0.34 apfu) and Mg (0.20-0.44 apfu) aside increased amounts of Fe_{total} (up to 0.24 apfu), Cs (up to 0.20 apfu; max. 3.65 wt.% Cs_2O) and Sc (max. 0.06 apfu; 0.68 wt.% Sc_2O_3). Breakdown products of brl I include brl II, phk II, bvn (0.01-0.10 apfu Na; 0.75-1.05 apfu Al), mil I (slightly Sc-enriched), epidote, sm, chlorite and kaolinite. Brl II, still Na-Mg-rich (up to 0.34 apfu Na; max. 0.32 apfu Mg) with moderate Fe_{total} (up to 0.10 apfu), but with low Sc and Cs, is quite rare and associates mostly with bvn. Phk II +mil I fill small cracklings in brl I. Bz is known solely from Kožichovice I-III, where forms thin laths (100 μm) in bvn and brl I. Bz is highly enriched in Na (up to 0.48 apfu) and Mg (up to 0.64 apfu), particularly in Ca (~0.10 apfu) and Cs (up to 0.01 apfu). Scandium content reaches 1.13-1.40 apfu, whereas Al is present in wide range (0.02-0.32 apfu). Phk I contains rare veinlets of Y-rich milarite (mil II) with 0.20-0.34 apfu Y+REE (up to 4.80 wt.% ΣY_2O_3 + REE_2O_3) and 0.11-0.22 apfu Al.

Calculation Si=6 apfu yielded O-type beryl with high enrichment in alkalies + Ca (0.21-0.40 apfu) in brl I. Contents of alkalies + Ca in bazzite (0.53-0.77 apfu) balanced with same amounts of (Fe + Mg), suggest a new mineral with ideal formula $NaBe_3ScMgSi_6O_{18}$. Such composition is close to non-pegmatitic source (Franz and Morteani 2002).

An occurrence of numerous alteration products of beryl could point on several alteration processes with different fluid composition and pH.

Mineralogy of the Třebíč pegmatites, enriched in Be, Sc, Y and Cs is partly similar to the Tørdal NYF pegmatites, Norway (Juve and Bergstøl 1990).

References

Franz G. and Morteani G. (2002): Rev Min Geochem 50:551–589.

Juve G. and Bergstøl S. (1990): Min Petrol 43:131–136.

Novák M. and Filip J. (2010): Can Min 48:519–532.

UNEXMIN: an autonomous underwater robot to deliver in-situ mineralogical information from flooded underground mines

[1]Norbert Zajzon[#] and [2]UNEXMIN team

[1] University of Miskolc, Faculty of Earth Science and Engineering, Istitute of Mineralogy and Geology, Egyetemváros, H-3515 Miskolc, Hungary [#]nzajzon@uni-miskolc.hu
[2] www.unexmin.eu

Key words: autonomous robotic explorer, 3D mapping, mineralogical information, water chemistry, geophysical data, flooded mines, multispectral camera, virtual-reality dataset

UNEXMIN (www.unexmin.eu) is an European Union funded Horizon 2020 project with a pan-European consortium, which aims to develop a fully autonomous robot family for underground flooded mines capable to deliver 3D maps, colour videos, water parameter data, geophysical and mineralogical information based on non-invasive measurements (Lopes et al. 2017a; 2017b).

Numerous flooded abandoned mines can be found in Europe which reassessment are crucial to support securing mineral resources for Europe to decrease its economical, thus political dependence of foreign countries. Usually abandoned mines still contain valuable ore resources as mine closure is rarely a cause of complete depletion of the ore. It more reflects the current level of mining technology and commodity prices on the market, so cut-off grades are significantly decrease(d) with time enlarge economically mineable materials in the mines. Many cases different minerals were not considered valuable during the closure of the mine (eg. hundred years ago fluorite was considered as waste in Mississippi Valley Type Cu-Pb-Zn mines) which are now even in the Critical Raw Materials list of the EU, thus exploration of abandoned mining areas can have great importance in Europe.

The project is aiming to develop a fully autonomous, battery powered (ca. 5 hours working time), 60 cm diameter, spherical robot which can access medieval mine parts where the corridors, shafts can be narrow. The robot is ca. 110 kg to have controllable neutral buoyancy, and it can handle pressures up to 500 m water depth and has a few kilometres operation range able to cover the majority of European flooded mines with its capabilities. Nearby the necessary navigation tools, which include multi-beam sonar, HD colour cameras and structured laser light systems capable to deliver 3D maps from the mine layout, some geo-scientific instruments will be placed on board regarding particular exploration needs. The list of scientific instruments is partially limited due to weight, space and size limitations, and the difficulty to sense minerals thru relatively thick (few tens of cm to few m) water body. The scientific instrumentation can be grouped into three areas: 1) water testing methods (temperature, pressure, pH, EC and water sampling) 2) geophysical methods (magnetic field measurement (strength and direction), natural (integral) γ-ray activity and sub-bottom sonar) and 3) optical mineralogical methods (UV fluorescent imaging and multispectral unit). For detailed description of geo-scientific instrumentation please see Papp et al. in this volume.

The UX-1 system will be tested in four different mines in Europe with increasing challenges including Kaatiala pegmatite mine (Finland), Idrija Hg-mine (Slovenia), Ugeiriça U-mine (Portugal) and Ecton Cu-Zn/Pb mine (United Kingdom).

Acknowledgment: The UNEXMIN project has received funding from the European Union's Horizon 2020 research and innovation programme under Grant Agreement No. 690008.

REFERENCES

Lopes L. et al. (2017a): Energy Proc 125:41–49.
Lopes L. et al. (2017b): Eur Geol 44:54–57.
Papp R.Z. et al. (2018): this volume.

Recent supergene minerals from abandoned mines of the Au-Ag-Pb-Zn deposit Muzhievo (Ukraine)

[1]Yuliia Ostapchuk, [1]Leonid Z. Skakun[#], [2]Jarmila Luptáková[#], [2]Adrian Biroň and [2]Stanislav Jeleň

[1] Department of Geology, Ivan Franko University, Lviv, 250005 Ukraine [#] lzskakun@gmail.com
[2] Earth Science Institute, Slovak Academy of Sciences, Ďumbierska 1, 974 11 Banská Bystrica, Slovakia [#] luptakova@savbb.sk

Key words: Berehovo ore field, zinc sulfate crystalline hydrates, speleothem, hypergene oxidation

The Muzhievo Au-Ag-Pb-Zn epithermal deposit is located in the Berehovo area of the Transcarpathian region near the village of Muzhievo, in the southwestern part of the Berehovo Lowland (southwestern Ukraine). According to age and geological position, the deposit is similar to the known epithermal deposits of central Slovakia and Oas-Gutâi Mountains (Romania).

The ores contain sulfide, quartz, quartz-sulfide, quartz-barite and carbonate in veins, veinlets, disseminated mineralization and stockworks (Vityk et al. 1994). Main ore minerals are pyrite, sphalerite, and galena. Quartz, chalcopyrite, wurtzite, marcasite, pyrrhotite, baryte, carbonates, Sb-sulfosalts, Ag-sulfosalts, and fluorite are widespread (Skakun et al. 1992; Emetz and Skakun 2001).

In the vicinity of the deposit, hundreds of exploratory boreholes were drilled to a depth of 2 km. Exploratory mining works were carried out on five horizons (+90, +130, +160, +210, +230 m). Mine works with a total length of more than 30 km were dug out.

Exploration of the deposit was performed since 1964 until 2000 and was followed by conservation of the infrastructure since 2001 below the horizon +230 m. Since sulfide ore bodies are isolated from above by a clay layer, there is no primary oxidation zone. Only the recent mining activity started oxidation of the ores as new channels for water infiltration were opened.

Unique occurrences of crystalline zinc sulfate hydrates were discovered during the inspection of the deposit (mine #2, drift #131, 130 m horizon) in August 2015. They form stalactites, stalagmites, antholites, coralites, spherulites, tubes, and fibrous aggregates on side walls, bottom and ceiling of the drift.

The area of formation of zinc sulfates is characteristic by a very low groundwater flow. Water is released from cracks. The temperature in the drift is constant around 14 °C. An important factor is presence of natural ventilation in the drift with maximum air humidity.

The XRD, XRF, Raman and EPMA analyses were used to identify individual secondary minerals. The paragenesis includes goslarite, bianchite, dietrichite-halotrichite, gunningite, boyleite, and gypsum. Dehydrated forms of zinc sulfates were also detected as these minerals rapidly dehydrate when ambient conditions change.

Acknowledgment: This work was supported by APVV-15-0083, ITMS: 26220120064.

References

Vityk M.O. et al. (1994): Econ Geol 89:547–565.

Emetz A. and Skakun L. (2001): Biul. Państw. Instytutu Geologicznego 396:43–44.

Skakun L.Z. et al. (1992): Ivan Franko Univ. Herald. Geology. 11:128–145 (in Ukrainian)

Joint 5th Central-European Mineralogical Conference and
7th Mineral Sciences in the Carpathians Conference
Banská Štiavnica 2018

Sharyginite and shulamitite in high temperature metacarbonate xenoliths of basalt at Balatoncsicsó, Balaton Highland Volcanic Field, Hungary

[1]Sándor Szakáll[#] and [2]Béla Fehér

[1] University of Miskolc, Institute of Mineralogy and Geology, H-3515 Miskolc-Egyetemváros, Hungary [#] askszs@uni-miskolc.hu
[2] Herman Ottó Museum, Department of Mineralogy, Kossuth u. 13, H-3525 Miskolc, Hungary

Key words: sharyginite, shulamitite, metacarbonate xenolith, basalt, Balatoncsicsó, Hungary

Two rare oxides from the brownmillerite subgroup of the perovskite supergroup, namely shulamitite (orthorhombic $Ca_3TiFeAlO_8$) and sharyginite (orthorhombic $Ca_3TiFe_2O_8$), were identified in metacarbonate xenoliths of basalt of the Balaton Highland Volcanic Field. They were originally described in high temperature conditions in the Hatrurim Complex, Israel (Sharygin et al. 2013) and at Bellerberg volcano, Eifel Mts., Germany (Juroszek et al. 2017), respectively. Based on the $CaTiO_3$–$Ca_2Fe_2O_5$ diagram for some larnite-bearing rocks of the Hatrurim Complex, where sharyginite was also identified, the minimum temperature of formation was estimated from Fe-perovskite–$Ca_3TiFe_2O_8$ mineral paragenesis. This temperature is in the range of 1170–1200 °C (Sharygin et al. 2008). The broad compositional variations for shulamitite and its Fe-analogue, sharyginite, suggest the existence of the isomorphic series between $Ca_3TiFeAlO_8$ and $Ca_3TiFe_2O_8$. The appearance of minerals of this series in metacarbonate rocks around the world could be an indicator of high temperature (>1170 ºC) of their formation.

The Fenyves Hill occurrence is a small basalt eruption in the northern margin of the Balaton Highland Volcanic Field. Metacarbonate xenoliths up to 2–4 cm in diameter, which contain brown, black and white parts, can be found in the basalt at Balatoncsicsó. The brown and black zones consist of mainly sharyginite-shulamitite solid solution, magnesioferrite, fluorapatite, in addition with some primary unidentified Ca-Mg-Fe-(Al) silicates. The white part of xenoliths is intensely altered by low-temperature retrograde processes. They are sometimes replaced by hydrated Ca-Al or Mg-Al silicates. The sharyginite and shulamitite form individual prismatic crystals up to 60 μm in length. The chemical analyses represent compositions close to the borderline between them, e.g.: SiO_2 0.64, TiO_2 19.01, Al_2O_3 6.12, Fe_2O_3 29.97, CaO 44.37, total 100.12 wt% correspond to $Ca_{3.12}Ti_{0.94}Fe_{1.48}Al_{0.47}Si_{0.04}O_8$ (sharyginite) and SiO_2 0.84, TiO_2 17.90, Al_2O_3 6.54, Fe_2O_3 29.54, CaO 44.08, MnO 0.15, total 99.05 wt% correspond to $Ca_{3.13}Ti_{0.89}Fe_{1.47}Mn_{0.01}Al_{0.51}Si_{0.06}O_8$ (shulamitite).

Magnesioferrite forms subhedral or euhedral, mainly isometric grains up to 40 μm. There are rarely octahedral and hexakis octahedral crystals up to 10–15 μm in the cavities of matrix. Chlormayenite appears not only inclusions in sharyginite-shulamitite, but it was also found as discrete isometric grains. Fluorapatite shows various chemical compositions, where phosphate can be substituted by sulphate and silicate anions. Additional primary phases could be such Al silicates, which contain a few percent sulphate/ phosphate anions. Mineral paragenesis of metacarbonate xenoliths in Balatoncsicsó confirm their high temperature origin. This is the first high temperature xenoliths from the area to date.

References

Juroszek R. et al. (2017): Mineral Mag 81: 737–742.
Sharygin V.V. et al. (2008): Russian Geol Geoph 49: 709–726.
Sharygin V.V. et al. (2013): Eur J Mineral 25: 97–111.

Joint 5th Central-European Mineralogical Conference and
7th Mineral Sciences in the Carpathians Conference

Vonsenite from Nagylóc-Zsunypuszta, Cserhát Mts., Hungary: The first borate mineral of postvolcanic origin from the Carpathian-Pannonian Region

[1]Sándor Szakáll[#], [2]Béla Fehér, [1]Ferenc Kristály, [3]Zsolt Kasztovszky and [3]Boglárka Maróti

[1] University of Miskolc, Institute of Mineralogy and Geology, H-3515 Miskolc-Egyetemváros, Hungary, [#] askszs@uni-miskolc.hu
[2] Herman Ottó Museum, Department of Mineralogy, Kossuth u. 13, H-3525 Miskolc, Hungary
[3] Hungarian Academy of Sciences, Institute of Isotopes, Department of Nuclear Research, Konkoly-Thege Miklós út 29-33, H-1121 Budapest, Hungary

Key words: vonsenite, borate, postvolcanic, Cserhát Mts., Hungary

Borate minerals occur not only in sediments, but also in some high-temperature contact-metamorphic rocks, especially in skarns (Anovitz and Grew 1996). Less often they appear in postvolcanic formations, especially in connection with potassium-rich volcanics. Such occurrences are known for example in Campania, Latium, and Aeolian Islands, all in Italy. The most famous postvolcanic borate locality is the La Fossa Crater, Aeolian Islands, where vonsenite is the most abundant borate mineral.

The boron concentration of Neogene Carpathian-Pannonian volcanics are between 4.4–90.3 ppm. The highest boron concentration was proved by prompt gamma activation analysis from the Cserhát Mts. (Gméling 2010).

The borate mineral vonsenite, an orthorhombic $Fe^{2+}{}_2Fe^{3+}(BO_3)O_2$, was identified in trachyandesite, especially sanidine-rich miarolitic cavities at Zsunyi Quarry, Zsunypuszta, near Nagylóc, Cserhát Mts. The main cavity-filling phases are plagioclases (with bytownite-anorthite composition), which are commonly covered by euhedral sanidine. Accessory minerals are: magnetite, ilmenite, quartz, rutile, fluorapatite, rare zircon, baddeleyite and monazite-(Ce). Vonsenite was detected by XRD, EPMA, PGAA and neutron radiograph examinations. It forms black, opaque needles with size of 0.1–0.5 mm, but it rarely reaches 1–2 mm in length. It frequently occurs as sprays or parallel intergrowths of acicular crystals. Vonsenite crystals are always covered by smectite crusts. The EPMA detected a few wt% MgO and TiO_2, where Fe^{2+} is substitutes by Mg, while Fe^{3+} is replaced by Al + Ti^{4+}. Chemical zoning in vonsenite was not observed. A representative electron-microprobe analysis of vonsenite: TiO_2 4.59, B_2O_3* 14.00, Al_2O_3 0.69, Fe_2O_3** 24.80, FeO** 53.62, MgO 2.29, total 99.99 wt%, which corresponds to $(Fe^{2+}{}_{1.86}Mg_{0.14})_{\Sigma=2.00}$ $(Fe^{3+}{}_{0.77}Ti_{0.14}Al_{0.03})_{\Sigma=0.94}$ BO_5. Remarks: *B_2O_3 calculated from the stoichiometry (B = 1 apfu); **Fe_2O_3/FeO ratio calculated from the equation Fe^{2+} + Mg = 2 apfu. The Fe^{2+}–Mg substitution is very frequent in vonsenite, because this mineral forms a series with its Mg analogue, ludwigite. The boron content was proved by neutron radiograph examination.

Vonsenite of Nagylóc-Zsunypuszta has postvolcanic origin, its appearance is confined to sanidine-rich miarolitic cavities. No other borate minerals can be found in this paragenesis. Vonsenite deposited from boron-rich, post-magmatic fluids. Probably the low aluminum content of the hydrothermal fluids was the reason why no tourmaline was formed, which is a more common boron mineral in such environment.

References

Anovitz L.M., Grew E.S. (eds.) (1996): Boron: Mineralogy, Petrology, and Geochemistry. Rev Mineral 33, Mineralogical Society of America.

Gméling K. (2010): Boron geochemistry of Miocene-Quaternary calc-alkaline volcanics of the Carpathian-Pannonian Region in connection with subduction formations: prompt gamma activation analysis. PhD thesis. Eötvös University, Budapest (in Hungarian).

Joint 5th Central-European Mineralogical Conference and
7th Mineral Sciences in the Carpathians Conference
Banská Štiavnica 2018

Authigenic barite crystals from the eupelagic sediments of CCFZ (IOM H22 area, Clarion-Clipperton Fracture Zone, Pacific)

[1]Łukasz Maciąg[#], [1]Dominik Zawadzki, [1]Ryszard Kotliński, [1]Ryszard K. Borówka, [2]Rafał Wróbel

[1] University of Szczecin, Faculty of Geosciences, Mickiewicza 16A, 70-383 Szczecin, Poland
[#]lukasz.maciag@usz.edu.pl
[2] West Pomeranian University of Technology, Faculty of Chemical Technology and Engineering, Piastów 42, 71-065 Szczecin, Poland

Key words: barite, eupelagic sediments, Clarion-Clipperton, Pacific, polymetallic nodules

INTRODUCTION

Barite is important accessory mineral, being extensively found in the recent years in the deep-sea sediments, covering abyssal parts of the oceanic basins (Griffith and Paytan 2012).

Authigenic barite crystals are formed mainly under the supersaturation conditions, directly water column. Barite is especially important indicator for the oscillatory fluctuations of environmental conditions (oxic-anoxic changes) (Liguori et al. 2016; Paytan and Griffith 2007).

The major mechanism for barite formation is derived from the degradation of organic matter (OM) and later precipitation, due to release of SO_4^{2-} during burial diagenesis. The flux and preservation of these crystals in sediments is expected to reflect the productivity in water column, as its formation (Paytan et al. 2002; Paytan and Griffith 2007; Horner et al. 2017).

Barite in the deep-sea sediments is often associated with carbonates, biogenic silica (diatoms, radiolarian), Fe−Mn oxy-hydroxides and clay minerals. Presence of planktonic and benthic organisms may also strongly induce the precipitation of barite crystals. It remains stable under the oxidizing conditions, being however demineralized under the reducing one (Griffith and Paytan 2012; Liguori et al. 2016).

The oxidizing conditions are predominating diagenetic barite formation. It shows usually smaller crystal dimensions and precipitates when reduction of sulphates takes place. During these processes barium is being released directly to the pore waters.

Potentially, if Ba reaches an oxic layer of sediment, it can re-precipitate as a diagenetic type (Liguori et al. 2016).

Clarion−Clipperton Fracture Zone (CCFZ) is located in the abyssal basin of NE Pacific, covering about 5.5 mln km^2 of seafloor, in water depths of 3700−5700 m, increasing along the E−W transect (Fig. 1).

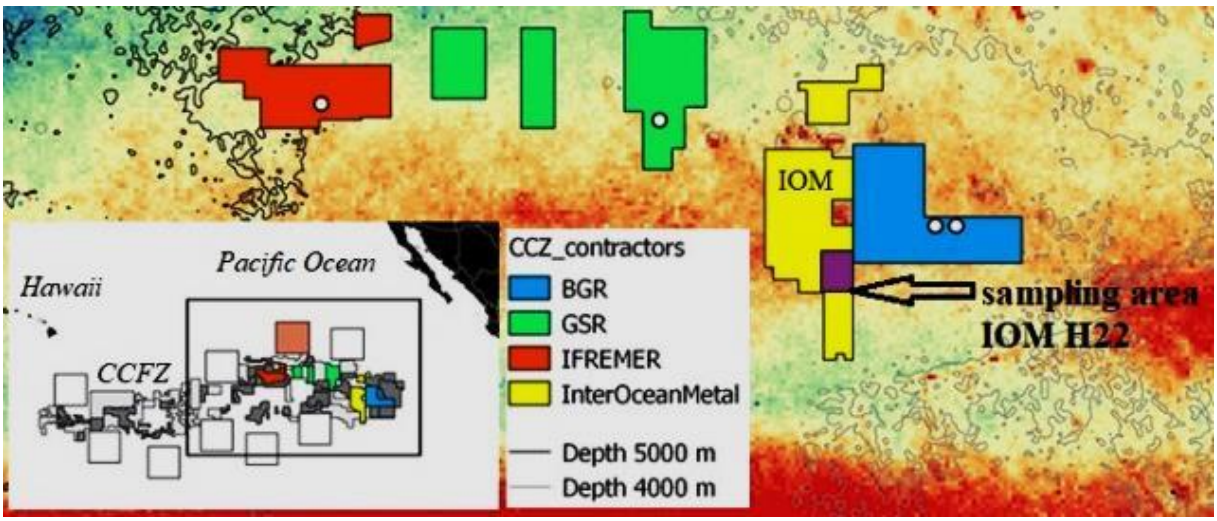

Fig. 1. Location of the investigation area. The IOM H22 polymetallic nodules field marked by violet rectangle. Map basing on Vanreusel et al. (2016).

The seabed is composed mainly of MORB tholeiitic basalts, covered by 100−300 m thick sediments of age $Cr-Q_H$ (Kotliński 2011).

The CCFZ area is under law jurisdiction of International Seabed Authority (ISA), being the largest and economically most promising deep oceanic deposit. Several contracts for polymetallic nodules exploration were approved here in recent years (Abramowski and Kotliński 2011; Kotliński et al. 2015).

The IOM H22 polymetallic nodule field is about 5180 km^2, with the water depths from 4300 to 4500 m. It is located in the Eastern part of CCFZ (Fig. 1). The seabed is covered mainly by Ng_M-Q_H siliceous clayey silts, minor by calcareous oozes, both belonging stratigraphically to the Clipperton formation.

MATERIAL AND METHODS

The samples of siliceous clayey silts were collected using box corer in 2014, by research vessel "Yuzhmorgeologiya", during IOM cruise to the H22 polymetallic nodules prospective field. The sediments were divided into the three major depth intervals: 0-5, 10-15 and 25-30 cm. In some cases, the layers above 30 cm were also recovered and described.

The total number of 34 samples was analysed. Sediments preparation, mineral separation (using sedimentary methods) and the biogenic elements content estimation were conducted at the Faculty of Geosciences, University of Szczecin, Poland. Nutrients were analysed using Variomax CNS spectrometer.

SEM images, chemical analysis and XRD data were obtained at the Faculty of Chemical Technology and Engineering, West Pomeranian University of Technology, Szczecin, Poland, using SEM Hitachi SU 8070 with the EDX Thermo Scientific Fisher NORAN 7 and XRD PANalytical Empyrean.

The barite content in bulk sediments was estimated basing on XRD data. The complete mineralogical results were obtained using RockJock Software (Eberl 2003).

RESULTS

Several well preserved, euhedral, elongated and barrel-like diagenetic barite crystals were identified (Fig. 2).

Measured crystal dimensions varied from <5ηm up to 100 ηm. The EDS analysis revealed some chemical impurities in barite, including admixtures of Sr (1.52 wt %), Si (1.26 wt %), Fe (0.53 wt %), Ca (0.09 wt %) and K (0.09 wt %).

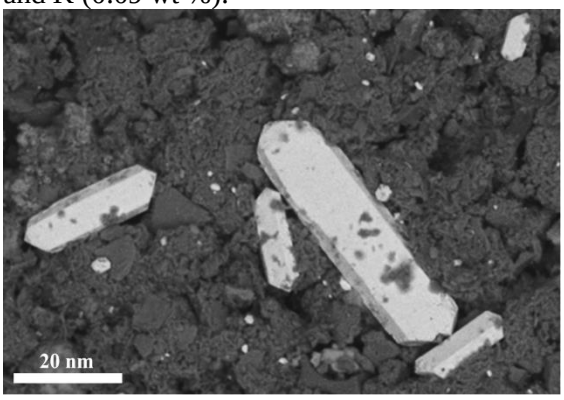

Fig. 2. The representative SEM image of euhedral barite crystals from the IOM H22 polymetallic nodules field, Clarion-Clipperton Fracture Zone, Eastern Pacific.

Barite content in sediments varied from 1.1 to 3.4 %, with mean 1.6%, showing good positive correlation − expressed by the Pearson's coefficient − with content of clay minerals (+0.83). The negative correlation (-0.78) was found with amorphic phase (mainly siliceous frustules of diatoms and radiolarian skeletons) and biogenic elements content, -0.66 for nitrogene, -0.62 for total carbon, respectively.

The insignificant (-0.06) correlation of barite vs sulphur content confirm S depletion during burial diagenesis.

The siliceous OM degradation, clay minerals formation and presence of Fe−Mn oxy-hydroxides, definitely predominate authigenic barite formation during early burial diagenesis.

The significant increase of barite content, up to 3> wt %, was observed in the sediment layers from depths of 30 cm and more, confirming diagenetic formation processes. Some traces of authigenic gypsum and celestite (not mentioned here) may also reflect the early burial diagenesis.

Acknowledgments:

We thank the General Director of Interoceanmetal Joint Organization prof. Tomasz Abramowski for cooperation and results publication ability.

The research was partially financed from the IOM contract No. 501-2.3/2-14

and the University of Szczecin statutory funds No. 503-1100-230342.

REFERENCES

Abramowski T. and Kotliński R. (2011): Górnictwo i Geoinż. 35(4/1): 41−61.
Eberl D.D. (2003): User's Guide to RockJock. USGS, Colorado.
Griffith E.M. and Paytan A. (2012): Sedimentology 59(6): 1817−1835.
Horner T.J. et al. (2017): Nat. Communicat. 8: 1−11.
Kotliński R. (2011): Górnictwo i Geoinż. 35(4/1): 195−214.
Kotliński R. et al. (2015): Geol. and Mar. Res. of World Oc. 2: 65−80.
Liguori B.T.P. et al. (2016): An. Acad. Bras. Cienc. 88(4): 2093–2103.
Paytan A. et al. (2002): Geology 30(8): 747−750.
Paytan A. and Griffith E.M. (2007): Deep-Sea Res. II 54: 687−705.
Vanreusel A. et al. (2016): Nature Sc. Rep. 6: 1−6.

Joint 5th Central-European Mineralogical Conference and
7th Mineral Sciences in the Carpathians Conference

Tourmaline (schorl−elbaite−dravite) from the pegmatitic aplite, Lisiec Hill, Strzegom, Poland

[1]Łukasz Maciąg [#], [2]Rafał Wróbel

[1] University of Szczecin, Faculty of Geosciences, Marine Geology Unit, Mickiewicza 16A, 70-383 Szczecin, Poland [#] lukasz.maciag@usz.edu.pl
[2] West Pomeranian University of Technology, Faculty of Chemical Technology and Engineering, Piastów 42, 71-065 Szczecin, Poland

Key words: tourmaline, aplite, pegmatite, schorl-elbaite-dravite, zonation, Strzegom

INTRODUCTION

The tourmaline supergroup members are extensively studied in recent years, being the most widespread of cyclosilicate minerals, commonly found in several magmatic rocks, especially in pegmatites and aplites (Bačík 2015; Bosi et. al 2017; Bosi et al. 2018; Pieczka et al. 2018).

Tourmalines general empirical formula $XY_3Z_6T_6O_{18}(BO_3)_3V_3W$ represents many constituents: X = Na^+, K^+, Ca^{2+}, □ (= vacancy); Y = Al^{3+}, Fe^{3+}, Cr^{3+}, V^{3+}, Mg^{2+}, Fe^{2+}, Mn^{2+}, Li^+; Z = Al^{3+}, Fe^{3+}, Cr^{3+}, V^{3+}, Mg^{2+}, Fe^{2+}; T = Si^{4+}, Al^{3+}, B^{3+}; B = B^{3+}; V = $(OH)^-$, O^{2-}; W = (OH), F^-, O^{2-}. Group structure may be regarded as a ZO_6 octahedral three-dimensional framework surrounding the "islands" of XO_9, YO_6, BO_3 and TO_4 polyhedral groups.

Tourmalines show significant structural and chemical complexity, revolving important petrogenetic information about host rocks and conditions of their formation (Bačík 2015; Bosi et al. 2018).

The occurrence of tourmalines in the post-magmatic and metamorphic rocks from Strzegom, Poland, is known from several localities and was reported long ago (Traube 1888 *vide* Pieczka and Kraczka 1988). Local granites, pegmatites and aplites are the host rocks for some of well-known tourmalines, especially from the schorl group (Janeczek 1985).

The few peraluminous pegmatite aplite dykes, exceeding 1 m of thickness, were identified among the amphibolite from SW cover of the Strzegom-Sobótka Granitic Massif. The dykes lie on a short distance, as a roof part of granite. The contacts with amphibolite show, however, no evidence of chemical interaction with the dykes (Puziewicz 1988).

The aplite dykes are made of two generations of coarse and fine-grained pegmatite intercalations. So-called "younger aplite" is almost free from tourmalines, containing nests of andalusite crystals and garnet-tourmaline schlieren. The "Older aplite" contains more tourmalines (Puziewicz 1981).

Both rocks show porphyritic texture, dominated by the alkali feldspar (orthoclase) with several types of pertites, plagioclase, biotite, muscovite, chlorite, garnet (~$Alm_{50}Sps_{50}$) and andalusite. There are visible traces of alteration in type of sericitization and kaolinization (Puziewicz 1981; Pieczka and Kraczka 1988).

The solid inclusions in form of euhedral spessartine-almandine garnet, albite, quartz, monazite, zircon, epidote, rutile, magnetite, hematite, goethite and andalusite were also identified (Pieczka and Kraczka 1988; Kozłowski 2003).

Mentioned tourmalines show directional orientation of poles and many schlieren clusters suggesting their fluidal movement (Puziewicz 1981; Kozłowski 1984).

Several analyses of the fluid inclusions confirmed their metasomatic-hydrothermal origin and formation under T=410-480°C, pressure about 77-81 MPa (Kozłowski 1987; Kozłowski 2003).

The detailed chemical, XRD, IR and Mössbauer spectroscopy studies conducted by Pieczka and Kraczka (1988), revealed iron-rich nature of the Lisiec Hill tourmalines. Described crystals were showing zonal pleochroism parallel to crystal elongation, ranging mostly from colourless to dark olive-

brown and grey-green. The mineral unit cell parameters indicated they represented aluminium schorls, as a member of series schorl-olenite.

Mentioned authors observed also insignificant occupancy of the *Y* octahedral by Mg ions (about 10%), small role of dravite component and domination of Fe and Al at the *Y* sites, typical of aluminium "elbaite" schorls.

MATERIAL AND METHODS

The pegmatitic aplite samples were collected in 2008 near the Lisiec Hill, Strzegom, Poland. Several loose rock blocks containing tourmalines were picked up along field road (Fig. 1).

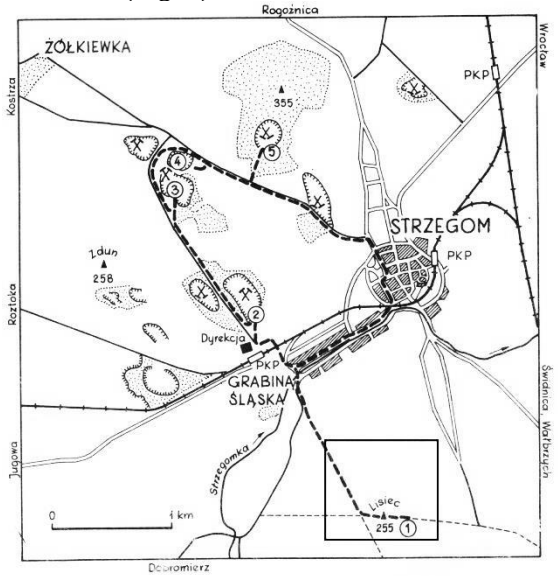

Fig. 1: The location of Lisiec Hill, Strzegom, Poland (Żaba 1991). Sampling area marked by rectangle.

The visual description, microscopic observations and material separation, including preparation of polished sections, were done at the Faculty of Geosciences, University of Szczecin, Poland.

Loose crystals (N=10) were separated from crushed aplite samples and investigated using SEM Hitachi SU 8070 with EDX Thermo Scientific Fisher NORAN 7 at the Faculty of Chemical Technology and Engineering, West Pomeranian University of Technology, Szczecin, Poland.

The chemical analysis presented here is basing on 18 revised data points from the EDS. To observe tourmalines zonation, two polished sections were prepared and chemical distribution maps were registered (Fig. 2).

The chemical data were normalized (12 *X*+*Y*+*Z* cations) and classified using CLASTOUR software (Yavuz et al. 2002). Fe was calculated as FeO_t. B_2O_3 and OH^- were estimated basing on stoichiometry.

RESULTS

Two major identified textural groups of tourmaline assemblages has been identified and investigated:

1) massive, schorl-type (length up to 30 mm), freely distributed, black-brownish colour, non-opaque and non-pleochroic, associated dominantly with coarse feldspar and quartz;

2) fine elbaite and dravite-type (length <5mm), distributed in clusters and patches, opaque and pleochroic, brown to greenish, located within fine mass of feldspar and quartz. The second group of tourmalines were often cracked, crushed and fractured.

The chemical analysis revealed domination of oxy-schorl, elbaite and oxy-dravite members.

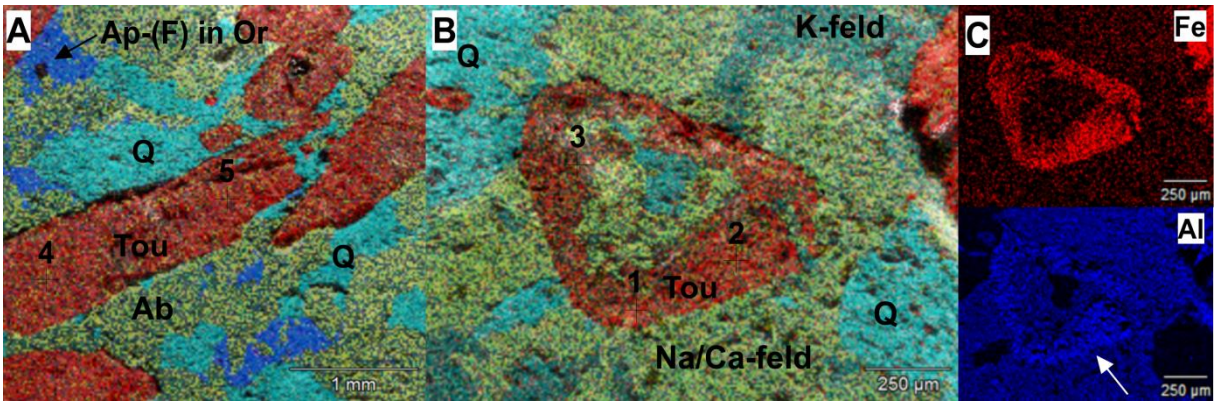

Fig. 2: The representative EDS chemical maps of analysed samples. Visible cracks and some apatite grains (A); Fe and Al zonation (B and C). Q-quartz, Tou-tourmaline, Ab-albite, Or-orthoclase, Ap-apatite.

Tab. 1: The representative chemical data of identified tourmaline members from the Lisiec Hill, Strzegom,

id	SiO_2	Al_2O_3	FeO_t	MnO	TiO_2	CaO	Na_2O	K_2O	MgO	Cl^-	B_2O_3	$H2O^-$	∑	type
N = 6 samples (10 analysis points); wt %														
L3_1	39.72	37.81	4.51	0.00	0.00	0.00	2.76	0.00	0.00	0.24	11.16	3.78	99.98	elbaite
L5_1	38.07	39.14	3.27	0.00	0.23	0.00	1.87	0.00	2.30	0.00	11.22	3.86	99.96	elbaite
L5_2	39.60	36.12	3.03	0.00	0.20	0.17	3.61	0.14	2.02	0.12	11.16	3.78	99.95	elbaite
L8_1	37.81	36.08	0.82	0.00	0.19	0.49	6.71	0.28	1.96	0.94	11.09	3.58	99.95	elbaite
L8_2	38.96	40.81	1.11	0.00	0.00	0.00	3.69	0.19	0.00	0.00	11.31	3.90	99.97	elbaite
L9_1	38.33	38.05	2.19	0.00	0.00	0.00	4.70	0.19	1.57	0.00	11.10	3.83	99.96	elbaite
L9_2	36.09	40.09	0.96	0.00	0.00	0.00	5.62	0.21	2.01	0.00	11.14	3.84	99.96	elbaite
L11_1	38.56	38.58	0.39	0.18	0.23	0.19	4.17	0.00	2.33	0.00	11.40	3.92	99.95	elbaite
L12_3	36.56	39.02	1.64	0.00	0.24	0.00	4.40	0.00	3.20	0.00	11.08	3.81	99.95	elbaite
L12_5	38.56	37.52	2.75	0.00	0.25	0.00	3.91	0.00	2.02	0.00	11.12	3.83	99.96	elbaite
mean	38.23	38.32	2.07	0.02	0.13	0.09	4.14	0.10	1.74	0.13	11.18	3.81	99.96	
st. dev.	1.11	1.46	1.25	0.05	0.11	0.15	1.30	0.11	0.96	0.28	0.10	0.09		
N = 2 samples (4 analysis points); wt %														
L6_3	37.79	36.61	2.05	0.15	0.19	0.00	3.99	0.00	4.34	0.00	11.04	3.80	99.96	oxy-dravite
L12_4	38.96	34.87	2.69	0.00	0.20	0.00	4.58	0.14	3.62	0.00	11.08	3.82	99.96	oxy-dravite
mean	38.38	35.74	2.37	0.08	0.20	0.00	4.29	0.07	3.98	0.00	11.06	3.81	99.96	
st. dev	0.59	0.87	0.32	0.08	0.01	0.00	0.30	0.07	0.36	0.00	0.02	0.01		
N = 2 samples (4 analysis points); wt %														
L1_1	36.91	36.68	4.85	0.00	0.22	0.18	3.99	0.00	2.45	0.00	10.90	3.76	99.94	oxy-schorl
L1_3	35.90	35.15	6.85	0.00	0.43	0.36	4.38	0.00	2.58	0.16	10.52	3.63	99.96	oxy-schorl
L2_1	36.77	35.26	7.14	0.15	0.41	0.17	3.47	0.14	1.83	0.24	10.74	3.63	99.95	oxy-schorl
L3_4	38.34	33.28	11.05	0.00	0.51	0.00	2.37	0.00	0.00	0.00	10.72	3.69	99.96	oxy-schorl
mean	36.98	35.09	7.47	0.04	0.39	0.18	3.55	0.04	1.72	0.10	10.72	3.68	99.95	
st. dev.	0.88	1.21	2.25	0.06	0.11	0.13	0.76	0.06	1.03	0.10	0.13	0.05		
Pieczka et al. 1988; wt %														
L_1988	35.50	33.40	13.06	0.28	0.54	0.46	1.31	0.05	1.40	0.00	10.30	3.59	99.89	schorl

The zonality of some crystals was observed, especially according to the Al and Fe distribution (see example Fig. 2B and C).

Some small grains of F-apatite had been identified for the first time in this locality (Fig. 2A). Olenite and (oxy)-foitite (not reported here) need to be confirmed by further research.

Several low Fe tourmaline members has been revealed, especially in group of elbaite and dravite.

The dominance of Al^{3+} in elbaite, comparing to oxy-schorl samples, may suggest lower substitution by Fe^{3+}.

The Mg^{2+} and Mn^{2+} occupancy of *Y* octahedral sites is insignificant, however, a bit higher was observed in the oxy-dravite. The Na^+ incorporation within *X* site in elbaite and dravite seems to be a bit higher, especially comparing to schorl (Tab. 1).

The structural model of analysed tourmalines need to be refined by additional XRD analysis and IR/Mössbauer spectra.

REFERENCES

Bačík P. (2015): The Canadian Mineralogist 53(3): 571–590.

Bosi F. et al. (2017): European Journal of Mineralogy 29(3): 445–455.

Bosi F. et al. (2018): Lithos: in press.

Janeczek J. (1985): Geol. Sudetica 20(2): 1−81.

Kozłowski A. (1984): Acta Univ. Wratislav. 834: 58–59.
Kozłowski A. (1987): Arch. Mineral. 42(2): 95–100.
Kozłowski A. (2003): Min. Soc. of Pol. Spec. Pap. 22: 126−128.
Pieczka A. and Kraczka J. (1988): Miner. Pol. 19(1): 25−38.
Pieczka A. et al. (2018): Minerals 8(126): 1–21.
Puziewicz J. (1981): Miner. Pol. 12(2): 69–75.
Traube M. (1888). Die Mineralien Schlesiens. Breslau.
Yavuz F. et al. (2002): Comp. & Geosc. 28(9): 1017–1036.
Żaba J. (1991): Zbieramy minerały i skały. Wydawnictwa Geologiczne.

Joint 5th Central-European Mineralogical Conference and
7th Mineral Sciences in the Carpathians Conference

New remarks on the Mn-columbite from Scheibengraben granitic pegmatite, Maršíkov, Czech Republic

[1]Łukasz Maciąg [#], [1]Adrianna Szaruga, [2]Rafał Wróbel

[1] University of Szczecin, Faculty of Geosciences, Mickiewicza 16A, 70-383 Szczecin, Poland
[#]lukasz.maciag@usz.edu.pl
[2] West Pomeranian University of Technology, Faculty of Chemical Technology and Engineering, Piastów 42, 71-065 Szczecin, Poland

Key words: Mn-columbite, granite, pegmatite, Scheibengraben, REE

INTRODUCTION

Columbite group minerals (CGM) are economically important accessory phases of granites and granitic pegmatites (Melcher et al. 2016).

CGM are showing intensive fractionation between Nb-Ta and Fe-Mn, giving detailed information about pegmatites formation and regional metamorphism history (Černý et al. 1992; Novák et al. 2003).

The empirical formula of cation ordered columbite is AB_2O_6, where commonly A = Fe^{2+}, Mn^{2+} and B = Nb^{5+}, Ta^{5+}. Other minor elements, such as Ca^{2+}, Sc^{3+}, Fe^{3+}, Ti^{4+}, Sn^{4+}, W^{6+}, and sometimes other REE, are additionally distributed over A and B positions.

CGM show an orthorhombic crystal structure (space group No. 60, *Pbcn*, $a \approx 14.27$, $b \approx 5.73$, $c \approx 5.06$ Å, V = 412.8 Å^3).

Natural crystals, depending on conditions of formation and chemical composition, may show partial cation disorder (Balassone et al. 2015).

The beryl-columbite REE rich Scheibengraben pegmatite is located about 1.5 km E from Maršíkov near Šumperk, being part of the Hrubý Jeseník Mountains pegmatite field of N Moravia. Several irregular pegmatite bodies are hosted by metapelites, amphibolites and rare granodiorites. They were found mainly in the sillimanite and staurolite metamorphism zones (Černý et al. 1992; Novák and Rejl 1993; Novák et al. 2003).

Few pegmatite textural-paragenetic units were recognized here, consisting mainly from albite-cleavelandite, muscovite, quartz, K-feldspar and accessory minerals: F-apatite, garnet, beryl (aquamarine), zircon, schorl, gahnite and other.

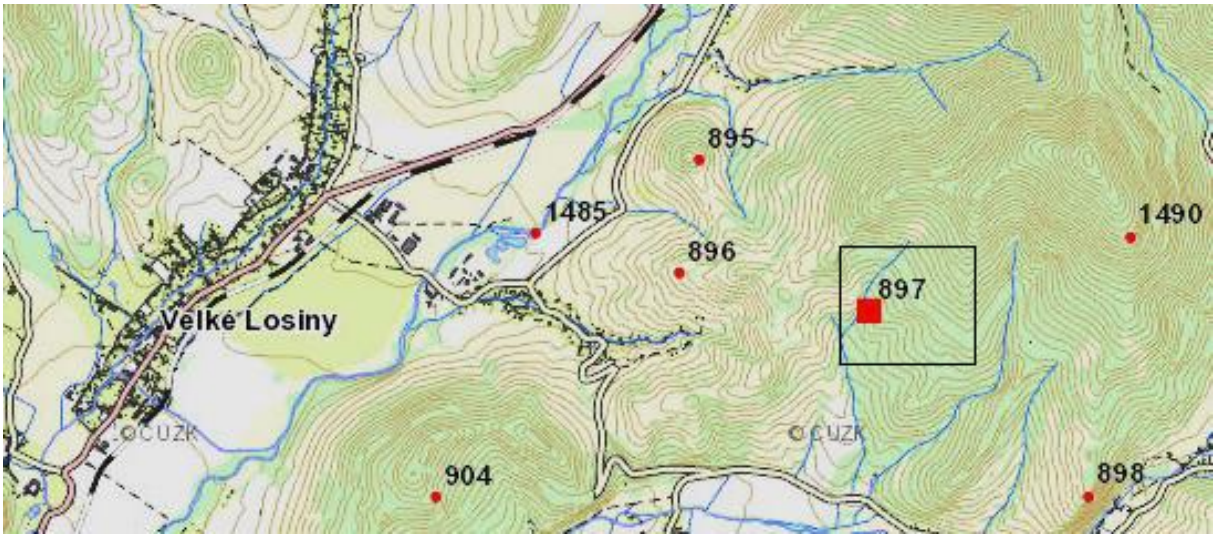

Fig. 1: The sampling location marked by black rectangle (www.lokality.geology.cz).

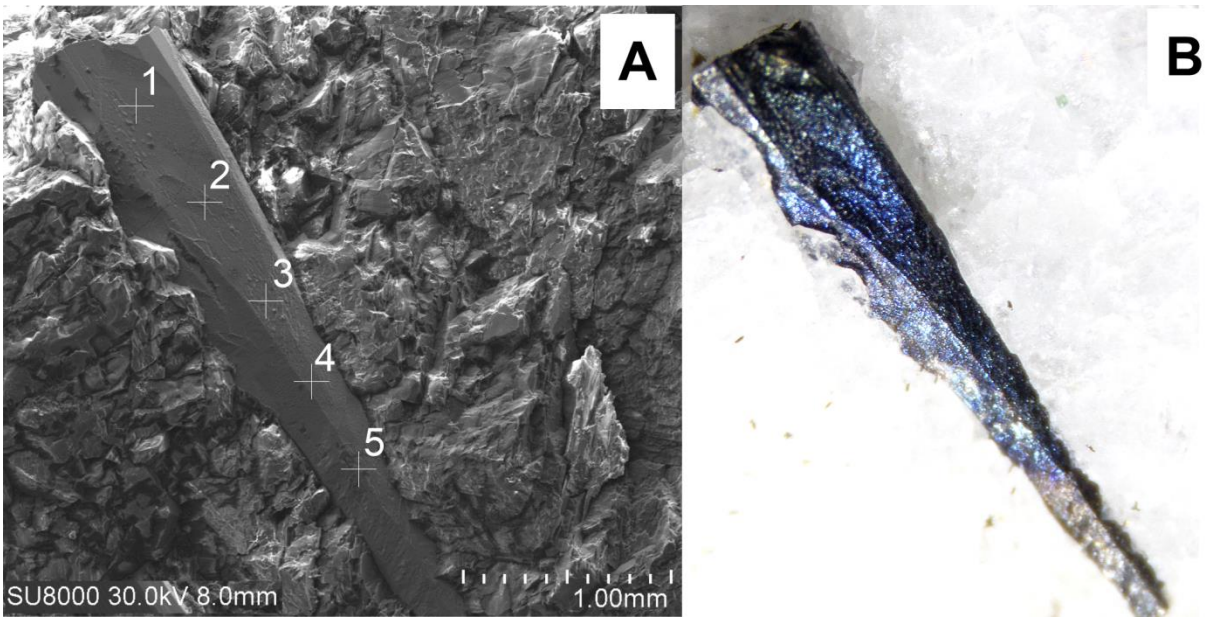

Fig. 2: The SEM photography (A) of a representative Mn-columbite crystal in albite matrix, with included EDS sampling points; the optical microscope image of the same specimen (B) revealing intensive blue-violet pleochroism.

The Nb-Ta oxides are relatively common in here, showing distinctive oscillatory and patchy zonation. Extreme Nb-Ta fractionation of the CGM from the Scheibengraben pegmatite is among the highest ever recorded within single pegmatite body, including Li-rich complex pegmatites (Novák et al. 2003).

Material and Methods

The pegmatite samples containing Nb-Ta oxides were collected in summer 2016 in the forest dumps near small abandoned quarry of Střelecký důl (Fig. 1.).

The visual description, photos and material separation was done at the Faculty of Geosciences, University of Szczecin, Poland.

The crystal samples were preliminary investigated using SEM Hitachi SU 8070 with the EDX Thermo Scientific Fisher NORAN 7, at the Faculty of Chemical Technology and Engineering, West Pomeranian University of Technology, Szczecin, Poland.

Presented chemical analysis was performed basing on the five data points from EDX (work in progress) from the one representative crystal (Fig. 2).

The chemical data were normalized on 12 cations and 24 oxygens per formula.

The calculations and theoretical unit cell dimensions were prepared using NBTA software (Yavuz 2001). Fe^{3+} content was estimated with Droop method (1987).

Results

The analysis of the well-developed, black-blueish-violet, pleochroic, orthorhombic Mn-columbite crystal revealed slight decrease of Fe, Nb and Ta towards ending, along the {010} rim. The highest Mn content was observed in the crystal ending. TiO_2 was distributed uniformly in range of 1.00-1.24 wt %.

The Nb_2O_5 and Ta_2O_5 contents were varying from 56.21-58.39 wt % and 9.86-12.08 wt %, respectively.

The MnO domination over FeO_t was revealed, in contents of 15.12-19.31 wt % and 12.12-14.49 wt %, respectively.

The SnO_2 and WO_2 were below 0.01 wt %. Complete chemical data are presented in the Tab. 1.

The Calculated (*abc*) unit cell dimensions are: $a \approx 14.33$ to 14.35; $b \approx 5.74$ and $c \approx 5.07$ Å, with $V \approx 417.32$ Å^3. Due to increase of *a* length towards crystal ending, some increase of V was observed (Tab. 1).

According to the Ta/(Ta+Nb) and Mn/(Mn+Fe) and *a/c* unit cell dimensions, analysed crystal needs to be considered as a intermediately fractionated and well ordered, similar to Mn-columbites investigated by Novák et al. (2003) (Fig. 3A and C).

Tab. 1: The EDS chemical data of analysed Mn-columbite crystal. The unit cell dimensions calculated after Yavuz (2001).

		M_1	M_2	M_3	M_4	M_5	mean	std. dev.
TiO_2		1.11	1.00	1.12	1.24	1.00	1.09	0.09
SnO_2		<0.01	<0.01	<0.01	<0.01	<0.01	<0.01	<0.01
WO_2		<0.01	<0.01	<0.01	<0.01	<0.01	<0.01	<0.01
MnO	[wt %]	15.12	15.96	16.40	19.31	18.92	17.14	1.67
FeO_t		14.06	14.33	14.49	12.12	12.60	13.52	0.97
Nb_2O_5		58.39	56.61	56.21	57.45	56.45	57.02	0.80
Ta_2O_5		11.30	12.08	11.76	9.86	11.01	11.20	0.77
Total		99.98	99.98	99.98	99.98	99.98	99.98	0.00
Ta/(Ta+Nb)		0.16	0.18	0.17	0.15	0.16	0.16	0.01
Mn/(Mn+Fe)		0.52	0.53	0.53	0.61	0.60	0.56	0.04
a		14.33	14.34	14.34	14.35	14.35	14.34	0.01
b	Å	5.74	5.74	5.74	5.74	5.74	5.74	0.00
c		5.07	5.07	5.07	5.07	5.07	5.07	0.00
V	Å³	417.03	417.32	417.32	417.61	417.61	417.38	0.22

The Ti content increase, along with the Ta/(Ta+Nb) decrease, was also revealed (Fig. 3B). Comparing to Černý et al. (1992) and Novák et al. (2003), titanium contents are here however a bit higher.

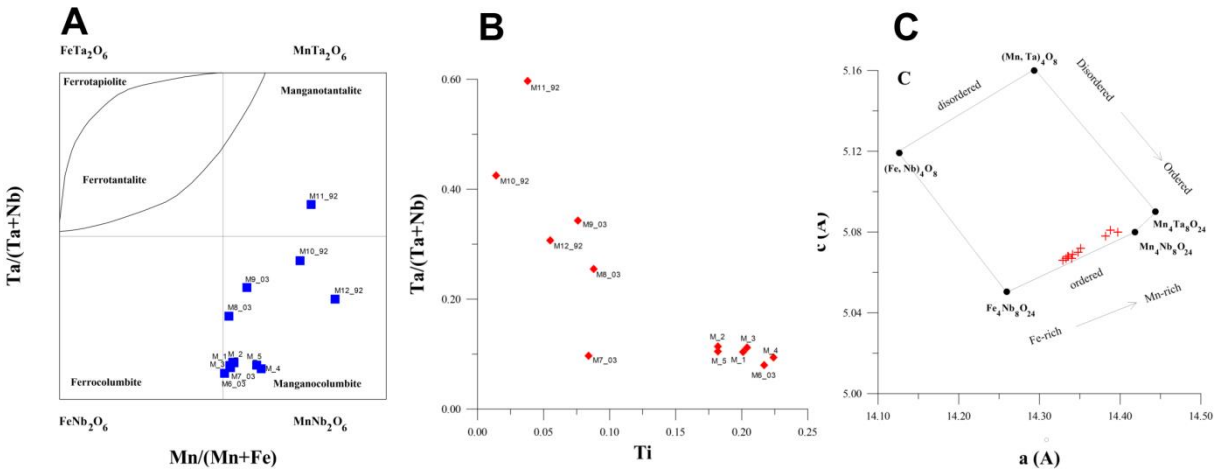

Fig. 3: The chemical composition of analysed Mn-columbite crystal according to the Ta-Nb, Mn-Fe relations (A) and Ti content (B). The structural state (C) basing on Černý and Turnock (1971). Mx_92 and Mx_03 data of Mn-columbite samples investigated by Černý et al. (1992) and Novák et al. (2003), respectively.

REFERENCES

Balassone G. et al. (2015): N. Jb. Miner. Abh. (J. Min. Geochem.) 192(3): 275−287.

Černý P. and Turnock A.C. (1971): Can. Mineral. 10: 755−772.

Černý P. et al. (1992): Can. Mineral. 30: 699−718.

Droop G.T.R. (1987): Min. Mag. 51: 431−435.

Melcher F. et al. (2016): Ore Geol. Rev.: 1–42.

Novák M. and Rejl L. (1993): Acta Mus. Moraviae, Sci. Nat. 78: 13−18.

Novák M. et al. (2003): Eur. J. of Min. 15(3): 565–574.

Yavuz F. (2001): Comp. & Geosc. 27: 241−248.

List of Authors

Bold = first author

Joint 5th Central-European Mineralogical Conference and 7th Mineral Sciences in the Carpathians Conference - Book of Contributions and Abstracts

Editors: Martin Ondrejka, Jan Cempírek and Peter Bačík

ISBN 978-80-223-4548-4